Final Project Report

Development and Utilization of Test Facility for the Study of Candle Filter Surface Regeneration

Research sponsored by the U.S. Department of Energy,
National Energy Technology Laboratory for the period of
10/1/99 to 12/31/2002

Report Prepared by

Bruce S. Kang (project P.I.) and Eric K. Johnson (project co-P.I.)

Mechanical and Aerospace Engineering Department
West Virginia University
Morgantown, WV 26506

April 29, 2003 (first edition)
July 14, 2003 (Final edition)

for

National Energy Technology Laboratory
U.S. Department of Energy
under contract **DE-FC26-99FT40203**

Table of Contents

Chapter 5 Influence of Reservoir Pressure on Surface Regeneration in RTTF

Chapter 6 Discussion on RTTF-Long Term Test Results

ABSTRACT

Hot gas particulate filtration is a basic component in advanced power generation systems such as Integrated Gasification Combined Cycle (IGCC) and Pressurized Fluidized Bed Combustion (PFBC). These systems require effective particulate removal to protect the downstream gas turbine and also to meet environmental emission requirements. The ceramic barrier filter is one of the options for hot gas filtration. Hot gases flow through ceramic candle filters leaving ash deposited on the outer surface of the filter. A process known as surface regeneration removes the deposited ash periodically by using a high pressure pulse of gas to back flush the filter. After this cleaning process has been completed there may be some residual ash on the filter surface. This residual ash may grow and this may then lead to mechanical failure of the filter.

A Room Temperature Test Facility (RTTF) and a High Temperature Test Facility (HTTF) were built to investigate the ash characteristics during surface regeneration at room and selected high temperatures. The RTTF system was used to gain experience with the selected instrumentation and develop an operating procedure to be used later at elevated temperatures. The HTTF system is capable of conducting surface regeneration tests of a single candle filter at temperatures up to 1500^{o}F. In order to obtain sequential digital images of ash particle distribution during the surface regeneration process, a high resolution, high speed image acquisition system was integrated into the HTTF system. The regeneration pressure and the transient pressure difference between the inside of the candle filter and the chamber during regeneration were measured using a high speed PC data acquisition system. The control variables for the high temperature regeneration tests were (1) face velocity, (2) pressure of the back pulse, and (3) cyclic ash built-up time. Coal ash sample obtained from the Power System Development Facility (PSDF) at Wilsonville, AL was used at the elevated temperatures regeneration tests. The basic test conditions were (1) Face velocity: 5 cm/s or 7 cm/sec (2) Regeneration pressure: 95 psi, and (3) Build-up time: 20 minutes.

A number of cyclic regeneration tests were conducted at 1,100, 1,200, 1,300, and 1,400 ^{o}F. The surface regeneration tests indicated no temperature dependence from room temperature tests up to 1,200 ^{o}F. Above 1300 ^{o}F, the ash layer showed greater cohesive strength and only the loose particles were removed during the initial few cycles of surface regeneration. It appears that the ash cake can continue to grow as the pressure difference between the chamber and filter pressure increases slowly. This may then lead to the inevitable candle filter failure due to bridging between filters.

EXCUTIVE SUMMARY

The objective of this project was to develop a system for a fundamental study of the ash characteristics during surface regeneration. A room temperature test facility, RTTF, was constructed. This system was used to gain experience with the selected instrumentation and develop an operating procedure to be used later at elevated temperatures. The major accomplishment was the coordinating the optical system, pressure readings, and the initiation of the surface regeneration process. In the development of the RTTF, The face velocity of the fluidized gas, the regeneration pressure of the back pulse and the time to build up ash on the surface of the candle filter were identified as the important parameters to be studied. Two types of ceramic candle filters were used in the study. Each candle filter was subjected to several cycles of ash build-up followed by a thorough study of the surface regeneration process, at different parametric conditions. The pressure histories in the chamber and filter system during build-up and regeneration were then analyzed. The size distribution and the movement of the ash particles during the surface regeneration process were studied. Effects of each of the parameters on the performance of the regeneration process are presented. A comparative study between the two candle filters with different characteristics is presented. The work in the RTTF system is reported in Part I of this report. In addition, conference papers were presented, references S.1 to S.7 and several masters theses were written. These references are listed at the end of the summary section.

The high temperature test facility, HTTF, was then developed based on the knowledge gained from working with the RTTF. The system is capable of conducting surface regeneration tests of a single candle filter at temperatures up to 1500^{o}F. A high resolution, high-speed image acquisition system was integrated into the HTTF system to obtain sequential digital images of ash particle distribution during the surface regeneration process. The regeneration pressure and the transient pressure difference between the inside of the candle filter and the chamber during regeneration were measured using a high speed PC data acquisition system. The control variables for the high temperature regeneration tests were (1) face velocity, (2) pressure of the back pulse, (3) cyclic ash built-up time and, (4) temperature of the hot gas being filtered. Tests were conducted up to, and including, 1500^{0}F.

The results of these HTTF tests appear to be reasonable on a macroscopic time scale, but rather chaotic on a microscopic time scale. It is the investigators opinion that the HTTF and associated equipment operated as desired and produced reliable results for the conditions selected. The HTTF test results suggested that the ash characteristics changed significantly and an additional surface regeneration phenomenon was detected. Time did not allow for an attempt to optimize the surface regeneration process at high temperatures. The work with the HTTF system is reported in Part II of this report. In addition, conference paper was presented, (S.2) and several theses have been completed or in preparation, S.8 to S.13.

Conference Proceedings

S.1 A Study of Ash Particle Distribution Characteristics of Candle Filter Surface Regeneration at Room Temperature," V. Vasudevan, B. Kang, and E. K. Johnson, 5th International Symposium on Gas Cleaning at High Temperature, Morgantown, WV 2002.

S.2 "A High Temperature Test Facility for Studying Ash Particle Distribution Characteristics of a Candle Filter During Surface Regeneration," J. Rincon, B. Kang, and E. K. Johnson, 5th International Symposium on Gas Cleaning at High Temperature, Morgantown, WV 2002.

S.3 "Investigation of Unburned Carbon on the Structure of Residual Ash," E. K. Johnson, S. Simha, B. S-J Kang, and R. A. Dennis, Proceedings of the 16th International Fluidized Bed Conference, May 2001.

S.4 "Basic Candle Filter Surface Regneration Investigation," B.S-J Kang, E. K. Johnson, S. Gregory, and R. A. Dennis, Proceedings, High Temperature Gas Cleaning Conference, Vol. II, 1999, Published by the Institut for Mechanische Verfahrenstechnik and Mechanik Universitat, Karlsruhe, Germany, 1999.

S.5 Test Facility for the Investigation of Surface Regeneration on Candle Filters," B.S-J Kang, E. K. Johnson, J. Barberio and S. Gregory, Proceedings of the Advanced Coal-Based Power and Environmental Systems '98, USDOE, 1998

S.6 Strength Characteristics of Filter Ash Deposits," J. Barberio, B. S-J Kang, and E. K. Johnson, Symposium on High-Temperature Prticulate Cleanup for Advanced Coal-Based Power Systems, USDOE-EPRI, Birmingham, AL, April 20-23, 1998.

S.7 "Development of High Temperature Facility for Filter Characterization During Filter Regeneration," E. K. Johnson, B. S-J Kang, J. Barberio, and J. Mei, Proceedings of the Advanced Coal-Based Power and Environmental Systems, USDOE, Pittsburgh, PA, July 22-24, 1997.

M.S Theses

S.8 "Numerical Simulation of Filter Ash Deposits," R. Mallela, West Virginia University, December 1997.

S.9 "Investigation of the Formation of Residual Ash on Candle Filters," S. Simha, West Virginia University, December 1998.

S.10 "Development of Instrumentation for the Investigation of Surface Regeneration for Candle Filters," S. Gregory, West Virginia University, 2001.

S.11 "Study of Candle Filter Surface Regeneration Characteristics at Room Temperature," V. Vasudevan, West Virginia University, May 2003.

S-12 "Development of a High Temperature Test Facility to Investigate Ash Characteristics During Surface Regeneration at High Temperatures, J. Rincon, WVU, May 2003.

S-13 "Non-intrusive Optical Studies of Particle Motion and Size Distribution," M. Zhang, West Virginia University, December , 2003 (est.).

Part I - Room Temperature Test Facility

STUDY ON CANDLE FILTER SURFACE REGENERATION CHARACTERISTICS AT ROOM TEMPERATURE

Part I Summary

Ceramic barrier filtration is a leading technology employed in hot gas filtration. Hot gases loaded with ash particle flow through the ceramic candle filters and deposit ash on their outer surface. The deposited ash is periodically removed using back pulse cleaning jet, known as surface regeneration. The cleaning done by this technique still leaves some residual ash on the filter surface, which over a period of time, sinters and forms a solid cake, which leads to mechanical failure of the candle filter.

A room temperature testing facility (RTTF) was built to gain more insight into the surface regeneration process before testing commenced at high temperature. RTTF was instrumented to obtain pressure histories during the surface regeneration process and a high-resolution high-speed imaging system was integrated in order to obtain pictures of the surface regeneration process. The objective of this research has been to utilize the RTTF to study the surface regeneration process at the convenience of room temperature conditions.

The face velocity of the fluidized gas, the regeneration pressure of the back pulse and the time to build up ash on the surface of the candle filter were identified as the important parameters to be studied. Two types of ceramic candle filters were used in the study. Each candle filter was subjected to several cycles of ash build-up followed by a thorough study of the surface regeneration process, at different parametric conditions. The pressure histories in the chamber and filter system during build-up and regeneration were then analyzed. The size distribution and the movement of the ash particles during the surface regeneration process were studied. Effects of each of the parameters on the performance of the regeneration process are presented. A comparative study between the two candle filters with different characteristics is presented.

Chapter 1

Introduction

1.0 Introduction

Coal reserves are abundant and an effective long-term usage of coal is strategically critical to energy security and global economics. The production of electricity from coal must however be accomplished as efficiently and cleanly as possible. Unlike the combustion of clean fuels, such as distillate oil and natural gas, coal combustion and gasification can produce significant amounts of particulate and release high levels of sulfur, nitrogen, and alkali. A new generation of "ultra-clean high efficiency" systems have significantly reduced the amount of the pollutants associated with coal fired plants built before 1970s.

Integrated gasification combined-cycle (IGCC) and pressurized fluidized-bed combustion (PFBC) are two examples of types of new-generation advanced coal fired power plants. Both of these power systems have demonstrated the ability to surpass existing new source performance standards, in some case by orders of magnitude, for all criterion pollutants. In these advanced power plants, the gas stream from the combusted coal drives a high efficiency gas turbine, and the steam generated from the heat of reaction drives a steam turbine. Therefore, for these systems, it is necessary to produce an acceptable environment for the high temperature turbine.

In IGCC systems (Figure 1.0.a), fuel gas, which is composed of hydrogen and carbon oxides, is generated in a gasifier by coal reacting with steam and air or oxygen. The pressurized gas is then cleaned and fed to a high-efficiency combustion gas turbine/generator. The gas clean up temperatures in this system are usually lower, 325 to

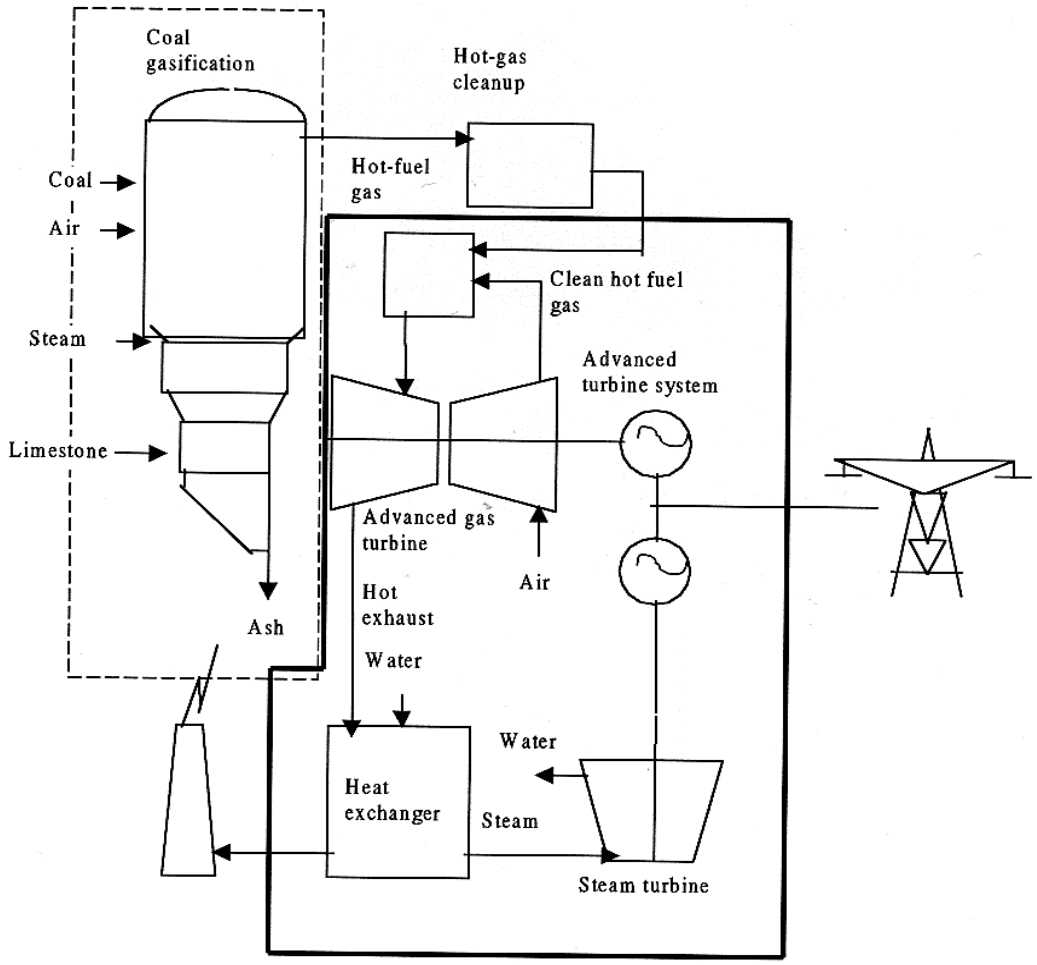

Figure 1.0.a
Schematic representation of IGCC system [5]

650 ^{o}C (about 600 to 1200 ^{o}F). The hot turbine exhaust produces steam to drive a steam turbine/generator. In a PFBC system (Figure 1.0.b) jets of air in a fluidized bed suspend a mixture of the coal and limestone or dolomite during combustion, converting the mixture into a suspension of red-hot particles that flow like a fluid. The limestone captures sulfur

oxides that are released by the burning coal. The gas clean up temperatures are higher compared to the IGCC and are in the range of 815 to 871 ^{o}C (about 1500 to 1600 ^{o}F).

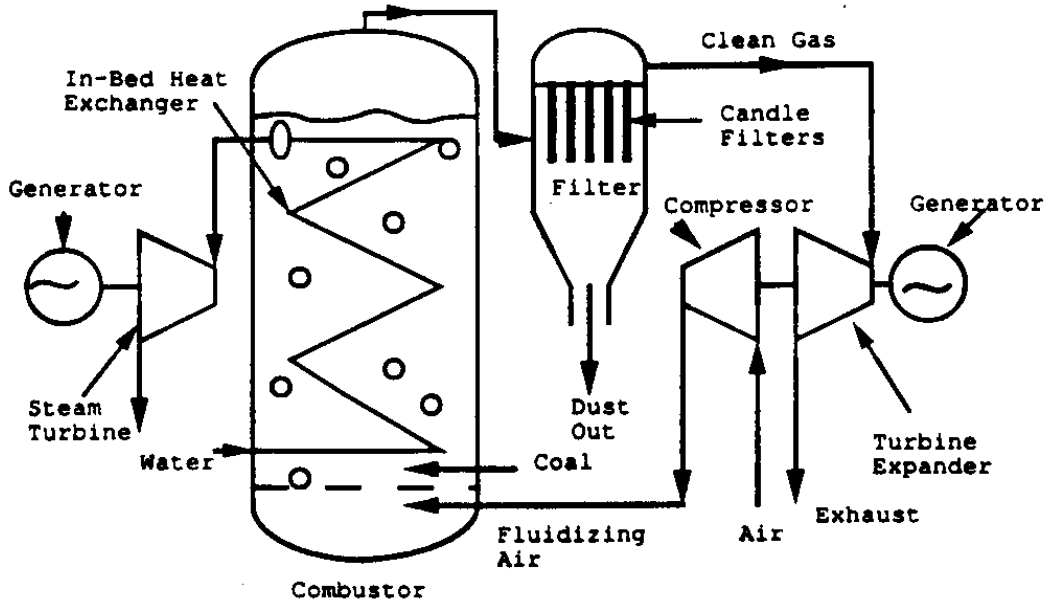

Figure 1.0.b
Schematic representation of PFBC system [20]

In these plants, coal-derived gases are cleaned prior to or during combustion at elevated pressures and temperatures, which makes them compatible with gas turbine power generation systems. These advanced coal based power generation systems require efficient hot-gas cleanup systems to protect the gas turbine and to control emissions. "Hot-gas cleanup improves overall system efficiency by as much as three percentages" [5].

Rotating and stationary airfoils in the hot-gas path are the parts of the gas turbine most sensitive to contaminants. To protect these airfoils, hot-gas cleanup systems for

IGCC and PFBC power generation systems must clean the raw gas to certain levels (Table 1.0.a). The following have been identified as the major factors that affect the airfoils in the hot-gas path:

Deposition: Accumulation of small particles on airfoil surfaces. The more the number of particles, the more are the chances of deposition.

Erosion: Rapid wear of turbine airfoils due to particulates. If too many larger particles enter the turbine, erosion will be heavy.

Corrosion: Rapid chemical attack of airfoil material after breakdown of surface coatings. [5]

Therefore, removal of particles in the gas stream is a necessary condition for the new power plants to be successful.

Numerous methods for achieving hot-gas particulate removal at high temperature and pressure are emerging. The leading technology for particle removal is the ceramic barrier filter, with a variety of ceramic filter element forms, (like ceramic candle, cross-flow, tube, or bag filter elements).

Concern	**Particulate Limits**
Erosion	All particles with less than 10 micron diameters, with 90% less than 5 microns
Deposition	Less than 100 parts per million weight
Corrosion	Total alkali (sodium plus potassium) less than 20 parts per million weight
Environmental	0.03 pound per MMBtu, higher heating value

Table 1.0.a
Guidance for contaminants in gases from coal based combustion systems [5]

Ceramic barrier filters have emerged as the most promising choice for hot gas cleaning because of their resistance to attack by aggressive gases and their ability to withstand high temperatures up to 875 ^{o}C. "A recent survey of 34 organizations, including utilities, filter manufacturers, power generation system constructors, government agencies, universities and research institutes, indicated a 65% preference for high-temperature gas filtration technologies over conventional low-temperature separators"[7]. The performance of ceramic filters has been investigated extensively, and laboratory results have confirmed excellent particle collection and cake detachment at high temperatures.

Although this technology shows a lot of promise, there are some problems that persist. During the filtration process an ash cake builds up on the surface of the candle filters, causing the pressure drop to increase. An excessive accumulation of the ash cake on the surface of the filter results in abnormal pressure drops and bridging. Bridging is defined as accumulation of ash that fill spaces between filters that can result in filter breakage. In the long run, ash accumulations reduce the performance of the hot gas filtration, and in turn the power plant. The filter medium is cleaned, by a pulse of compressed gas. The overall effort of this research, at West Virginia University, has been focussed on the comprehensive understanding of the filter surface regeneration (cleaning) process. The specific problem to be addressed is to determine the optimum process conditions for filter regeneration, or cleaning.

The final goal of this research program is to build a high temperature test facility (HTTF) to test candle filters in a high temperature environment that would operate in conditions close to the ones existing in power plants. A room temperature testing facility

(RTTF) was initially built in order to gain valuable insights regarding: (1) the instrumentation for surface regeneration process, (2) the operational information that could be used for the high temperature system, (3) to correct or avoid any unforeseen problems in the high temperature system.

The RTTF was built and instrumented to enable room temperature surface regeneration studies. The control features in the system allowed the operator to control important parameters in the regeneration process, such as flow rates and back pulse pressure and duration. The PC-based data acquisition system allowed the synchronization of the controls and various sensors to collect useful pressure data associated with the surface regeneration process. An optical/imaging system was developed in order to obtain high resolution images during the surface regeneration process. The optical system has been integrated with the PC-based data acquisition system to coordinate the surface regeneration process with the imaging system.

The data obtained was useful

a) in determining the strength of the ash layer under different parametric conditions,

b) in obtaining the images of the surface regeneration process.

1.1 Objectives

The objective of this study is to develop a comprehensive understanding of the ceramic candle filter surface regeneration process under room temperature conditions. In particular the optimal conditions will be determined. The results from the room temperature tests will be helpful in predicting, to an extent, the nature of results in high temperature tests.

The parameters that affect the regeneration characteristics have been identified as,

1) Regeneration pressure pulse
2) Face velocity of build up air
3) Time of ash layer build-up

In order to achieve the objectives, based on the above parameters a test matrix was developed and a series of tests were performed using the RTTF. Two brands of filters, "Lanxide-PRD-66$^{\rightarrow}$" and "Pall-442T$^{\rightarrow}$", were used as the testing filters. In this thesis, the two filters, "Lanxide-PRD-66$^{\rightarrow}$" and "Pall-442T$^{\rightarrow}$", are referred to as "Lanxide" and "Pall" filters respectively. After a preliminary cycle of tests, a testing protocol was developed and implemented.

The tests yielded pressure data and images of the surface regeneration process. The pressure data was used to obtain information regarding pressure drop during cleaning cycles, the pressure build-up in the chamber, the nature of regeneration, and the efficiency of cleaning process during the tests. The image data in addition helps us in obtaining time of crack initiation, the nature of surface regeneration and the particle size distribution.

Chapter 2

Literature Review

2.0 Hot gas filtration

Advanced coal power generation systems utilize combined cycle technology to achieve high thermal efficiency. Higher thermal efficiencies are achieved by operating a gas turbine (on the combustion gases) in addition to the conventional steam turbine, for power generation. IGCC and PFBC are two examples of such advanced power generating systems. These systems are widely anticipated as future technologies to produce electricity from coal [7].

The requirements placed on a hot gas cleaning system primarily relate to meeting environmental emission regulations for the power plant and satisfying turbine protection standards. "The dust emission limits required by environmental legislation vary from country to country, but a figure of less than 20ppmw is a reasonable guideline" [23]. Turbine protection standards that have been developed by the vendors usually do not allow any particle greater than 20μm diameter, and set restrictions on particle loading in the 0-20μm range. [16]

High operating temperatures and fuel gas characteristics impose additional conditions in the design of hot gas filtration systems. To maintain a high thermal efficiency, the gas cleaning should be carried out at a high temperature. For PFBC system hot gas clean up must be accomplished at 700-850 ^{o}C at pressures between 7-15 atm. The hot gas filtration system for IGCC should operate at a temperature of 350 ^{o}C at the least. Long term durability, alkali corrosion, cleanability, brittle failure, thermal shock and

particulate penetration into filter media have been recognized as major concerns related to hot gas filtration systems [7].

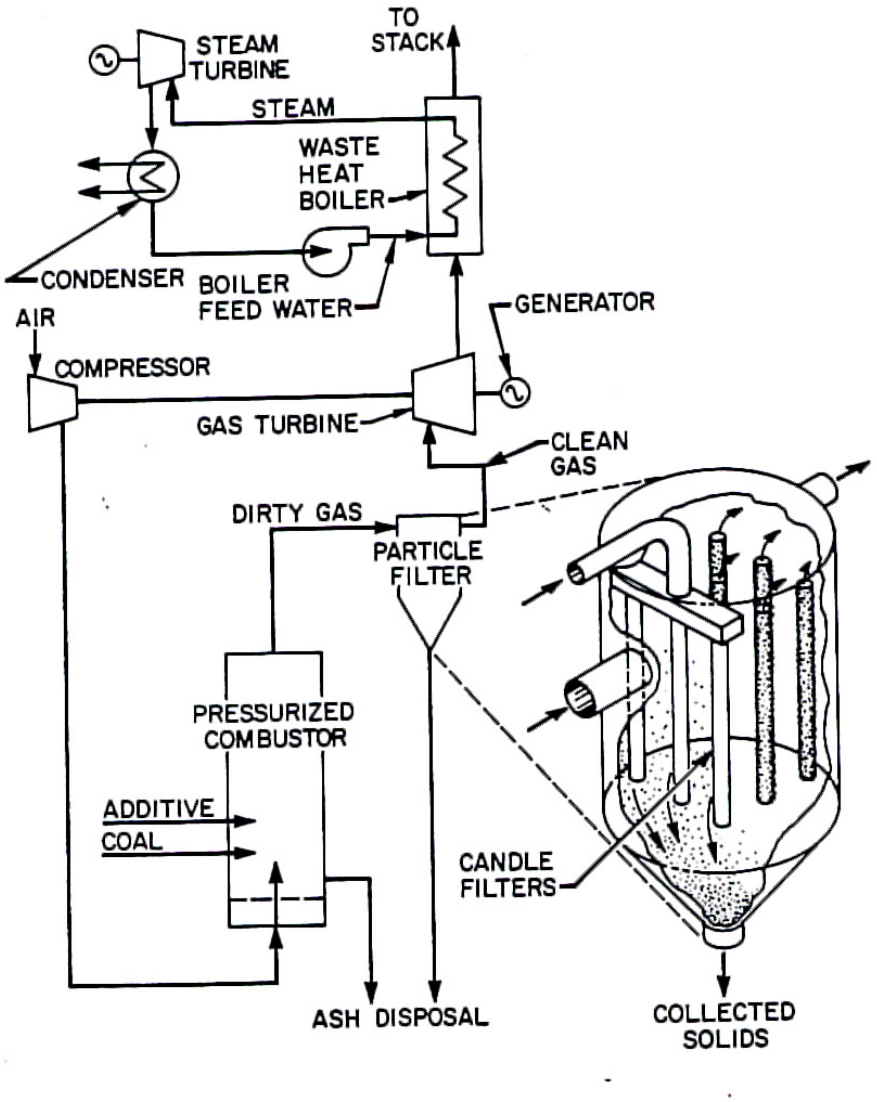

Figure 2.0.1
Schematic of advanced coal based power system with hot gas filtration [22]

Different types of particulate collection devices are being developed for application in advanced power generating systems. Some of the more prominent ones are:

- High performance mechanical collectors
- High efficiency barrier filtration filters
    1. bag filters
    2. ceramic candle filters
    3. ceramic cross flow filters
    4. metal candle filters
- Electrostatic precipitators
- Sonic agglomerators ahead of mechanical collectors
- Electrostatic agglomerators ahead of mechanical collectors [17].

An investigation on cleanability factors of ceramic candle filters, forms the basis of this study, hence only ceramic candle filters will be reviewed in this chapter.

2.1 Ceramic candle filters

Ceramic candle filters have emerged as one of the most promising hot gas filtration devices. Candle filters are usually long porous cylinders closed at one end and open at the other end. The open end is usually flanged to allow the mounting of the candle on a tube sheet plate. They are rigid with pore sizes ranging between 5 and 100 microns. Filters tested in this study are about 0.5 m long, 60 mm outer diameter and 10 mm wall thickness. Most filters used in industry are about 1.5 m long, 60 mm outer diameter and 10-15 mm wall thickness. [21,23]

The candle filters are formed from ceramic particles or fibers bundled with both organic and inorganic binders. Materials such as alumina/mullite, cordierite,

aluminosilicate foam, clay bonded silicon carbide, bonded or sintered silicon nitride, and cordierite-silicon nitride are used in these porous candle filters [14]. The filters are essentially stable at high temperatures and are not damaged by spark or incandescent particles. The filters have been found to withstand high temperatures of up to 1000 ^{o}C. A further characteristic of the ceramic structure is that filters are relatively inert to attack from aggressive chemical such as steam and acid gases. [7,21]

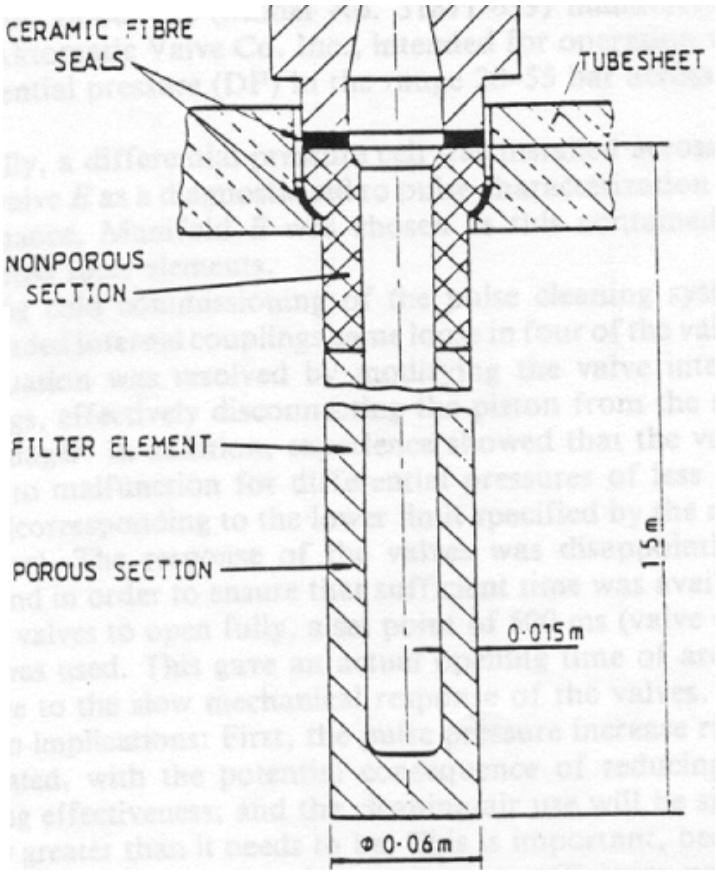

Figure 2.1.1
Ceramic candle filter and mounting system [20]

"Previously, ceramics were thought to be the only materials suitable for use under PFBC conditions, but metals are now being considered for two reasons: 1) advancements have been made in processing methods from corrosion resistant alloys, allowing them to be fabricated into metal filter media, 2) lower hot gas filter temperatures, associated with second generation PFBC are being considered that will provide lower-risk entry opportunities into the commercial market" [6].

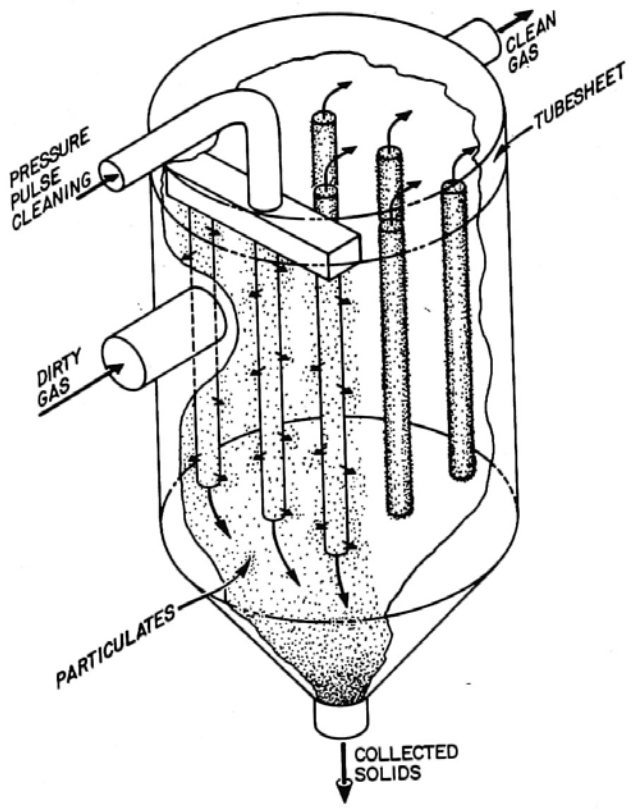

Figure 2.1.2
Hot gas filtration using candle filters [22]

The filter medium is designed to act as a surface filter so that dust is deposited on the outer candle surface and builds up into a cake. During filtration an ash cake develops on the surface of the candle filter and a linear increase in the pressure drop between the outer surface and the inside of the candle filter, have been observed [13]. The usefulness of filter in practice does not only depend on the cleaning efficiency by which it removes the incoming particles from the gas. This efficiency is very close to 100% for all but the most demanding applications. It depends to a much greater extent on its long-term pressure drop history. In order to maintain an acceptable total pressure drop across the filter, a reverse pulse removes the cake periodically. It is intended that the detached dust cakes then falls off into a collection bin, and the filter returns to a state approaching its original condition. This process of removing the cake from the filter surface by the reverse pulse has been termed as "surface regeneration". [11,13]

2.1.1 Candle filter failures

Ceramic candle filter systems have been observed to perform unsatisfactorily and even fail during operation. A progressive weakening of the candles has been cited as a concern in the Grimethorpe PFBC facility. The mechanism of which has not been fully identified. It has been suggested that improvement on the bond material and variation in the silicon carbide grit size could improve its physical properties. [20]

Mounting systems instability, distortion in the tube sheet holding the candle filters, thermal expansion and creep in the header sheet and mechanical shock due to the pulse jet have caused failures in the filter system. Thermal shock effects due to the cold air impingement during pulsed jet cleaning cycles have also been observed. [17,20]

Ash accumulation and bridging around the filter elements was a problem experienced at Grimethorpe PFBC testing facility. The problem was not solved adequately and was probably due to combination of effects involving ineffective cleaning, ineffective dust shedding form the body of the elements and insufficient element separation. The elements showed a tendency to bend. This is believed to be due to a combination of the earlier problem, ash accumulation around the elements, and pulsing. [20,23]

2.2 Surface regeneration

Pulse cleaning of rigid ceramic filter elements requires that the dust cake be dislodged from the outside surface. To apply an outward radial force to the dust cake the pressure drop during filtration has to be neutralized. Internal stress is applied to the dust layer and a pressure drop across the filter and the dust cake is built up by a sudden reverse flow. [11,12,13]

Ideally upon the application of reverse pressure pulse, the ash cake should dislodge completely from the filter. The most common of all the assumptions in the problem of cake detachment is that the dust cake detaches from the filter medium, when it experiences a tensile stress sufficient to overcome either the strength of the adhesive bond between the cake and the medium or the internal cohesion of the cake. In theory, as soon as the strength of this adhesive or cohesive bond is exceeded, the cake detaches everywhere simultaneously. [11,12,13]

When a reverse flow of cleaning gas is imposed, there will be a total pressure difference across the medium plus the cake, ΔP_T. However, only part of this pressure difference, ΔP_C, acts across the filter cake and it is shown that,

$$\Delta P_C/\Delta P_T = R_C/ R_{C+}R_M$$

Where R_C and R_M, are the resistance to flow (pressure difference divided by face velocity) of the cake and the medium, respectively. The total resistance ($R_{C+}R_M$) can be obtained from the pressure drop at a given flow rate immediately prior to cleaning, while R_M can be obtained from the pressure drop immediately after cleaning. [11,12]

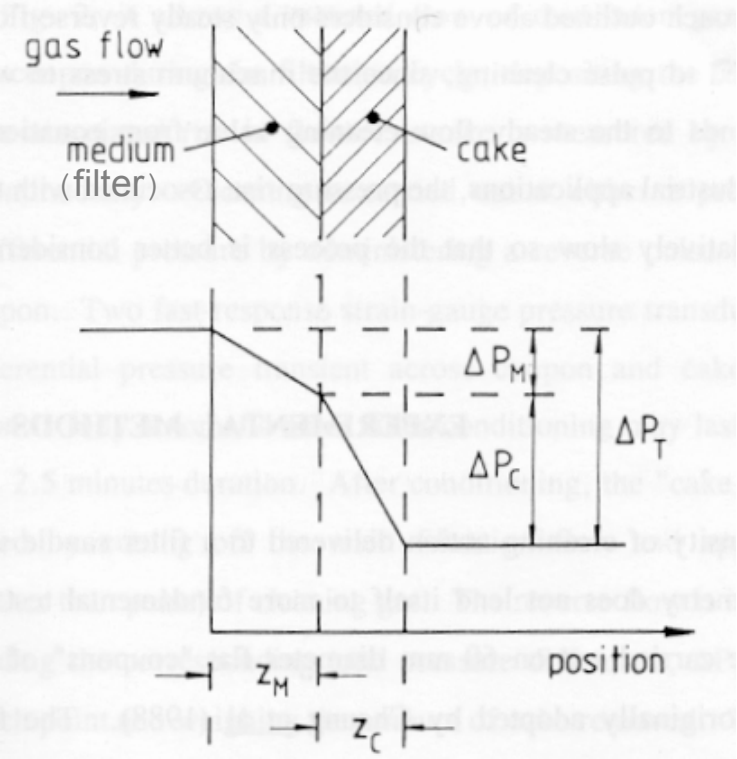

Figure 2.2.1
Pressure distribution in medium and cake during reverse flow [11]

In practice, however, neither the adhesive/cohesive cake strength nor the applied stress is uniform across the filter surface, so "patchy" cleaning is often the result. It has also been observed that the dislodgment of the dust layer does not occur directly at the interface between the filter element surface and dust cake, but somewhere inside the dust layer itself. This leaves a thin layer of dust that remains on the surface (after cleaning) and is termed as the residual layer. The layer of ash that builds on top of the residual layer and dislodges when reverse pulse is applied is called as the temporary layer. The sum of pressure drop due to the residual ash layer and the pressure drop of the medium is termed as the baseline pressure. This is pressure drop after all the elements are cleaned and is dependent on a large set of parameters, mainly the interaction of the dust cake with the filter element surface and the residual dust layer permeability.

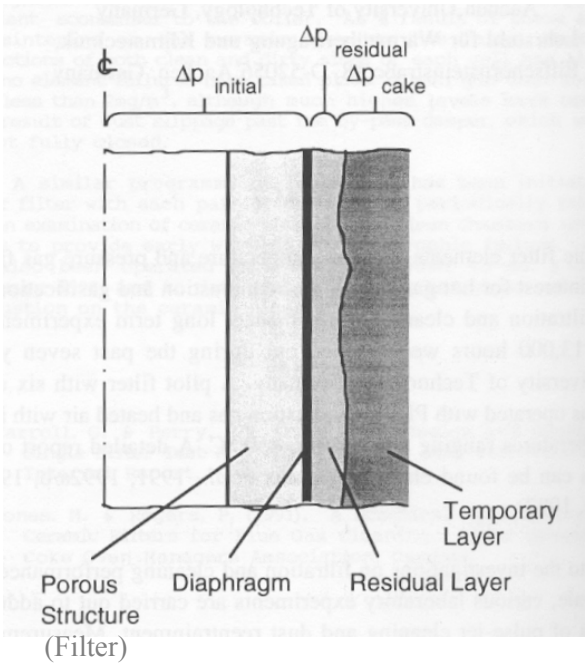

Figure 2.2.2
Filtration model [11]

During filtration, the pressure drop increases linearly [13]. With a sufficiently strong pulse the entire dust layer accumulated can be removed. Experiments show that a specific threshold pulse is necessary to achieve cleaning at certain operating conditions. Pulse pressures below this threshold fail to remove any dust cake. This results in a permanent building of the dust layer. The pressure generated by a pulse inside the filter cavity must always exceed the pressure drop of the filter to achieve a local flow reversal. [11,13]

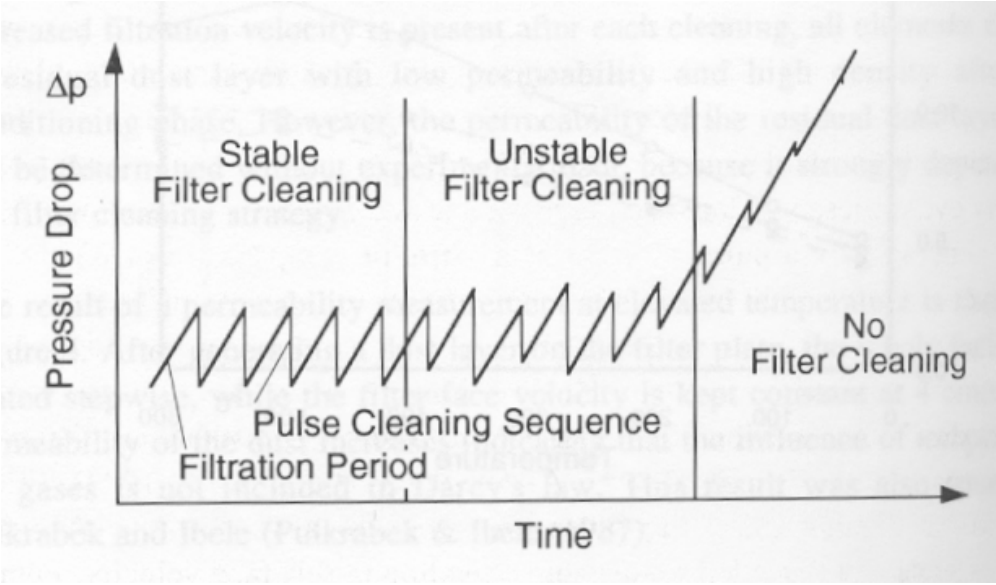

Figure 2.2.3
Filtration model [13]

In repeated cycles of filtration and cleaning, pulse pressures slightly above threshold pressure seem to provide sufficient cleaning. Since, the amount of dust settling on the surface is larger than the dust removed from surface by the cleaning pulse, an increasing residual layer occurs. This in turn causes increased pressure drop, as depicted in the "unstable filter cleaning" region of Figure 2.2.3. If the pulse pressure is not

increased at this point, the operation turns into a failure as shown in the right hand section of the Figure 2.2.3.

Stringer and Leitch showed that in the cleaning operation, the desirable situation is for the cake to fracture within the cake itself, leaving a thin layer of residual dust. They suggest that this is the best way to operate because the filter/dust cake interface is stable since further impregnation does not occur. For a long-term stable operation of the filter element, successful pulse cleaning of the filter is essential. The baseline pressure drop should not keep increasing with time and completely resist the cleaning pulse process. [20]

2.2.1 Pressure Histories during surface regeneration

The pressure histories for the filter and chamber observed during surface regeneration illustrate an important factor in the analysis of cleaning process. Measurements of transient pressure differences in the candle filters have been carried out experimentally by a number of researchers.

Laux *et al,* at the Aachen University of Technology-Germany, experimentally recorded the pressure histories while testing a cold filter element. The transient pressure values measured, by Laux *et al* at the center of the element are shown in Figure 2.2.4. All the pressure pulse settings employed in their tests, reversed the pressure differential across the filter. It can be seen that a 2 bar pulse generates only little over-pressure, relative to the 6 bar pulse. [13]

Berbner and Loffler obtained pressure traces during regeneration at the University of Karlsruhe-Germany. They obtained pressure traces for different pulse durations and

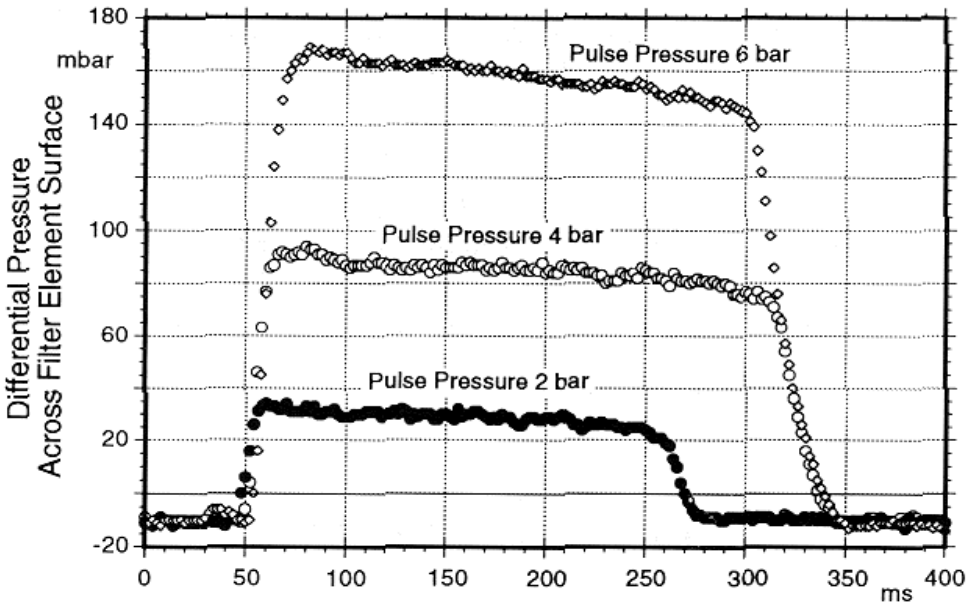

Figure 2.2.4
Transient pressure across the filter element during pulse
- for different pulse pressure[11]

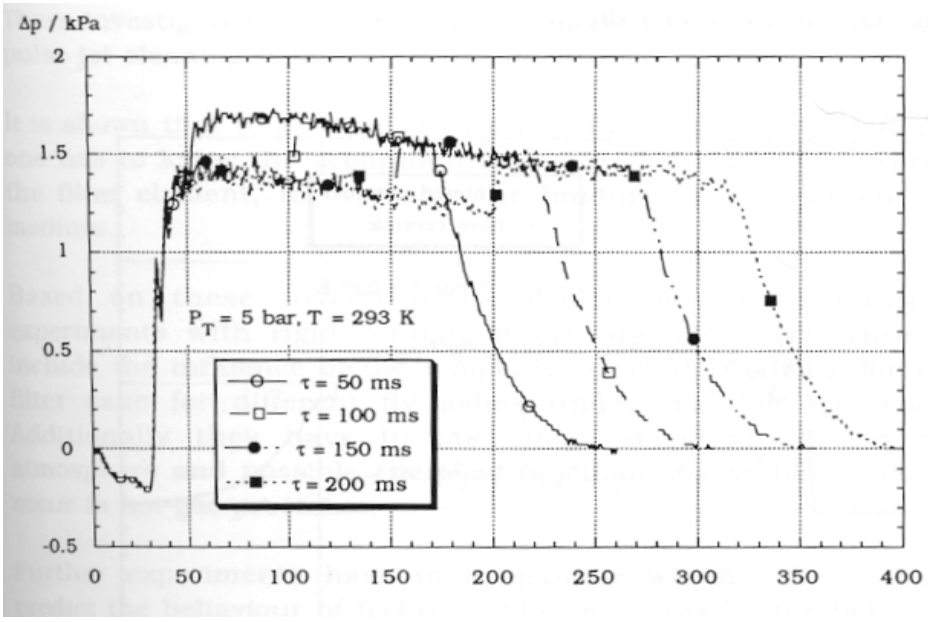

Figure 2.2.5
Transient pressure across the filter element during pulse
- for different pulse duration [2]

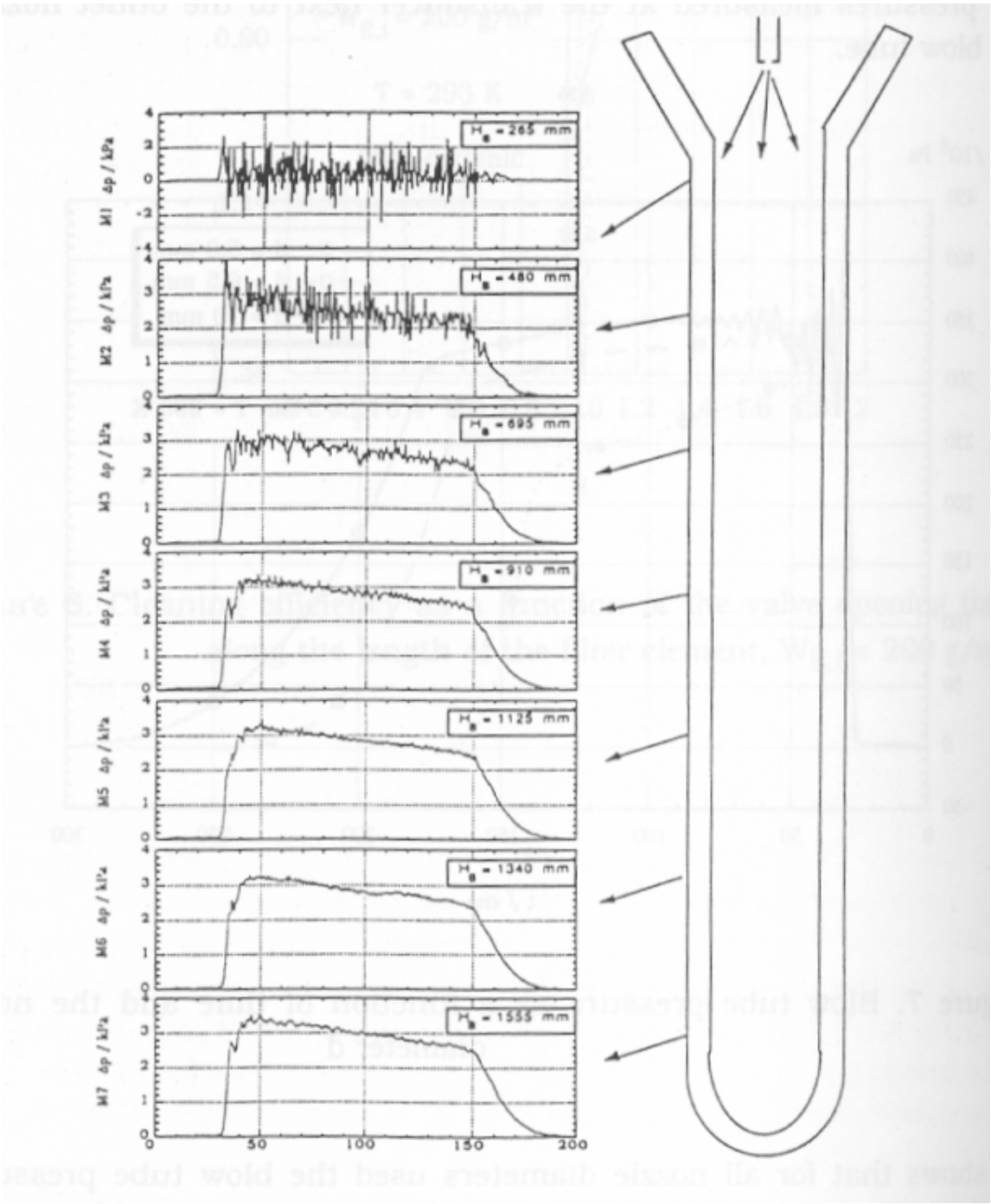

Figure 2.2.6
Transient pressure across the filter element during pulse, along the length of the filter[2]

also for different lengths along the candle filter element, under ambient conditions. The valve opening time did not seem to have any significant influence over the pressure peaks in the filter element (Figure 2.2.5). The cleaning jet was loosing energy progressively as it traveled along the filter length and the time the peak pressure occurred lagged relative to the top of the filter. [2]

Zhongli Ji et al measured the transient pressures in a three-filter system. They have examined the effect of reservoir pressure on the transient pressure in the filter element. The pressure transducer was mounted on the inner surface of the candle filter to measure the transient pressure (Figure 2.2.7). [8]

They divide the whole transient pressure pulse into three parts: 1) zero (gauge) pressure part, 2) positive (gauge) pressure part and 3) negative (gauge) pressure part. In the first part, the pressure in the filter element is zero, and this corresponds to the delay time just before pulse jet is activated. In the second part, is the positive pressure pulse that generates the reverse pulse flow to dislodge the dust cake on the surface of the filter element to perform the pulse jet cleaning. In the third part, having longer acting time, the authors defined this as the "interim process" between the pulse-jet cleaning and normal filtration in which the transient pressure inside the filter element is much lower than the outside of the filter element. The interim process may cause a fraction of particles removed to re-deposit on the candle surface. Especially smaller particles with lesser inertia are easily re-deposited to form a thin and dense layer on the filter, thus increasing the residual pressure drop across the filter. This process of re-deposition of small particles during the interim process has been termed as the re-entrainment process. The study on

the interim process may have very important effects on the long-term stable operation of the filter unit. [8]

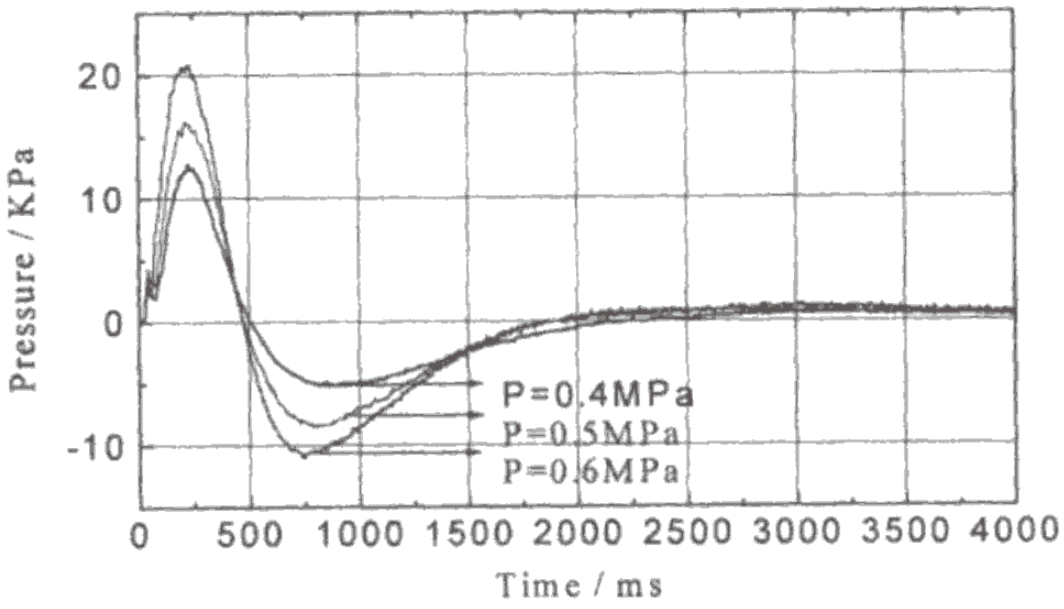

Figure 2.2.7
Transient pressure across the filter element during pulse,
- for the different pulse pressures [8]

2.2.2 Surface Regeneration Efficiencies

Different methods have been employed to calculate the efficiency of the cleaning process. The efficiency discussed here relates to how well the filter is cleaned during the surface regeneration process.

Berbner and Loffler [2] have proposed a method to calculate the efficiency, by calculating the ratio of the removed to the remaining dust fraction between two successive pressure pulses. This efficiency is termed as the incremental efficiency, R:

$$R = 1 - \frac{W_{E,i}}{W_{R,i}}$$

Where: $W_{E,i}$ = Incremental areal dust density just before cleaning process

$W_{R,i}$ = Incremental areal dust density just after cleaning process

i = sample location on the candle filter

Chiang [4] presented a residual pressure drop formulation γ, this γ fraction represents the residual filter pressure drop when filtration occurs cyclically. Where

$$\gamma = \frac{\Delta P_{final} - \Delta P_{clean}}{\Delta P_{initial} - \Delta P_{clean}}$$

ΔP_{final} = Pressure drop across the candle filter just after cleaning process

$\Delta P_{initial}$ = Pressure drop across the candle filter just before cleaning process

ΔP_{clean} = Pressure drop across the candle filter with no ash [4].

When comparing tests with the same face velocity, the pressure drop caused by the ash can be used as an indication of how much ash is on the filter. Simple algebraic manipulation leads to:

$$\eta = \frac{\Delta P_{initial} - \Delta P_{final}}{\Delta P_{initial} - \Delta P_{clean}}$$

This efficiency is the change in pressure drop caused by the removal of ash divided by the pressure drop caused by the ash before surface regeneration.

The efficiency η is good for comparing results within a certain ash build-up thickness, i.e. comparing thick ash results to thick ash results, or thin ash results to thin ash results. However, when comparing thin ash results to thick ash results this efficiency was found to be misleading. [24]

A new variable, ϕ, was introduced to compare the thin ash tests to the thick ash tests. Using the equation:

$$\phi = \frac{\Delta P_{final}(\delta_1) - \Delta P_{final}(\delta_2)}{\Delta P_{initial}(\delta_1) - \Delta P_{initial}(\delta_2)}$$

Where δ_1 is the ash thickness for a thick ash and δ_2 is the ash thickness for a thin ash. The only independent variable being changed in these tests is the ash thickness. The other variables were kept constant. [24]

2.3 Factors influencing surface regeneration process

The cleaning process of candle filter system is affected by a number of factors. It can be broadly categorized based on the filter system design, the filter element properties, ash properties and surface regeneration characteristics. The filter system design factors include the pulse jet delivery system, the filter arrangements, nozzle design, etc. The filter properties that affect the cleaning process include the filter material, strength, porosity, surface characteristics, and the shape. Ash properties are characterized by the chemical composition, interaction with the filter material, size and filtration characteristics. The surface regeneration characteristics deal with the effect of reservoir pressure, filtration velocity, the build-up time, the type of cake detachment and ash cake

characteristics. For a successful and optimal cleaning system, all the factors mentioned above needs to be assessed and optimized in a holistic manner.

In order to obtain optimal conditions of pulse jet cleaning for a given filter system with the same filter and same ash it is important to study the effect of surface regeneration parameters. Mechanism of residual ash growth and ash re-entrainment can be studied and correlated to the change of surface regeneration characteristics.

a) Cake thickness and detachment

A thicker dust cake brings about a better cleaning. In thicker dust cakes, the jetting gas is less likely to escape in large quantities through cracks, thus an uniform regeneration distribution is achieved. Although a higher pressure drop is observed, the cleaning is found to be more efficient. The cake detaches as thicker pieces and fall with less fine dust, reducing chances of re-entrainment and brings about an improvement in cleaning. It has been observed that for thin filter cakes, the residual pressure drop increases rapidly. [3]

b) Cleaning time interval

The cleaning time interval is the filtration period when ash cake growth occurs, and will be referred to as build-up time. If the cake is allowed to grow for a longer period, the average pressure drop across the filter unit increases, but there are two counterbalancing effects on the cake removal process itself. Firstly, less pressurized cleaning gas is required if the filter is cleaned less often. Secondly, provided that the cake

removal stress is not affected by the increased cake thickness, less cleaning flow is required at each cleaning event.

c) Filtration velocity

A high filtration velocity results in a dense dust cake, therefore the removal of a dust cake at high filtration velocity is more difficult than that collected at a lower filtration velocity. Filtering at higher face velocity is marked with high residual pressure and extremely reduced cycle times. Also if the dust loading is low for a given filtration velocity, then the pressure drop will be lower. [3,9,12]

d) Regeneration pressure

Cleaning efficiency is found to increase with increasing pulse reservoir pressure or the regeneration pulse pressure. A higher regeneration pulse pressure imparts a higher stress on the ash cake. An extended regeneration pressure pulse duration does not seem to have an effect on the cleaning. It has been concluded that an increase in the reservoir pressure is more effective than to extend the valve opening time. [3,9,11,12,13]

e) Particle properties

The particle sizes and their distribution along with the material composition play a very important role in the filtration and surface regeneration properties. The role played by particle size and distribution will be discussed in detail assuming a constant chemical composition. Cake detachment stress decreases strongly with increase in particle size

[12]. Smaller particles have a greater tendency to be re-entrained immediately after the surface regeneration. [3,8]

Investigations have been undertaken to study the possibility of sintering of ash particles to the filter surface under high process temperatures. Sintering on the surface increases the pressure drop and may eventually lead to the system breakdown. Ash particles sinter by viscous flow mechanism. The rate of sintering for different sizes of particles for a given viscosity (10^8 Nsm^{-2}) has been plotted in Figure 2.3.1 [18]. It is obvious from the plot the sintering rate is higher for smaller particles. A study on particle size distribution especially during regeneration, is important.

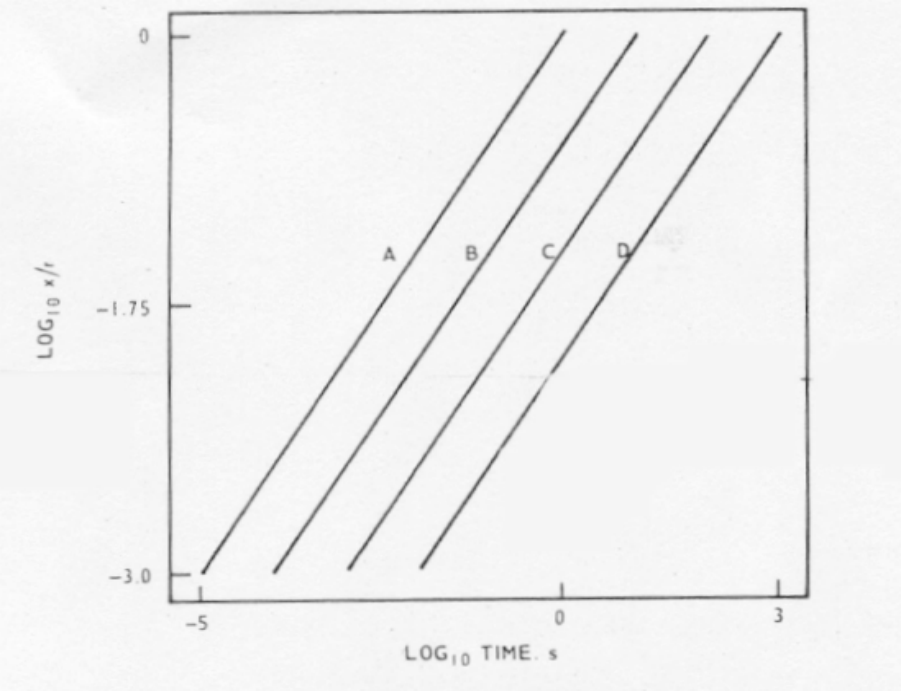

A 0.05 micron
B 0.50 micron
C 5.00 micron
D 50.0 micron

Figure 2.3.1
Sintering rate for different particle sizes [18]

f) Filter porosity

Filter porosity or permeability strongly influences cleaning efficiency. A higher permeability filter offers a higher cleaning efficiency. Cleaning air easily flows through the filter medium and enhances the cake dislodgment. The pressure pulse profile also differs with the porosity of the filter. [9]

g) Operating temperature

The surface forces, which bind the ash cake together alters with temperature. The operating temperatures have a strong effect on cake detachment stress. The mechanism of cake detachment however is same at all temperatures. [2,3]

2.4 Imaging the surface regeneration process

Observing the cleaning process and simultaneously measuring the pressure histories in the filter during the cleaning process, helps in obtaining several important information regarding the regeneration. A correlation can be established between the observed phenomena and the pressures developed. For example the crack initiation time can be matched with the pressure drop across the filter element. Video observations have been used to study the surface quality after regeneration. Several research groups have used video observations to study the regeneration process.

The particle sizes and distribution immediately on the application of the cleaning pulse has become a subject of interest because of the possible influence on the sintering of ash on filter surface. The more the smaller number of particles the higher the

probability of re-entrainment and faster the sintering rate. Imaging the surface regeneration event and analyzing the images can help in studying this mechanism in a better manner.

Kanaoka et al [9] used a high-speed video camera to monitor the regeneration process. The schematic of their experimental set up is shown in Figure 2.4.1. They used the imaging system to get images of the surface regeneration process. The images of the filter after the regeneration process were obtained to study the surface quality.

Laux et al [11] used a solenoid valve triggered camera that captures a frame every 20ms, to image the regeneration event and record it on a tape. Individual images (Figure 2.4.2) were processed on a personal computer with imaging software.

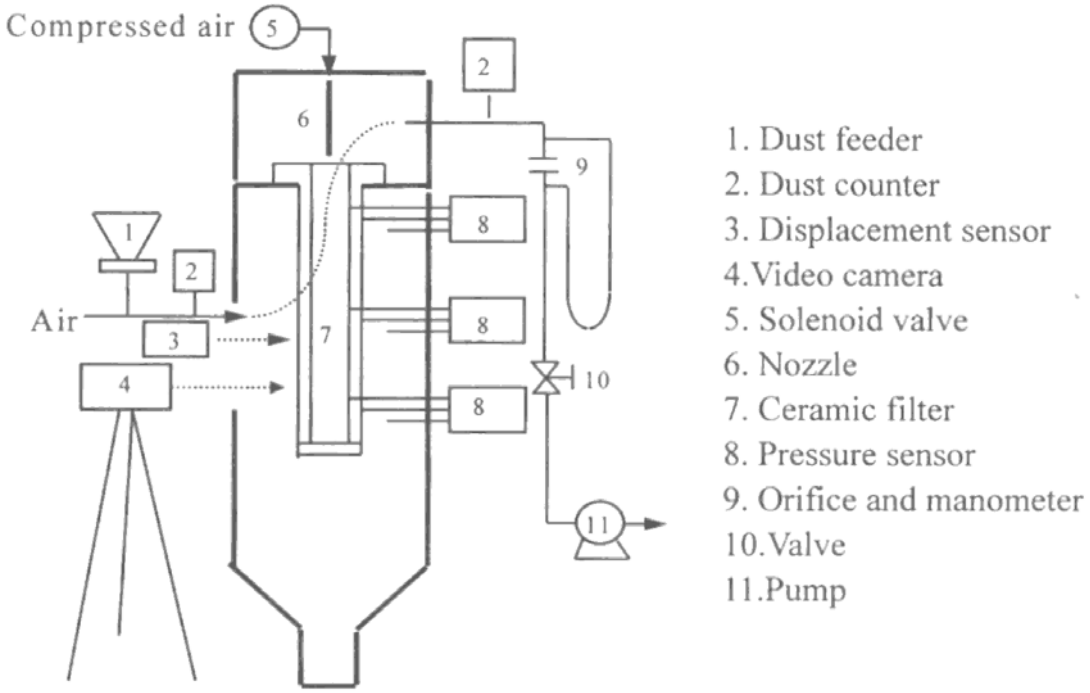

Figure 2.4.1
Schematic of experimental system imaging the candle filter regeneration [9]

Christ et al [1] used video observations to analyze the pulse cleaning event on a flat filter specimen. The camera captured a frame every 20ms and they correlated the image with pressures obtained using a high speed pressure transducer. Crack initiation time was observed and correlated with the pressure conditions (Figure 2.4.3). The cracks were found to start even before the pressure difference reaches its maximum value.

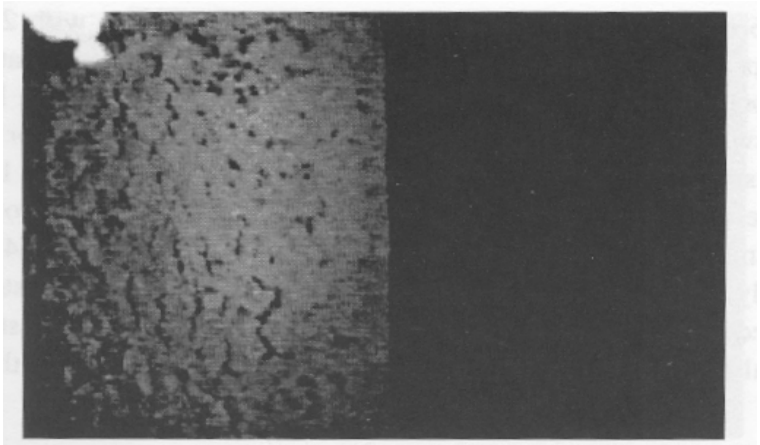

4 bar Pulse Approximately 20 ms after Cleaning Started

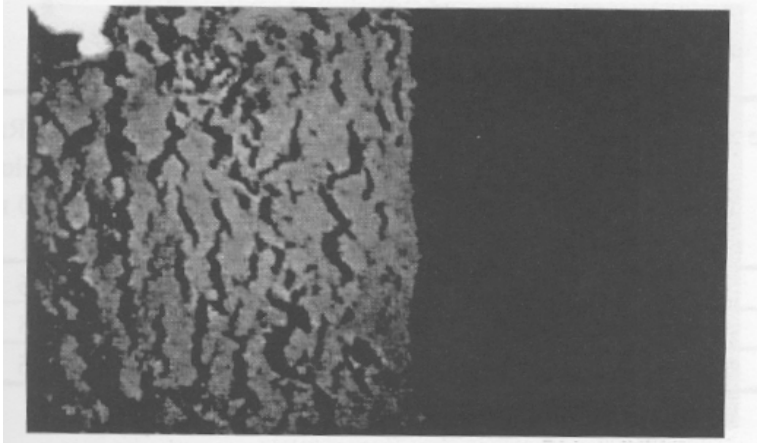

4 bar Pulse Approximately 40 ms after Cleaning Started

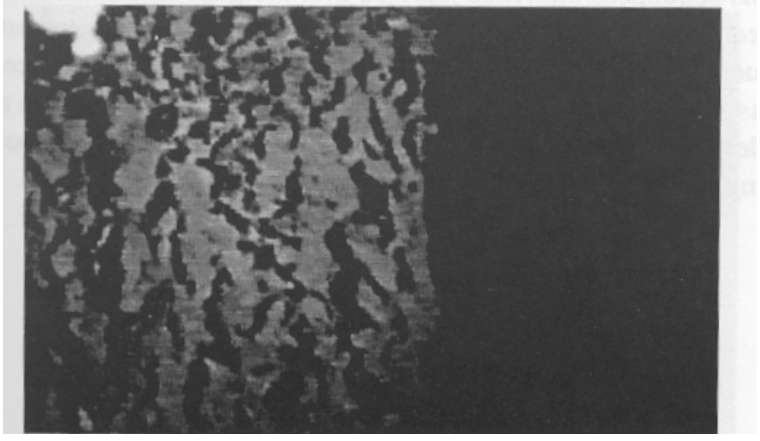

Figure 2.4.2
Images of candle filter surface regeneration [11]

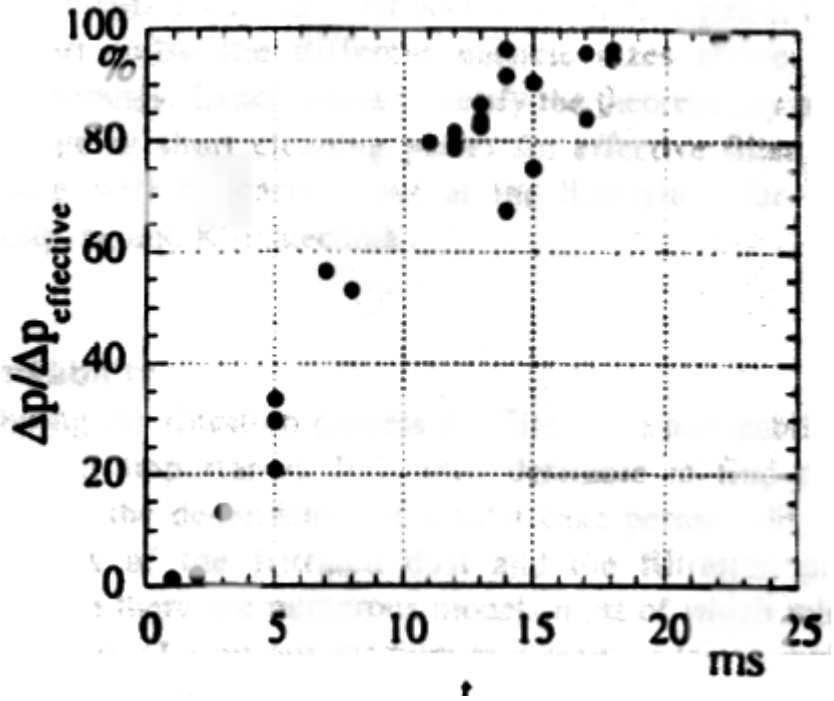

Figure 2.4.3
Crack initiation time and its relation to the pressure inside the flat specimen (of candle filter), maximum ash thickness = 5 mm [1]

Chapter 3

Room Temperature Testing Facility

3.0 Introduction

A room temperature testing facility (RTTF) was built and instrumented to perform surface regeneration studies under ambient temperatures. The facility is designed to hold a single candle filter element (about 60 mm diameter and 0.5 m length). A brief introduction to the chamber and instrumentation used in RTTF is provided in this chapter. The optical system used to capture the images of the surface regeneration process in RTTF is then discussed. The program written in MATLAB to measure, count and classify ash particles based on its size is also described in this chapter.

3.1 Chamber and instrumentation

The room temperature testing facility (RTTF) is primarily a square, airtight, chamber with a provision to house a candle filter (Figure 3.1.1). The room temperature chamber is made of aluminum and the chamber is divided into the cap region, chamber body and the bottom cone. The chamber is positioned on four steel legs. The chamber is 12 inches square and 24 inches tall, and has glass windows on three of its walls. There is an air inlet/outlet on its fourth wall. The cap region houses the nozzle that injects the reverse pulse jet and the exhaust. A header sheet houses the filter and is bolted between the chamber and the cap flanges. The bottom cone holds the ash and air inlet jets to fluidize the ash during the filtration phase. A special attachment to fluidize the ash is present in the bottom section.

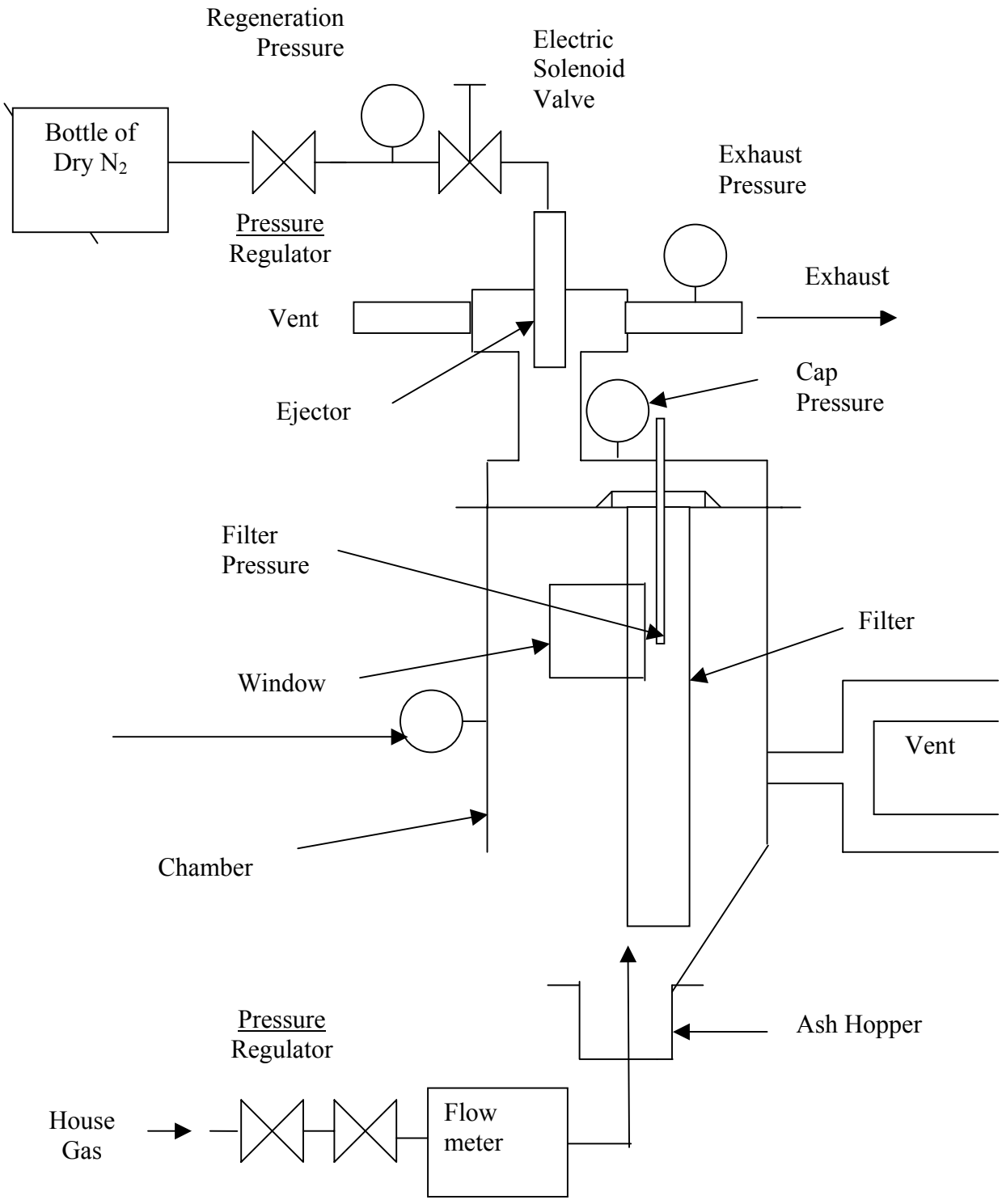

Figure 3.1.1
Schematic of RTTF chamber and instrumentation

Compressed air from a wall outlet (house gas) is regulated to fluidize the ash for a given flow condition. The filter collects the dust on its surface, as the air passes through the filter element, and escapes through the exhaust. A high-pressure dry nitrogen tank is used as a source to provide the reverse pulse jet and the regulator on the tank is used to obtain the desired regeneration pressure. When the solenoid valve opens high pressure nitrogen passes through the velocity tube and solenoid valve before expanding through a nozzle into the chamber. The electrically operated solenoid valve was opened for a 0.3 seconds period to provide a short high pressure cleaning pulse. There are vents on the cap and chamber, which were used to release the pressure differentials in the chamber and cap regions, and to maintain ambient pressure conditions.

Pressure transducers located at the chamber, cap, exhaust, velocity tube and inside the filter (refer Figure 3.1.1) were used to sense the pressure histories during the filtration process (or the build up period) and during the surface regeneration process. The pressure histories were recorded using a PC based data acquisition system (data acquisition board: Microstar Laboratories DAP 5200a/526 with a 300 MHz and 32 MB RAM) to collect the data in real time. A resolution of 0.00344 psi per division is obtained with this sensor-data acquisition combination. The data acquisition board was also used to control the solenoid valve to open/close to enable the surface regeneration. A high resolution high speed Charge Coupled Device (CCD) camera (1024 x 1024 with 256 MB on-board memory) was used to capture images of the surface regeneration process. The data acquisition board was used to trigger this camera too.

Two programs "calib.dap" and "fastak.dap" written in the data acquisition boards programming language have been used to record the data during build-up and

regeneration respectively. The filtration is a long and steady process without any sudden changes in the pressures, so a slower data acquisition rate sampled at every 0.25 second was used. The regeneration is a short process with sudden and large pressure variations, so a higher data acquisition rate sampled at the rate of 0.01 second during regeneration.

3.2 Optical system

An important objective of this project was to design an optical system to study the surface regeneration process, such as crack initiation time, type of regeneration and ash thickness. As discussed in Chapter 2, the study of particle size and distribution immediately after surface regeneration is very important. The two key components of the optical system are: 1) illumination, and 2) the imaging system. The objective in developing the optical system was to capture images in a vertical plane (radial plane) normal to the circumference of the candle filter. It is assumed that the effect of the reverse pulse jet is radially symmetric and thus this radial plane will serve as a representative plane. These images can be further processed to obtain the particle size, distributions and trajectories.

3.2.1 Illumination

Illumination or lighting is as important as the imaging system in designing the optical system. The performance of the imaging system is best when the illumination is evenly and brilliantly illuminated. A parallel light source system was built using a cylindrical lens and a bright halogen lamp (white light). Light stops are provided to further direct the light as a thin parallel beam. This light beam is designed to illuminate the focal plane of the imaging system.

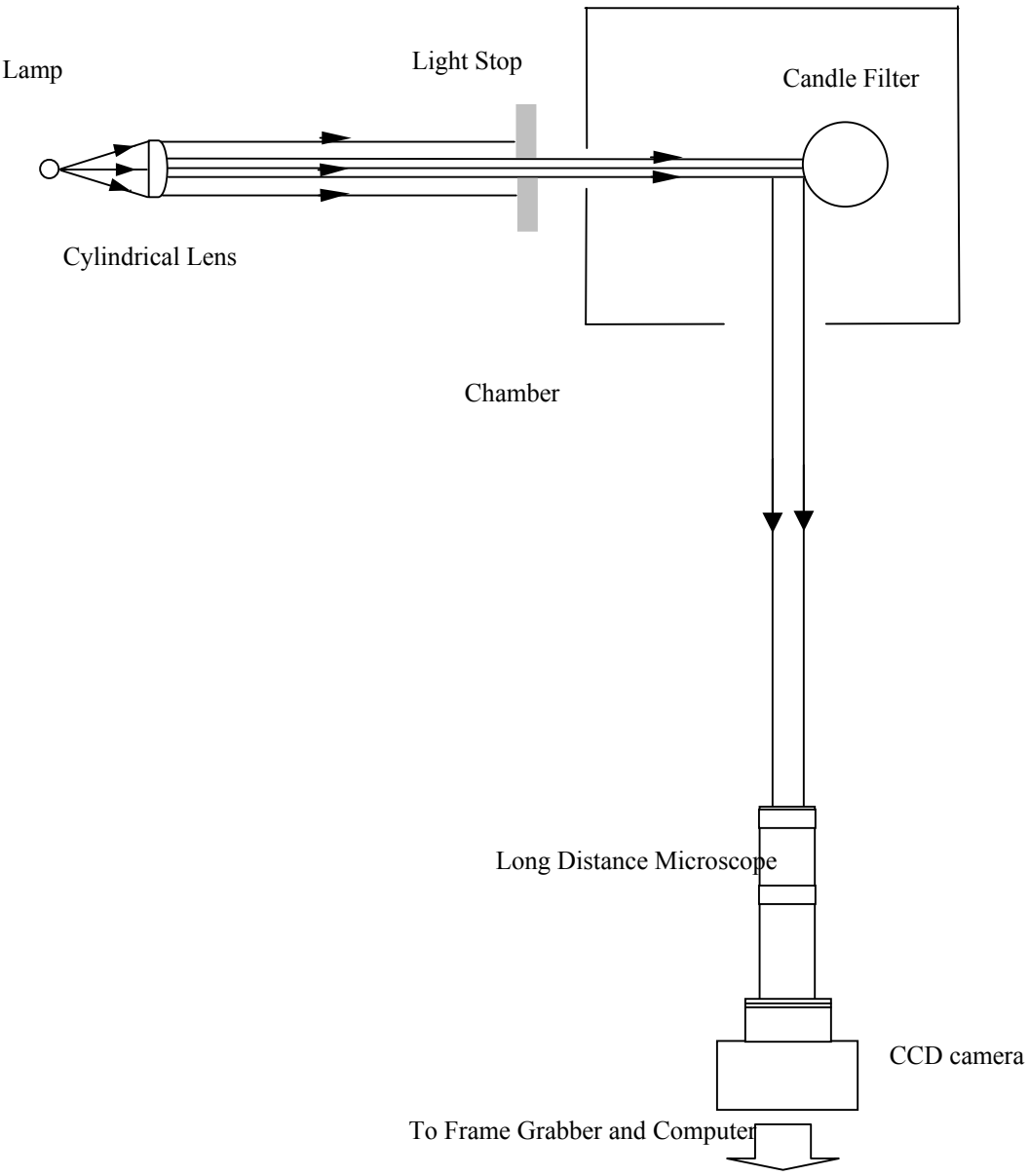

Figure 3.2.1
Schematic of optical system in RTTF

3.2.2 Imaging system

The imaging system consists of 1) a long distance microscope, 2) a high resolution & high speed camera and 3) an image acquisition board. The imaging system was designed to captured a 36 x 36 mm region, with a partial view of the filter surface . This helped in observing the surface and its immediately surrounding regions during filter regeneration.

1. Long distance microscope:

The long distance microscope is capable of imaging the region of interest, which is at a distance with sufficient magnification and resolution, on the camera's sensor. Infinity's Model K2, a commercial long distance microscope was used for this purpose.

Figure 3.2.2 Long distance microscope used in RTTF

2. CCD camera:

The CCD camera used in this study is a commercially available model, XYBION CCD-70. The camera has 1024 x 1024 pixels, and can capture images at 30 frames per second. The camera can be configured to capture 1024 horizontal pixels and 512 vertical pixels at 60 frames per second. An image acquisition board is used to transfer the captured images to the computer.

3. Image acquisition board:

4MEG VIDEO Model 12 (manufactured by Epix Inc) was the image acquisition board used in the RTTF imaging system. A 12 MIPS TMS320C25 digital signal processor is used to accelerate image processing functions. Analog and digital inputs can be sampled at rates up to 50 MHz. The pixel clock can be selected from either the video camera (or other external source) or an onboard generator. In order to maintain pixel accuracy the video camera was chosen as the pixel source. The Model 12 can generate a variety of capture or display video formats including RS-170, CCIR, RS-330, and RS-343, as well as nonstandard image formats as in the case of the RTTF's imaging system. An external TTL level trigger was used to initiate image sequence capture. The image acquisition board has been found to perform satisfactorily to capture the nonstandard 8 bit gray level images (1024 x 512 pixels resolution @ 60 frames/sec). The current configuration allows us to capture 512 consecutive images.

3.3 Particle counting program

The size of the ash particles during regeneration and their distribution immediately after the regeneration with time is an important factor that needs to be

studied. This factor is studied because of small particle reentrainment and possible sintering during the regeneration process. The estimation of the sizes and calculation of time distribution was initially performed manually. The manual estimation was time consuming and tedious, and thus could have resulted in some inaccuracies and in consistencies in the result obtained.

A program was developed using MATLAB^{TM} to enhance and process the images. The program assumes no two particles are overlapping each other and all particles are in the plane of focus. This helps us in obtaining a sufficiently accurate first estimate of the distribution.

The first step in this process is to enhance the images in order to get a clear distinction between the particles and the images. Then the images were converted to a binary image in order to facilitate the counting of ash particles and estimate their size. A scanning and counting algorithm was developed to detect, determine the size and the distribution of particles. Once the particle was detected a "nearest neighborhood" technique was applied to estimate the number of pixels covered by the particle. Then by using the predetermined scaling factor, which gives the resolution of a pixel in a given image, the size of the particle is determined. Then the location of the particle and its size are used to obtain the required results, in the format desired.

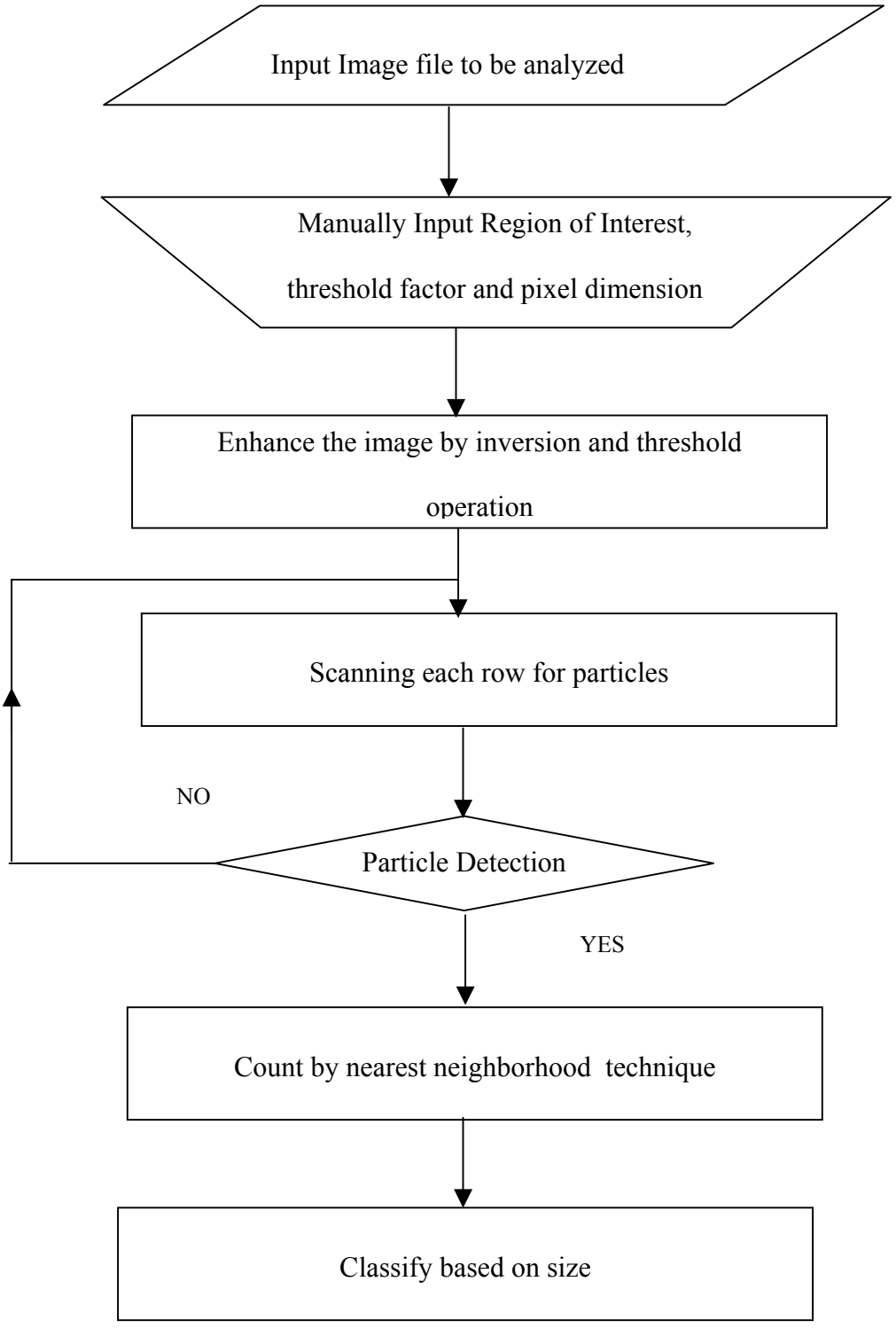

Figure 3.4.1
Flow chart for particle counting program

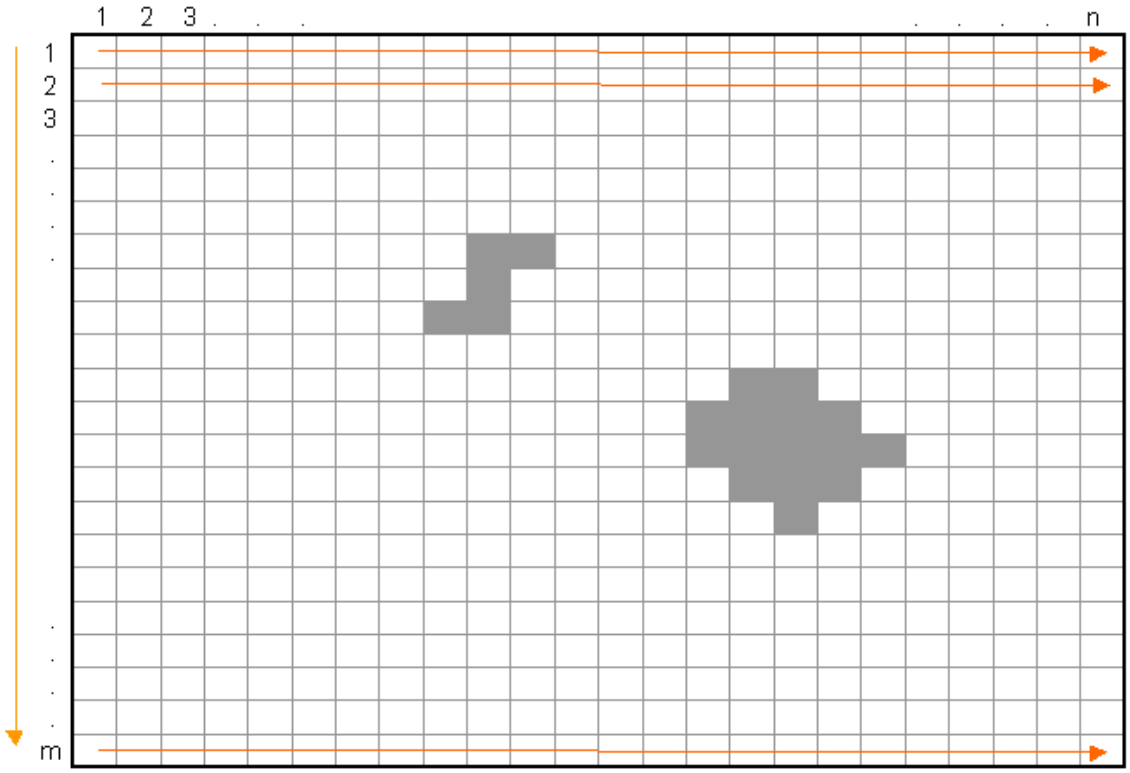

Figure 3.4.2
Image scanning for particle size / distribution estimation by the particle counting program

The program allows the user to estimate the size of the particle at a particular pixel coordinate, and offers flexibility to choose the size ranges for which the distributions are needed, and in choosing the Region of Interest (ROI).

The accuracy of the results obtained through this program was first verified by using synthetic images generated for the purpose. The program was then tested on images obtained during the regeneration process. The results were then compared with result obtained by manual estimation. A sample comparative result table is presented in the

Table 3.4.1. The standard deviation of the error percentage was to be less than 10% on an average.

The program is more reliable because, the results obtained when tested on synthetic images were very accurate. The error when the results were compared with manual estimation can be attributed to the fact that the manual counting of the particles is tedious and inconsistent (a perceptional variance on how many pixels a particle occupies is natural), and hence error prone. The program is more consistent since the rules are well defined. Also it is fast and less time consuming when compared to the manual estimation, giving us more time to analyze the data.

Time in sec	Sample1				Sample2				Sample3				Sample4			
	Manual Count	Matlab Count	Error	Error %	Manual Count	Matlab Count	Error	Error %	Manual Count	Matlab Count	Error	Error %	Manual Count	Matlab Count	Error	Error %
0	32	34	-2	-6.25%	11	13	-2	-18.18%	1	1	0	0.00%	2	2	0	0.00%
0.1	28	29	-1	-3.57%	3	5	-2		1	1	0	0.00%	0	0	0	0.00%
0.3	94	97	-3	-3.19%	20	22	-2	-10.00%	6	7	-1		7	11	-4	
0.4	73	76	-3	-4.11%	24	27	-3	-12.50%	19	18	1	5.26%	19	17	2	10.53%
0.5	51	54	-3	-5.88%	35	38	-3	-8.57%	34	29	5	14.71%	6	7	-1	-16.67%
0.6	44	47	-3	-6.82%	27	29	-2	-7.41%	15	17	-2	-13.33%	3	4	-1	
0.7	28	31	-3	-10.71%	19	22	-3	-15.79%	6	7	-1		1	1	0	0.00%
0.8	40	42	-2	-5.00%	15	17	-2	-13.33%	4	5	-1		3	3	0	0.00%
0.9	38	41	-3	-7.89%	17	18	-1	-5.88%	5	6	-1		0	0	0	0.00%
1	378	354	24	6.35%	145	154	-9	-6.21%	37	35	1	2.70%	8	7	1	
1.1	772	728	44	5.70%	303	313	-10	-3.30%	59	57	2	3.39%	9	10	-1	-11.11%
1.2	1156	1021	135	11.68%	411	394	17	4.14%	91	83	8	8.79%	21	22	-1	-4.76%
1.3	715	724	-9	-1.26%	246	224	22	8.94%	45	39	6	13.33%	12	14	-2	-16.67%
1.4	852	842	20	2.32%	302	291	11	3.64%	47	42	5	10.64%	9	11	-2	-22.22%
1.5	926	942	-16	-1.73%	344	327	17	4.94%	62	61	1	1.61%	11	13	-2	-18.18%
1.6	815	827	-12	-1.47%	342	324	18	5.26%	57	55	1	1.75%	17	18	-1	-5.88%
		Standard Deviation		5.89%		Standard Deviation		8.54%		Standard Deviation		7.48%		Standard Deviation		9.64%

Data in Shaded boxes have been discarded due to high error %, caused by very low particle count.

Table 3.4.1
Comparison of particle count - Manual vs. Matlab™ counts

Chapter 4

Room Temperature Tests

4.0 Introduction

Room temperature tests were performed on the candle filter(s) using the RTTF. The testing facility was primarily utilized to study the effects of different regeneration parameters on the performance of candle filters. A description of the long term tests and related testing matrix is provided in this chapter. The pressure drop across the filter was measured for different face velocities, for clean air through a clean filter. This gives us the resistance (a permeability measure) offered to the flow by the filter material. A description of these tests is also provided in this section.

4.1 Tests performed to evaluate the effect of regeneration parameters

As mentioned in the introduction, the objective was to study the influence of the following surface regeneration parameters, 1) effect of regeneration pressure, 2) effect of face velocity, and 3) effect of build-up time, on the surface regeneration process. Each test has two phases: a) the ash build-up phase and b) the regeneration phase. During the build-up phase, ash is fluidized in air and passed through the filter, the ash collects on the filter surface while the air passes through the filter. The velocity of the fluidizing air is described in terms of the face velocity. The higher the face velocity, the stronger is the ash cake. Also, it is expected that more ash will be fluidized and deposited with a higher face velocity, for the same period of time, compared to a lower face velocity. A longer build-up phase causes more ash deposit and hence a thicker ash. During the regeneration phase, a reverse regeneration pulse flows through the ash build-up for a very short period

of time. This reverse flow produces the tensile force to dislodge the ash cake. It is expected that a higher regeneration pressure causes a higher tensile force and hence results in a better clean up of the filter surface. The build-up face velocity contributes to the chamber pressure during surface regeneration phase and resists the regeneration pulse.

4.1.1 Testing procedure

As mentioned earlier, a room temperature surface regeneration test consisted of two phases, a) the build-up phase and b) the regeneration phase. A description of both the phases is provided in this section with the help of Figures 4.1.1 and 4.1.2.

The filter was installed and the ash hopper was filled with ash obtained from Wilsonville power plant. The ash hopper valve and the exhaust were then turned open. The side valve and the cap vent valve were closed. The solenoid valve used for the pressure pulse is also closed. This is done so that the air entering the chamber through the ash hopper fluidizes the ash, pass through the filter and finally flows out through the exhaust. The pressure regulator and the flow meter are set to obtain the required face velocity. The window shields are closed so that the fluidizing stream does not deposit ash on the window.

The data acquisition program "calib.dap" is then turned on, to record data from all the pressure transducers, sampled every 0.25 seconds. The valves are left open for a period of two minutes so that all the sensors read the atmospheric pressure. Then the valves are set as described in the earlier paragraph (Figure 4.1.1) and the compressed air outlet is turned on. This fluidizes the ash and the filtration process starts. The duration of

the build-up is determined by the test conditions. At the end of the specified time period the air outlet valve is turned off. Then all the valves are turned open and exhaust closed so that the chamber, filter and cap are have uniform atmospheric pressure. The data acquisition program "calib.dap" is then stopped.

The filter is now coated with an ash layer. The window shields are now opened and the windows are cleaned of any ash/dust, to aid the imaging process. The illumination devices are switched on and optical alignment checked. The camera and image acquisition board are configured to capture images on a trigger from the data acquisition board. The hose that was initially connected to the ash hopper valve (at the bottom of the chamber), is now connected to the valve on the side of chamber. This is done to prevent the ash from fluidizing and hinder the image acquisition process. The nitrogen tank that provides the regeneration pulse is turned on to the required pressure. The side and exhaust valves were turned open. The ash hopper and the cap vent valves were closed. The solenoid valve is configured to open only for a period of 0.3 seconds, by a trigger from the data acquisition board. Fig. 4.2 shows a schematic sketch of the regeneration process.

The compressed air outlet valve is turned on. The air now flows through the side inlet of the chamber, then passes through the filter and then flows out through the exhaust. The illumination is turned on, then camera alignment and focus adjusted. The data acquisition program for regeneration "fastak.dap" is started. This program triggers the imaging board to capture images and after 0.1 sec opens the solenoid valve for a period of 0.3 seconds. This program records pressure from all the pressure transducers every 0.01 seconds. High-pressure nitrogen flows through the solenoid valve and the

injector nozzle and flows through the filter from inside to the outset. This dislodges the ash cake. The data acquisition program is stopped after a couple of minutes. The nitrogen tank valve and the wall outlets are then closed. The system is then prepared for the next test.

The ash on the filter can be disturbed easily by mechanical forces. Therefore care is taken when opening the valves, window shields etc. It is difficult to keep the amount of fluidized ash a constant because the ash tends to stick to the walls. Therefore between tests the walls are gently cleaned with a brush. When cleaning the windows and the chamber walls the exhaust airflow is maintained so that the pressure drop across the filter aids in keeping the ash on the filter.

4.1.2 Testing matrix

The objective of performing the tests was to evaluate the performance of the candle filter under different testing conditions. The independent parameters employed in this study were 1) the regeneration pressure of the pulse jet, 2) the face velocity of the air passing through the filter depositing ash on the filter surface, and 3) the ash build-up time. The candle filter was subjected to repeated cycles of build-up and regeneration under varying parametric conditions. These tests are termed as the "Long Term Tests".

A thorough study was performed by repeated single cycle and multi cycle tests to 1) develop an understanding of the variables measured as well as controlled, and 2) to avoid any unforeseen problems that may affect the long term test results. Such a study eliminated what could have been an additional variable. A detailed description of this

study on the effect of the nitrogen tank pressure (or the "reservoir" pressure) is described in Chapter 5.

The room temperature test matrix was built based on the three regeneration parameters. A fundamental or base test condition was chosen with 95 psi regeneration pressure, 5 cm/s face velocity and 20 min build-up time. Based on this testing condition other conditions were formed varying the values of only one parameter at a time and the effect of each variable observed. The different regeneration pressures employed were 80 psi, 95 psi, 120 psi and 145 psi. The face velocities were 3cm/s, 5cm/s and 7cm/s . The build-up time selected was 10 min, 20 min, 45 min and 90 min. Thus 9 testing conditions were obtained for Lanxide filter and shown in Table 4.1.1.

Similar tests were performed on the Pall filter, for a comparative study with the Lanxide filter. High face velocity (7 cm/s), longer build-up time (45 min and 90 min) and lower regeneration pressure (80 psi) will cause difficulties in the regeneration process. The base test condition along with the four conditions, which will cause difficulties in regeneration, formed the 5 testing conditions for the Pall filter (ref Table 4.1.2).

4.2 Pressure drop across a clean filter for varying face velocities

The filters were tested without ash fluidization to measure the pressure drop across a clean filter as a function of face velocity (Figure 4.2.1). In these tests the regeneration pulse was not employed, only the fluidizing air was used. The valve on the side of chamber and the exhaust valves were the only valves opened on the chamber. The bottom ash hopper, the vents and the pulse jet valves were closed. When the wall outlet was opened the build-up air flowed through the side valve, then through the filter and

flowed out through the exhaust. The pressure regulator and the flow meter are set to obtain the required face velocities. The steady state pressure drop was measured for each face velocity and time-averaged to obtain the pressure drop for a given face velocity.

The results obtained through these tests are discussed in Chapter 6.

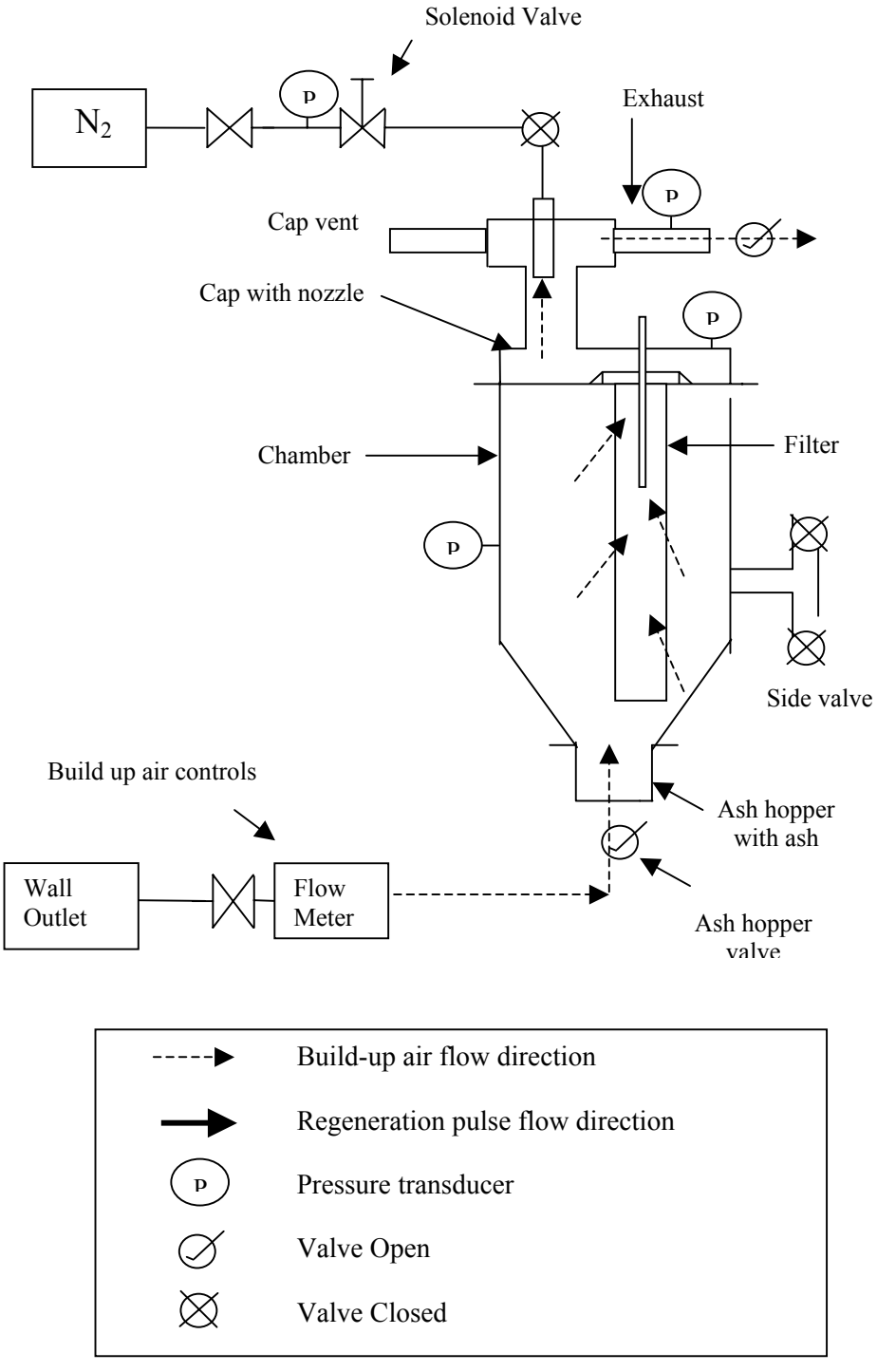

Figure 4.1.1
Schematic representation of build-up phase

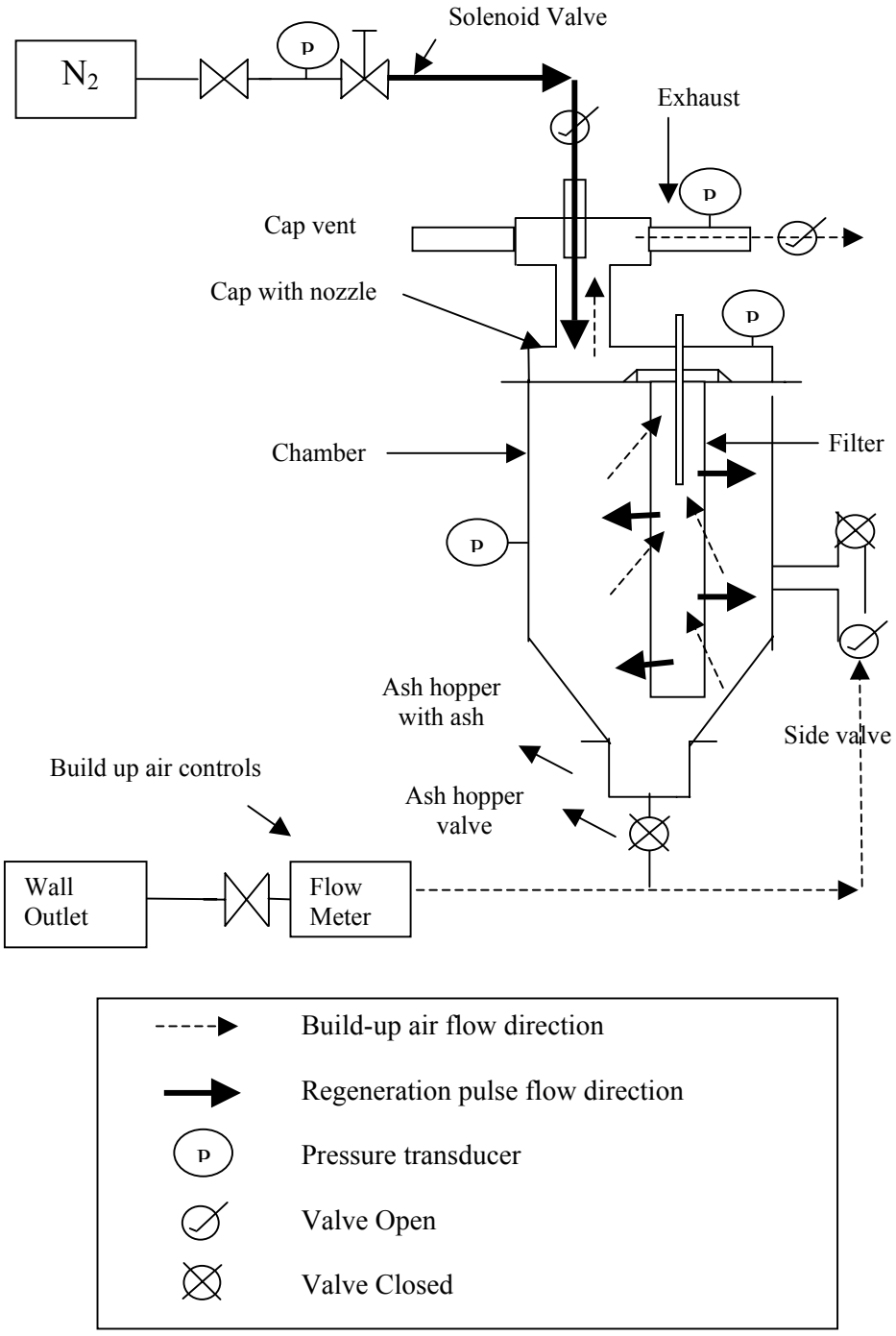

Figure 4.1.2.
Schematic representation of regeneration phase

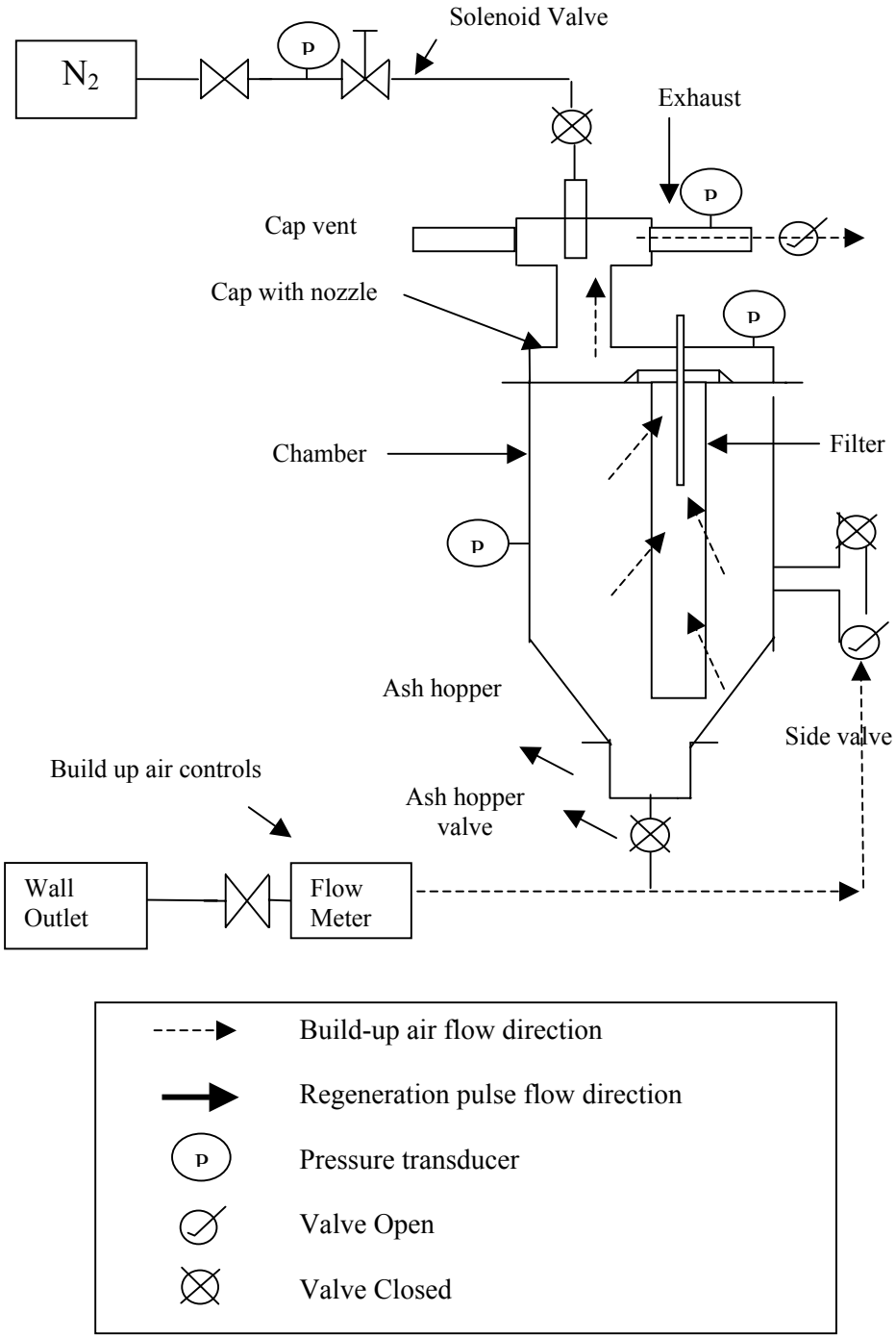

Figure 4.2.1
Schematic representation of pressure drop estimation across a clean filter

No.	Face Velocity (Cm/s)	Regeneration Pressure (psi)	Build-up Time (Min)
Base Condition - Lanxide Filter			
1	**5**	**95**	**20**
Effect of Face Velocity – Lanxide Filter			
2	**3**	95	20
3	**7**	95	20
Effect of Regeneration Pressure – Lanxide Filter			
4	5	**80**	20
5	5	**120**	20
6	5	**145**	20
Effect of Build-up Time – Lanxide Filter			
7	5	95	**10**
8	5	95	**45**
9	5	95	**90**

Table 4.1.1
Room temperature test matrix for Lanxide filter

No.	Face Velocity (Cm/s)	Regeneration Pressure (psi)	Build-up Time (Min)
Base Condition - Pall Filter			
1	**5**	**95**	**20**
Effect of Face Velocity – Pall Filter			
2	**7**	95	20
Effect of Reservoir Pressure – Pall Filter			
3	5	**80**	20
Effect of Build-up Time – Pall Filter			
4	5	95	**45**
5	5	95	**90**

Table 4.1.2.
Room temperature test matrix for Pall filter

Chapter 5

Influence of Reservoir Pressure on Surface Regeneration in RTTF

5.0 Introduction

The parameters included in the study of regeneration process for a given candle filter are the regeneration pressure, the filtration velocity or face velocity and the build-up time. While performing cycles of test on filters to study the surface regeneration process, the reservoir pressure was found to act as a variable. The study performed to understand the influence of reservoir pressure on surface regeneration in RTTF is discussed in this chapter.

5.1 Reservoir pressure

A commercially available high-pressure nitrogen tank/bottle stores and supplies the high-pressured gas required for the surface regeneration process. A pressure gauge on the tank reads the pressure of the compressed Nitrogen in the bottle. The full capacity of these tanks when full is about 2300-psig. A pressure regulator with a pressure gauge is used to obtain the desired regeneration pressure (the pressure at which reverse pulse is supplied *e.g.* 80 psig, 95 psig etc) during the tests. The high-pressure nitrogen passes through the regulator, a velocity tube and a solenoid valve before it is injected into the chamber. The solenoid valve is activated using a timed pulse from the data acquisition board. The valve opens for a 0.3 second period, for the regeneration to occur. A pressure transducer on the velocity tube measures the pressure profile of the reverse pulse gas, during surface regeneration. During the tests care was also taken to open the outlet valve by the same amount to maintain uniformity. The tanks were dispensed after the pressure

in the tank reached below 1000 psig. The reason for operating the reservoir at pressures between 1000 psig and 2300 psig was that, the pressures were assumed to be sufficiently high to provide a sufficiently steady and repeatable pressure pulse.

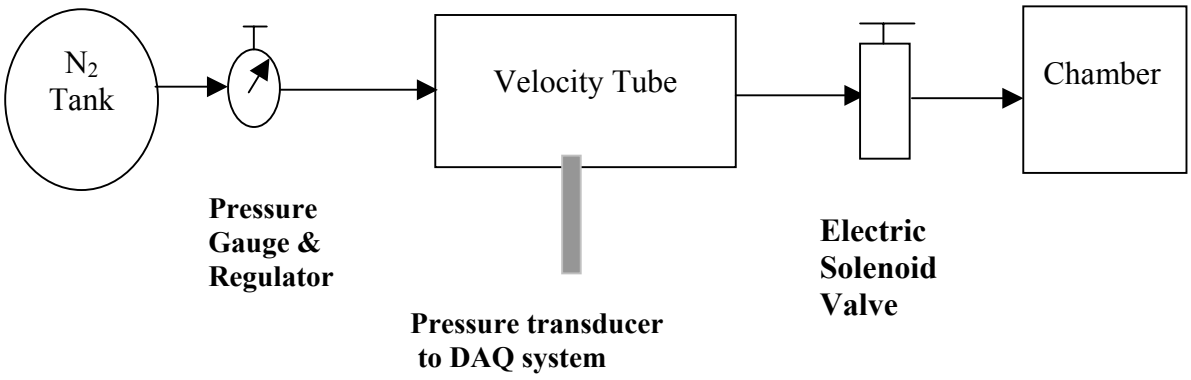

Figure 5.1.1
Schematic of reverse pulse gas flow

5.2 Influence of reservoir pressure

All experiments were performed based on this assumption. From the tests performed on Lanxide filter and Pall filter, for parametric conditions of 5cm/s-face velocity, 95 psig Reservoir pressure and 20 minutes build-up time, Pall filter's performance was better. That is the pulse jet cleaned the Pall filter more efficiently with less residual ash build up for the same number of cycles.

It was then decided to compare the filters for parametric conditions of 7cm/s-face velocity, 95 psig Reservoir pressure and 20 minutes build up time. Lanxide filter had stopped regenerating after 11 cycles, due to residual ash build up resulting in large pressure drops. Pall filter was expected to run for longer cycles before it stopped regenerating. But even during the first cycle of testing, the Pall filter failed to regenerate. The pressure in the tank (reservoir pressure) was 1200 psig during this test. In order to make it regenerate the outlet valve was opened much more than the usual amount, but this also does not seem to help the filter to regenerate. The old nitrogen tank was then replaced with a new one (with a reservoir pressure of about 2300-psig) and the testing recommenced. This cycle of testing continued for 19 cycles, before the filter stopped regenerating due to residual ash build up causing a large pressure drop.

The above observation suggested that the reservoir pressure could have an effect on the regeneration process. A study was therefore undertaken to study the possible effect of reservoir pressure on the regeneration process in RTTF.

5.3 Experiment

In order to study the effect of reservoir pressure on the regeneration pulse, a small experiment was designed. The transducer in the velocity tube measures the pressure of the pulse jet. The pressure profiles as measured by the transducer were recorded for each of the regeneration pressures (80, 95, 120 & 145 psig), to study the effects of varying reservoir pressures from 700 psig to 2400 psig (in steps of 100 psig). Figures 5.3.1, 5.3.2, 5.3.3 and 5.3.4 are the plots that show the variation in pressure profiles for varying reservoir pressures for 80, 95, 120 and 145 psig respectively.

5.4 Conclusion

The pulse jet profile was observed to have a steep fall when the solenoid valve was opened and then it was observed to increase with two different gradients: 1) a relatively slow increasing period when the solenoid valve was opened, from 0.06 to 0.43 sec., and 2) a faster increasing period once the solenoid valve was shut till the steady state pressure was reached. The rate at which the first pressure gradient increased was found to vary with varying reservoir pressures. A higher reservoir pressure caused a steep rise while a lower reservoir pressure had a relatively lower gradient. In order to ensure that the reservoir pressure did not influence the testing and sufficient repeatability was ensured for testing cycles, it was decided to maintain the reservoir pressure between 1600 psig and 2000 psig. The pressure slope during the first gradient phase did not differ significantly by a great extent in this range, and all tests henceforth were performed with the reservoir pressure between 1600 and 2000 psig.

This phenomenon of the reservoir pressure, which affected the surface cleaning/regeneration of the candle filter, may be unique to the RTTF design, and it may not be experienced in any other design.

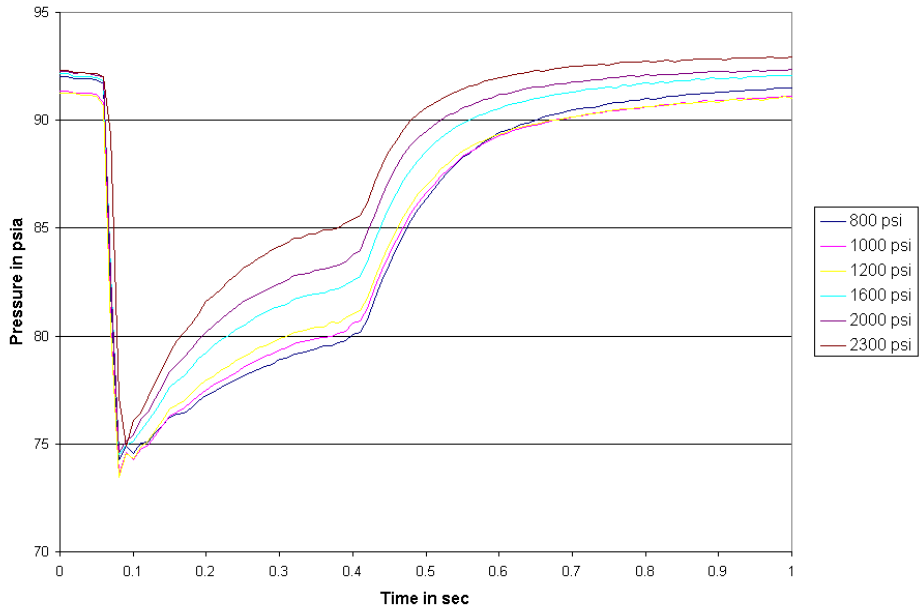

Figure 5.3.1
Effect of reservoir pressure (800 to 2300psig) for regeneration pressure 80psig

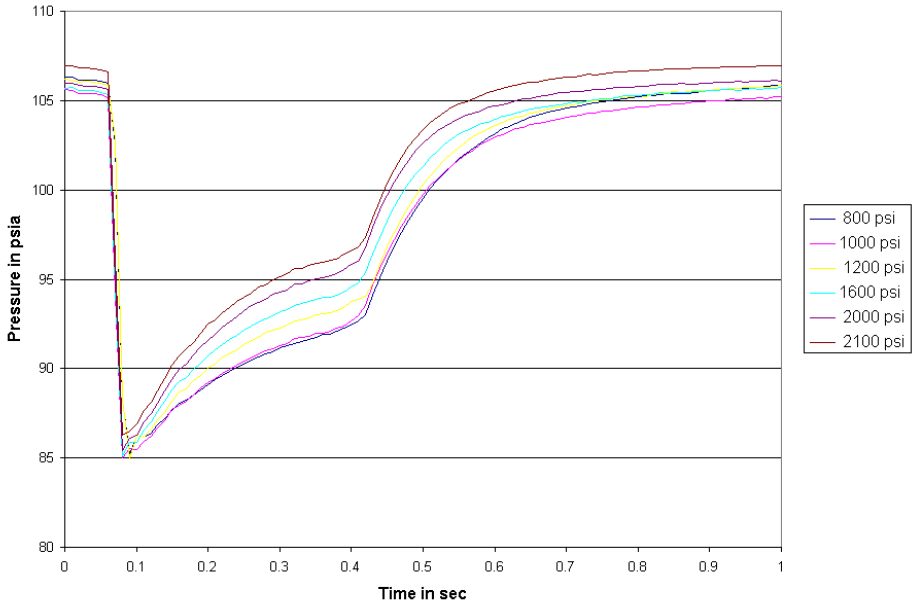

Figure 5.3.2
Effect of reservoir pressure (800 to 2100psig) for regeneration pressure 95psig

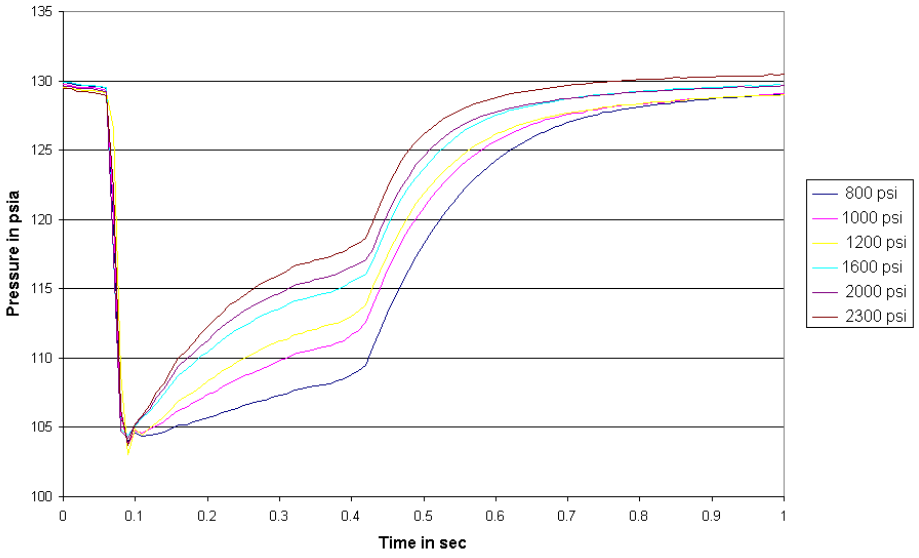

Figure 5.3.3
Effect of reservoir pressure (800 to 2300psig) for regeneration pressure 120psig

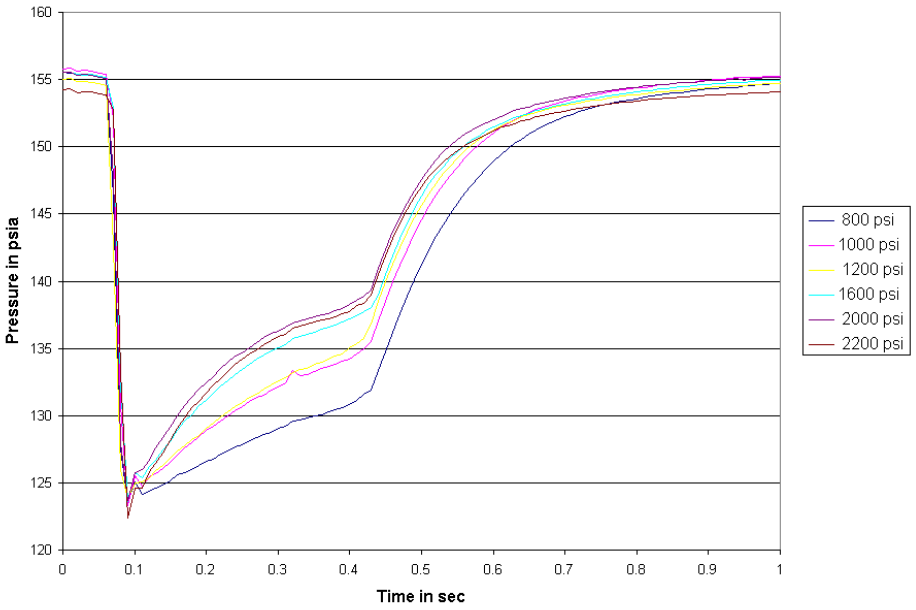

Figure 5.3.4
Effect of reservoir pressure (800 to 2200psig) for regeneration pressure 145psig

Chapter 6

Discussion on RTTF-Long Term Test Results

6.0 Introduction

In this chapter the results from the tests performed on the candle filter under room temperature conditions are discussed. The candle filter was subjected to continuos and repeated cycles of build-up and regeneration. These continuos cycles of tests have been termed as “Long Term Tests”. Each test cycle was performed to study the effect of the regeneration parameters. The independent regeneration parameters considered in the study were 1) the regeneration pressure of the pulse jet, 2) the face velocity of the air passing through the filter depositing ash on the filter surface, and 3) the ash build-up time. Initially a test was performed taking a particular set of parametric values as the "base" condition. Varying the value of one parameter at a time and keeping the other parameters constant, the other tests were performed. The "base" testing condition was used as the reference for comparison and to study the effect of each of the parameters.

The “base” test upon which all other tests are compared was performed with a regeneration pressure of 95 psig, face velocity of 5 cm/s and a build-up time of 20 minutes. Other tests were performed by each of the three parameters one at a time,

(a) the regeneration pressure was varied (80 psig, 120 psig, and 145 psig),

(b) the face velocity was varied (3 cm/s and 7 cm/s), and,

(c) the build-up time was varied (10 min, 45 min, and 90 min).

All these tests were performed on the same filter in order to maintain consistency. All of the above mentioned tests were performed using only one type of commercially available filter.

In order to study the role of different filter types, tests were performed on two branded filters. All the tests mentioned above were performed on the Lanxide→, a low permeability filter. In order to study the effect on the Pall→, a high permeability filter, comparative tests were performed. High face velocity (7 cm/s), longer build-up time (45 min and 90 min) and lower regeneration pressure (80 psi) were observed to cause difficulties in the regeneration process in Lanxide→, the low permeability filter. So these conditions along with the "base' condition were selected and tests performed on both the filters to obtain details on how Pall→, high permeability filter regenerated in comparison to the low permeability filter. The testing matrices for the low (Lanxide) and high (Pall) permeability filters are presented in Tables 6.0.1 and 6.0.2.

A discussion on the factors that influence the surface regeneration was presented in Chapter 2. The regeneration pressure, face velocity and the build-up time have been identified among the chief factors that influence the surface regeneration process of a given filter and ash. These factors were therefore chosen as the independent parameters. The filter type also influenced the regeneration process and hence considered as an independent variable. The effect of these parameters on the formation of residual ash on the filter surface and the regeneration efficiency was studied, by analyzing data obtained using extensive instrumentation of the RTTF. This data is termed as the "characteristic data", and this is used to infer the efficiency of the regeneration process. A brief description of the independent parameters, the characteristic data and related terms used to describe the regeneration process, and how they relate to the RTTF testing is presented in this chapter.

The pressure drop across a clean filter is a measure of its permeability. The filters used in the RTTF study were subjected to tests that measure their pressure drop as a function of the face velocity to gain knowledge on their respective permeability. Clean air flowed from the chamber through the filter wall to the exhaust. The steady state pressure drop was measured for different face velocities and averaged to obtain the pressure drop for each of the face velocities. Results obtained from these permeability tests are also presented in this chapter. A major portion of this chapter is devoted to discuss the results obtained when the filters were subjected to the long term tests under different conditions. The effect of each of the independent parameter on the regeneration is discussed by the presenting the characteristic data measured.

No.	Face Velocity (cm/s)	Regeneration Pressure (psi)	**Build-up Time (min)**	**Test-I Cycles**	**Test-II Cycles**	**Remarks**
Base - Lanxide Filter						
1	5	95	20	26	25	Repetitive Regeneration
Effect of Face Velocity – Lanxide Filter						
2	**3**	95	20	13	15	Repetitive Regeneration
3	**7**	95	20	11	7	Stopped
Effect of Regeneration Pressure – Lanxide Filter						
4	5	**80**	20	17	24	Repetitive Regeneration
5	5	**120**	20	11	14	Repetitive Regeneration
6	5	**145**	20	10	15	Repetitive Regeneration
Effect of Build-up Time – Lanxide Filter						
7	5	95	**10**	14	15	Repetitive Regeneration
8	5	95	**45**	12	5	***
9	5	95	**90**	14	1	Stopped Regenerating

Table 6.0.1
Results from room temperature tests - Lanxide filter

*** Test-I: Repetitive Regeneration / Test-II: Stopped Regenerating

No.	Face Velocity (cm/s)	Regeneration Pressure (psi)	Build-up Time (min)	Test-I Cycles	Test-II Cycles	Remarks
Base Condition – Pall Filter						
10	5	95	20	12	22	Repetitive Regeneration
Effect of Face Velocity – Pall Filter						
11	**7**	95	20	19	15	**Stopped Regenerating**
Effect of Reservoir Pressure – Pall Filter						
12	5	**80**	20	-	24	Repetitive Regeneration
Effect of Build-up Time – Pall Filter						
13	5	95	**45**	-	16	Repetitive Regeneration
14	5	95	**90**	-	3	**Stopped Regenerating**

Table 6.0.2
Results from room temperature tests - Pall filter

6.1 Independent parameters and the dependent regeneration characteristics

In this section a brief discussion on the independent parameters used in this study is presented at first. Then the significance of the dependent characteristic data set is discussed with relevance to the surface regeneration process in RTTF. This is done to facilitate the understanding of results presented. The terms and definitions used to describe the various aspects of the surface regeneration process are also presented here.

6.1.1 Independent parameters

This section explains the parameters used in the RTTF study. The three parameters: the regeneration pressure, face velocity of the fluidizing air stream, and the build-up time influences the surface regeneration process of a candle filter. The filter type itself imposes an additional variable, hence the filter itself was chosen as a parameter to be studied.

1. Regeneration pressure

Regeneration is the process by which a high-pressured reverse pulse is subjected on the candle filter for a very short period of time, and the regeneration pressure is the magnitude of this pulse, measured here in psia. A higher regeneration pulse pressure imparts a higher stress on the ash-cake. Cleaning efficiency is expected to increase with increasing the regeneration pulse pressure. A higher regeneration pressure is expected to dislodge the deposited ash-cake better than a relatively lower regeneration pressure. The regeneration pressures used in the study were (a) 80 psig, (b) 95 psig, (c) 120 psig and (d) 145 psig. The 95 psig condition, as mentioned earlier was taken as the base condition.

2. Face velocity

The face velocity is the velocity at which the air stream mixed with ash dust passes the wall of the candle filter. A higher face velocity has found to result in denser, thicker and stronger cake formation by the ash particles collecting on the surface of the filter during the filtration process, while a lower face velocity results in thinner deposit and weaker ash cake. A higher face velocity also causes an increased chamber pressure in RTTF. This results in more compaction of the ash particles and also a higher resistance to the regeneration pressure. The face velocities employed in the study were (a) 3 cm/s, (b) 5 cm/s and (c) 7cm/s. A face velocity of 5 cm/s was taken as the base condition, and the effect of higher face velocity (7 cm/s) and lower face velocity (3 cm/s) were studied.

3. Build-up time

Build-up time is the time interval between successive regenerations, in effect this is the length of time during which the ash gets deposited on the filter before regeneration pulse is effected. A longer build-up time results in more ash being collected on the surface of the filter. The build-up time used in the study were (a) 10 min, (b) 20 min, (c) 45 min and (d) 90 min**.** The 20 min build-up time condition was used as the base condition.

4. Filter types

The study involved comparing two different types/brands of filters. A complete cycle of tests was performed on the Lanxide filter (ceramic composite candle filter, PRD-

66). The test conditions, for which, the Lanxide filter had difficulty in regenerating, were employed on the Pall filter (monolithic silicon carbide filter, Pall 442T). The permeability (as a function of pressure drop) of both the filters was also experimentally determined.

6.1.2 Dependent regeneration characteristics

The effectiveness of the regeneration process under different parametric conditions is characterized and modeled based on the data obtained. The different regeneration characteristics and their relevance are discussed in this section.

1. Number of test cycles and reason for ending the long term test

The number of testing cycles performed on the candle filter without residual ash accumulation is an indicator on the effectiveness of the parametric conditions. It becomes more relevant when associated with the criterion for ending the test cycles. The test cycles were ended for one of the following two reasons; (a) the filter stopped regenerating or (b) the filter kept repeatedly regenerating without any significant residual ash build-up. If the number of cycles was large and the filter was regenerating without any signs of increasing residual ash build-up, then the corresponding condition is desirable for the regeneration process. If the filter stopped regenerating after certain number of test cycles, then the number of cycles becomes significant. For both of the above mentioned cases, the more the number of cycles, the better the filter's performance.

2. Increase of chamber pressure (P_c) during the build-up phase

During the build-up phase, the air stream with fluidized ash passes through the candle filter depositing ash on the candle surface. The deposited ash obstructs the pores on the filter. The resistance associated with the deposited ash decreases the flow rate. This causes the chamber pressure to increase. This increase in pressure is directly related to the amount of ash on the filter. During repeated cycles, if the surface regeneration process is efficient there will be little or no residual ash on the filter. And, the chamber pressure build-up between cycles will be identical or as close as possible. If the cleaning process is not efficient, there will be more residual ash. This residual ash on the filter surface will cause a semi permanent obstruction to the airflow, and as more ash is accumulated during build-up phase, the chamber pressure increase is relatively bigger than the previous cycle. With continued residual ash layer growth, the chamber pressure continues to increase.

A study on chamber pressure increase should help us gauge the increase in the ash deposit on the filter surface. If during a long term test the chamber pressure does not increase with successive test cycles then it should indicate that the residual ash layer is not growing. On the contrary if the chamber pressure keeps increasing then it indicates residual ash growth or improper regeneration. It is desired that the chamber pressure does not increase between successive test cycles.

3. Pressure difference, ΔP (P_f-Pc), between filter (P_f) and chamber(Pc) during regeneration

In the RTTF the filter pressure is maintained slightly lower than the chamber pressure to cause a positive flow between the chamber and the filter. A negative exhaust

pressure maintains the lowered filter pressure. The pressure difference across a new (i.e. very clean) filter is the lowest possible pressure drop, ΔP_N across the filter wall, for a given flow condition (i.e. face velocity). ΔP_N is negative since the flow is from chamber to the filter. In RTTF the same filter is used for all the tests. After every test cycle the filters are cleaned manually by using high-pressure air. This may not result in filter that is as clean as a new filter. When this filter is subjected to flow conditions a pressure drop develops that is slightly higher in magnitude than the ΔP_N, and this is due to some ash that was not removed even by the manual cleaning. This pressure drop is denoted by ΔP_C, and is also negative.

During the build-up phase, the chamber pressure increases (although the pressure inside the filter also increases, however the chamber pressure increase is much larger) and increases the pressure drop ΔP (Pf-Pc). The increase in the ΔP value is a function of the build-up conditions. At the start of the regeneration phase the initial pressure difference between the filter and the chamber ($\Delta P_{initial}$), is the resistance offered by the ash collected on the filter, the residual ash and the flow conditions. When the cleaning pulse is applied (0.3 sec), the pressure inside the filter increases and the flow occurs from inside the filter to the chamber. This causes the pressure difference (ΔP) to increase, cause a sign change and reaches a positive maximum (ΔP_{max}).

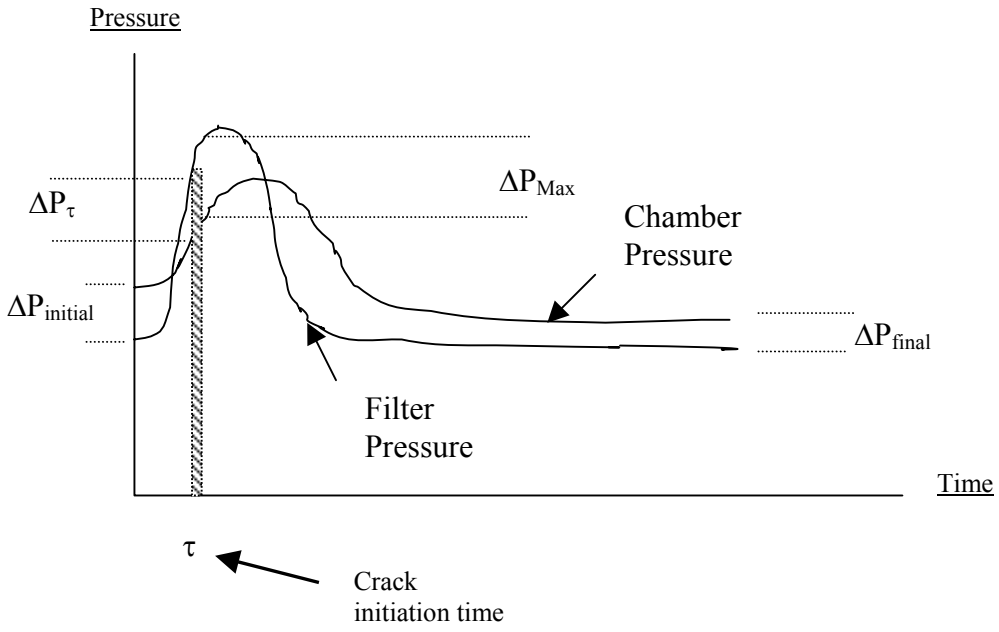

Figure 6.1.1.
Schematic of chamber and filter pressure profiles during regeneration

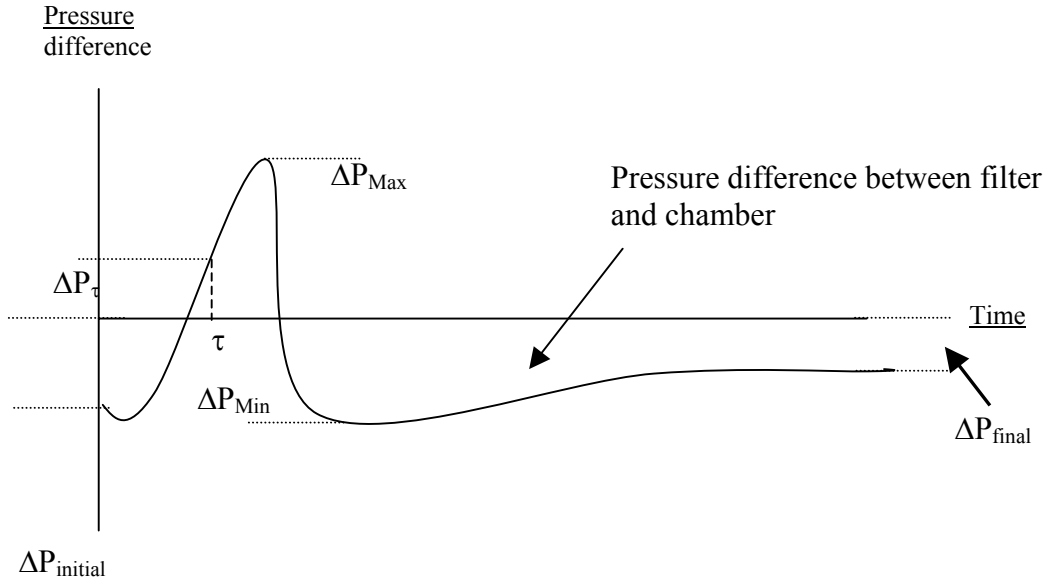

Figure 6.1.2.
Schematic of the pressure difference between the filter and the chamber during regeneration

During this period the ash collected on the filter is regenerated. Due to the short duration of pulse, the ΔP starts decreasing and now reaches a minimum value (ΔP_{min}). This ΔP-min value is even lower than the initial pressure difference ($\Delta P_{initial}$), and during this period the flow from chamber to the filter is expected to be the fastest. With so many ash particles regenerated the probability of re-entrainment is highest during this phase. Then the pressure difference reaches a stable final value (ΔP_{final}). The pressure profiles of the chamber the filter and the pressure difference during the regeneration process are presented in Figures 6.1.1 and 6.1.2. Study on the ΔP curve profile provides information about the cleaning process.

a. $\Delta P_{initial}$:

If the magnitude of $\Delta P_{initial}$ value is low then the ash and the flow conditions do not resist the flow as much. The cleaning pulse has to overcome the $\Delta P_{initial}$ to regenerate and thus defines the magnitude necessary for an efficient regeneration. During repeated cycles of building up, the $\Delta P_{initial}$ variation is a measure of resistance due to residual ash. If the value does not change then it can be perceived that there is little residual ash build-up, while if it increases then it is an indicator of residual ash build-up.

b. ΔP_{final}:

The ΔP_{final} value is measured after the filter has been regenerated and is now the pressure difference after the cleaning. This magnitude should be low if the regeneration has cleaned most of the ash, but if there is a lot of ash then the magnitude will be high.

c. ΔP_{max}:

If the magnitude of the regeneration pulse is sufficient to overcome the resistance offered by the ash and the flow, then this value is positive large number. If the resistance starts to build-up this value starts to decrease and becomes a negative number when the filter can no longer regenerate. Hence, it is undesirable to find the ΔP_{max} value becoming small and reducing below zero.

d. ΔP_{min}:

The ΔP_{min}, value is always found to occur during the transition from the cleaning pulse to the stable filtration condition. Immediately after the regeneration pulse (0.3 sec) the chamber is filled with the reverse pulse gas in addition to the build-up air. This causes a temporary pressure increase in the chamber and hence causes the ΔP value to decrease further. ΔP_{min} is the lowest value that occurs during this transitory phase. This pressure drop causes a flow from chamber to filter during this phase. The flow rate is higher because the porosity is reduced therefore reducing the area of flow, and by continuity equation the velocity increases. The particles that are present around the filter have a high probability to be sucked back on to the filter surface due to this flow. The flow is directly proportional to the pressure difference. Therefore if the magnitude of ΔP_{min} is large, it is detrimental to the regeneration process.

e. Efficiencies:

The efficiency of the regeneration process has been defined as (from Chapter 2);

$$\eta = \frac{\text{Cleaning in the current pulse}}{\text{Maximum possibleCleaning}}$$

Which in terms of pressure difference is,

$$\eta = \frac{\Delta P_{initial} - \Delta P_{final}}{\Delta P_{initial} - \Delta P_{clean}}$$

where,

ΔP_{final} = Pressure drop across the candle filter just after cleaning process

$\Delta P_{initial}$ = Pressure drop across the candle filter just before cleaning process

ΔP_{clean} = Pressure drop across the candle filter with no ash

In the long term tests the ΔP_{clean} value is slightly modified. In RTTF test facility, the same filter was used for all tests. The filter is used after and may not be as clean as a new filter. In RTTF the filter was cleaned by compressed air sent from both inside and outside of the filter, manually. This however does not result in a filter that is as clean as a new filter. Therefore the pressure drop is greater in the cleaned filter. In order to differentiate the pressure drop in a new filter and the cleaned filter, ΔP_N and ΔP_C are used. The new efficiencies are calculated based on ΔP_N and ΔP_C. This is because the filters surface cleanliness is limited to the extent of the cleaning performed on it. Therefore two efficiencies are now calculated,

$$\eta_{new} = \frac{\Delta P_{initial} - \Delta P_{final}}{\Delta P_{initial} - \Delta P_N}$$

$$\eta_{cleaned} = \frac{\Delta P_{initial} - \Delta P_{final}}{\Delta P_{initial} - \Delta P_{C}}$$

If the efficiencies comes close to zero or negative, then $\Delta P_{initial}$ is equal or less than ΔP_{final}, which means the ash has not been removed from the filter surface.

The efficiencies 'η' do not perform satisfactorily, when a thick ash regeneration and thin ash regeneration are compared. The $\Delta P_{initial}$ value is dependent on the ash thickness. If thick ash forms, then ΔP-initial is large, and if thin ash forms $\Delta P_{initial}$ is small. All other values remaining the same, the efficiency η is high for thick ash compared to thin ash. This efficiency is based on the amount of ash removed and the resistances overcome by the regeneration pulse. η does not indicate how clean the filter is after the pulse.

A cleaning factor 'F' is introduced, to compare the how clean the filter is after the pulse, irrespective of the type of ash removal. F is the ratio of final ΔP to the clean or new ΔP.

$$F_N = \frac{\Delta P_{final}}{\Delta P_{new}}$$

$$F_C = \frac{\Delta P_{final}}{\Delta P_{cleaned}}$$

The cleaning factor is a measure of how clean the filter is, and if F_N/F_C is equal to 1, then the filter is as clean as a new/cleaned filter. Higher F value indicates that filter is not clean.

4. Distribution of particles less than 100 microns during regeneration

The particle sizes during regeneration are important because of their possible influence on the sintering of ash on the filter surface, at high temperature. In Chapter 2, the relationship between the larger number of smaller particles and (a) the increased probability of re-entrainment and (b) the faster sintering rate, was discussed.

In Chapter 2 it was discussed that during regeneration a period exists between the pulse-jet cleaning and normal filtration, during which the transient pressure inside the filter element is much lower than the outside of the filter element. This causes a flow from the outside of the filter element to the inside and this may cause a fraction of particles in air to re-deposit on the candle surface. Especially the smaller particles (less than 100μ, or even 250μ) are more prone to be re-deposited on the filter.

The images captured during the regeneration process are processed to get the particle size information. The particles are classified based on their size and a distribution pattern obtained. A distribution pattern of particles less than 100μ is analyzed to arrive at conclusions regarding the regeneration process. A larger number of these particles

increases the probability of re-entrainment and also increases the probability of sintering, at higher temperatures.

5. The thickness of ash deposit during build-up

The amount of ash deposited on the filter determines the nature of regeneration, whether - thick, thin or partially thick-thin. The ash thickness is obtained from the images of the regeneration process. It is important to observe this parameter as it can also be used as an indicator of performance as the parameters are varied. The ash thickness has been categorized as thick and thin ash. A thin ash layer is less than 1-1.5mm thick, and a thick ash is 1.5 mm or more.

6. The type of regeneration

The regeneration process can be classified based on the way the ash cake is removed from the filter. The regeneration can be characterized as (a) Thick ash Regeneration, (b) Partial Thick-Thin Ash Regeneration and (c) Thin Ash Regeneration. Each type of regeneration is discussed and associated images presented in Figures 6.1.3,6.1.4 and 6.1.5 at the end of this section.

(a) Thick ash regeneration

This type of regeneration occurs usually when a thick layer of ash is deposited on the filter surface. The regeneration is characterized by few long cracks (usually vertical) that initiate and form large chunks of ash cake that fall down or slide on the surface of the filter during the regeneration process (Figure 6.1.3). The amount of small particles that are less than 100 and 250μ is generally low. In good thick ash regeneration there are no visible ashy patches, but as the ability to regenerate lowers there are very thick residual

ash patches. This usually leads to a total failure of regeneration process and the filter system in turn.

(b) Thin ash regeneration

This type of regeneration occurs usually when a thin layer of ash is deposited. The ash cake explodes into small and medium chunks of ash, due to the action of regeneration pulse. A large number of cracks form horizontally relative to the filter surface. This type of regeneration usually has smaller particles around the filter for a longer period of time. Also the ash between the cracks is not removed totally leaving some residual on the surface.

(c) Partially thick-thin ash regeneration

In some cases although the ash cake initially cracks like a thick ash, but the chunks loose strength immediately and disintegrate into medium and smaller sized particles. This occurs usually when there is a transition from thin ash to thick ash regeneration, or improper thick ash build-up with low resistance.

The thin ash regeneration and the partially thick-thin ash regeneration usually have a large number of particles less than 100μ and this causes an increased probability for sintering and re-entrainment.

0.0 sec

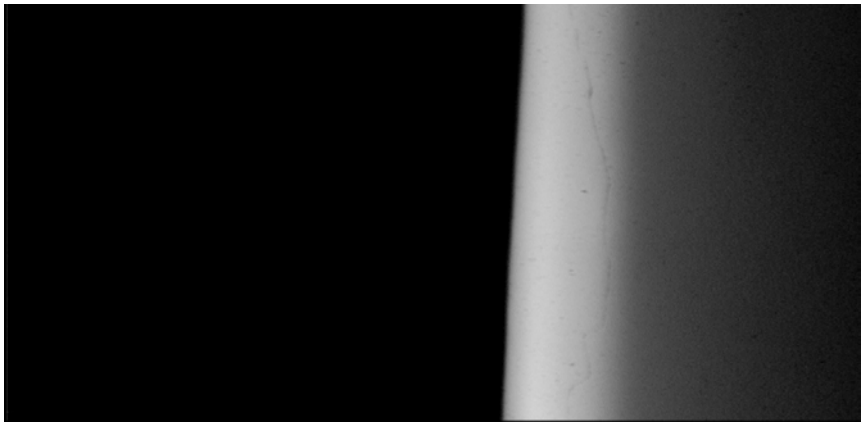

0.2 sec

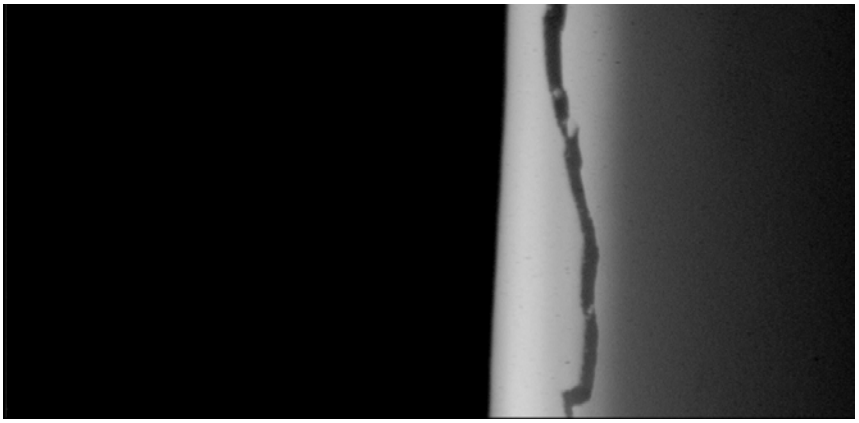

0.267 sec

Figure 6.1.3.a.
Images of thick ash regeneration sequence with corresponding time after regeneration. (Contd.)

0.333 sec

0.367 sec

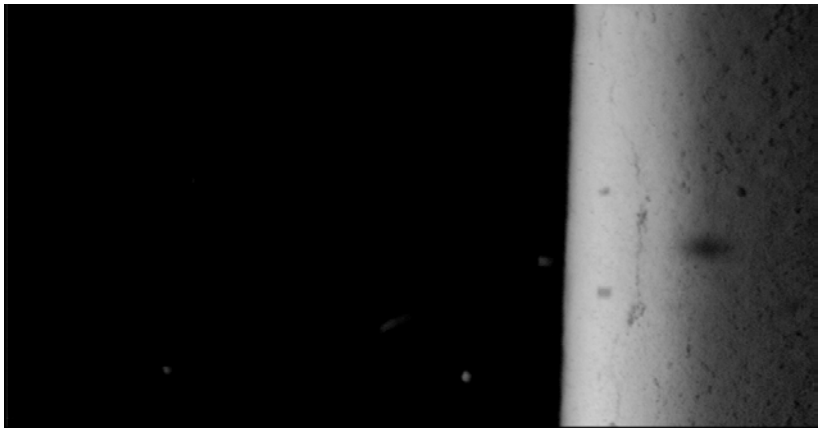

0.4 sec

Figure 6.1.3.b.
Images of thick ash regeneration sequence with corresponding time after regeneration

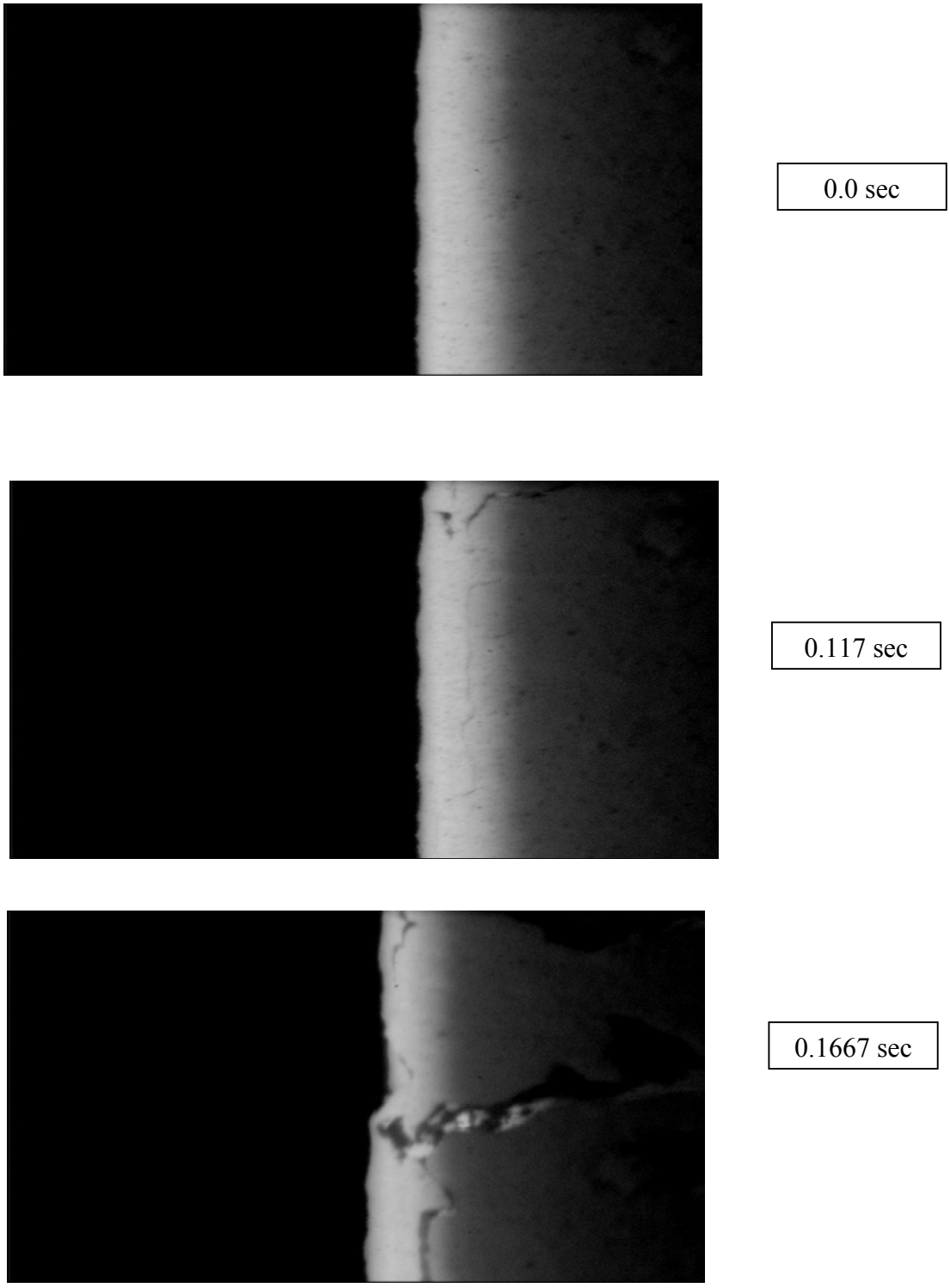

Figure 6.1.4.a.
Images of partial thick-thin ash regeneration sequence with corresponding time after regeneration. (Contd.)

0.2117 sec

0.1833 sec

0.2113sec

Figure 6.1.4.b
Images of partial thick-thin ash regeneration sequence with corresponding time after regeneration.

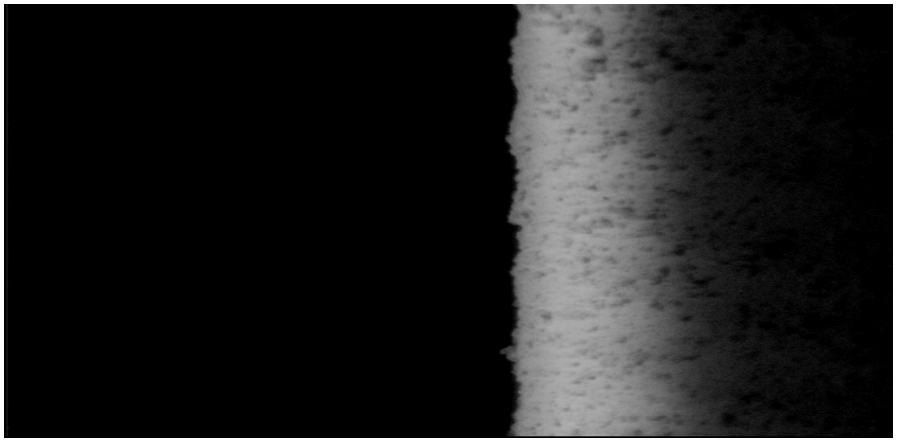

0.0 sec

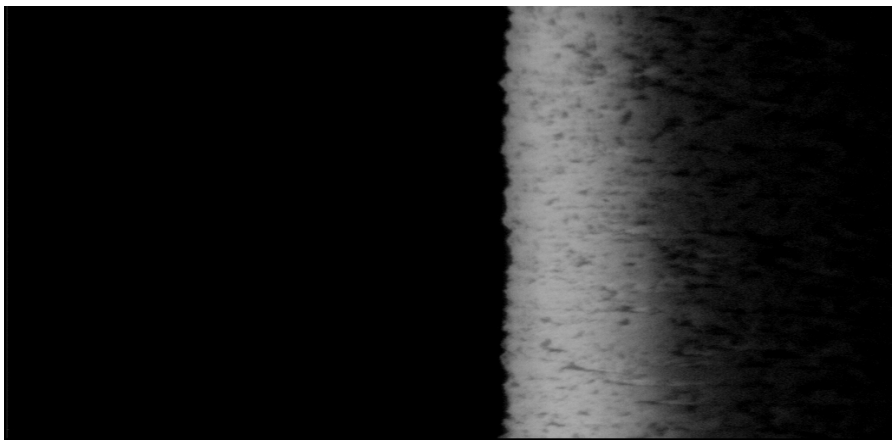

0.117 sec

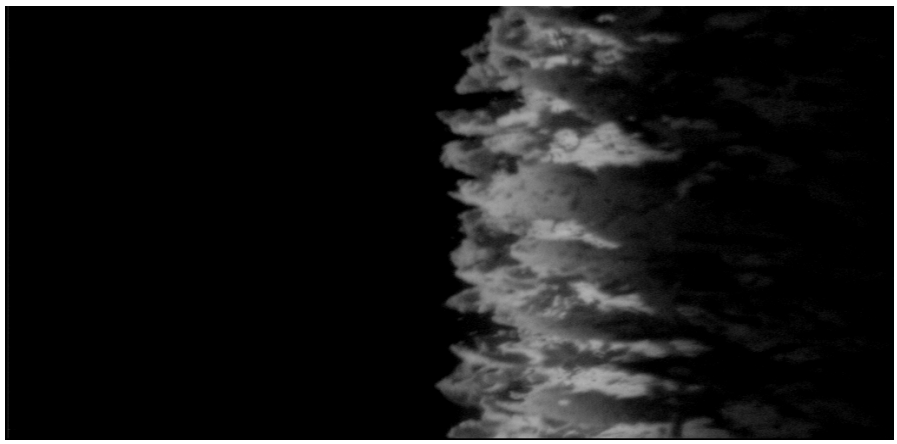

0.1667 sec

Figure 6.1.5.a.
Images of thin ash regeneration sequence with corresponding time after regeneration. (Contd.)

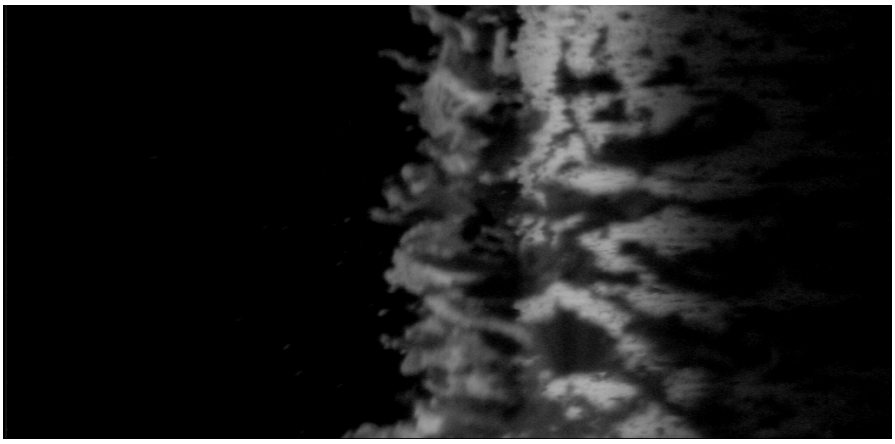

0.2 sec

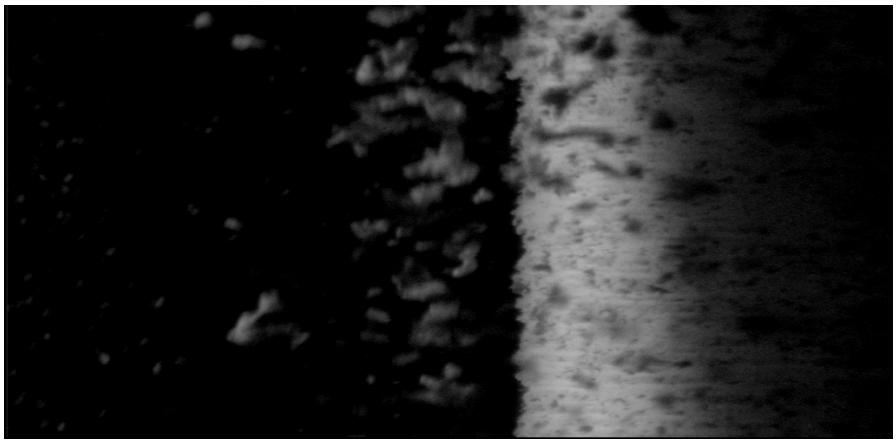

0.2833 sec

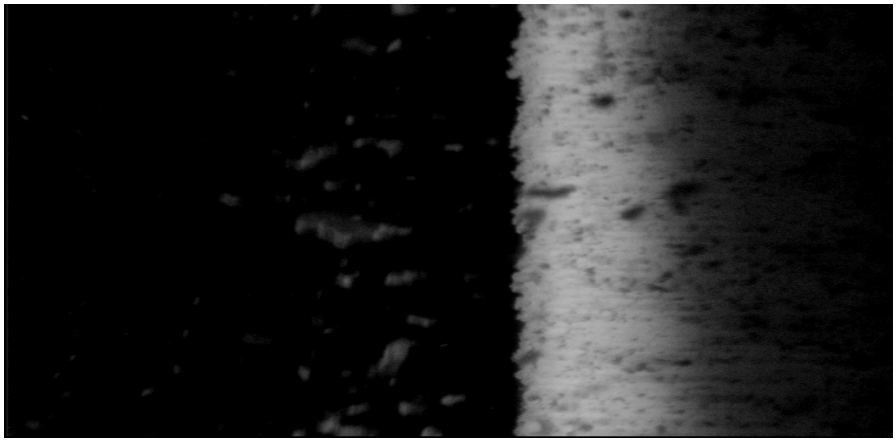

0.35 sec

Figure 6.1.5.b.
Images of thin ash regeneration sequence with corresponding time after regeneration.

7. Crack initiation time

The formation of cracks on the surface of the ash layer is an indicator of the start of the cleaning process by the back pulse. It has been observed that the crack initiation time does not correspond to the maximum ΔP, but it occurs slightly before ΔP reaches the maximum value. It is quite logical to associate the crack initiation to some threshold value of ΔP, and can be safely assumed that the crack will not initiate if this threshold pressure has not been reached. A longer crack initiation time indicates that the strength of the ash cake is greater, and hence takes longer for the ΔP to build-up to reach the threshold condition. Since the pulse jet period is fixed, there is an inherent time limit.

7. Surface quality

The purpose of the study on regeneration is to find how effectively the process removes the ash on the surface. Visible observation and a high resolution imaging system are used in examining and recording the quality of the filter surface, immediately after the regeneration process. A cleaner surface indicates efficient cleaning while a dirty/patchy surface indicates inefficient cleaning. Large residual chunks are also observed in cases with partial regeneration. It is very important to take this observation into consideration when analyzing the overall performance of the regeneration process. Images of candle filters with varied degree of ash accumulation are shown in Figures 6.1.6 and 6.1.7.

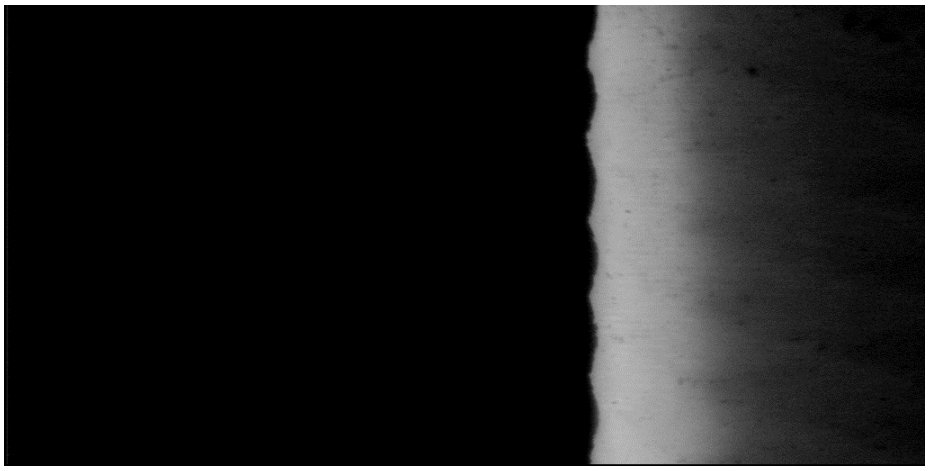

Clean Filter

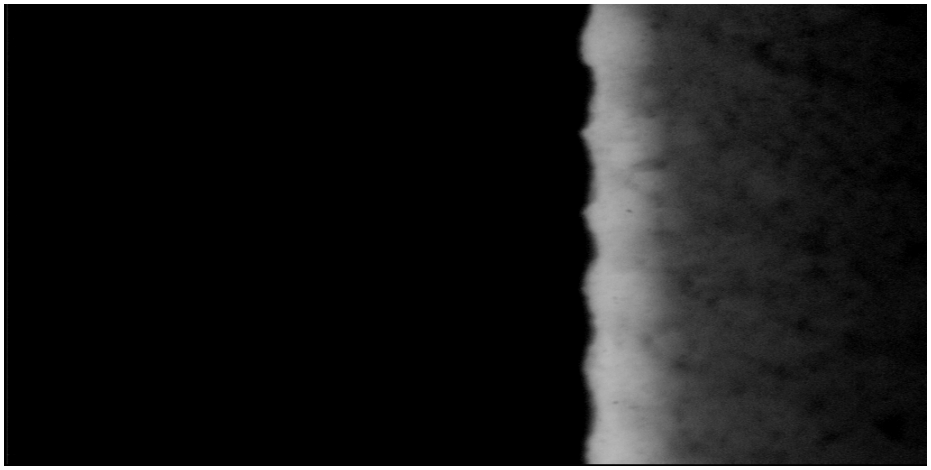

Ash collection on ridges

Figure 6.1.6.a.
Images of surface quality of the Lanxide filter. (Contd.)

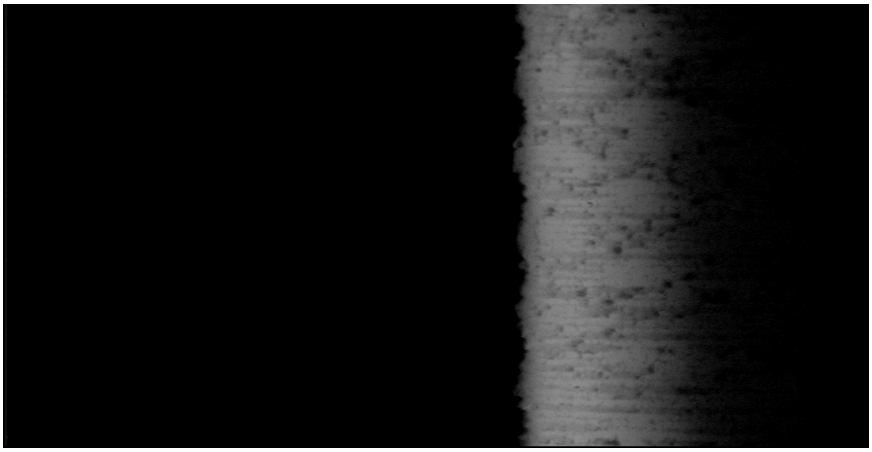

Thin
Uncleaned
Residual Ash

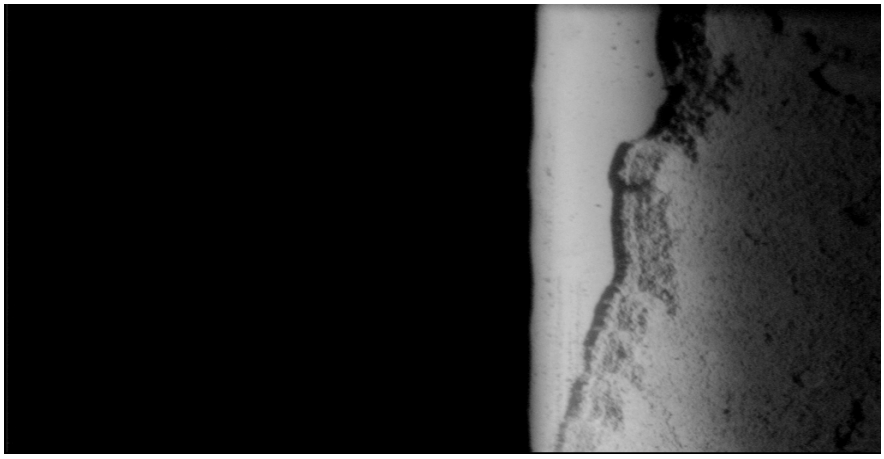

Thick
uncleaned
Residual Ash

Figure 6.1.6.b.
Images of surface quality of the Lanxide filter.

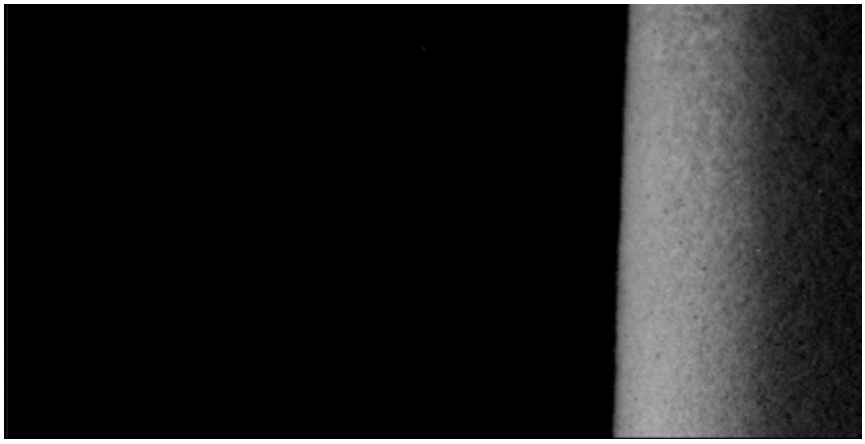

Clean Filter

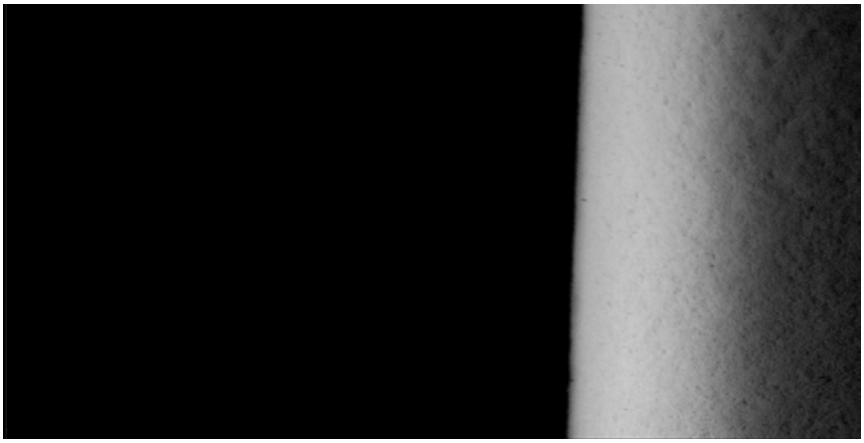

Residual Ash growth

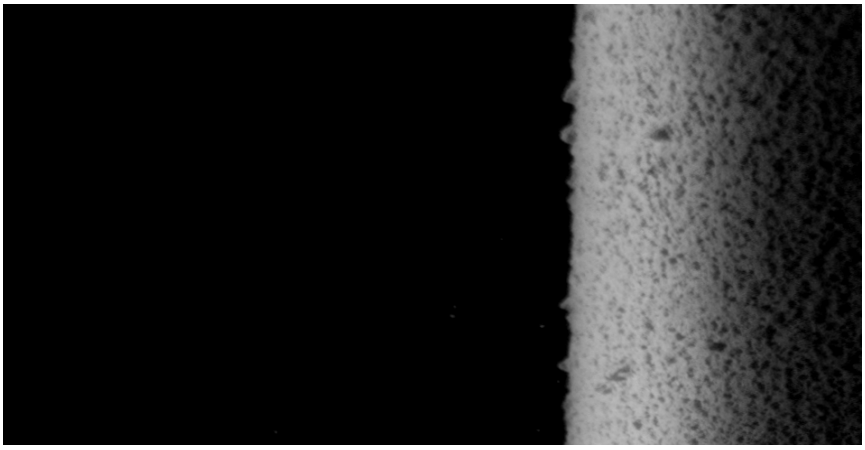

More Residual Ash growth

Figure 6.1.7.a.
Images of surface quality of the Pall filter. (Contd.)

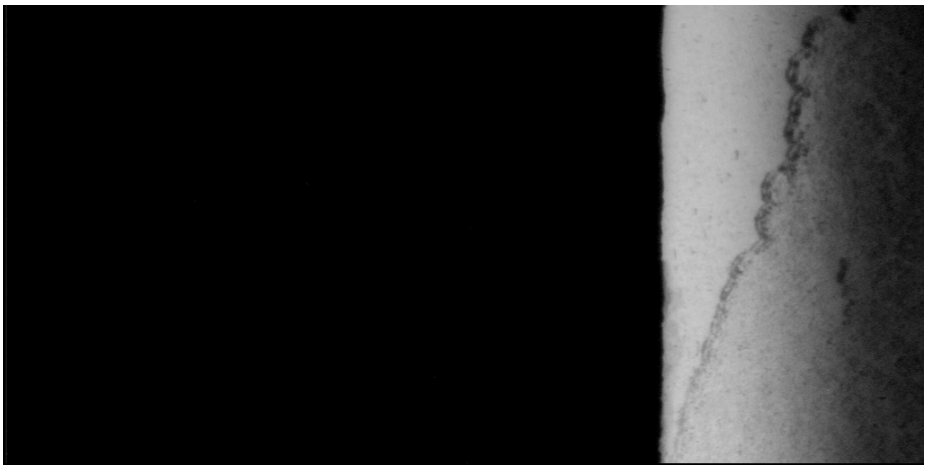

Patchy
Cleaning

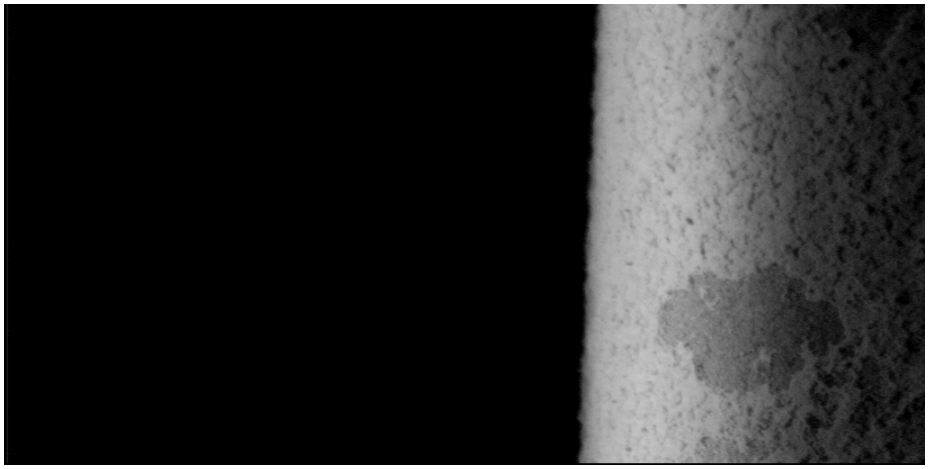

Patchy
Cleaning

Figure 6.1.7.b.
Images of surface quality of the Pall filter.

The independent variables and the regeneration characteristics have been discussed in order to get a better understanding when interpreting the results.

6.2 Effect of regeneration pressure on the regeneration process

The filter was subjected to long term test cycles under four different regeneration pressure conditions. The 95 psi regeneration pressure corresponds to the base condition. The face velocity was 5 cm/s and the build-up time 20 minutes. The other regeneration pressure conditions selected were 80 psi, 120psi and 145 psi, respectively. The effect of each of the pressure conditions is discussed through the regeneration characteristic factors discussed in section 6.1.2. With all other factors maintained the same, the 80 psi condition is expected to have a relatively higher difficulty to regenerate and the145 psi condition is expected to have the lowest difficulty to regenerate. The results obtained are discussed in this section.

6.2.1 Number of test cycles and reason for ending

The reason the tests were ended was primarily due to repeated regeneration in all four conditions. In the case of 120 psi and 145 psi regeneration pressure conditions the tests were stopped after it was observed that the filter was not building up ash and the pressure conditions also did not vary. The filter was partially regenerating, though continuously for the 80 psi condition. Although some residual ash was building up on the ridges of the filter, repeated partial regeneration kept occurring. Therefore after 24 testing cycles the long term test was stopped. The 95 psi condition did not result in as much residual ash on the filter surface, but had some patchy residuals. This condition was

stopped after 25 cycles, due to repetitive regeneration. The results are part of Table 6.2.1. The ash thickness column is shaded when thin ash was observed.

Reg. Pressure	Test Status	Number of cycles	Stopped due to	Ash Thickness in mm	Type of Regeneration	Crack initiation Time	Surface Quality
80	Begin	24	**repeated partial regen.**	0.7-1.4	Thin	0.1-0.1667	very clean
	During			0.35	Thin	0.117-0.133	residaul ash on ridges
	End			0.175	Thin	0.117-0.133	repeated partial regen.
95	Begin	25	Repetitive Regeneration	0.7-1.05	Thin	0.1-0.13	clean
	During			0.35-0.35	Thin	0.117-0.13	patchy residuals
	End			0.35-0.525	Thin	0.117-0.15	more residual
120	Begin	14	Repetitive Regeneration	0.7-1.05	Thin	0.117-0.13	clean
	During			0.35	Part Thick/Thin	0.117-0.13	mostly clean
	End			0.35-1.05	Thin	0.117-0.13	mostly clean
145	Begin	15	Repetitive Regeneration	1.05	Thin	0.117-0.13	clean
	During			0.525-0.7	Thin	0.117-0.13	clean
	End			0.7-1.05	Thin	0.117-0.13	mostly clean

Table 6.2.1.
Effect of regeneration pressure
Comparative table of regeneration characteristics

6.2.2 Increase of chamber pressure (P_c) during the build-up phase

The chamber pressure increases with more ash deposition on the surface of the filter. The chamber pressure at the end of build-up phase is the resistance offered to the cleaning pulse, in addition to the resistance offered by the filter medium and the ash deposit. The ideal condition will be that the chamber pressure profile does not increase with successive tests. The observations from the tests performed at four different condition show that in the 80 psi and 95 psi regeneration cases, the chamber pressure increases with successive tests. The chamber pressure profiles of these two cases are shown in Figure 6.2.1 and 6.2.2. This chamber pressure profile indicates that there may be a residual ash build-up or improper cleaning. The chamber pressure profile (Figure 6.2.3 and 6.2.4) for 120 psi and 145 psi do not display as much pressure increase. The 120 psi and the 145 psi pressure conditions show favorable results as far as this regeneration characteristic is concerned.

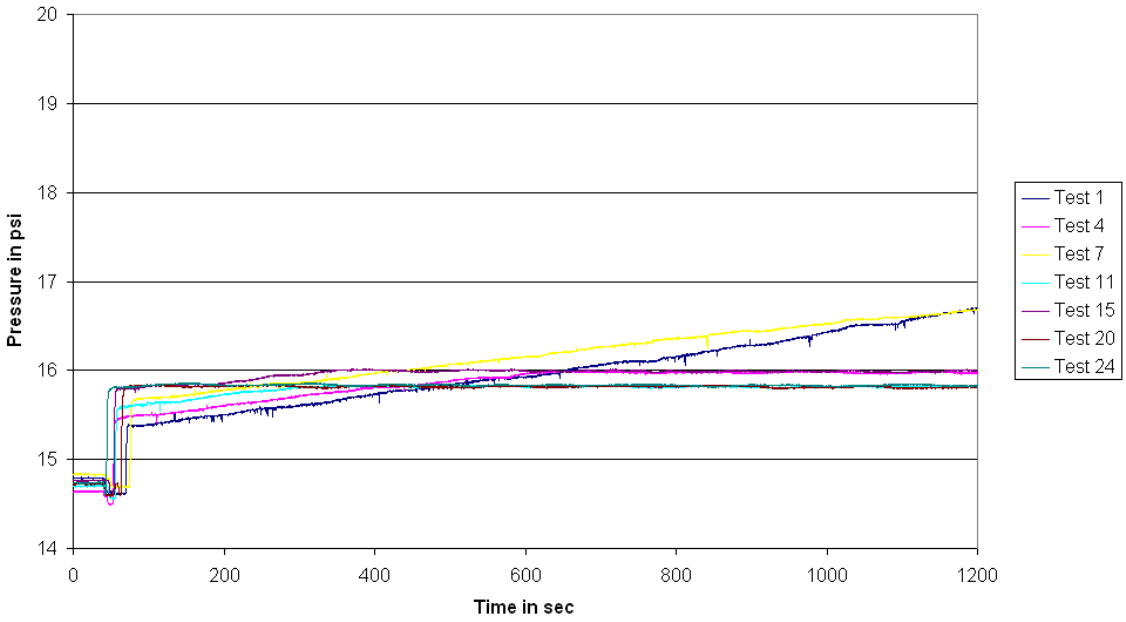

Figure 6.2.1.
Effect of regeneration pressure - Lanxide filter
Comparative plot of chamber pressure increase during build-up
80 psi regeneration pressure, 5 cm/s face velocity, 20 minute build-up time

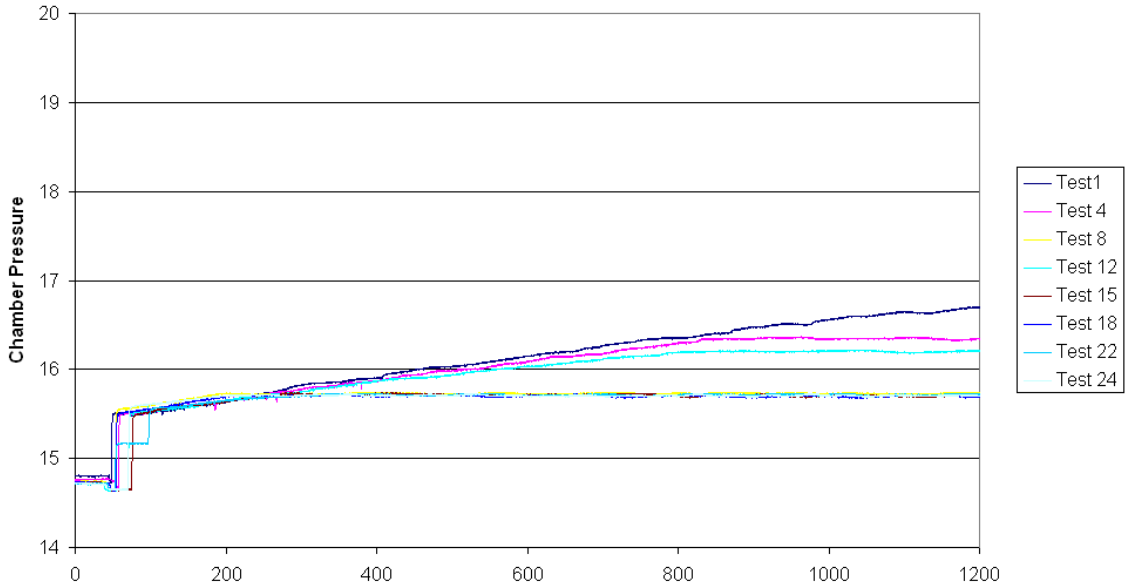

Figure 6.2.2.
Effect of regeneration pressure - Lanxide filter
Comparative plot of chamber pressure increase during build-up
95 psi regeneration pressure, 5 cm/s face velocity, 20 minute build-up time

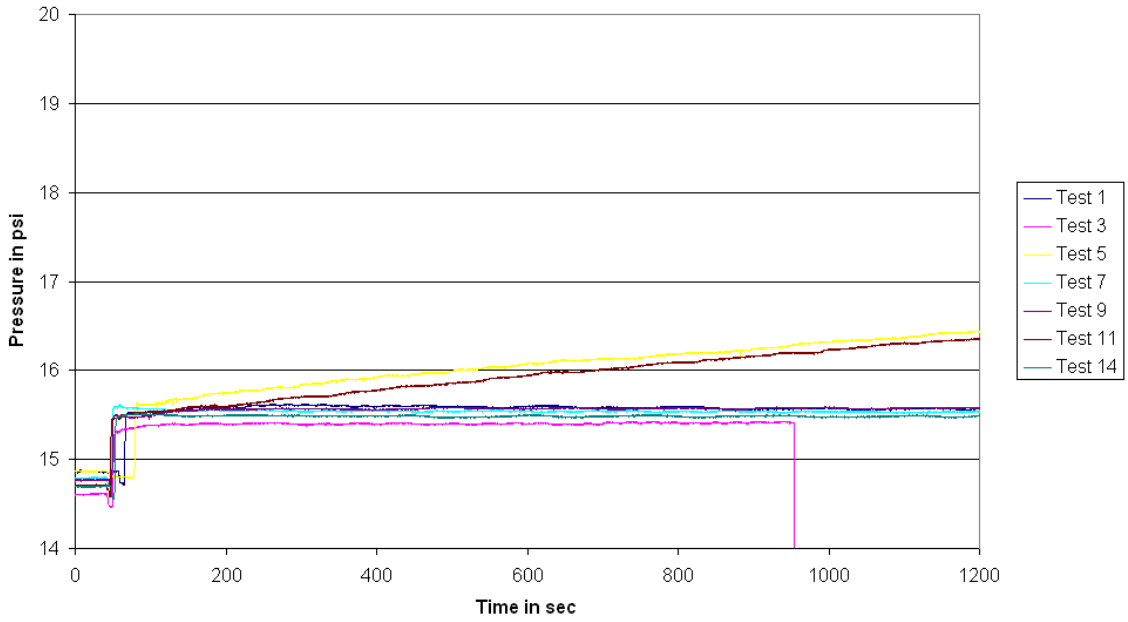

Figure 6.2.3.
Effect of regeneration pressure - Lanxide filter
Comparative plot of chamber pressure increase during build-up
120 psi regeneration pressure, 5 cm/s face velocity, 20 minute build-up time

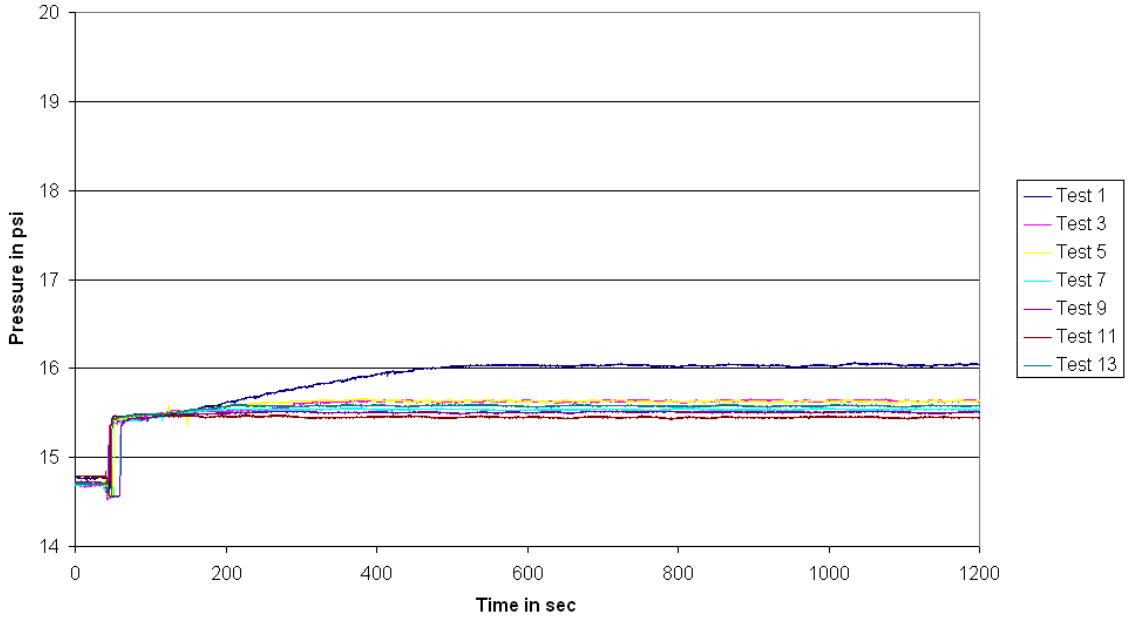

Figure 6.2.4.
Effect of regeneration pressure - Lanxide filter
Comparative plot of chamber pressure increase during build-up
145 psi regeneration pressure, 5 cm/s face velocity, 20 minute build-up time

6.2.3 Pressure difference, ΔP (P_f-Pc), between filter (P_f) and chamber (Pc) during regeneration

A study on the pressure difference (ΔP) profile helps us to determine how effective the regeneration process was. All the important factors associated with the ΔP profile has been discussed in sec 6.1.2. The ΔP profiles of the long term tests performed to study the effect of regeneration pressure are discussed here. The pressure difference profiles for 80 psi, 95 psi, 120 psi and 145 psi are shown in Figures 6.2.5 to 6.2.8. From the pressure profiles the $\Delta P_{initial}$, ΔP_{final}, ΔP_{max}, ΔP_{min}, the efficiencies and the cleaning factors are obtained and are also presented along with the above Figures. The effectiveness of the regeneration process is discussed.

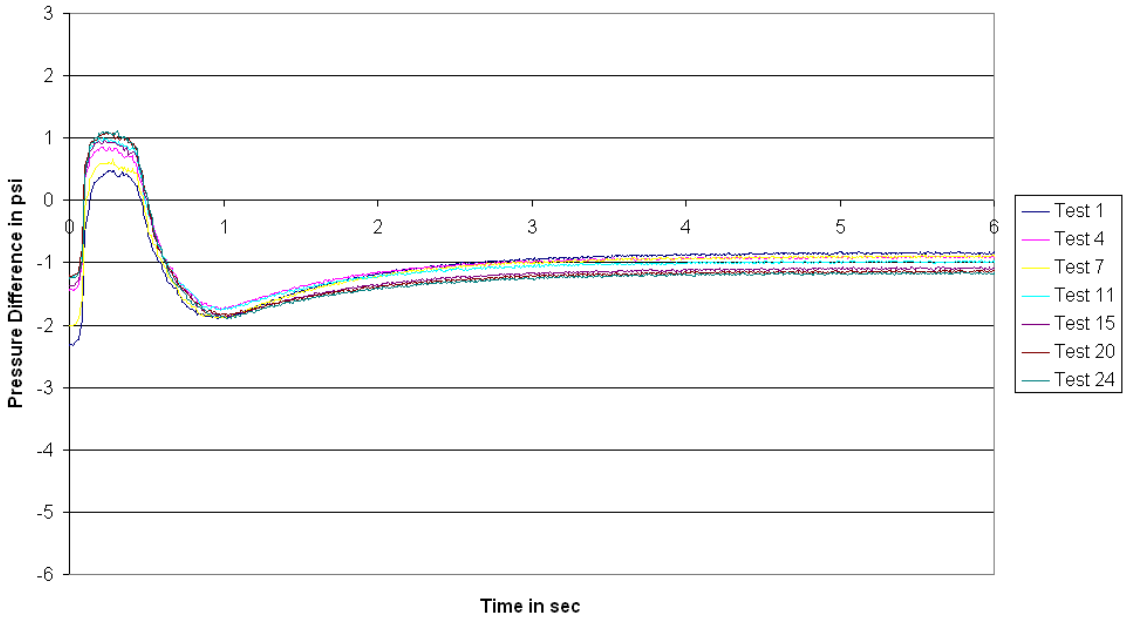

	Test 1	Test 4	Test 7	Test 11	Test 15	Test 20	Test 24
ΔP new (psi)	-0.34978	-0.34978	-0.34978	-0.34978	-0.34978	-0.34978	-0.34978
ΔP cleaned (psi)	-0.77162	-0.77162	-0.77162	-0.77162	-0.77162	-0.77162	-0.77162
ΔP initial @ t=0 (psi)	-2.32146	-1.43974	-2.00754	-1.23078	-1.3673	-1.2073	-1.25286
ΔP initial @ t=5 (psi)	-0.82948	-0.90866	-0.90874	-0.98698	-1.09834	-1.16394	-1.18336
Time @ ΔP max (sec)	0.26	0.26	0.28	0.22	0.29	0.24	0.31
ΔP max (psi)	0.46926	0.8499	0.65872	0.99764	0.9353	1.08184	1.11376
Time @ ΔP min (sec)	0.96	0.99	0.92	0.98	1.01	1.03	1.05
ΔP min (psi)	-1.89094	-1.74516	-1.88054	-1.76034	-1.88026	-1.84412	-1.89286
Efficiency-clean	0.962667	0.794887	0.889054	0.53097	0.451518	0.099523	0.144419
Efficiency-new	0.756705	0.487247	0.662822	0.276731	0.264329	0.050564	0.076959
Factor-c	1.074985	1.1776	1.177704	1.279101	1.423421	1.508437	1.533605
Factor-n	2.371431	2.597802	2.598031	2.821714	3.140085	3.327631	3.383152

Figure 6.2.5.
Effect of regeneration pressure - Lanxide filter
Comparative plot of pressure difference (ΔP: Pf-Pc) change during regeneration and corresponding analysis table for
80 psi regeneration pressure, 5 cm/s face velocity, 20 minute build-up time

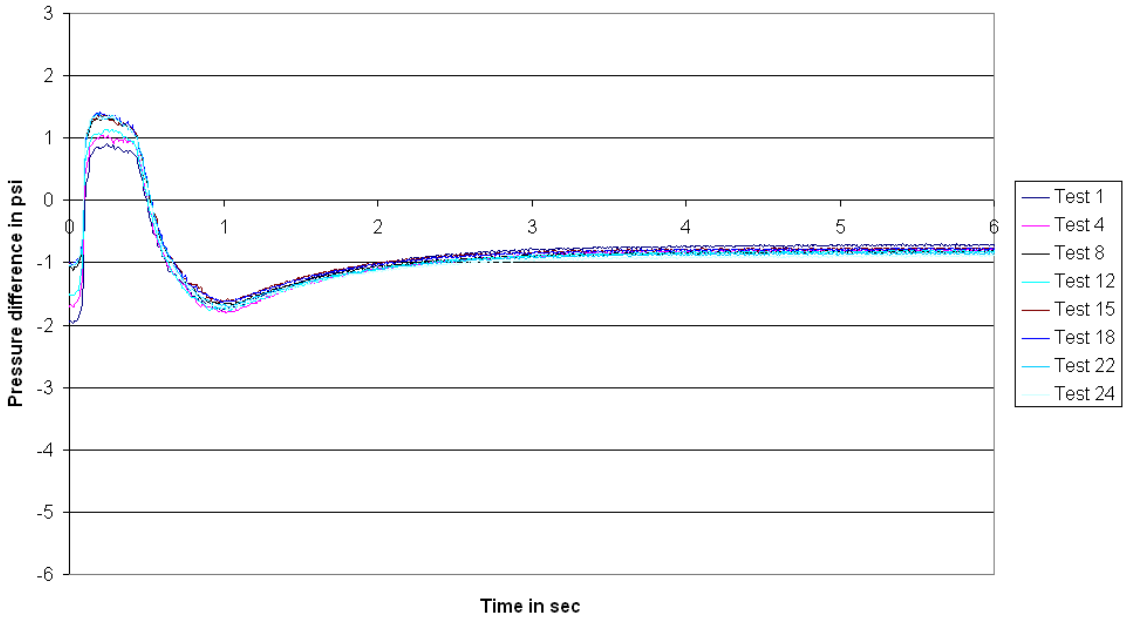

	Test 1	Test 4	Test 8	Test 12	Test 15	Test 18	Test 22	Test 24
ΔP new (psi)	-0.34978	-0.34978	-0.34978	-0.34978	-0.34978	-0.34978	-0.34978	-0.34978
ΔP cleaned (psi)	-0.78702	-0.78702	-0.78702	-0.78702	-0.78702	-0.78702	-0.78702	-0.78702
ΔP initial @ t=0 (psi)	-1.94848	-1.70232	-1.06656	-1.5146	-1.01064	-0.99012	-1.0259	-1.03348
ΔP initial @ t=5 (psi)	-0.7367	-0.81544	-0.82716	-0.82608	-0.77356	-0.77698	-0.84696	-0.899
Time @ ΔP max (sec)	0.24	0.22	0.24	0.24	0.2	0.2	0.19	0.26
ΔP max (psi)	0.90554	1.04566	1.35588	1.13994	1.35742	1.41752	1.40018	1.38776
Time @ ΔP min (sec)	0.98	1.02	1.05	1.04	0.97	0.99	1.04	1.03
ΔP min (psi)	-1.7665	-1.8096	-1.66952	-1.75564	-1.6275	-1.62946	-1.70752	-1.73794
Efficiency-clean	1.043325	0.96895	0.856407	0.946315	1.060191	1.049434	0.749079	0.545646
Efficiency-new	0.757979	0.655715	0.333994	0.591096	0.358745	0.332855	0.264657	0.196695
Factor-c	0.936063	1.036111	1.051003	1.04963	0.982898	0.987243	1.076161	1.142284
Factor-n	2.106179	2.331292	2.364798	2.361711	2.211559	2.221337	2.421405	2.570185

Figure 6.2.6.
Effect of regeneration pressure - Lanxide filter
Comparative plot of pressure difference (ΔP: Pf-Pc) change during regeneration and corresponding analysis table for
95 psi regeneration pressure, 5 cm/s face velocity, 20 minute build-up time

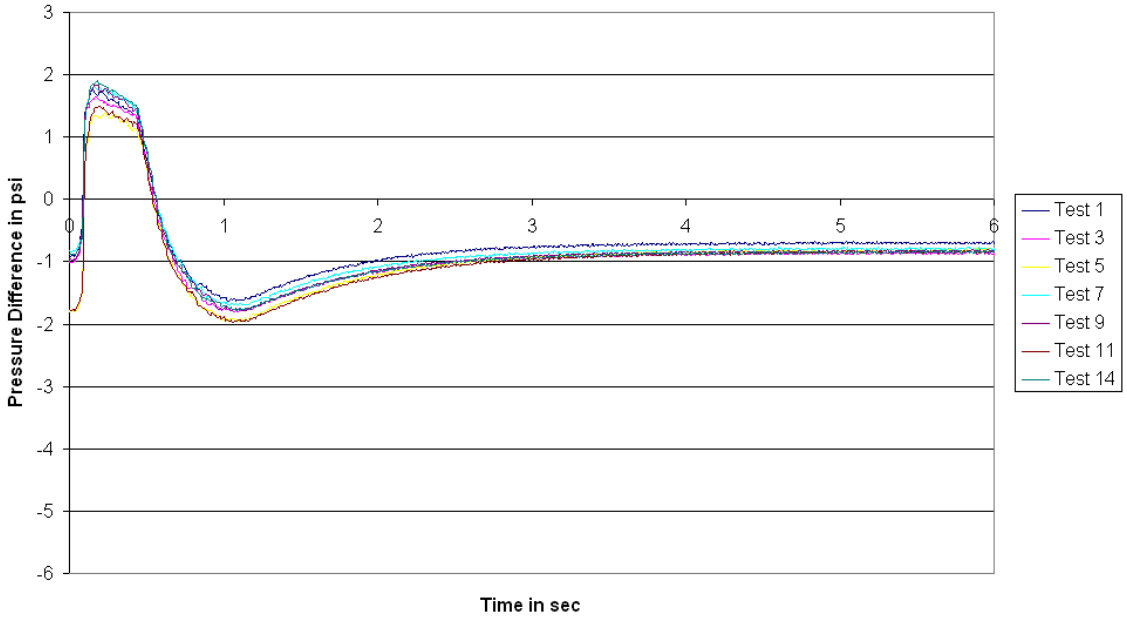

	Test 1	Test 3	Test 5	Test 7	Test 9	Test 11	Test 14
ΔP new (psi)	-0.34978	-0.34978	-0.34978	-0.34978	-0.34978	-0.34978	-0.34978
ΔP cleaned (psi)	-0.855	-0.855	-0.855	-0.855	-0.855	-0.855	-0.855
ΔP initial @ t=0 (psi)	-0.91156	-0.99214	-1.80834	-0.82818	-0.96306	-1.767	-0.87184
ΔP initial @ t=5 (psi)	-0.69842	-0.85412	-0.84048	-0.78262	-0.84116	-0.8392	-0.83886
Time @ ΔP max (sec)	0.15	0.17	0.23	0.16	0.16	0.2	0.18
ΔP max (psi)	1.7526	1.63698	1.38922	1.80508	1.83744	1.50164	1.91096
Time @ ΔP min (sec)	1.03	1.07	1.03	1.14	1.05	1.06	1.09
ΔP min (psi)	-1.62794	-1.8021	-1.95662	-1.69606	-1.79182	-1.96146	-1.77672
Efficiency-clean	3.768388	1.006417	1.015231	-1.69873	1.128077	1.017325	1.958432
Efficiency-new	0.379401	0.214864	0.663572	0.095234	0.198767	0.654662	0.063173
Factor-c	0.816865	0.998971	0.983018	0.915345	0.983813	0.98152	0.981123
Factor-n	1.996739	2.441875	2.40288	2.237461	2.404824	2.39922	2.398248

Figure 6.2.7.
Effect of regeneration pressure - Lanxide filter
Comparative plot of pressure difference (ΔP: Pf-Pc) change during regeneration and corresponding analysis table for
120 psi regeneration pressure, 5 cm/s face velocity, 20 minute build-up time

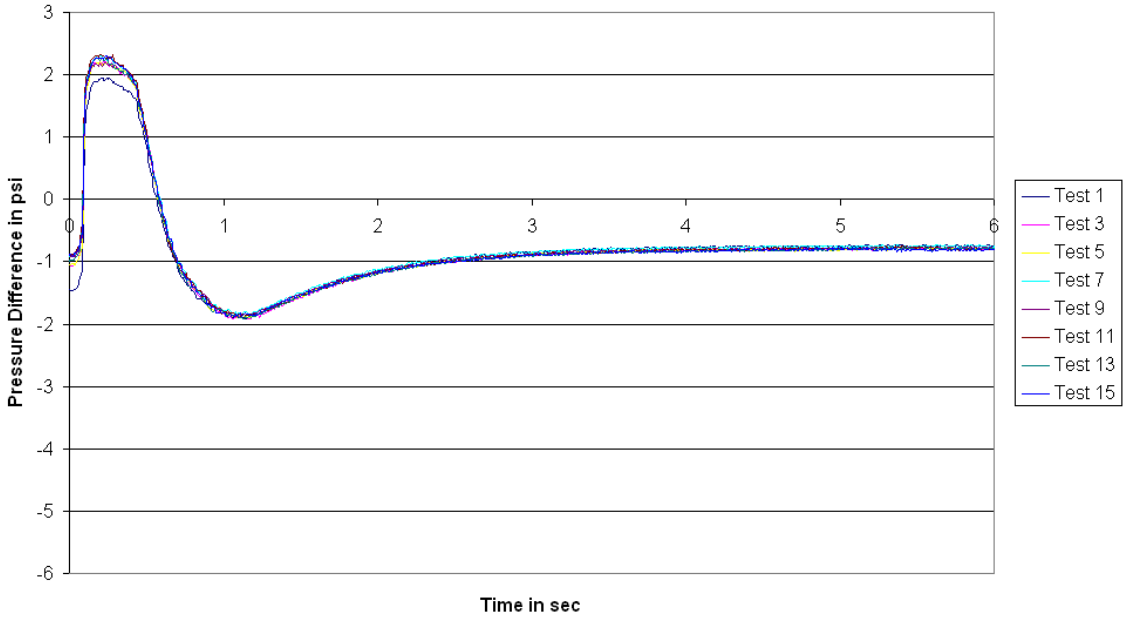

	Test 1	Test 3	Test 5	Test 7	Test 9	Test 11	Test 13	Test 15
ΔP new (psi)	-0.34978	-0.34978	-0.34978	-0.34978	-0.34978	-0.34978	-0.34978	-0.34978
ΔP cleaned (psi)	-0.8041	-0.8041	-0.8041	-0.8041	-0.8041	-0.8041	-0.8041	-0.8041
ΔP initial @ t=0 (psi)	-1.45256	-1.04968	-1.03892	-0.89704	-0.90476	-0.8881	-0.98398	-0.8885
ΔP initial @ t=5 (psi)	-0.76746	-0.78866	-0.79622	-0.74778	-0.78396	-0.79698	-0.80504	-0.79738
Time @ ΔP max (sec)	0.21	0.22	0.2	0.22	0.23	0.28	0.19	0.24
ΔP max (psi)	1.94866	2.23184	2.21216	2.29738	2.19328	2.32018	2.2677	2.29714
Time @ ΔP min (sec)	1.15	1.06	1.09	1.12	1.14	1.14	1.13	1.07
ΔP min (psi)	-1.90718	-1.91858	-1.8988	-1.84964	-1.87142	-1.88028	-1.91228	-1.877
Efficiency-clean	1.056503	1.062872	1.033558	1.605982	1.200079	1.084762	0.994774	1.079621
Efficiency-new	0.621248	0.372939	0.352178	0.272741	0.217666	0.169267	0.282151	0.169142
Factor-c	0.954434	0.980798	0.9902	0.929959	0.974953	0.991145	1.001169	0.991643
Factor-n	2.19412	2.254729	2.276343	2.137856	2.241292	2.278516	2.301559	2.279659

Figure 6.2.8.
Effect of regeneration pressure - Lanxide filter
Comparative plot of pressure difference (ΔP: Pf-Pc) change during regeneration and corresponding analysis table for
145 psi regeneration pressure, 5 cm/s face velocity, 20 minute build-up time

a. $\Delta P_{initial}$

It is expected that if the $\Delta P_{initial}$ value is low, then the ash and flow conditions do not resist the flow as much. On studying the plot of $\Delta P_{initial}$ values as the test cycle progresses, for the different parametric conditions the following observations are noted. The $\Delta P_{initial}$ value is low for the 145 psi and the 120 psi conditions right from the beginning to the end. The two drops in the 120 psi condition correspond to the 5th and the 11th cycles when it built thick ash. If these two tests are neglected from the analysis, the $\Delta P_{initial}$ values for the 120 psi and the 145 psi conditions are low. The $\Delta P_{initial}$ values for the 80 psi and the 95 psi indicate a large pressure drop at the beginning, but the value becomes low as the test cycles increase. The four conditions do not show any significant changes among themselves when evaluated based on $\Delta P_{initial}$.

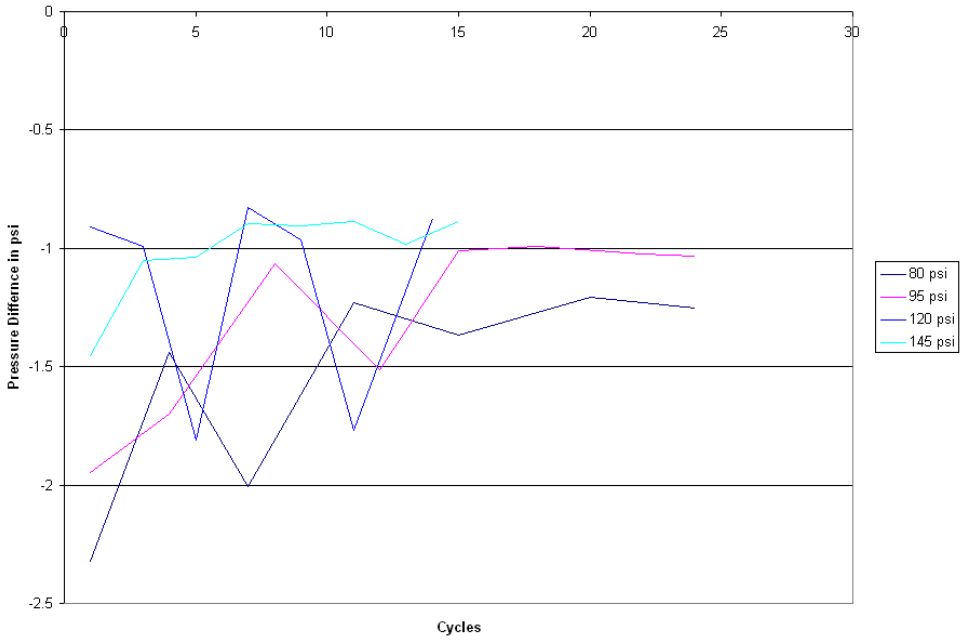

Figure 6.2.9.
Effect of regeneration pressure
Lanxide filter - long term tests
Comparative plot of initial pressure difference ($\Delta P_{initial}$)

b. ΔP_{final}

The ΔP_{final} value is measured after the filter has been regenerated and is now the pressure difference after the cleaning. This magnitude remains low after repeated testing cycles if the regeneration has cleaned the filter with the same consistency. If the magnitude of pressure drop starts to increase then it indicates ineffective cleaning. In the comparative study from the Figure 6.2.10, it is observed that in the 95 psi, 120 psi and 145 psi conditions the pressure drop does not increase. While for the 80 psi condition the pressure drop (magnitude) keeps increasing very distinctly.

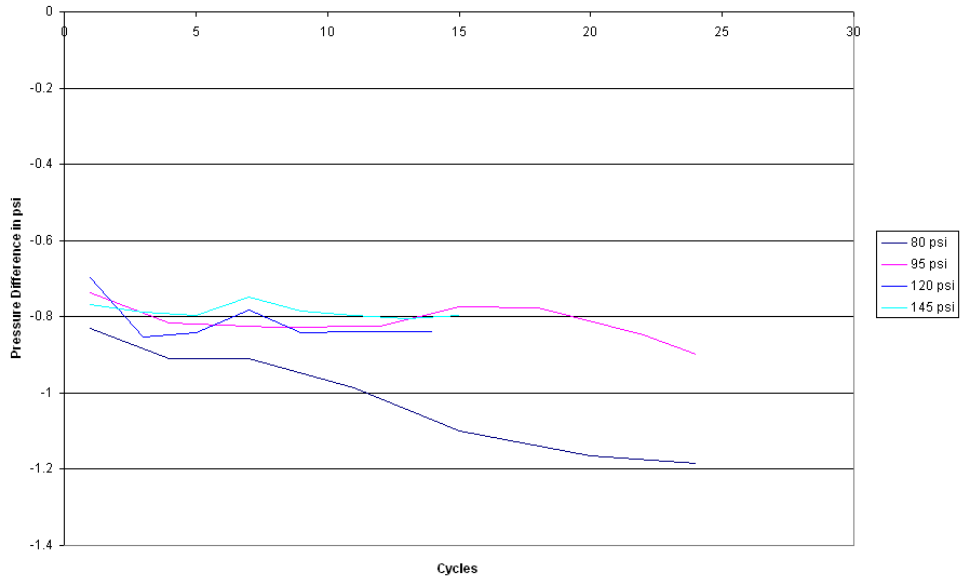

Figure 6.2.10.
Effect of regeneration pressure
Lanxide filter - long term tests
Comparative plot of final pressure difference (ΔP_{final})

c. ΔP_{max}

ΔP_{max} corresponds to the maximum pressure difference and if the magnitude of the regeneration pulse is sufficient to overcome the resistance offered by the ash and the flow, then this value is positive large number. As expected the plot corresponding to the 145 psi condition has the largest ΔP-maximum while the plot corresponding to the 80 psi condition has the lowest ΔP-maximum. Since all conditions kept regenerating continuously the ΔP-maximum was always positive for all the conditions.

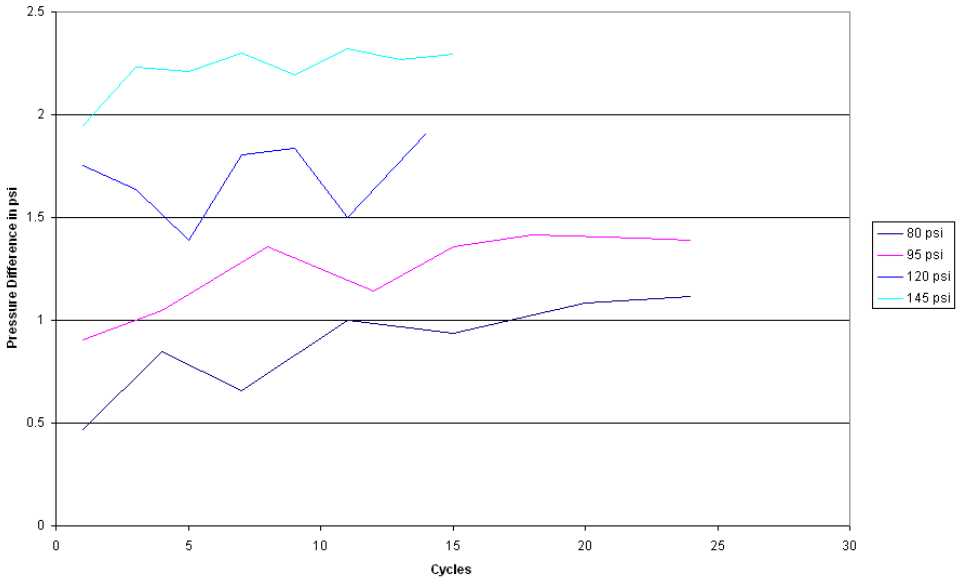

Figure 6.2.11.
Effect of regeneration pressure
Lanxide filter - long term tests
Comparative plot of maximum pressure difference (ΔP_{max})

d. ΔP_{min}

The ΔP_{max} values were all found to lie within the same range of values in all four conditions. Thus all four conditions may have the same probability of re-entrainment.

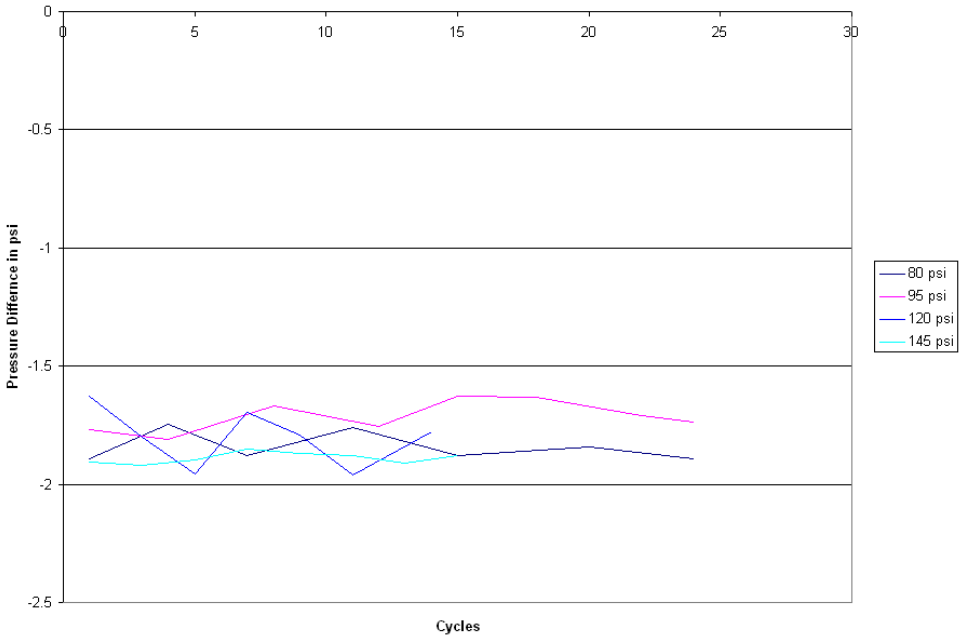

Figure 6.2.12.
Effect of regeneration pressure
Lanxide filter - long term tests
Comparative plot of minimum pressure difference (ΔP_{min})

e. Efficiency η:

The regeneration in all the cases were tending towards thin type regeneration. The test cycles in some sporadic cases showed tendency towards thick type and partial thick-thin type. These changes affect the ΔP-initial value and thus the efficiency values (η_{new} and $\eta_{cleaned}$). The $\eta_{cleaned}$ value for test 7 in the 120 psi condition is negative because of the value of ΔP-initial. It is difficult to arrive at the most efficient filter based on the value of

η alone as presented in the graphs. It is observed that the η–new values are reducing with more test cycles in all four cases. But the efficiencies are generally low for the 80 psi condition and decreases in both η_{new} and $\eta_{cleaned}$ conditions.

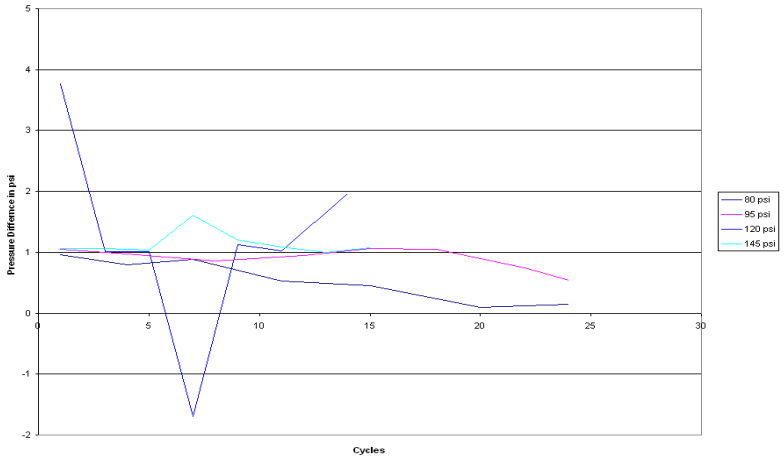

Figure 6.2.13.
Effect of regeneration pressure
Lanxide filter - long term tests
Comparative plot of efficiency based on ΔP_C (η_C)

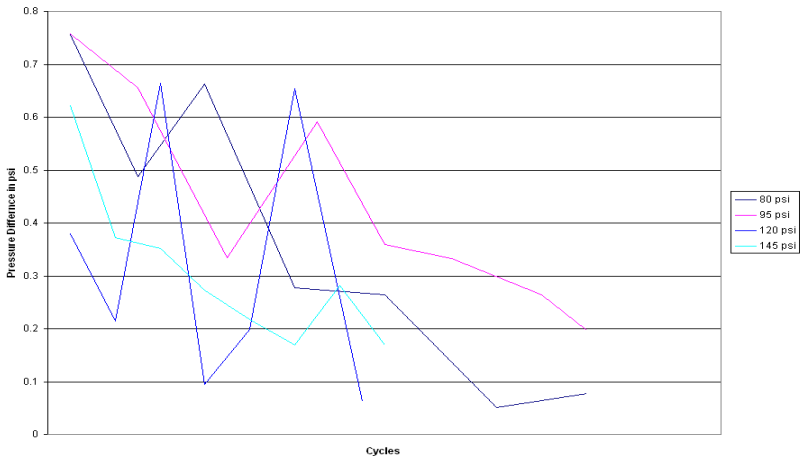

Figure 6.2.14.
Effect of regeneration pressure
Lanxide filter - long term tests
Comparative plot of efficiency based on ΔP_N (η_N)

f. Cleaning Factor F:

The cleaning factor F is the ratio of final pressure difference to the pressure drop across a clean/new filter. This factor when measured with progressing test cycles show a measure of how much residual ash is collecting on the filter. The F_N (cleaning factor when measured with respect to a new filter) and the F_C (cleaning factor when measured with respect to a cleaned filter) are plotted for all the four conditions. It is very clear from the plot that the factor keeps increasing for the 80 psi condition. The other three conditions exhibit almost the same values.

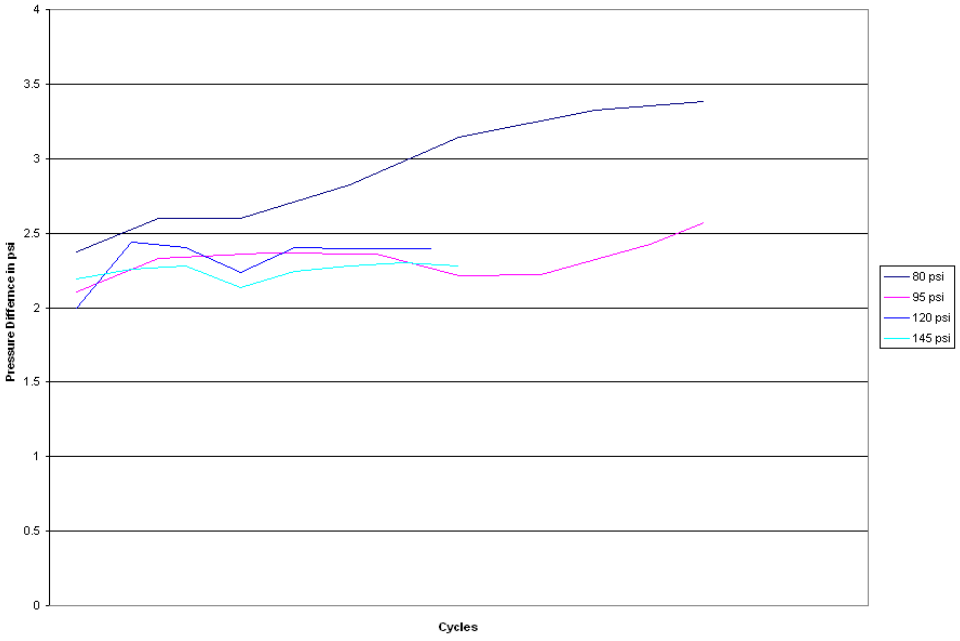

Figure 6.2.15.
Effect of regeneration pressure
Lanxide filter - long term tests
Comparative plot of cleaning factor based on ΔP_C (F_C)

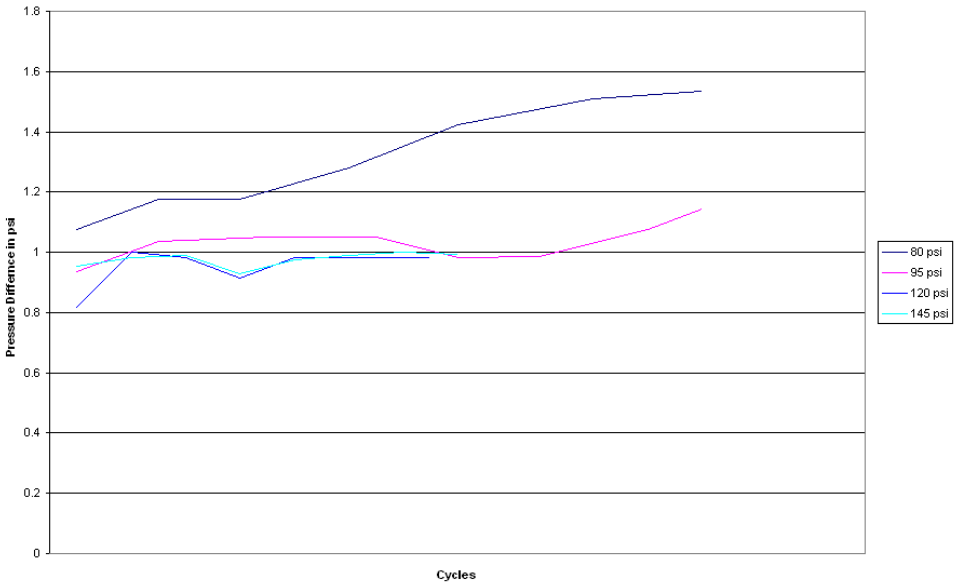

Figure 6.2.16.
Effect of regeneration pressure
Lanxide filter - long term tests
Comparative plot of cleaning factor based on ΔP_N (F_N)

From analyzing the pressure difference profiles it can be concluded that although all the four parameters seem to perform similarly in some cases, but the 80 psi condition shows an indication of residual ash growth. The efficiencies and cleaning factors also indicate the same for the 80 psi condition.

6.2.4 Distribution of particles less than 100 microns during regeneration

The particle count for size less than 100 microns, do not show much difference while comparing the four cases Figures 6.2.17 to 6.2.20. All the four regeneration conditions exhibit thin ash regeneration. The formation of thin ash and resulting thin ash failure may be influenced more by the build-up conditions. The particle count is significantly higher in all cases and this can be attributed to the thin type regeneration observed in all cases.

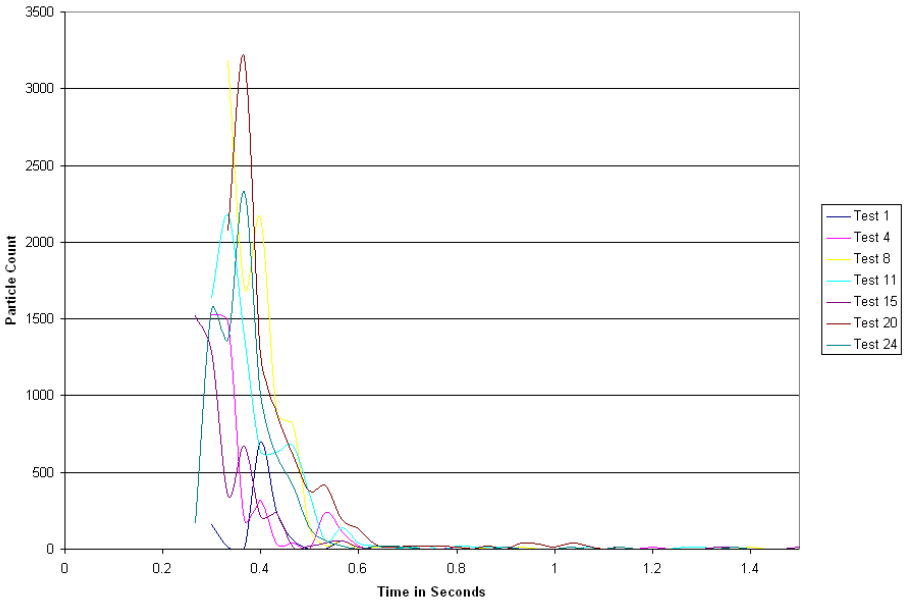

Figure 6.2.17.
Effect of regeneration pressure on Lanxide filter - long term tests
Particle count: less than 100 microns
80 psi Regeneration Pressure, 5 cm/s face velocity, 20 min build-up time

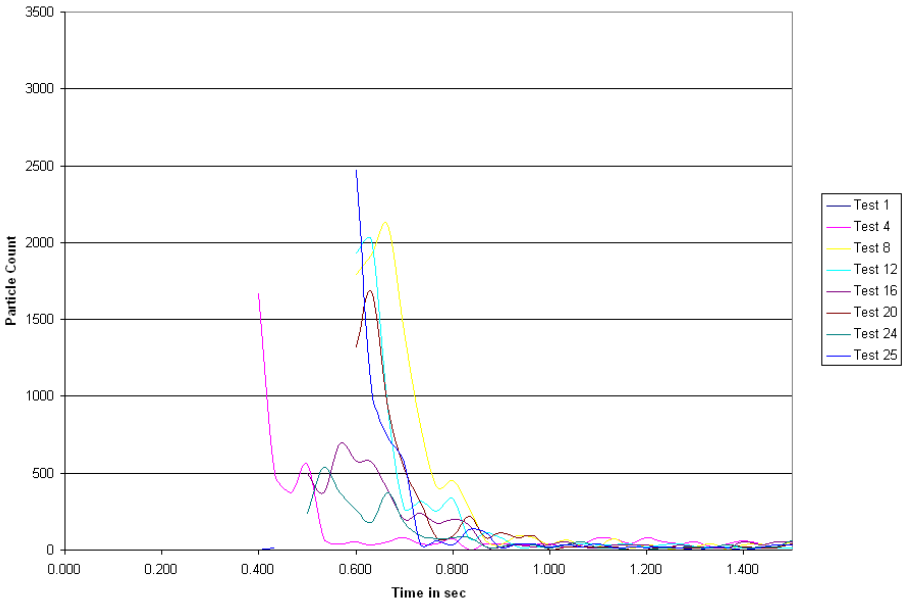

Figure 6.2.18.
Effect of regeneration pressure on Lanxide filter - long term tests
Particle count: less than 100 microns
95 psi Regeneration Pressure, 5 cm/s face velocity, 20 min build-up time

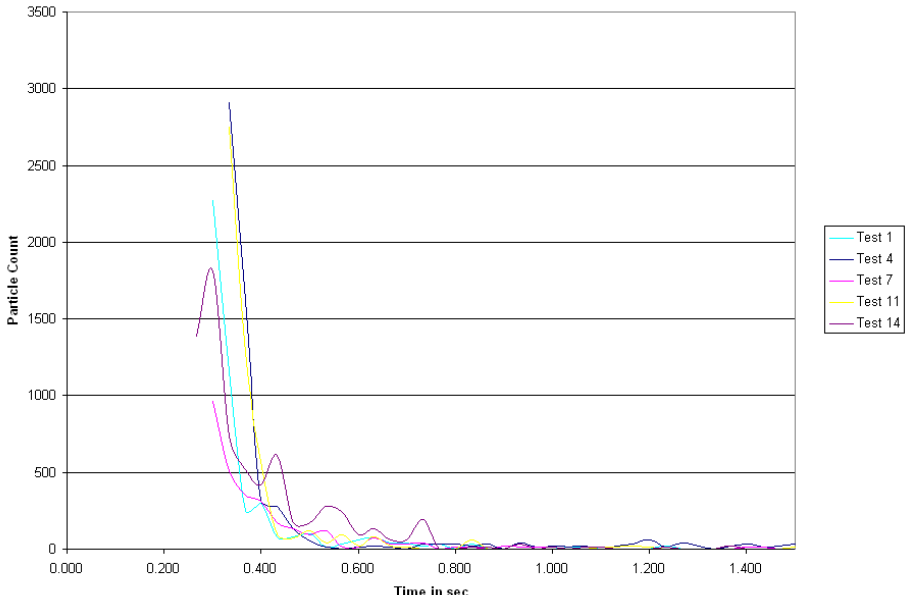

Figure 6.2.19.
Effect of regeneration pressure on Lanxide filter - long term tests
Particle count: less than 100 microns
120 psi Regeneration Pressure, 5 cm/s face velocity, 20 min build-up time

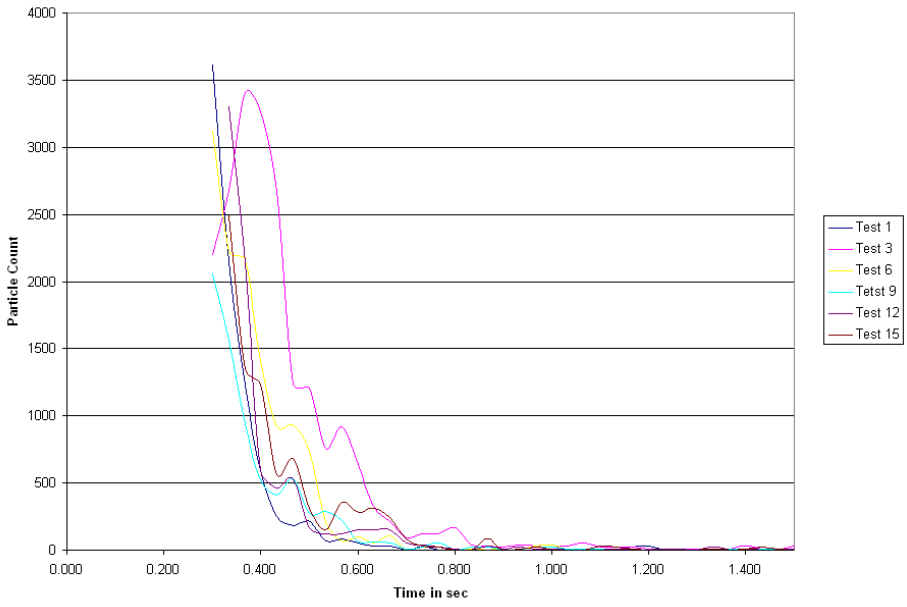

Figure 6.2.20.
Effect of regeneration pressure on Lanxide filter - long term tests
Particle count: less than 100 microns
145 psi Regeneration Pressure, 5 cm/s face velocity, 20 min build-up time

6.2.5 The thickness of ash deposit during build-up

It is observed (from Table 6.2.1) that the regeneration pressure does not seem to influence the thickness of the ash deposit. The ash thickness was thin in all four cases. The build-up conditions: especially the face velocity and the build-up interval can be the influencing factors as far as the formation of ash on the surface more than the regeneration pressure.

6.2.6 The type of regeneration

The type of regeneration process is dependent on the thickness of the ash deposit. The ash deposited on the filter surface was thin and the type of regeneration observed was predominantly thin type (Table 6.2.1). This type of regeneration generates a large amount of small particles, and is detrimental to the regeneration process overall.

6.2.7 Crack initiation time

A longer crack initiation time indicates that the ash resists the regeneration pulse and the pressure inside the filter builds up to a higher value to dislodge the ash cake. The crack initiation time is low (Table 6.2.1), and almost the same in nearly all pressure conditions, even with continued testing. Therefore the resistance offered by the built up ash cake is not difficult to overcome in all conditions.

6.2.8 Surface quality

The surface deterioration was observed in the 80-psi regeneration condition the most. Although the 80 psi condition did not have a large residual ash cake forming, there were patchy residuals on its surface and also there was ash on the filter surface contours. The filter was dirty, but the ash was not thick or strong enough to prevent surface regeneration. The 120 psi and 145 psi conditions resulted in filters that appeared to be mostty clean. The surface quality, for all four conditions have been denoted in Table 6.2.1. The filter quality imaged after every few testing cycles for all four conditions are shown in Figures 6.2.21 to 6.2.24.

Test 1
Clean Filter

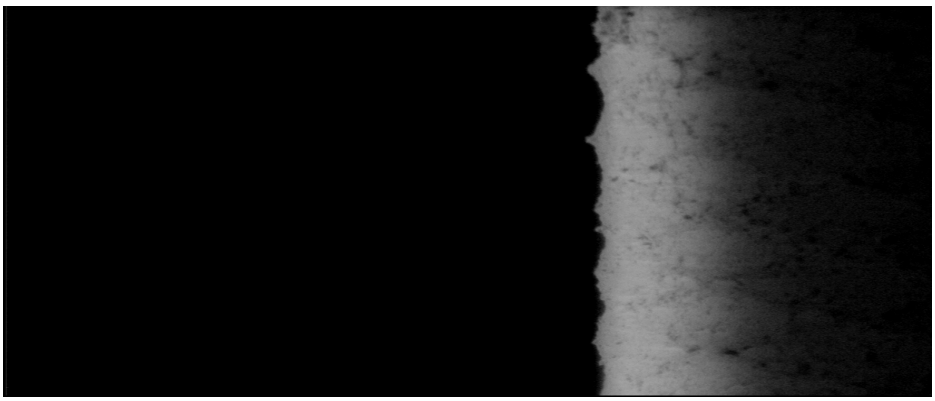

Test 4
Ash on Ridges

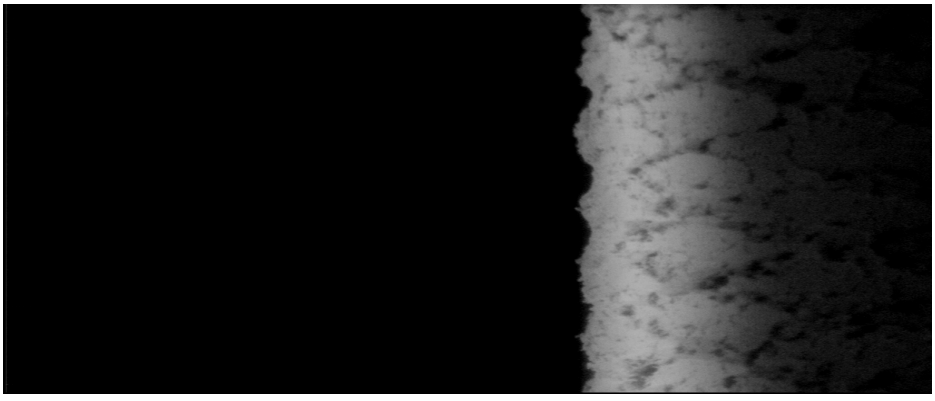

Test 8
Ash on
Ridges

Figure 6.2.21a
Effect of regeneration pressure on Lanxide filter
Surface quality during long term test cycles
80 psi regeneration pressure, 5 cm/s face velocity, 20 min build-up time. (Contd.)

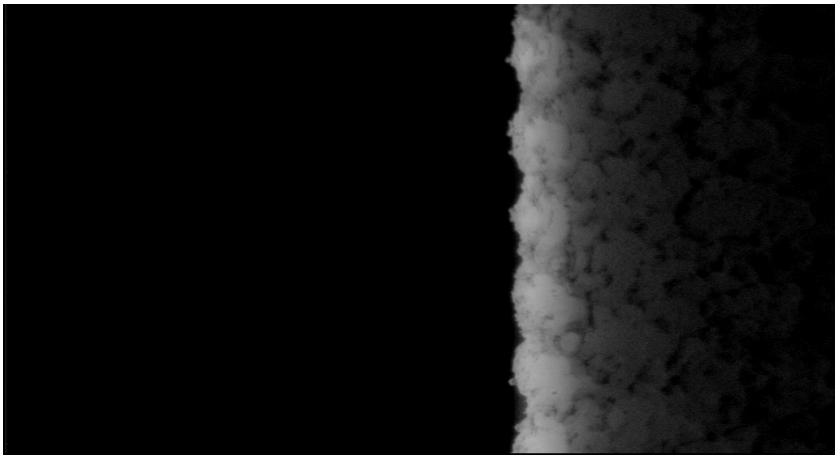

Test 15
More Ash on
Ridges

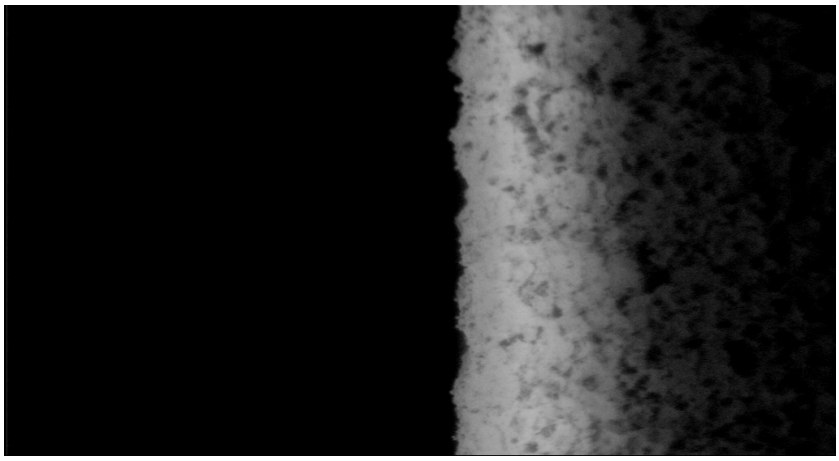

Test 24
Thin
Residual

Figure 6.2.21b
Effect of regeneration pressure on Lanxide filter
Surface quality during long term test cycles
80 psi regeneration pressure, 5 cm/s face velocity, 20 min build-up time.

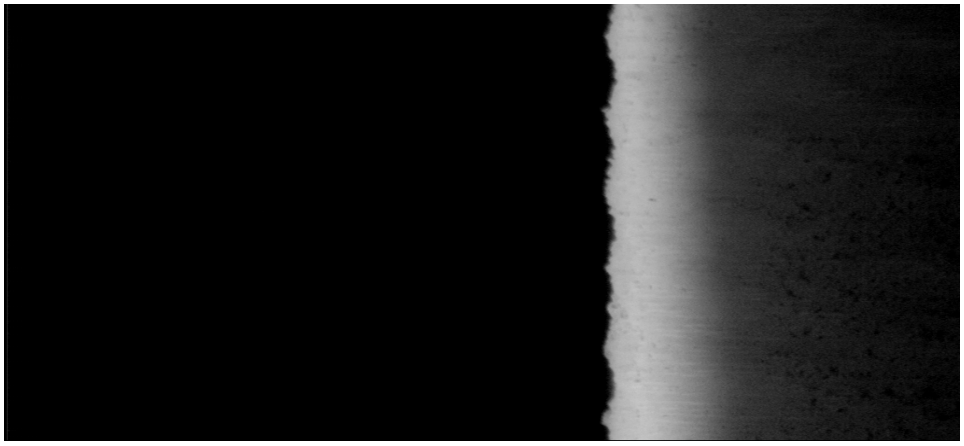

Test 1
Clean Filter

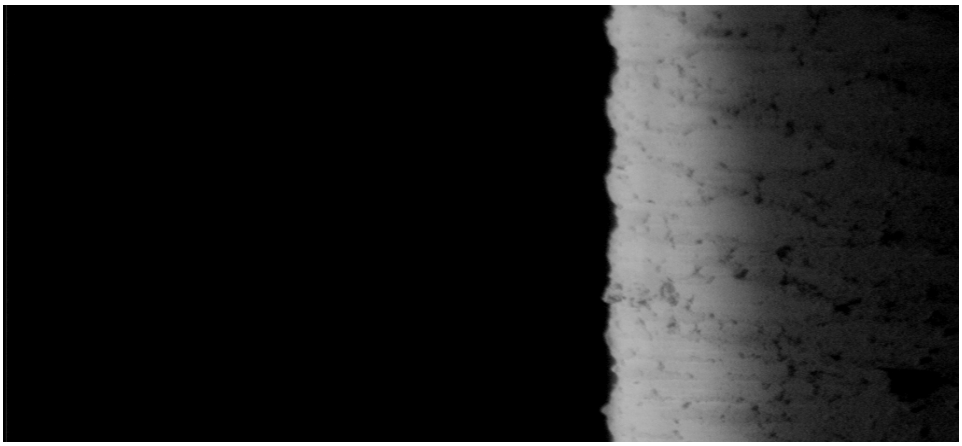

Test 4
Little
Residual

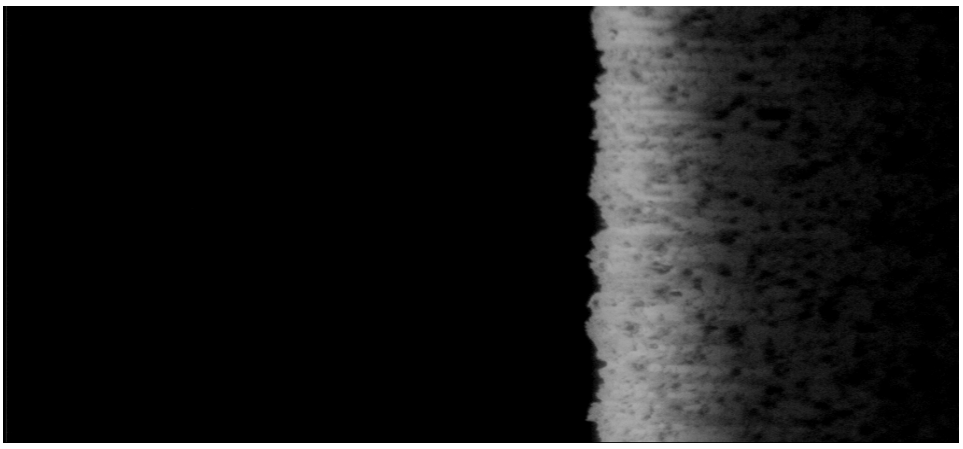

Test 8
Residual ash
typical of thin
ash regeneration.

Figure 6.2.22a
Effect of regeneration pressure on Lanxide filter
Surface quality during long term test cycles
95 psi regeneration pressure, 5 cm/s face velocity, 20 min build-up time. (Contd.)

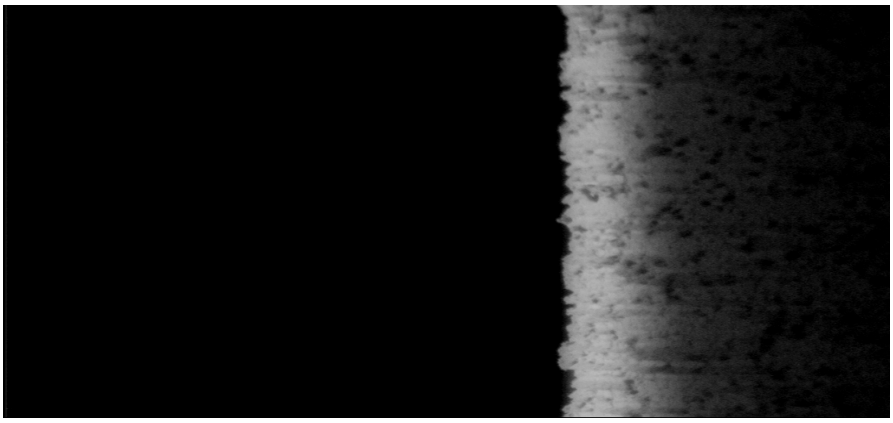

Test 16
More thin ash
type residuals

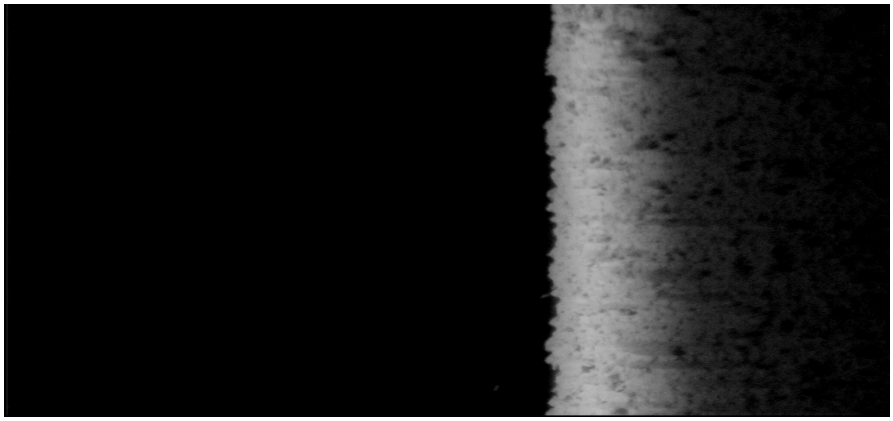

Test 20
Dirty Filter

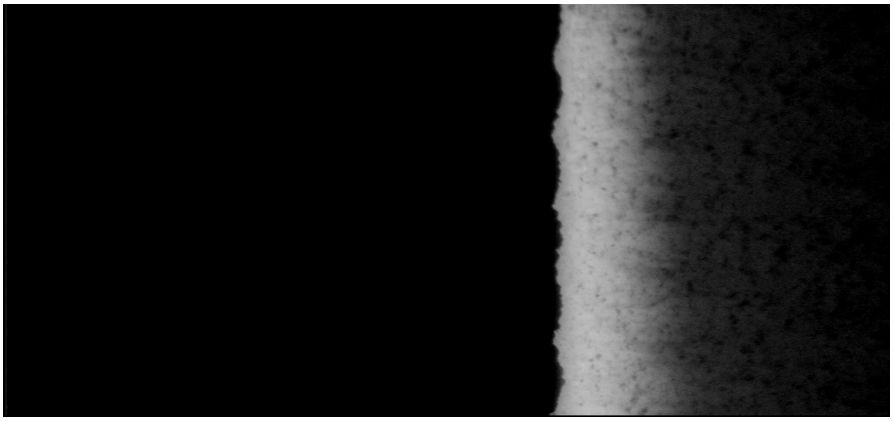

Test 25
Dirty Filter

Figure 6.2.22b
Effect of regeneration pressure on Lanxide filter
Surface quality during long term test cycles
95 psi regeneration pressure, 5 cm/s face velocity, 20 min build-up time.

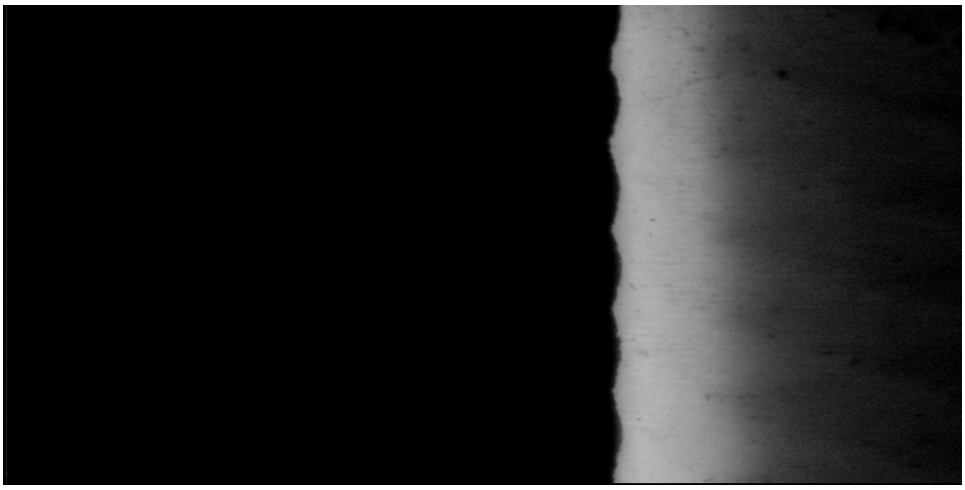

Test 1
Clean Filter

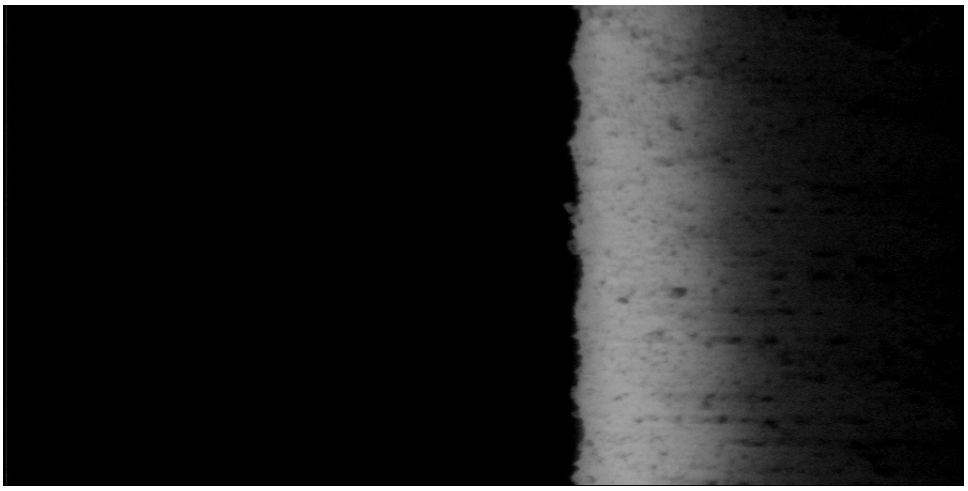

Test 6
Little Residual
Ash

Figure 6.2.23a
Effect of regeneration pressure on Lanxide filter
Surface quality during long term test cycles
145 psi regeneration pressure, 5 cm/s face velocity, 20 min build-up time. (Contd.)

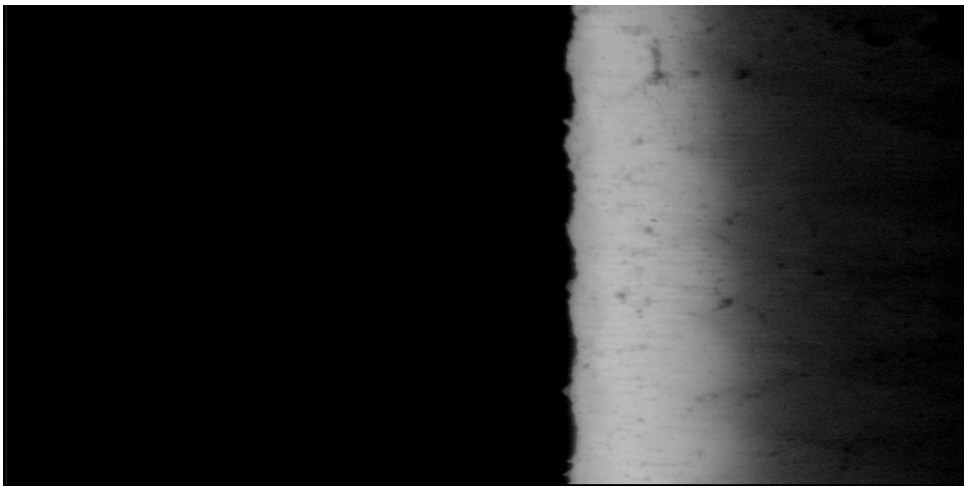

Test 12
Little Residual
Ash

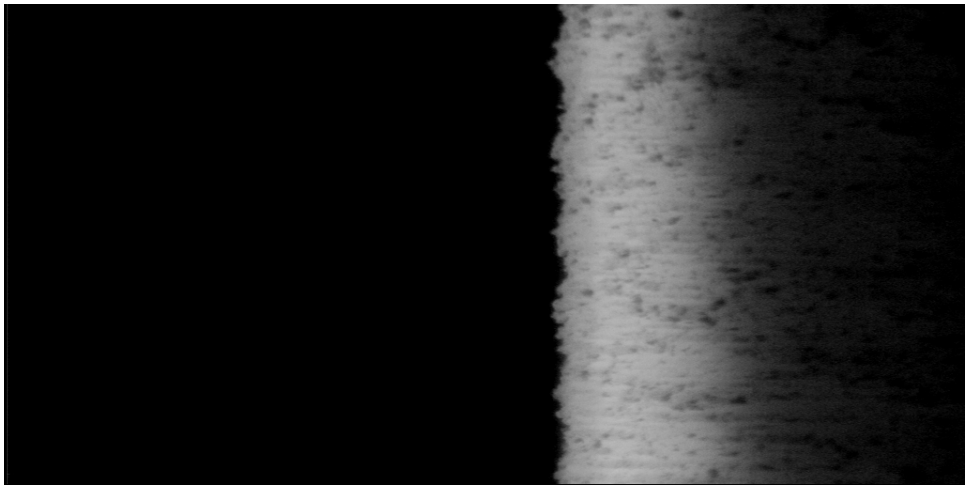

Test 15
Thin Residual

Figure 6.2.23b
Effect of regeneration pressure on Lanxide filter
Surface quality during long term test cycles
145 psi regeneration pressure, 5 cm/s face velocity, 20 min build-up time.

On comparison of all data obtained from all the test conditions the 120 psi and the 145 psi conditions have resulted in regeneration process that is more desirable. The 95 psi condition was not as satisfactory due to the chamber pressure build-up and due to the formation of residual ash. The 80 psi condition had repeated partial regeneration, which by itself is not desirable.

6.3 Effect of face velocity on the regeneration process

The filter was subjected to long term test cycles under three different face velocity values. The 5 cm/s face velocity with 95 psi regeneration pressure and 20 minute build-up time was the base condition. The effect of face velocity was studied by increasing (to 7 cm/s) and decreasing (3 cm/s), the face velocity value with respect to the base condition. The role of face velocity in the regeneration process was discussed in Chapter 2 and section 6.1.2. A lower face velocity is expected to build a thinner and weaker ash, while a higher face velocity is expected to build a thicker and stronger ash. The results obtained are discussed in this section**.**

6.3.1 Number of test cycles and reason for ending

The 3 cm/s and 5 cm/s conditions of face velocity resulted in a regeneration process that displayed repetitive regeneration. Both these conditions were stopped for this reason after 15 and 25 cycles respectively. The 7 cm/s condition resulted in formation of thick ash build up, which eventually failed to regenerate, and stopped on the 7^{th} cycle. A brief overview of results is presented in Table 6.3.1. Based on this observation, the 7

cm/s is not a desirable condition for surface regeneration. The 3 cm/s and the 5 cm/s conditions appear more desirable.

Face Velocity	Test Status	Number of cycles	Stopped due to	Ash Thickness in mm	Type of Regeneration	Crack initiation Time	Surface Quality
3cm/s face velocity	Begin	15	Repetitive Regeneration	0.7-1.05	Thin	0.1-0.13	clean
	During			0.35-0.35	Part Thick/Thin	0.117-0.13	patchy residuals
	End			0.35-0.525	Thin	0.15-0.117	some very thin patches
5cm/s face velocity	Begin	25	Repetitive Regeneration	0.7-1.05	Thin	0.1-0.13	clean
	During			0.35-0.35	Thin	0.117-0.13	patchy residuals
	End			0.35-0.525	Thin	0.117-0.15	more residual
7cm/s face velocity	Begin	7	**Stopped Regenerating**	1.75	Thick	0.2167	clean
	During			1.4	Thick	0.2-0.25	clean
	End			1.75	Thick	0.2833	big patches, stopped

Table 6.3.1.
Effect of face velocity
Comparative table of regeneration characteristics

`6.3.2 Increase of chamber pressure (P_c) during the build-up phase

The chamber pressure increases with more ash deposition on the surface of the filter. The chamber pressure increase for successive cycles was not significant for the 3 cm/s condition. For the 5 cm/s condition the increase was marginal especially when compared to the 7 cm/s condition. The 7 cm/s eventually failed to regenerate. The increase in residual ash can be attributed to the formation of thick ash cake due to high face velocity. These thick ash layers did not regenerate thoroughly and formed thick residual ash cake with successive cycles. In the 3 cm/s and 5 cm/s conditions the chamber pressure at the end of 15 cycles did not even cross 16 psia, while in the 7 cm/s condition

even during the first cycle the chamber pressure reached close to 18 psia and by the 7th cycle reached 19.5 psia. The graphs are shown in Figure 6.3.1, 6.3.2 and 6.3.3.

The 3 cm/s and the 5 cm/s displayed favorable surface regeneration characteristic as compared to the 7 cm/s condition.

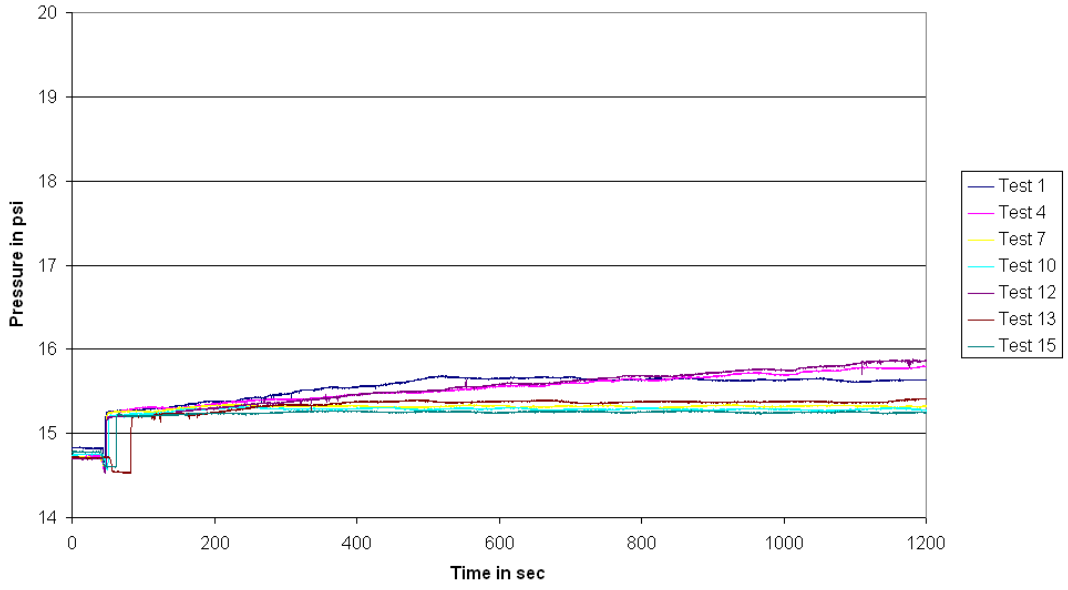

Figure 6.3.1.
Effect of face velocity - Lanxide filter
Comparative plot of chamber pressure increase during build-up
95 psi regeneration pressure, 3 cm/s face velocity, 20 minute build-up time

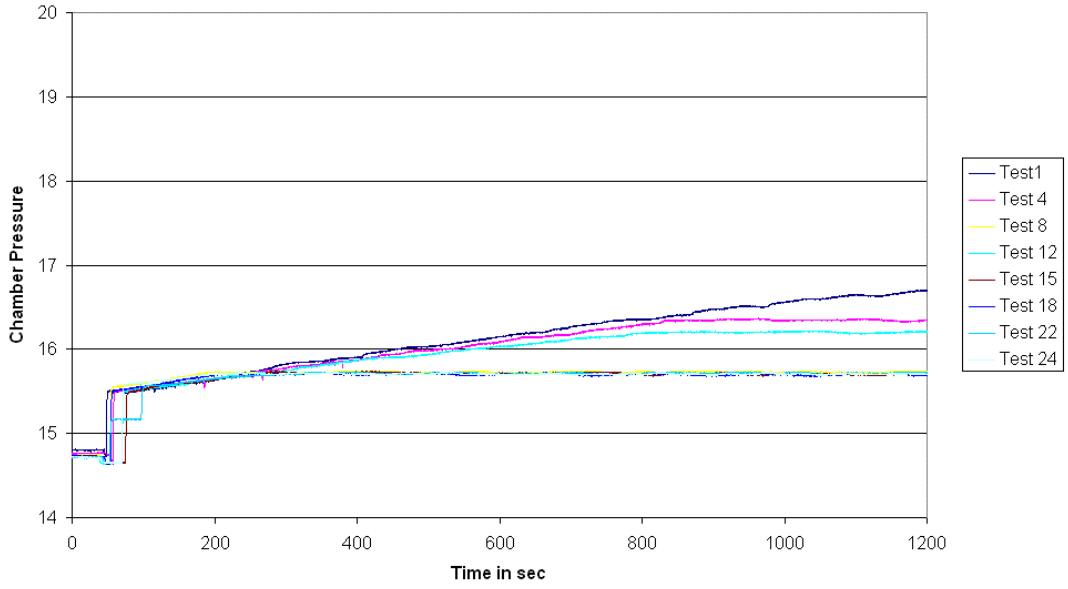

Figure 6.3.2.
Effect of face velocity - Lanxide filter
Comparative plot of chamber pressure increase during build-up
95 psi regeneration pressure, 5 cm/s face velocity, 20 minute build-up time

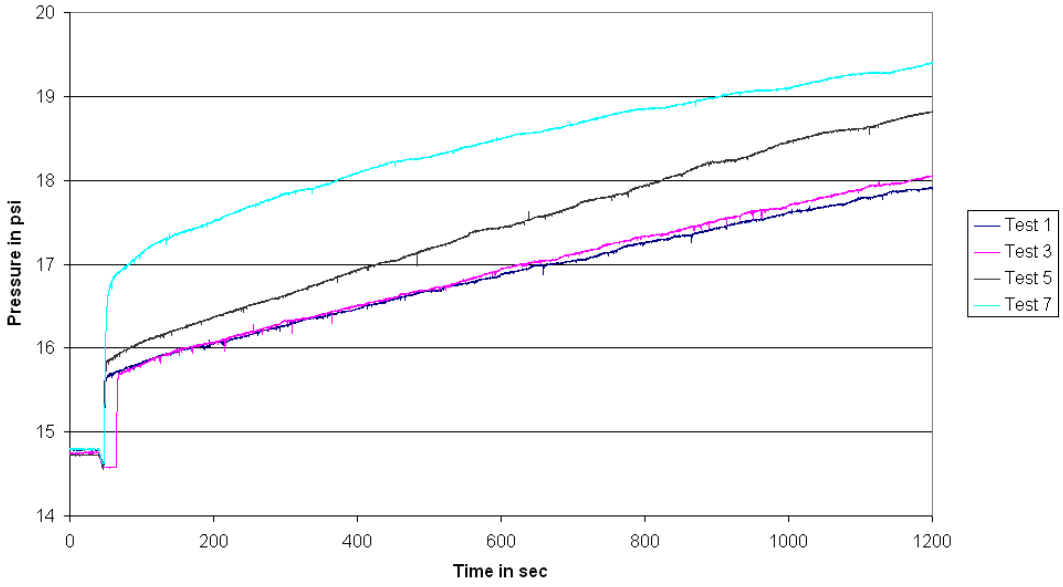

Figure 6.3.3.
Effect of face velocity - Lanxide filter
Comparative plot of chamber pressure increase during build-up
95 psi regeneration pressure, 7 cm/s face velocity, 20 minute build-up time

6.3.3 Pressure difference, ΔP (P_f-Pc), between filter (P_f) and chamber (Pc) during regeneration

In this section the effectiveness of the regeneration process is discussed through the results obtained from the pressure difference curves. The pressure difference profiles for 3 cm/s, 5 cm/s and 7 cm/s are shown in Figures 6.3.4 to 6.3.6. The associated tabular column giving the values of $\Delta P_{initial}$, ΔP_{final}, ΔP_{max}, ΔP_{min}, the efficiencies and the cleaning factors are presented. Then the influence of the tested parameter is discussed through the ΔP variables.

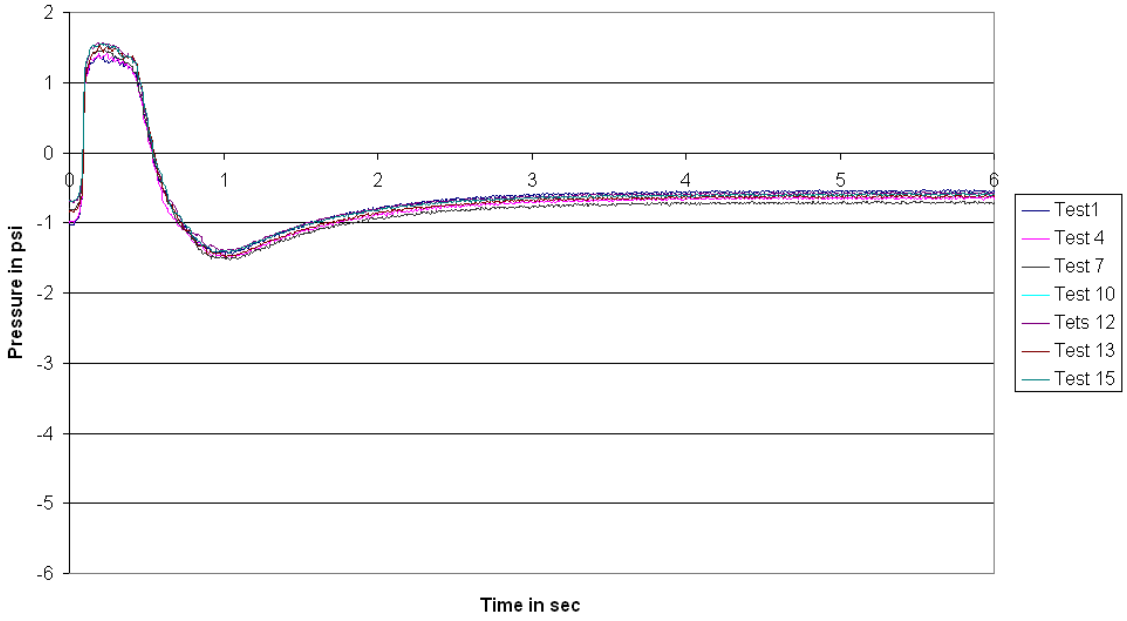

	Test1	Test 4	Test 7	Test 10	Test 13	Test 15
ΔP new (psi)	-0.22056	-0.22056	-0.22056	-0.22056	-0.22056	-0.22056
ΔP cleaned (psi)	-0.6566	-0.6566	-0.6566	-0.6566	-0.6566	-0.6566
ΔP initial @ t=0 (psi)	-1.0173	-1.0022	-0.7976	-0.69438	-0.84674	-0.67586
ΔP initial @ t=5 (psi)	-0.55108	-0.66936	-0.70636	-0.58726	-0.62566	-0.58584
Time @ ΔP max (sec)	0.19	0.24	0.23	0.19	0.2	0.21
ΔP max (psi)	1.38202	1.4101	1.4598	1.5658	1.52522	1.54842
Time @ ΔP min (sec)	1.01	1.03	1.04	1.02	1.02	1.04
ΔP min (psi)	-1.44754	-1.5061	-1.52576	-1.41558	-1.48598	-1.42296
Efficiency-clean	1.292542	0.963079	0.647092	2.835363	1.162722	4.673936
Efficiency-new	0.585163	0.425825	0.158119	0.22608	0.353064	0.197718
Factor-c	0.839293	1.019433	1.075784	0.894395	0.952878	0.892233
Factor-n	2.498496	3.034756	3.202507	2.66253	2.836628	2.656092

Figure 6.3.4.
Effect of face velocity - Lanxide filter
Comparative plot of pressure difference (ΔP: Pf-Pc) change during regeneration and corresponding analysis table for
95 psi regeneration pressure, 3 cm/s face velocity, 20 minute build-up time

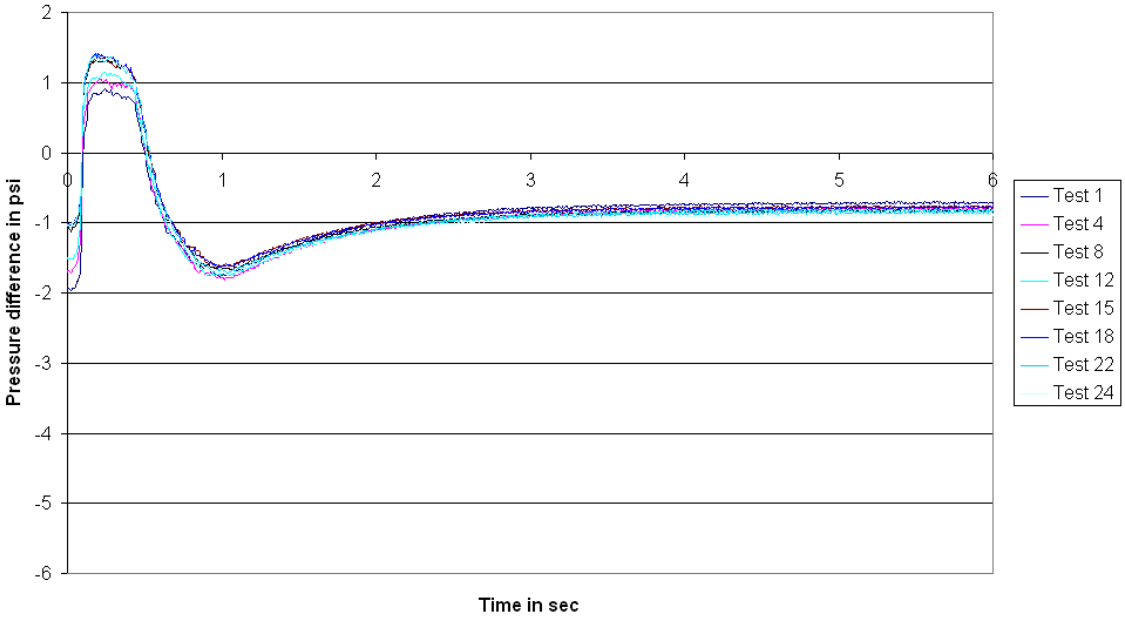

	Test 1	Test 4	Test 8	Test 12	Test 15	Test 18	Test 22	Test 24
ΔP new (psi)	-0.34978	-0.34978	-0.34978	-0.34978	-0.34978	-0.34978	-0.34978	-0.34978
ΔP cleaned (psi)	-0.78702	-0.78702	-0.78702	-0.78702	-0.78702	-0.78702	-0.78702	-0.78702
ΔP initial @ t=0 (psi)	-1.94848	-1.70232	-1.06656	-1.5146	-1.01064	-0.99012	-1.0259	-1.03348
ΔP initial @ t=5 (psi)	-0.7367	-0.81544	-0.82716	-0.82608	-0.77356	-0.77698	-0.84696	-0.899
Time @ ΔP max (sec)	0.24	0.22	0.24	0.24	0.2	0.2	0.19	0.26
ΔP max (psi)	0.90554	1.04566	1.35588	1.13994	1.35742	1.41752	1.40018	1.38776
Time @ ΔP min (sec)	0.98	1.02	1.05	1.04	0.97	0.99	1.04	1.03
ΔP min (psi)	-1.7665	-1.8096	-1.66952	-1.75564	-1.6275	-1.62946	-1.70752	-1.73794
Efficiency-clean	1.043325	0.96895	0.856407	0.946315	1.060191	1.049434	0.749079	0.545646
Efficiency-new	0.757979	0.655715	0.333994	0.591096	0.358745	0.332855	0.264657	0.196695
Factor-c	0.936063	1.036111	1.051003	1.04963	0.982898	0.987243	1.076161	2.570185
Factor-n	2.106179	2.331292	2.364798	2.361711	2.211559	2.221337	2.421405	1.142284

Figure 6.3.5.
Effect of face velocity - Lanxide filter
Comparative plot of pressure difference (ΔP: Pf-Pc) change during regeneration and corresponding analysis table for
95 psi regeneration pressure, 5 cm/s face velocity, 20 minute build-up time

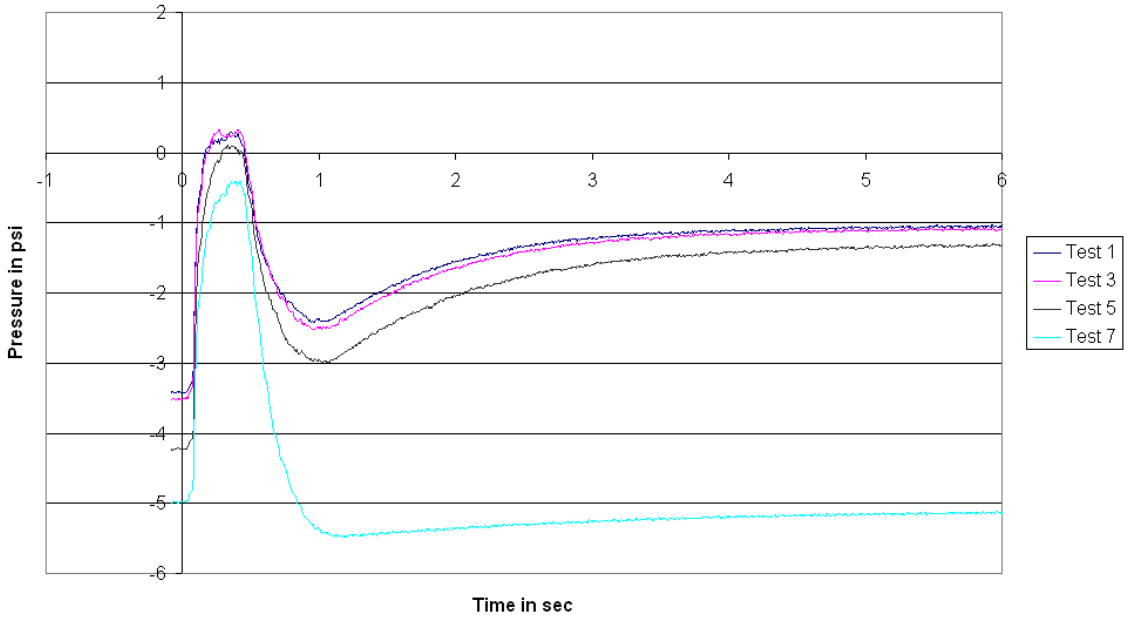

	Test 1	Test 3	Test 5	Test 7
ΔP new (psi)	-0.479	-0.479	-0.479	-0.479
ΔP cleaned (psi)	-1.10834	-1.10834	-1.10834	-1.10834
ΔP initial @ t=0 (psi)	-3.4155	-3.51778	-4.2306	-4.9797
ΔP initial @ t=5 (psi)	-1.0662	-1.10472	-1.349	-5.16658
Time @ ΔP max (sec)	0.36	0.27	0.33	0.38
ΔP max (psi)	0.28526	0.32782	0.11428	-0.41346
Time @ ΔP min (sec)	0.96	0.95	1.05	1.17
ΔP min (psi)	-2.42318	-2.52008	-2.99	-5.48268
Efficiency-clean	1.018265	1.001502	0.922921	-0.04827
Efficiency-new	0.800033	0.794087	0.768098	-0.04152
Factor-c	0.961979	0.996734	1.217136	4.661548
Factor-n	2.225906	2.306324	2.816307	10.78627

Figure 6.3.6.
Effect of face velocity - Lanxide filter
Comparative plot of pressure difference (ΔP: Pf-Pc) change during regeneration and corresponding analysis table for
95 psi regeneration pressure, 7 cm/s face velocity, 20 minute build-up time

a. $\Delta P_{initial}$

The ΔP-initial value is low and remains less than 1 psi in magnitude for the 3 cm/s condition. The 5 cm/s condition starts close to -2 psi and fluctuates between -2 psi and -1 psi. The 7 cm/s starts close to -3.5 psi even in the first cycle. This can be attributed to the large face velocity fluidizing and depositing a lot of ash. The chamber pressure is also increased due to the combined effect of more flow into the chamber and more resistance to flow out through the filter. The initial pressure drop increases further till the 7th cycle. The filter did not regenerate on the 7th cycle. The increased initial pressure indicates increased resistance to the regeneration pulse.

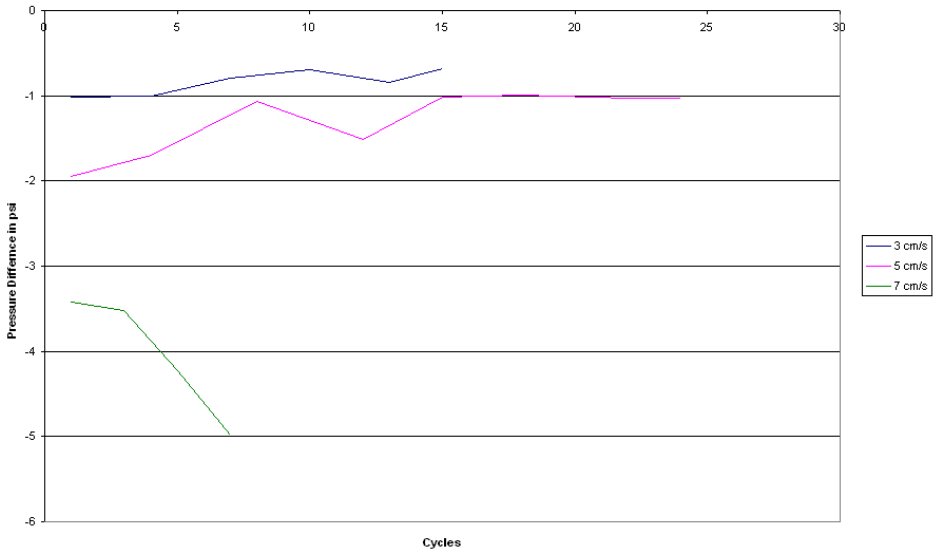

Figure 6.3.7.
Effect of face velocity
Lanxide filter - long term tests
Comparative plot of initial pressure difference ($\Delta P_{initial}$)

b. ΔP_{final}

The ΔP_{final} value is an indicator of how effective the cleaning is after the regeneration. If the pressure drop is consistent then it indicates repetitive cleaning which results in a filter with the same amount of residual ash. A lower magnitude indicates a lesser residual ash. If the magnitude of pressure drop starts to increase then it indicates ineffective cleaning. The 3 cm/s and 5 cm/s show consistent low values (less than 1psi drop). The 5 cm/s has a more pressure drop because of greater ash loading and larger flow rate. The 7 cm/s initially has a pressure drop of -1 psi which gradually increases to nearly -5 psi. The 7cm/s test conditions are characterized with large residual ash deposits.

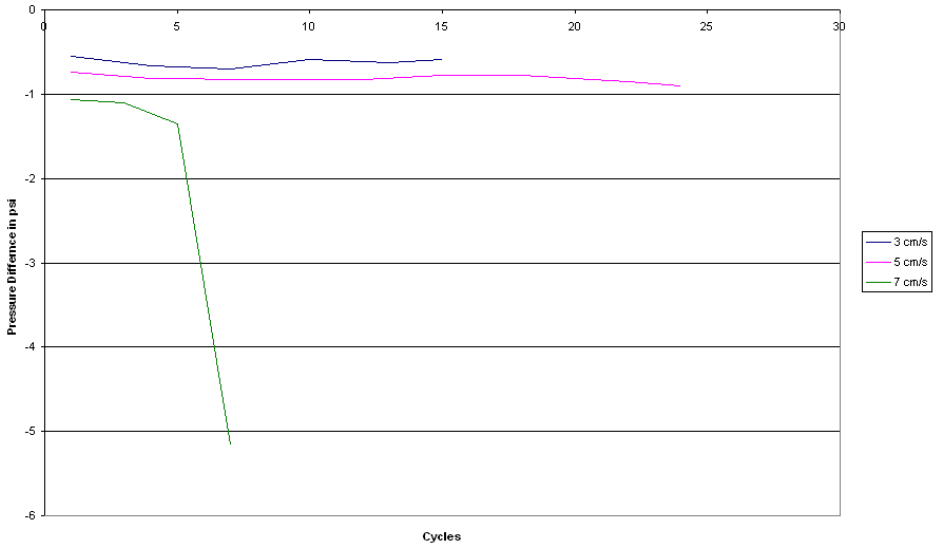

Figure 6.3.8.
Effect of face velocity
Lanxide filter - long term tests
Comparative plot of final pressure difference (ΔP_{final})

c. ΔP_{max}

Higher ΔP_{max} indicates that the regeneration pulse is able to overcome the resistance easily. If the regeneration pulse is not sufficient to overcome the ash and flow resistance then the maximum pressure drop is negative. That is the pressure inside the filter is not sufficiently high to cause a flow from the filter to the chamber. The 3 cm/s and the 5 cm/s have been found to have consistent positive ΔP-max values. In the 7 cm/s tests the value is found to start at a low value and keeps decreasing till it becomes negative in its 7th cycle when the filter failed to regenerate.

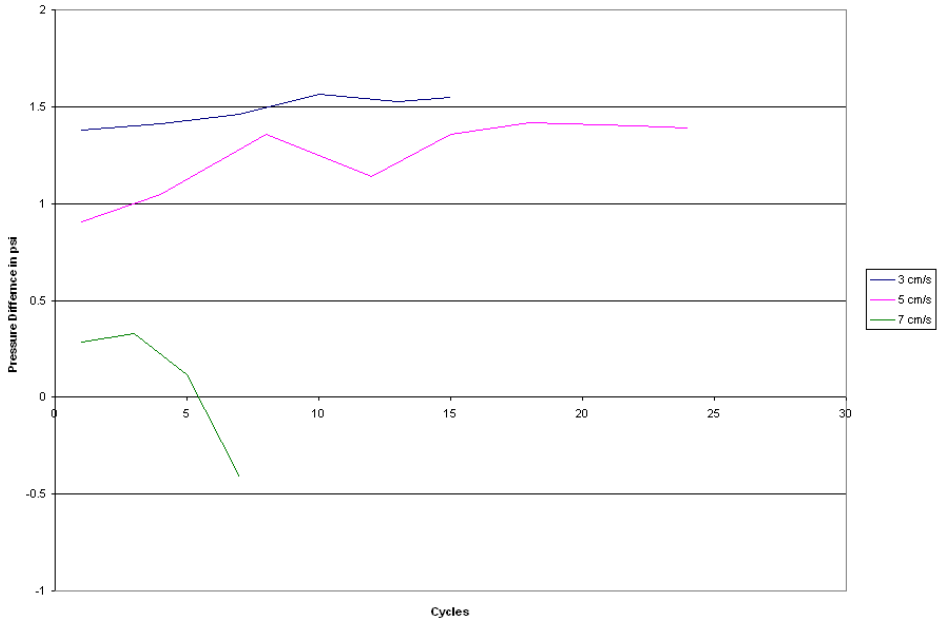

Figure 6.3.9.
Effect of face velocity
Lanxide filter - long term tests
Comparative plot of maximum pressure difference (ΔP_{max})

d. ΔP_{min}

The ΔP_{min} values are significant as this has a direct relation with the re-entrainment flow. If this magnitude is large then it means a larger pressure drop for flow from chamber to filter during the transient period. This value is low and consistent for the 3 cm/s and the 5 cm/s conditions. The magnitude in the 7cm/s the value keeps increasing. The ΔP-minimum values seem to have a direct relation with the values of the ΔP-final values, which in turn is directly related with insufficient ash removal. With the flow area reduced the chances for higher re-entrainment velocities and flow rates are possible, especially in areas that have regenerated (clean spots).

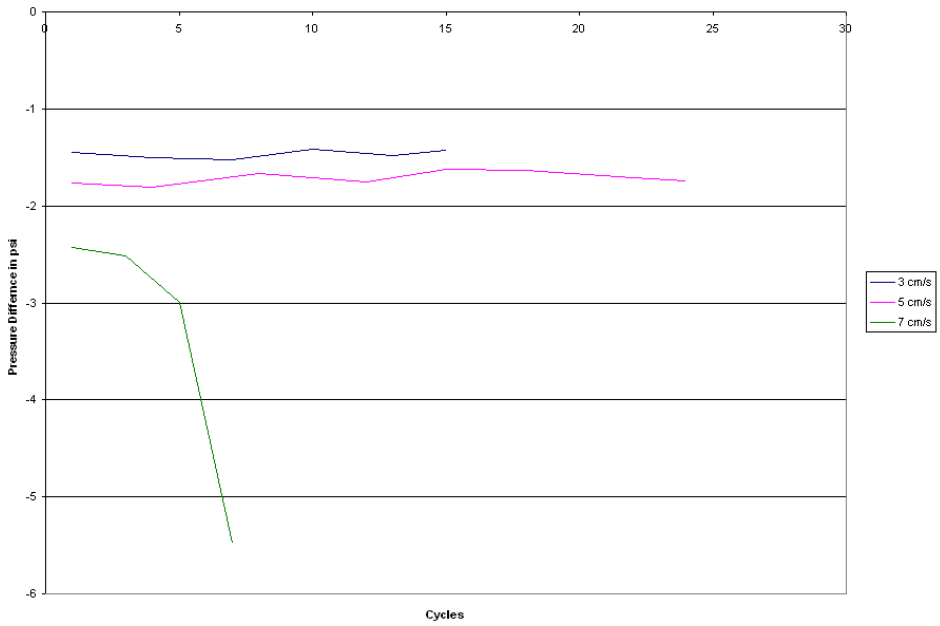

Figure 6.3.10.
Effect of face velocity
Lanxide filter - long term tests
Comparative plot of minimum pressure difference (ΔP_{min})

e. Efficiency η:

The regeneration in 3cm/s and the 5 cm/s were of the thin type regeneration. The 7cm/s condition was thick type regeneration. In this method of efficiency calculation thick ash regeneration will have higher value because of higher initial pressure drop, since this efficiency is an indicator of the amount of resistance overcome. The 7cm/s condition builds residual ash and fails to regenerate. The corresponding test efficiency is negative. The η_N values are decreasing for all cases, but the η_C values are increasing for 3cm/s, stable for 5 cm/s and decreasing for 7 cm/s.

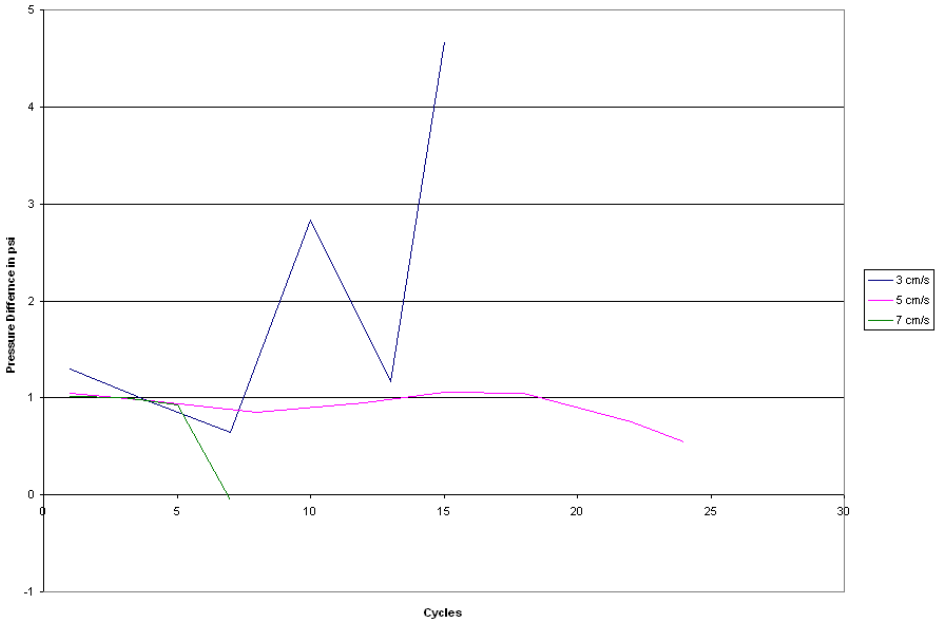

Figure 6.3.11.
Effect of face velocity
Lanxide filter - long term tests
Comparative plot of efficiency based on ΔP_C (η_C)

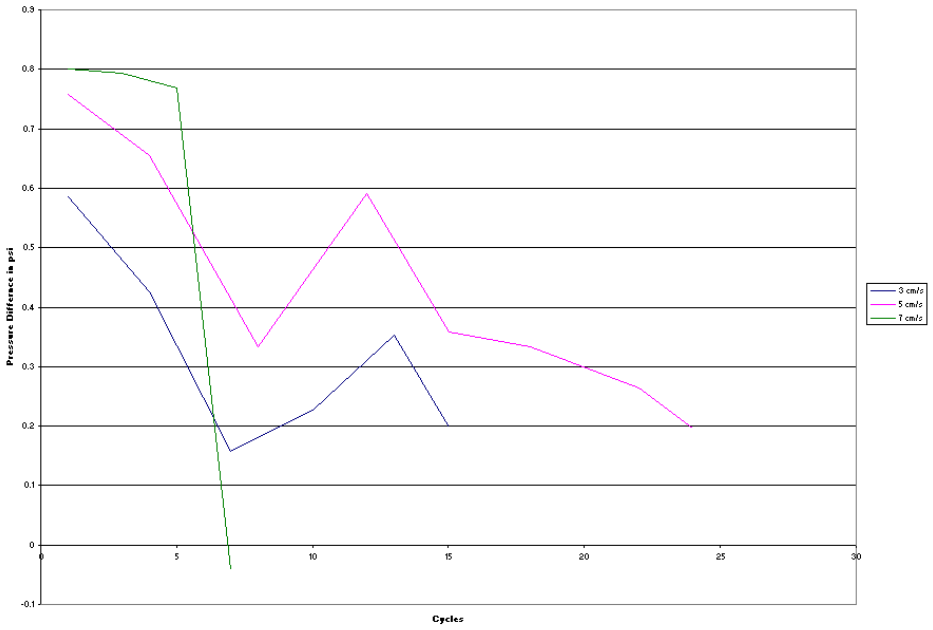

Figure 6.3.12.
Effect of face velocity
Lanxide filter - long term tests
Comparative plot of efficiency based on ΔP_N (η_N)

f. Cleaning Factor F:

The cleaning factor F indicates how clean the filter is with every testing cycle and indicates how much residual ash is collecting on the filter. The F_N (cleaning factor when measured with respect to a new filter) and the F_C (cleaning factor when measured with respect to a cleaned filter) are plotted for all the conditions. It is noted from the plot that the factor increases for the 7cm/s condition, while it is stable for the other two conditions. This increase indicates insufficient cleaning and increasing residual pressure drop.

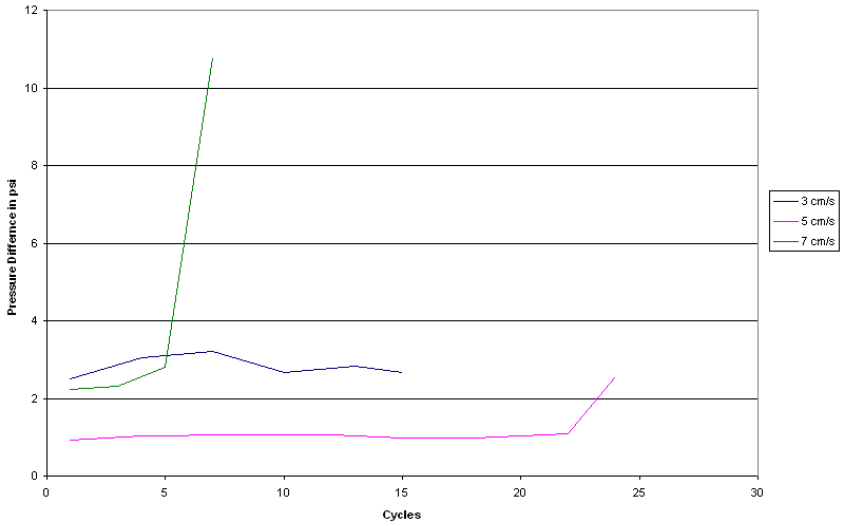

Figure 6.3.13.
Effect of face velocity
Lanxide filter - long term tests
Comparative plot of cleaning factor based on ΔP_C (F_C)

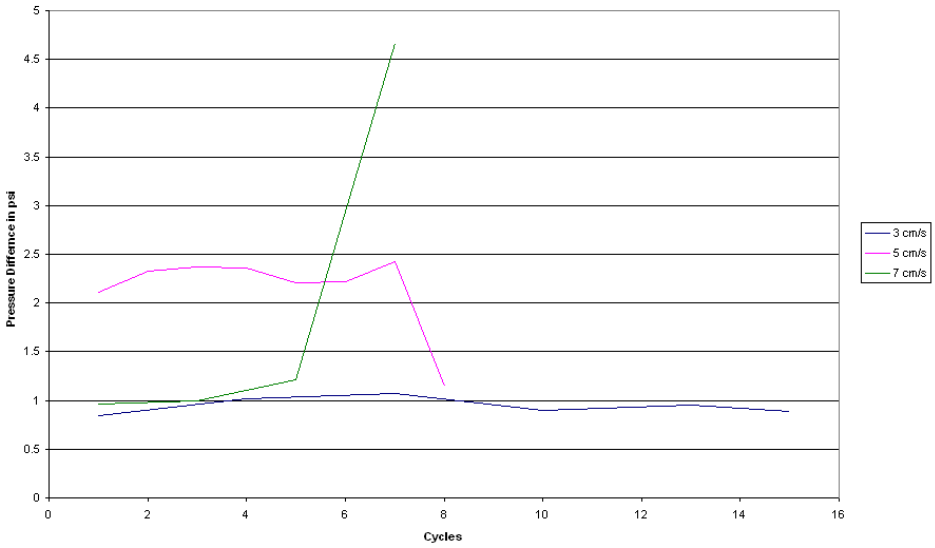

Figure 6.3.14.
Effect of face velocity
Lanxide filter - long term tests
Comparative plot of cleaning factor based on ΔP_N (F_N)

6.3.4 Distribution of particles less than 100 microns during regeneration

The particle count for size less than 100 microns for the 3 cm/s case is higher when compared to the other two conditions. The next highest is the 5 cm/s case followed by the 7 cm/s condition. The amount of small particles being higher is not a desirable property. The larger number of particles for the 3cm/s and the 5 cm/s conditions may be attributed to the formation of thin ash that results in thin ash regeneration. The 7 cm/s condition results in thick ash failure and therefore the number of small particle is lower.

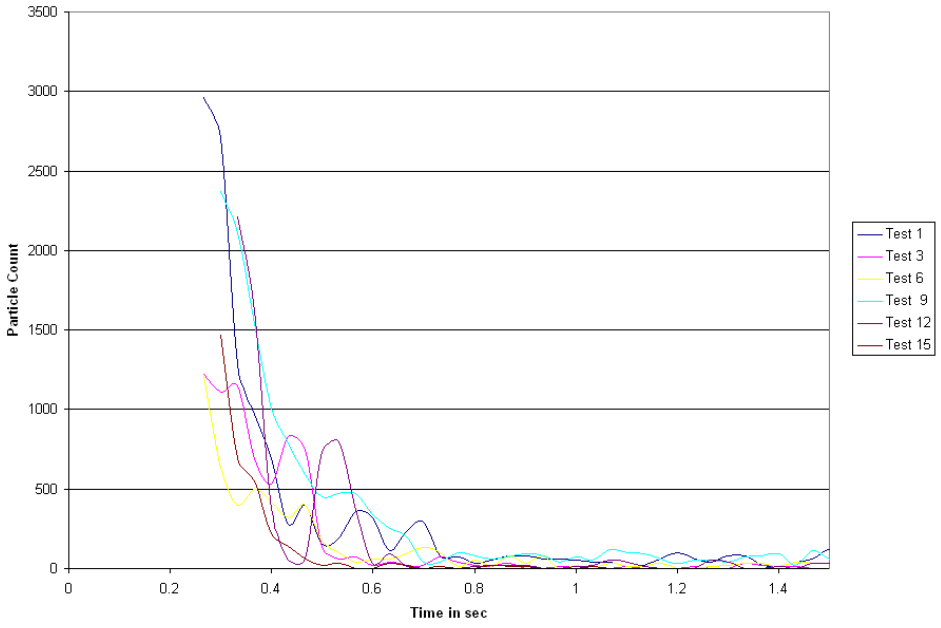

Figure 6.3.15.
Effect of face velocity on Lanxide filter - long term tests
Particle count: less than 100 microns
95 psi regeneration pressure, 3 cm/s face velocity, 20 min build-up time

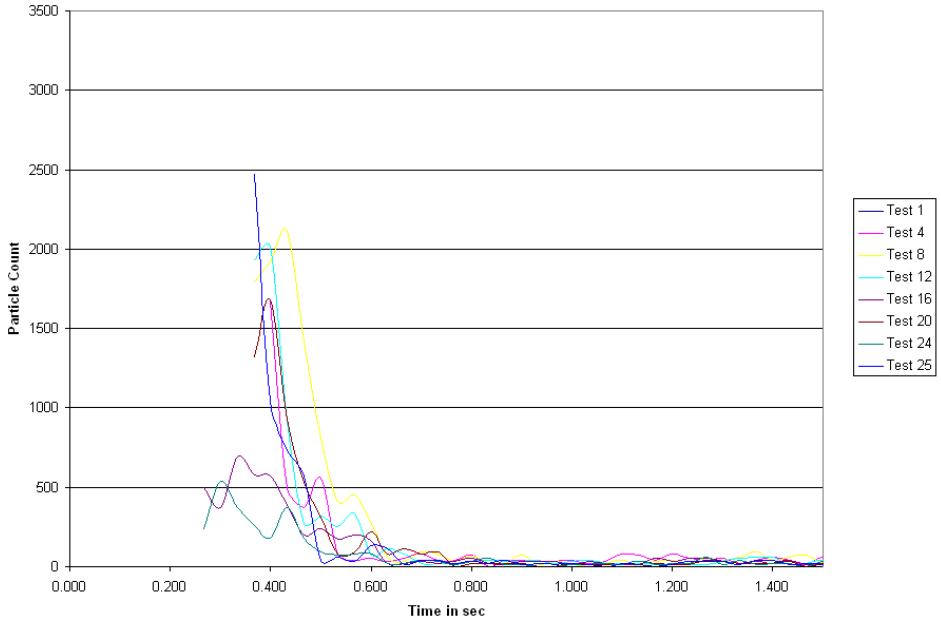

Figure 6.3.16.
Effect of face velocity on Lanxide filter - long term tests
Particle count: less than 100 microns
95 psi regeneration pressure, 5 cm/s face velocity, 20 min build-up time

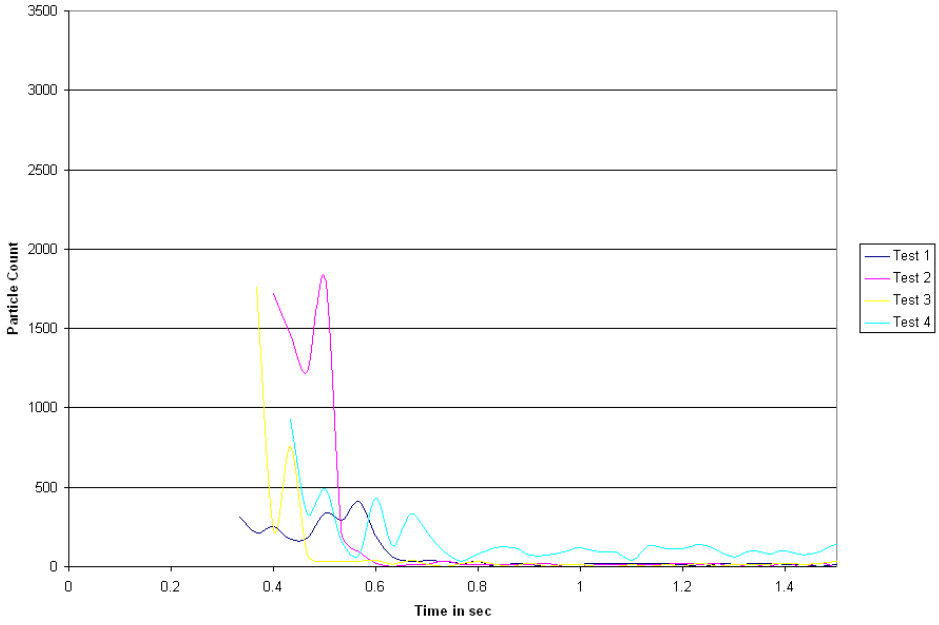

Figure 6.3.17.
Effect of face velocity on Lanxide filter - long term tests
Particle count: less than 100 microns
95 psi regeneration pressure, 7 cm/s face velocity, 20 min build-up time

6.3.5 The thickness of ash deposit during build-up

The face velocity influences in the ash formation. For lower face velocities 3 cm/s and 5 cm/s the ash formation is thin while for the 7 cm/s condition the ash formation is thick. More ash is fluidized due to higher face velocity in the 7 cm/s condition, resulting in thicker deposition. (ref. Table 6.3.1)

6.3.6 The type of regeneration

The type of regeneration is dependent on the thickness of the ash deposit. Due to the nature of ash deposition for the 3 cm/s and the 5 cm/s conditions, they exhibited thin type regeneration with ash regenerating as tiny particles. The 7 cm/s condition resulted in thick type regeneration, with ash regenerating as large pieces.(ref. Table 6.3.1)

6.3.7 Crack initiation time

A longer crack initiation time indicates that the ash resists the regeneration pulse and the pressure inside the filter builds up for a longer time to dislodge the ash cake. The crack initiation time is low for the 3 cm/s and the 5 cm/s condition. It is considerably longer for the 7 cm/s condition. The ash cake resistance is larger for this face velocity.

6.3.8 Surface Quality:

The 3 cm/s and the 5 cm/s condition resulted in predominantly thin ash cake and thin regeneration. The ash on the surface after repeated cycles of regeneration was observed to be thin patchy residuals. There was more residual ash in the 5 cm/s face velocity tests as compared to the 3 cm/s test. The 7 cm/s condition resulted in thick ash cakes, which after sometime became strong enough that there was thick patches that did not regenerate. The increasing residual ash growth is evident from increasing crack initiation time, large $\Delta P_{final,}$, and high cleaning factors

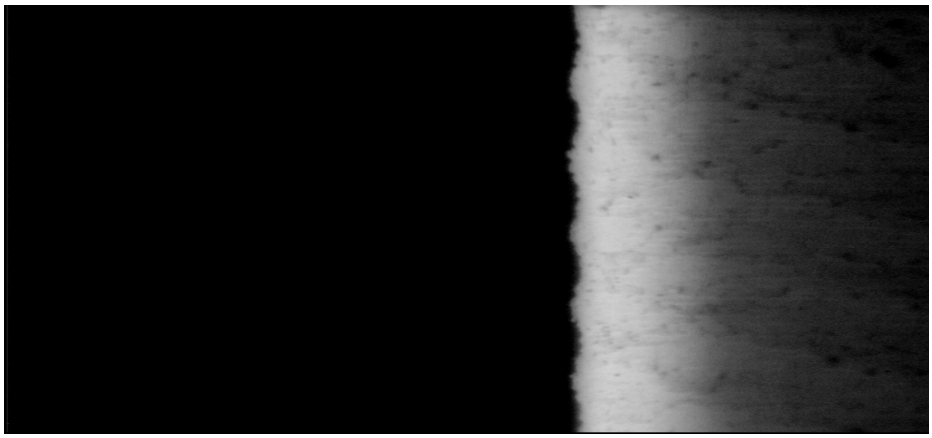

Test 1
Clean Filter

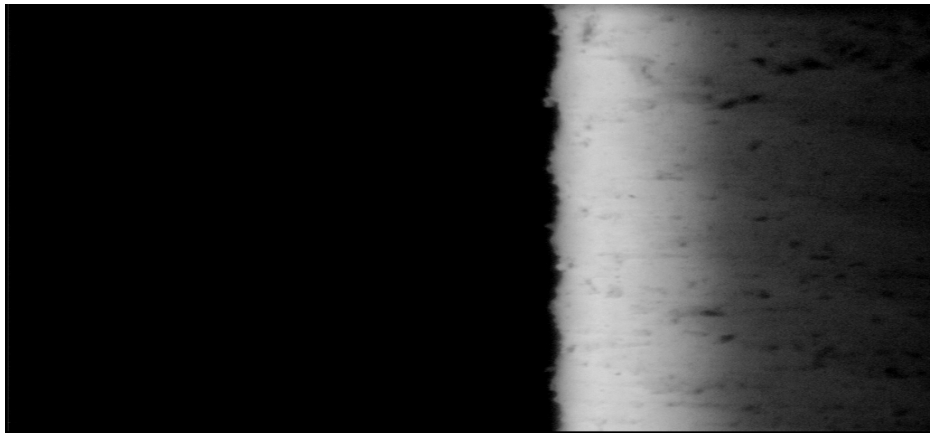

Test 3
Ash on Ridges

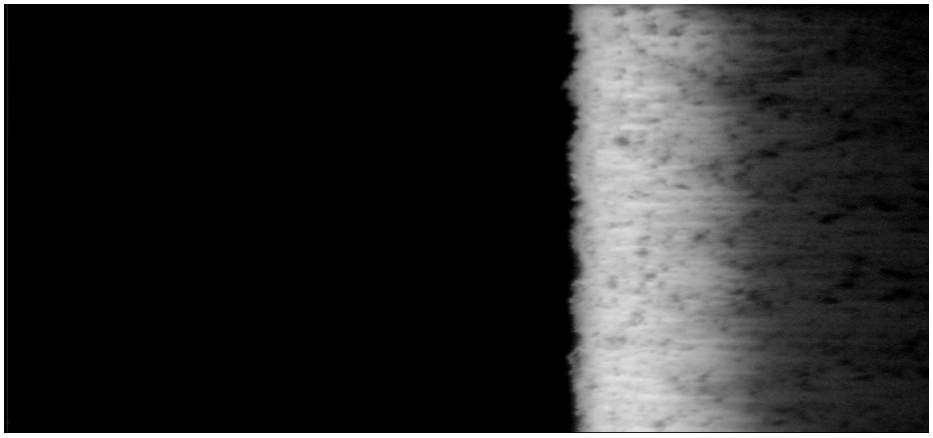

Test 6
Some Residual
Ash

Figure 6.3.18a
Effect of face velocity on Lanxide filter
Surface quality during long term test cycles
95 psi regeneration pressure, 3 cm/s face velocity, 20 min build-up time. (Contd.)

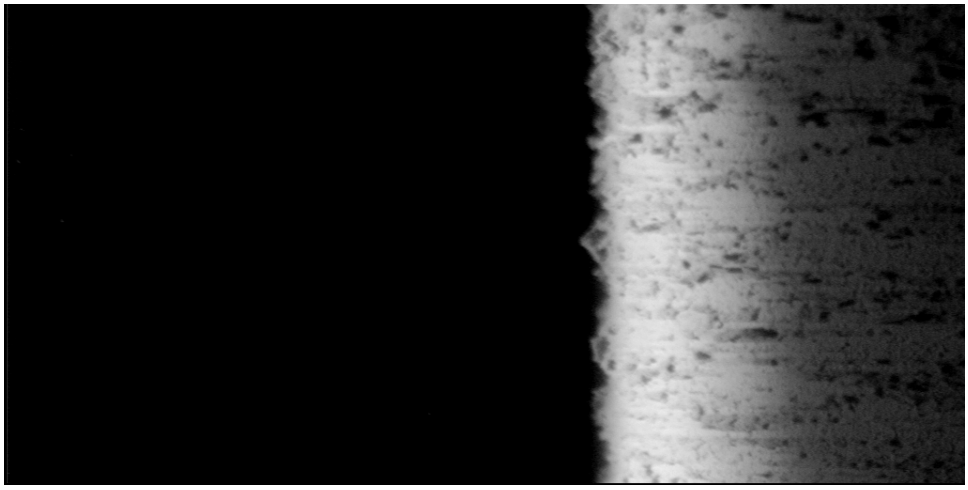

Test 9
More Residual
Ash

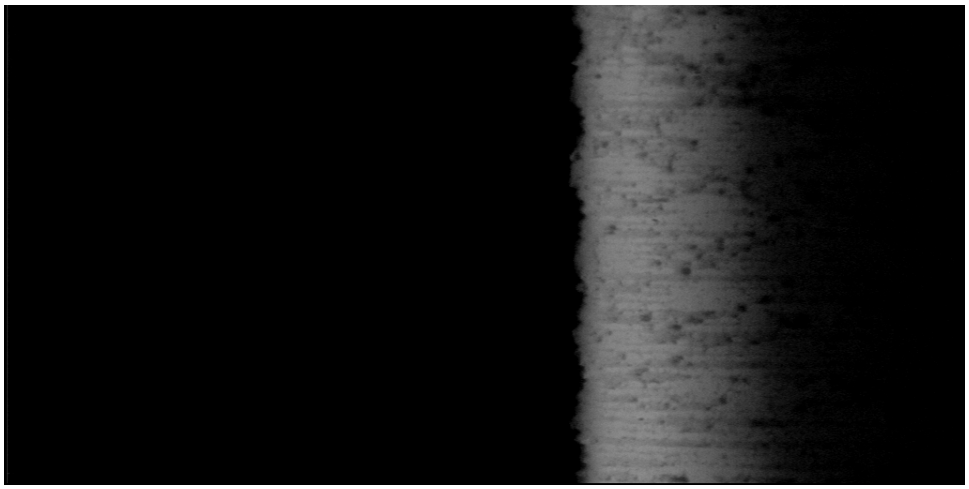

Test 15
More Ash

Figure 6.3.18b
Effect of face velocity on Lanxide filter
Surface quality during long term test cycles
95 psi regeneration pressure, 3 cm/s face velocity, 20 min build-up time.

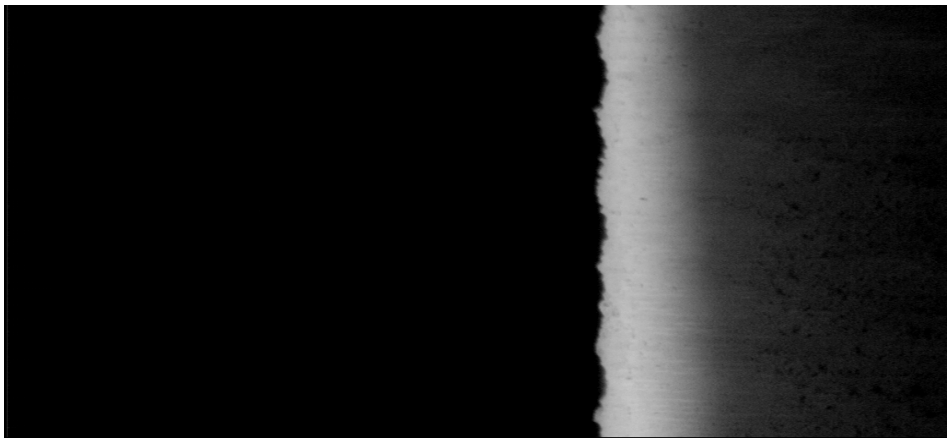

Test 1
Clean Filter

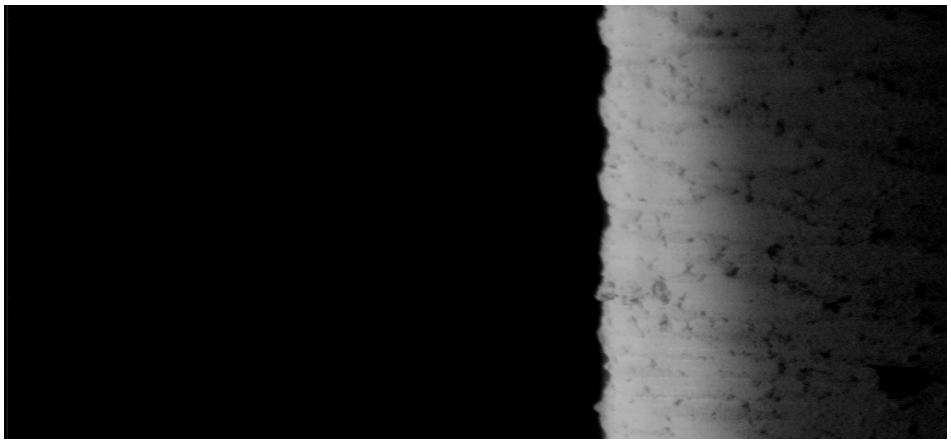

Test 4
Little
Residual

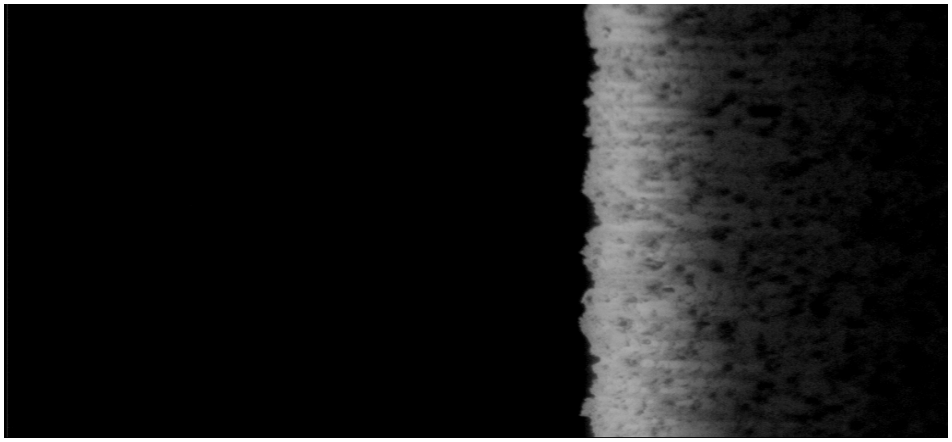

Test 8
Residual ash
typical of thin
ash

Figure 6.3.19a
Effect of face velocity on Lanxide filter
Surface quality during long term test cycles
95 psi regeneration pressure, 5 cm/s face velocity, 20 min build-up time. (Contd.)

Test 16
More thin
ash type

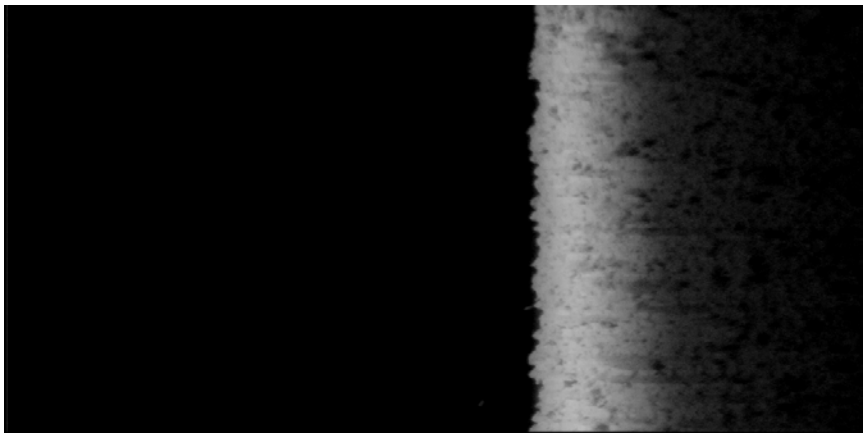

Test 20
Dirty Filter

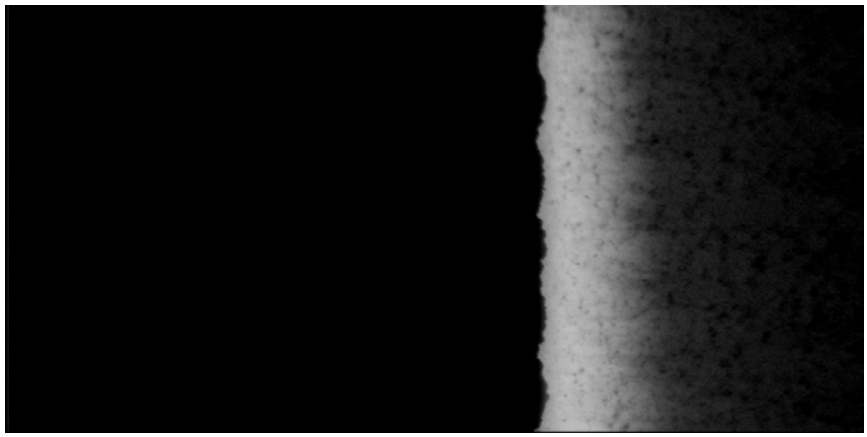

Test 25
Dirty Filter

Figure 6.3.19b
Effect of face velocity on Lanxide filter
Surface quality during long term test cycles
95 psi regeneration pressure, 5 cm/s face velocity, 20 min build-up time.

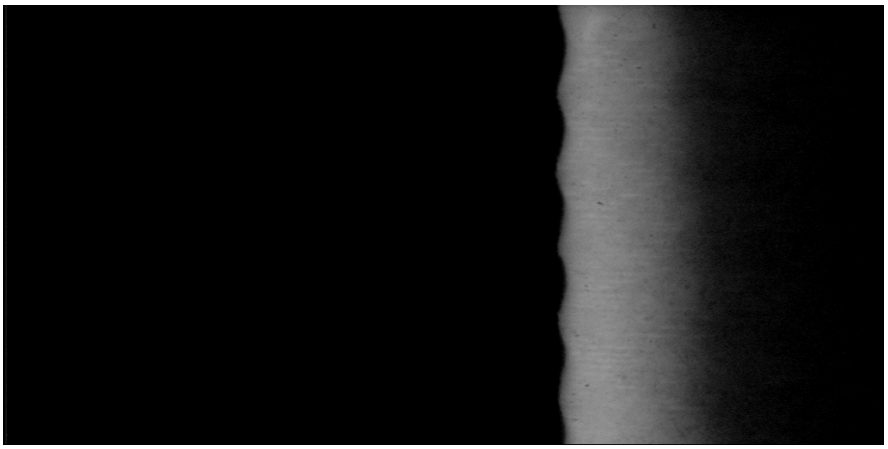

Test 1
Clean Filter

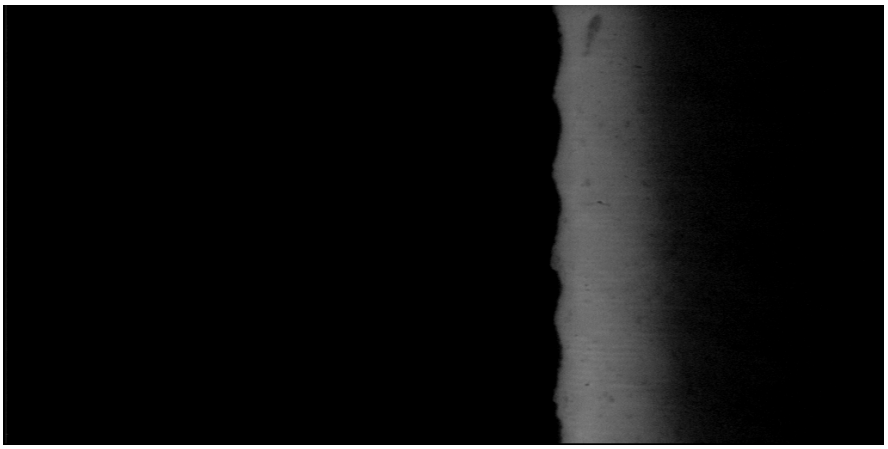

Test 3
Some Residual

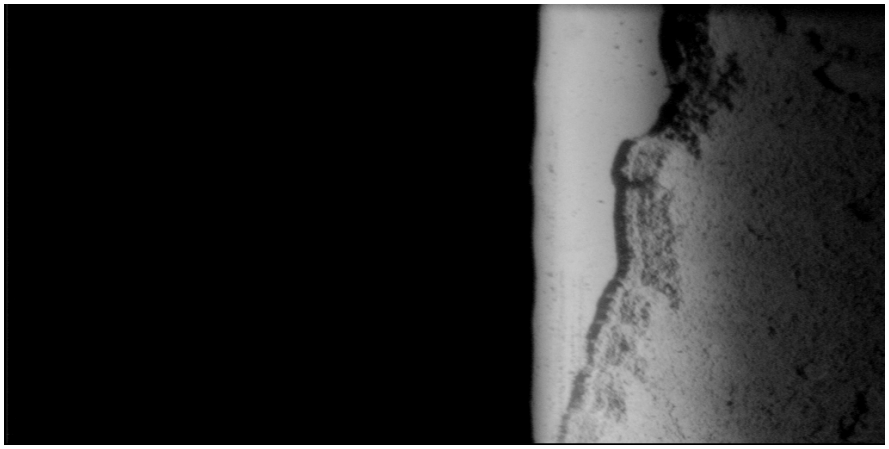

Test 4
Thick Residual
Layer

Figure 6.3.20a
Effect of face velocity on Lanxide filter
Surface quality during long term test cycles
95 psi regeneration pressure, 7 cm/s face velocity, 20 min build-up time. (Contd.)

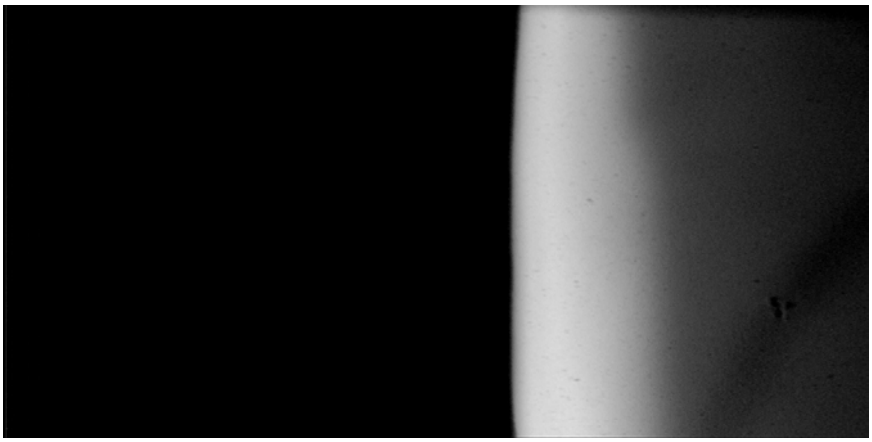

A

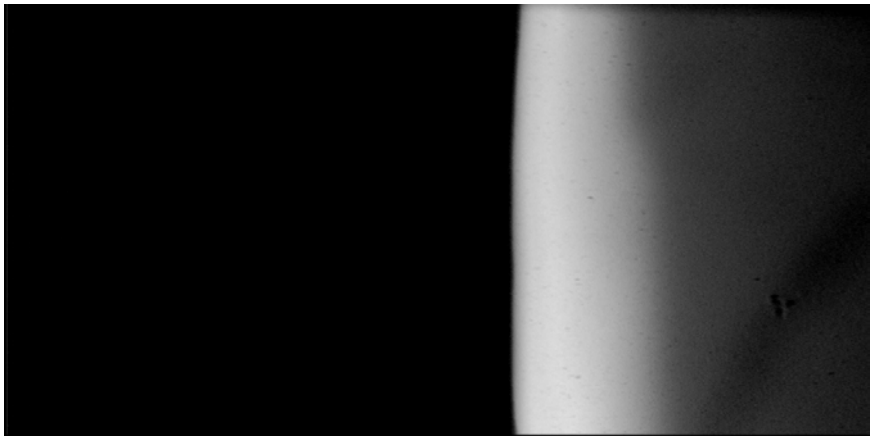

B

Test 6, No regeneration observed when comparing the images
A at 0.0 sec and B at 1.5 sec

Figure 6.3.20b
Effect of face velocity on Lanxide filter
Surface quality during long term test cycles
95 psi regeneration pressure, 7 cm/s face velocity, 20 min build-up time.

On comparison of all data obtained from all the test conditions the 7 cm/s condition is not desirable as it caused the failure of regeneration process. The other two conditions relatively seem to be better. But they result in thin ash cake formation and thin ash regeneration. This type of ash formation and regeneration is associated with larger small particles. This is also not desirable, especially at higher temperatures when sintering occurs.

6.3 Effect of build-up time on the regeneration process

Build-up time is the duration of the filtration time and the longer the build-up time more ash will be deposited on the candle filter. All parameters, except build-up time were kept a constant, i.e. the face velocity was 5 cm/s and the regeneration pressure was 95 psi. 20 minute build-up time with 95 psi regeneration pressure and 5 cm/s face velocity was the base condition. The effect of build-up time was studied by choosing one shorter duration (10 min) and two longer build-up duration (45 min and 90 min), as the parameter values. All other conditions remaining the same, a shorter duration build-up time will not build a thicker ash when compared to a longer duration build-up time.

6.4.1 Number of test cycles and reason for ending

The 10 min and the 20 min build-up time conditions of build-up time were stopped after the resultant regeneration process regenerated repetitively. Both these conditions were stopped after 15 and 25 cycles respectively. The 45 min and the 90 min built thick ash. In 45 min case, the filter had thick ash regeneration for the first test. In the second, third and fourth tests the top portion of the filter did not regenerate, while the

bottom half kept regenerating. Finally in the fifth cycle it totally stopped regenerating totally. For the 90 min build-up time the ash build-up was thick even in its first cycle and it failed to regenerate even in its first cycle.

Buildup Time	Test Status	Number of cycles	Stopped due to	Ash Thickness in mm	Type of Regeneration	Crack initiation Time	Surface Quality
10	Begin	15	Repetitive Regeneration	0.7-1.05	Thin	0.117	clean
	During			0.525-0.05	Thick/Thin	0.117-0.15	patchy residuals
	End			0.7-1.05	Thick/Thin	0.15-0.167	residual ash
20	Begin	25	Repetitive Regeneration	0.7-1.05	Thin	0.1-0.13	clean
	During			0.35-0.35	Thin	0.117-0.13	patchy residuals
	End			0.35-0.525	Thin	0.117-0.15	more residual
45	Begin	5	**Stopped Regenerating**	2.5	Thick	0.117	
	During						*Didn't regen. On top*
	End						Stopped Regenerating
90	Begin	1	**Stopped Regenerating**				
	During						*Didn't Regenerate*
	End						

Table 6.4.1.
Effect of build-up time
Comparative table of regeneration characteristics

6.4.2 Increase of chamber pressure (P_c) during the build-up phase

The chamber pressure did not increase significantly for the 10 min and the 20 min build-up conditions. The chamber pressure build-up for successive cycles for the 45 min build-up condition was large. Similarly the chamber pressure built up to nearly 22 psi even in the first cycle for 90 min build-up time.

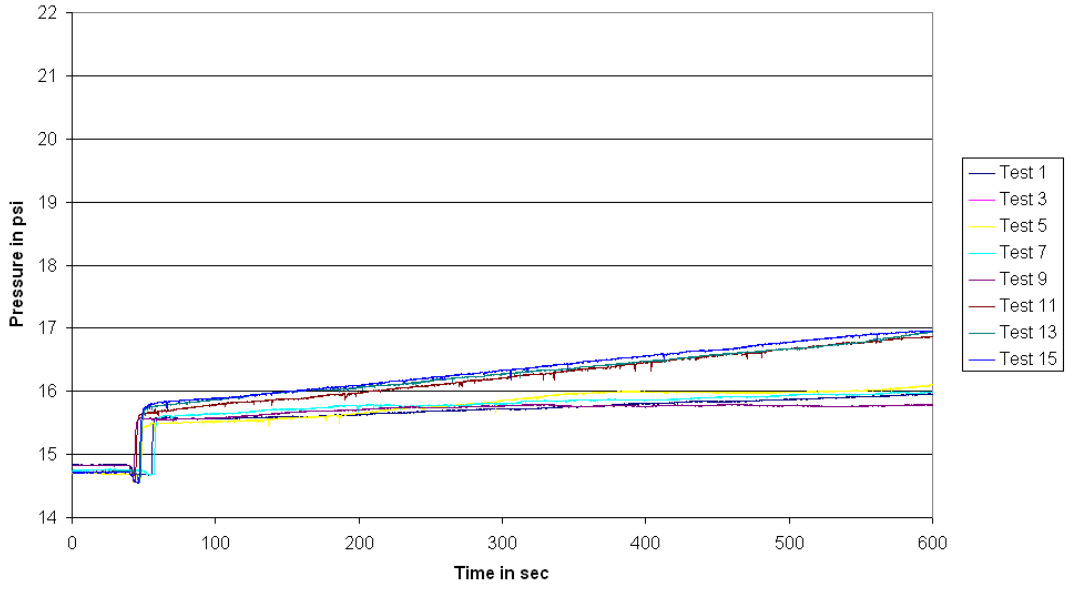

Figure 6.4.1
Effect of build-up time - Lanxide filter
Comparative plot of chamber pressure increase during build-up
95 psi regeneration pressure, 5 cm/s face velocity, 10 minute build-up time

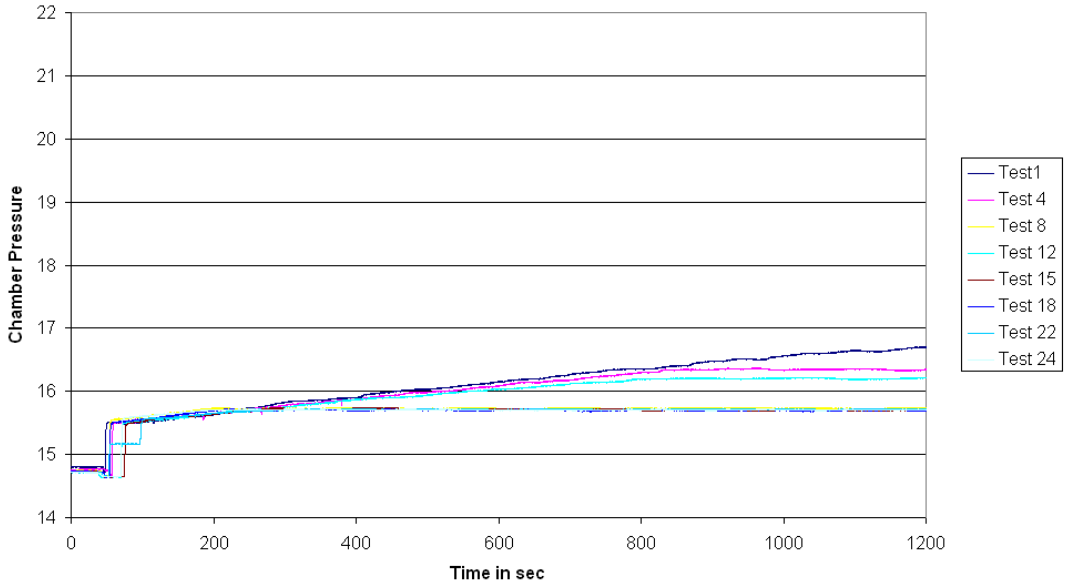

Figure 6.4.2
Effect of build-up time - Lanxide filter
Comparative plot of chamber pressure increase during build-up
95 psi regeneration pressure, 5 cm/s face velocity, 20 minute build-up time

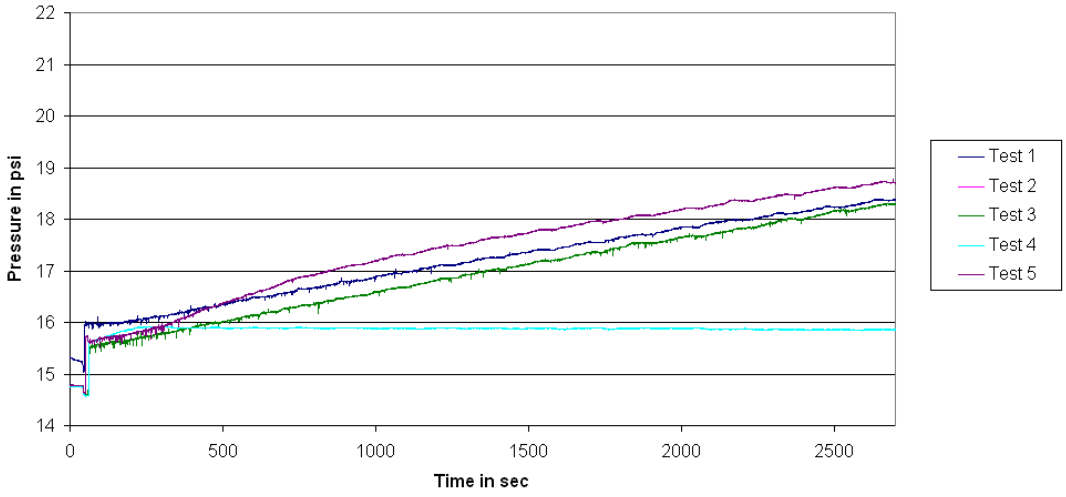

Figure 6.4.3
Effect of build-up time - Lanxide filter
Comparative plot of chamber pressure increase during build-up
95 psi regeneration pressure, 5 cm/s face velocity, 45 minute build-up time

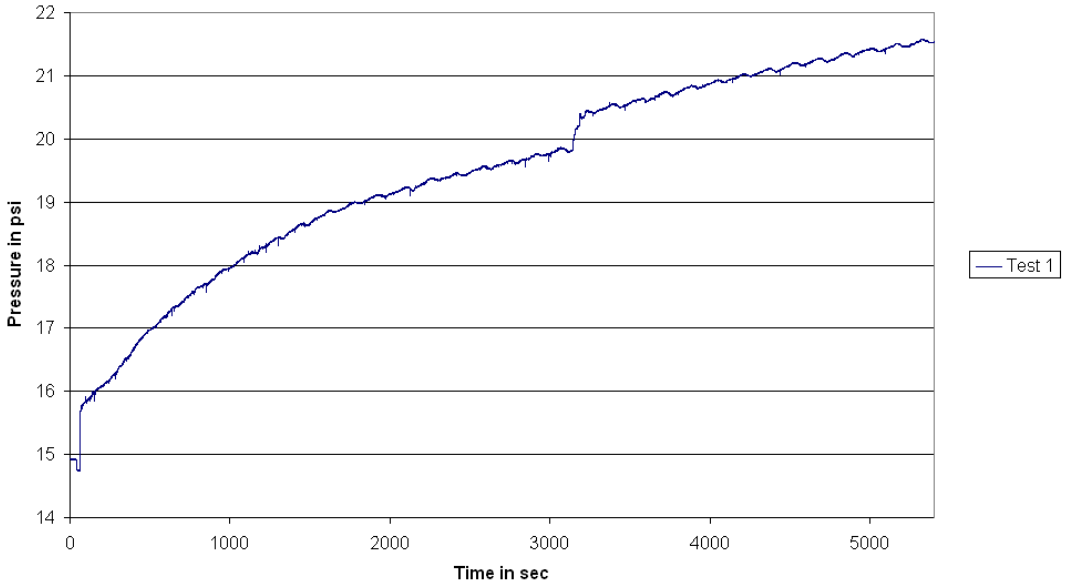

Figure 6.4.4
Effect of build-up time - Lanxide filter
Comparative plot of chamber pressure increase during build-up
95 psi regeneration pressure, 5 cm/s face velocity, 90 minute build-up time

6.4.3 Pressure difference, ΔP (P_f-Pc), between filter (P_f) and chamber(Pc) during regeneration

The analysis of the pressure drop, ΔP, across the filter, helps to determine the effectiveness of the regeneration process. The ΔP profiles, of the long term tests performed to study the effect of build-up time are discussed here. The pressure difference profiles for 10 min, 20 min, 45 min and 90 min build-up time are shown in Figures 6.4.5 to 6.4.8. In Table 6.4.1., the values of $\Delta P_{initial}$, ΔP_{final}, ΔP_{max}, ΔP_{min}, the efficiencies and the cleaning factors are presented. Then the influence of the tested parameter is discussed through the ΔP variables.

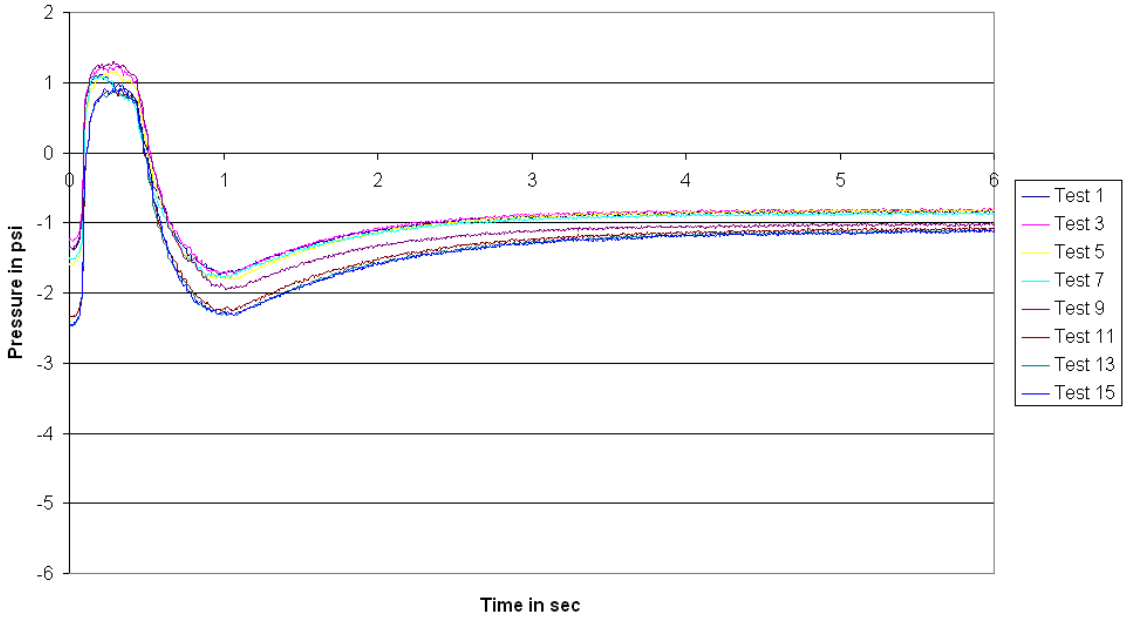

	Test 1	Test 3	Test 5	Test 7	Test 9	Test 11	Test 13	Test 15
ΔP new (psi)	-0.34978	-0.34978	-0.34978	-0.34978	-0.34978	-0.34978	-0.34978	-0.34978
ΔP cleaned (psi)	-0.78	-0.78	-0.78	-0.78	-0.78	-0.78	-0.78	-0.78
ΔP initial @ t=0 (psi)	-1.3852	-1.2421	-1.60218	-1.49836	-1.35668	-2.33242	-2.4498	-2.44406
ΔP initial @ t=5 (psi)	-0.83702	-0.8306	-0.84648	-0.8703	-1.03642	-1.08766	-1.11954	-1.15606
Time @ ΔP max (sec)	0.2	0.26	0.28	0.17	0.21	0.27	0.31	0.3
ΔP max (psi)	1.1122	1.2137	1.12506	1.06696	1.26022	0.87184	0.85282	0.90632
Time @ ΔP min (sec)	0.97	1.02	1.07	1.01	1.02	0.94	1.02	1.09
ΔP min (psi)	-1.7338	-1.72938	-1.80512	-1.7796	-1.94986	-2.25842	-2.32	-2.31794
Efficiency-clean	0.905783	0.8905	0.919142	0.874297	0.555351	0.801819	0.796658	0.774011
Efficiency-new	0.529428	0.461158	0.603402	0.546814	0.318065	0.62783	0.633451	0.615009
Factor-c	1.073103	1.064872	1.085231	1.115769	1.328744	1.394436	1.435308	1.482128
Factor-n	2.392988	2.374633	2.420033	2.488133	2.96306	3.109552	3.200695	3.305103

Figure 6.4.5.
Effect of build-up time - Lanxide filter
Comparative plot of pressure difference (ΔP: Pf-Pc) change during regeneration and corresponding analysis table for
95 psi regeneration pressure, 5 cm/s face velocity, 10 minute build-up time

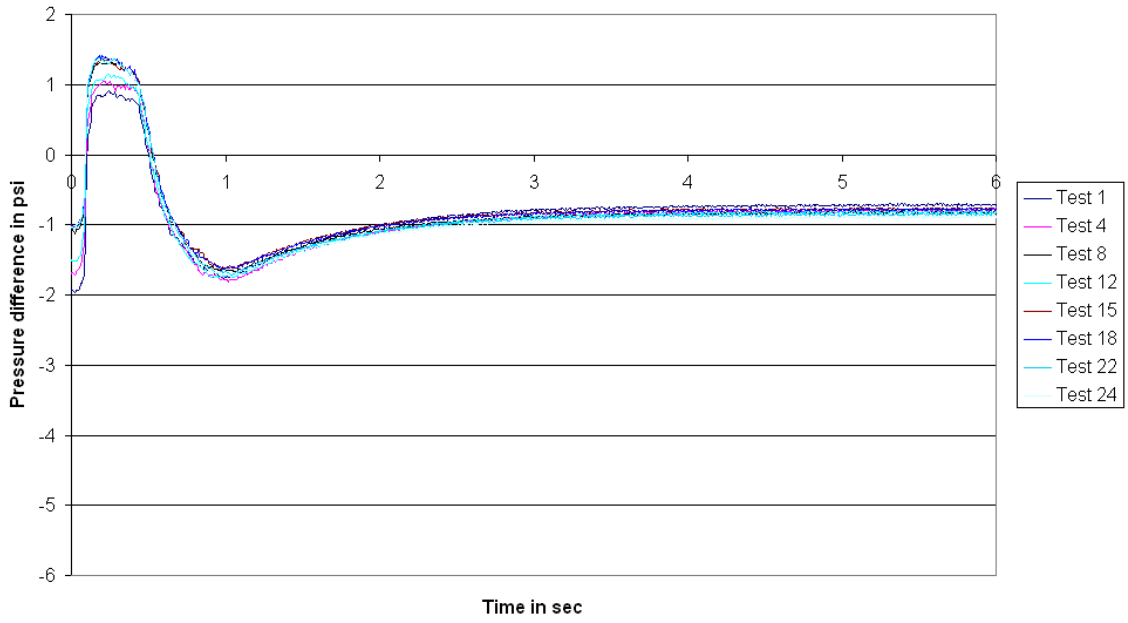

	Test 1	Test 4	Test 8	Test 12	Test 15	Test 18	Test 22	Test 24
ΔP new (psi)	-0.34978	-0.34978	-0.34978	-0.34978	-0.34978	-0.34978	-0.34978	-0.34978
ΔP cleaned (psi)	-0.78702	-0.78702	-0.78702	-0.78702	-0.78702	-0.78702	-0.78702	-0.78702
ΔP initial @ t=0 (psi)	-1.94848	-1.70232	-1.06656	-1.5146	-1.01064	-0.99012	-1.0259	-1.03348
ΔP initial @ t=5 (psi)	-0.7367	-0.81544	-0.82716	-0.82608	-0.77356	-0.77698	-0.84696	-0.899
Time @ ΔP max (sec)	0.24	0.22	0.24	0.24	0.2	0.2	0.19	0.26
ΔP max (psi)	0.90554	1.04566	1.35588	1.13994	1.35742	1.41752	1.40018	1.38776
Time @ ΔP min (sec)	0.98	1.02	1.05	1.04	0.97	0.99	1.04	1.03
ΔP min (psi)	-1.7665	-1.8096	-1.66952	-1.75564	-1.6275	-1.62946	-1.70752	-1.73794
Efficiency-clean	1.043325	0.96895	0.856407	0.946315	1.060191	1.049434	0.749079	0.545646
Efficiency-new	0.757979	0.655715	0.333994	0.591096	0.358745	0.332855	0.264657	0.196695
Factor-c	0.936063	1.036111	1.051003	1.04963	0.982898	0.987243	1.076161	1.142284
Factor-n	2.106179	2.331292	2.364798	2.361711	2.211559	2.221337	2.421405	2.570185

Figure 6.4.6
Effect of build-up time - Lanxide filter
Comparative plot of pressure difference (ΔP: Pf-Pc) change during regeneration and corresponding analysis table for
95 psi regeneration pressure, 5 cm/s face velocity, 20 minute build-up time

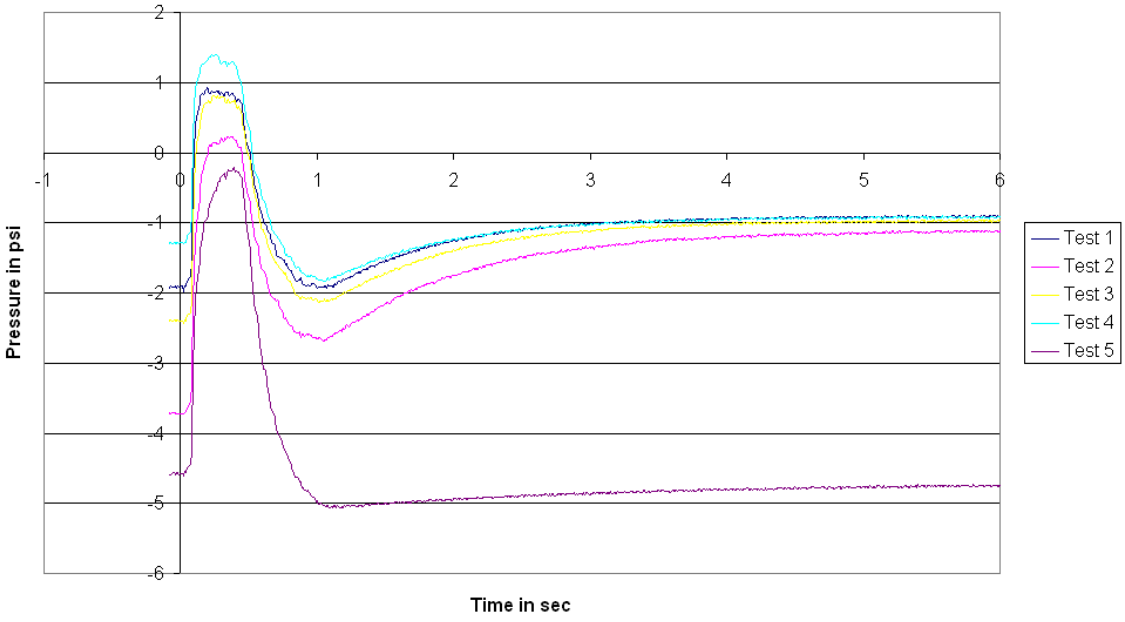

	Test 1	Test 2	Test 3	Test 4	Test 5
ΔP new (psi)	-0.3498	-0.3498	-0.3498	-0.3498	-0.3498
ΔP cleaned (psi)	-1.11956	-1.11956	-1.11956	-1.11956	-1.11956
ΔP initial @ t=0 (psi)	-1.92354	-3.72308	-2.3938	-1.27824	-4.57802
ΔP initial @ t=5 (psi)	-0.91708	-1.15148	-0.97694	-0.93282	-4.7605
Time @ ΔP max (sec)	0.19	0.37	0.24	0.26	0.39
ΔP max (psi)	0.92386	0.2243	0.81338	1.40258	-0.2021
Time @ ΔP min (sec)	1.07	1.05	1.02	1.06	1.11
ΔP min (psi)	-1.93238	-2.6811	-2.14002	-1.8387	-5.05938
Efficiency-clean	1.251847	0.98774	1.111926	2.176834	-0.05276
Efficiency-new	0.639534	0.762344	0.69318	0.372043	-0.04316
Factor-c	0.819143	1.028511	0.872611	0.833202	4.252117
Factor-n	2.621727	3.291824	2.792853	2.666724	13.60921

Figure 6.4.7.
Effect of build-up time - Lanxide filter
Comparative plot of pressure difference (ΔP: Pf-Pc) change during regeneration and corresponding analysis table for
95 psi regeneration pressure, 5 cm/s face velocity, 45 minute build-up time

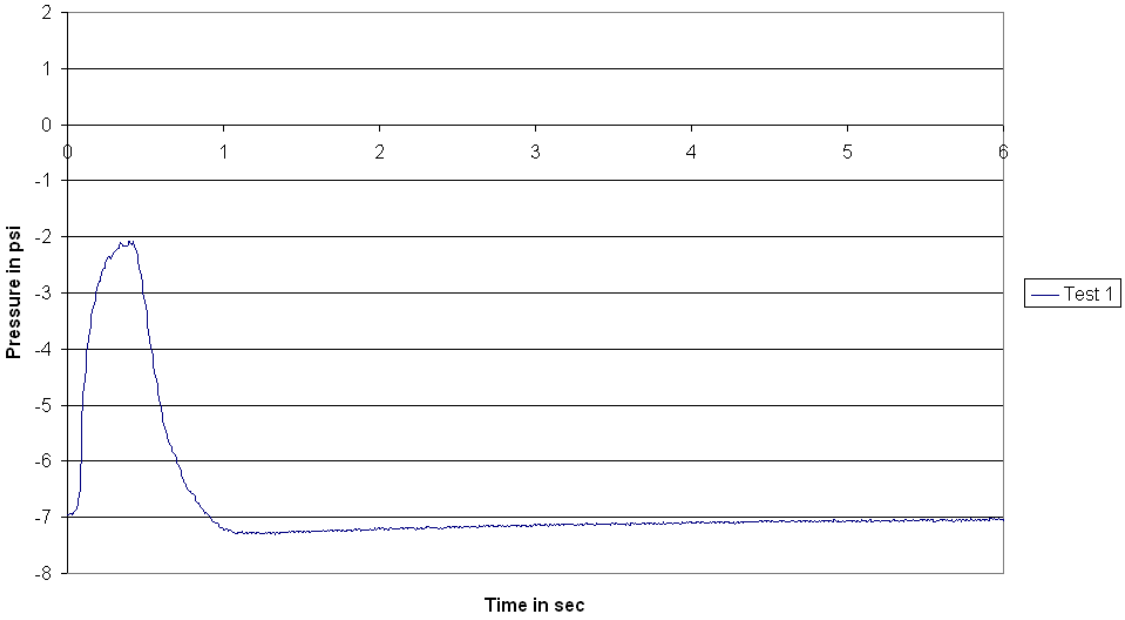

	Test 1
ΔP new (psi)	-0.3498
ΔP cleaned (psi)	-1.10892
ΔP initial @ t=0 (psi)	-6.96186
ΔP initial @ t=5 (psi)	-7.06446
Time @ ΔP max (sec)	0.4
ΔP max (psi)	-2.08474
Time @ ΔP min (sec)	1.33
ΔP min (psi)	-7.29934
Efficiency-clean	-0.01753
Efficiency-new	-0.01552
Factor-c	6.370577
Factor-n	20.19571

Figure 6.4.8.
Effect of build-up time - Lanxide filter
Comparative plot of pressure difference (ΔP: Pf-Pc) change during regeneration and corresponding analysis table for
95 psi regeneration pressure, 5 cm/s face velocity, 90 minute build-up time

a. $\Delta P_{initial}$

The $\Delta P_{initial}$ value for the 10 min build-up time is about -1.2 psi which gradually decreases to -2.5 psi. The 20 min build-up time is maintained between -1 and -2 psi. The 45 min build-up has larger magnitude initial pressure drop except in test 4 when it failed to build-up ash for reasons unknown. In the 5th test the initial pressure difference is greater than 4.5 psi. The filter failed to regenerate. Similarly the initial pressure difference is nearly 7 psi for the 90 min build-up time and the filter failed to regenerate. The particle loading extended over a period of time covers the filter pores and thus increases the chamber pressure. Both together resist the regeneration process.

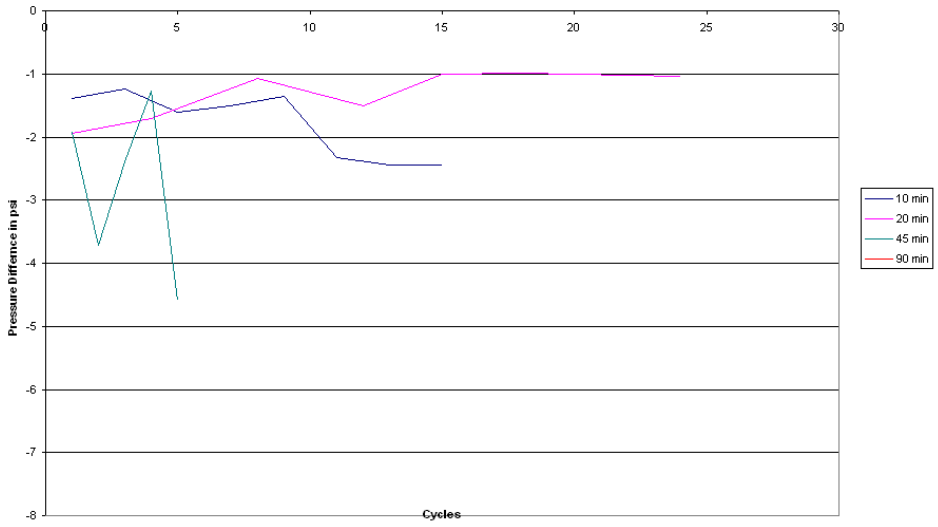

Figure 6.4.9.
Effect of build-up time
Lanxide filter - long term tests
Comparative plot of initial pressure difference ($\Delta P_{initial}$)

b. ΔP_{final}

The ΔP_{final} value is an indicator of how effective the cleaning is after the regeneration. The ΔP_{final} value for the 10 min and the 20 min build-up time interval is maintained at about -1 psi. For the 45 minute build-up case also the value was maintained close to -1 psi. It is to be noted that the filter did not regenerate on the top portion for the 2nd, 3rd and the 4th tests this value is low. The value for the 5th test (45 min build-up) and the 1st test (90 min build-up) are very high and these were the tests in which the filter failed to regenerate.

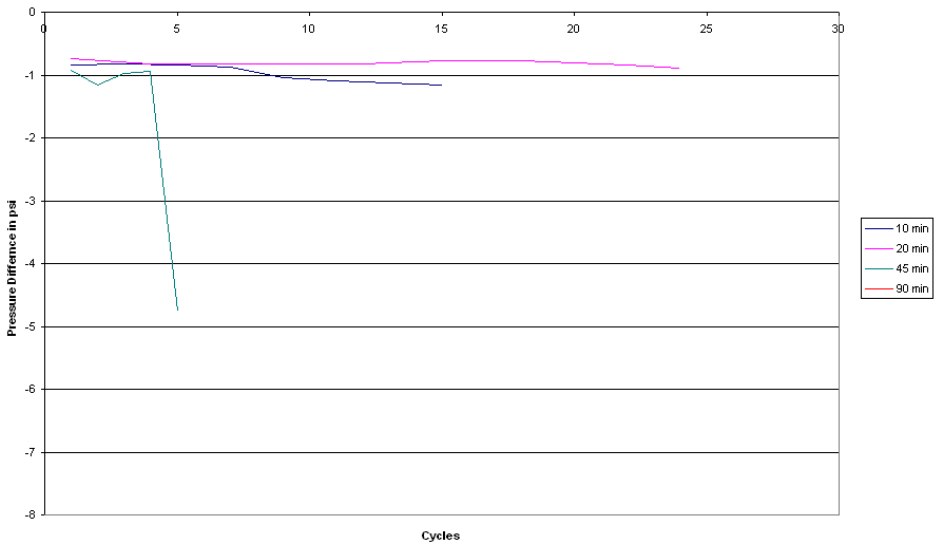

Figure 6.4.10.
Effect of build-up time
Lanxide filter - long term tests
Comparative plot of final pressure difference (ΔP_{final})

c. ΔP_{max}

The ΔP_{max} is about the same for the 10 min and the 20 min build-up are relatively high and consistent value indicating desirable regeneration characteristics. As expected in the 90 min build-up time case, the maximum pressure difference was negative since it did not regenerate. Similarly the value was negative in the 5th test of 45 min build-up time. The values for the 1st to 4th test are positive and low for the 45 min build-up.

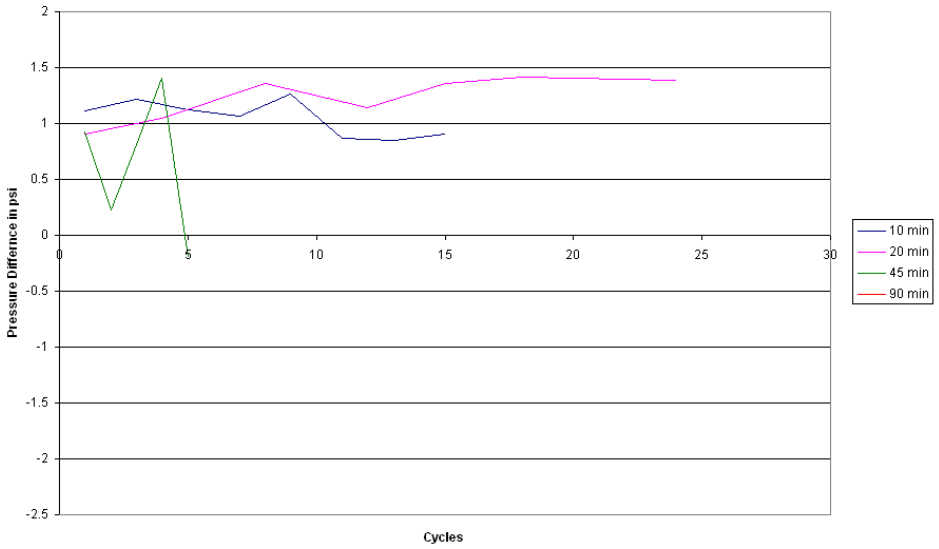

Figure 6.4.11.
Effect of build-up time
Lanxide filter - long term tests
Comparative plot of maximum pressure difference (ΔP_{max})

d. ΔP_{min}

The ΔP_{min} values are low and consistent for the 10 min and the 20 min conditions. The magnitude in the 45 min condition keeps increasing. This is due to the residual ash build-up. The corresponding value for the 90 min is also very low.

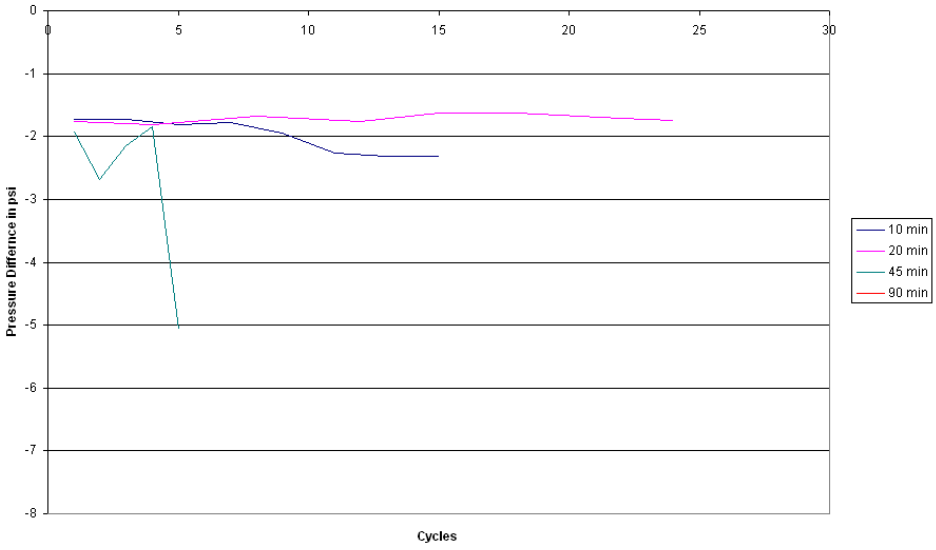

Figure 6.4.12.
Effect of build-up time
Lanxide filter - long term tests
Comparative plot of minimum pressure difference (ΔP_{min})

e. Efficiency η:

The ash build-up in the 10 min and the 20 min conditions were thin type. The efficiency for the 45 min test was high till the test in which the filter failed to regenerate. This is typical of thick ash formation as it has been noticed in the 7 cm/s condition. The efficiency was negative for the tests in which regeneration failed to occur. The efficiency (cleaned) was maintained near 1 for 10 min and 20 min tests, which indicate no or little residual ash build-up.

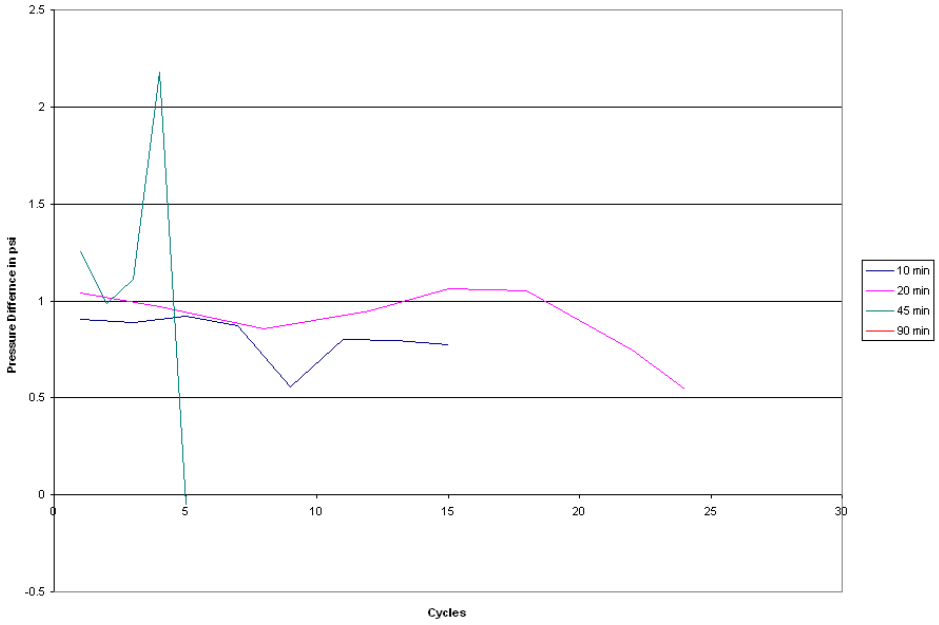

Figure 6.4.13.
Effect of build-up time
Lanxide filter - long term tests
Comparative plot of efficiency based on ΔP_C (η_C)

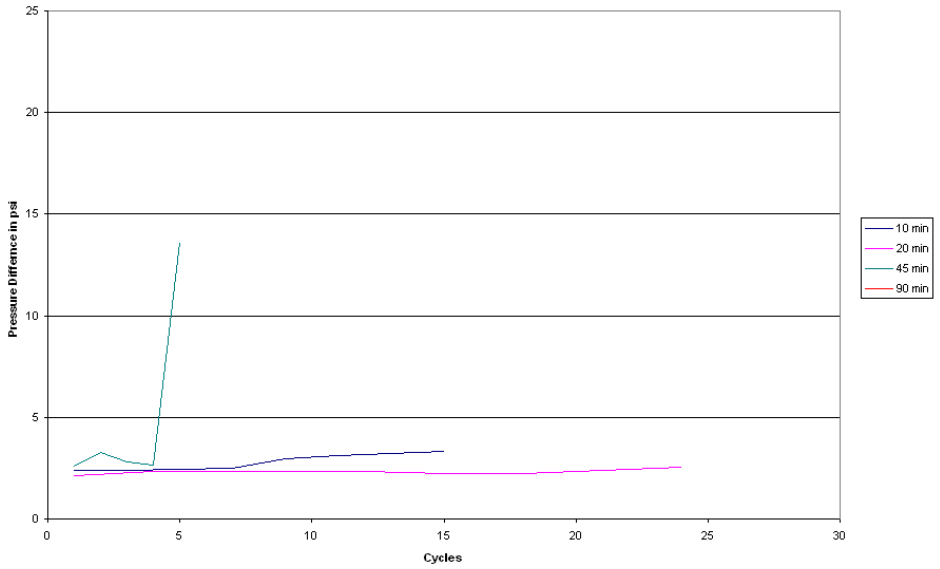

Figure 6.4.14.
Effect of build-up time
Lanxide filter - long term tests
Comparative plot of efficiency based on ΔP_N (η_N)

Cleaning Factor F:

The cleaning factor F indicates how clean the filter is with every testing cycle. The F_N (cleaning factor when measured with respect to a new filter) and the F_C (cleaning factor when measured with respect to a cleaned filter) are plotted for all the conditions. It is noted from the plot that the factor increases for the 45 min condition, while it is low and stable for the other 10 min and 20 min conditions. This increase indicates insufficient cleaning and increasing residual pressure drop for the 45 min build-up. The value is very high (F_C is close to 6.5 and F_N is close to 20) for the first test with the 90 min condition, when the filter failed to regenerate.

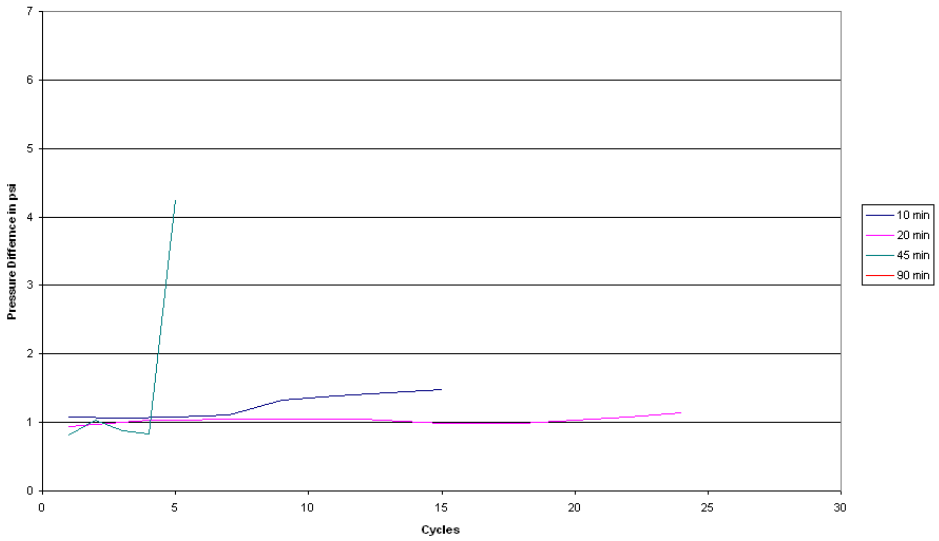

Figure 6.4.15.
Effect of build-up time
Lanxide filter - long term tests
Comparative plot of cleaning factor based on ΔP_C (F_C)

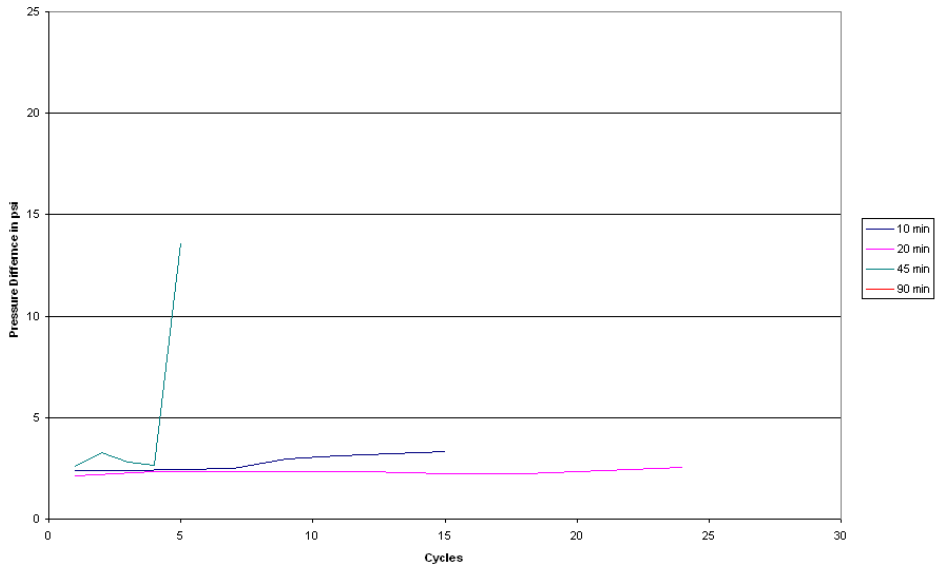

Figure 6.4.16.
Effect of build-up time
Lanxide filter - long term tests
Comparative plot of cleaning factor based on ΔP_N (F_N)

From the analysis of the pressure difference data, it is observed that the 45 min and the 90 min conditions are not suitable for effective regeneration.

6.4.4 Distribution of particles less than 100 microns during regeneration

The particle count for size less than 100 microns for the 10 min build-up condition was the highest of all four conditions. This can be attributed to the thin ash formation and thin type regeneration. The 20 min build-up time also has thin type ash formation and regeneration, also has a lot of particles but not quite as high as the 10 min condition. The 45 min build-up condition has thick ash regeneration and has low particle count. The observation was made for only one cycle as in the next four cycles the ash did not regenerate in the camera's area of view. It was also not possible to observe in the 90 min condition it did not regenerate at all.

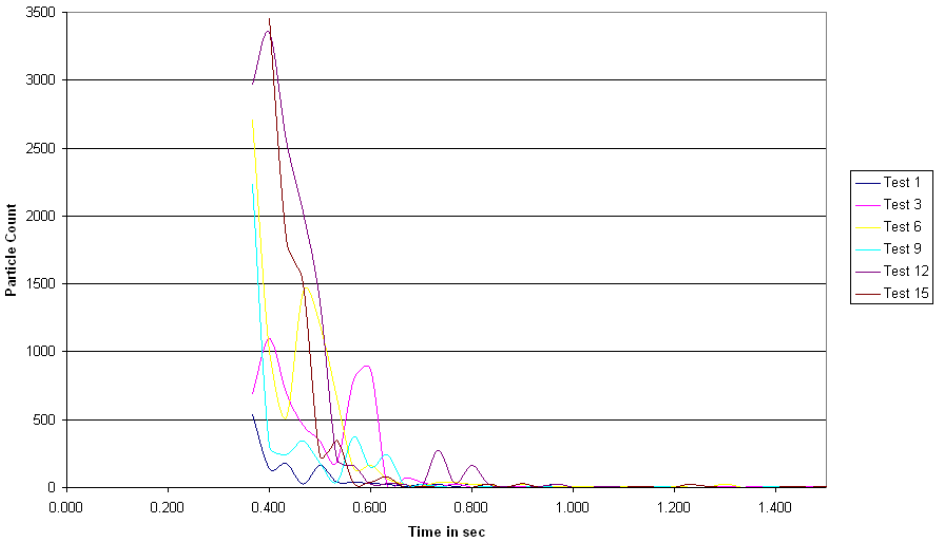

Figure 6.4.17.
Effect of build-up time on Lanxide filter - long term tests
Particle count: less than 100 microns
95 psi regeneration pressure, 5 cm/s face velocity, 10 min build-up time

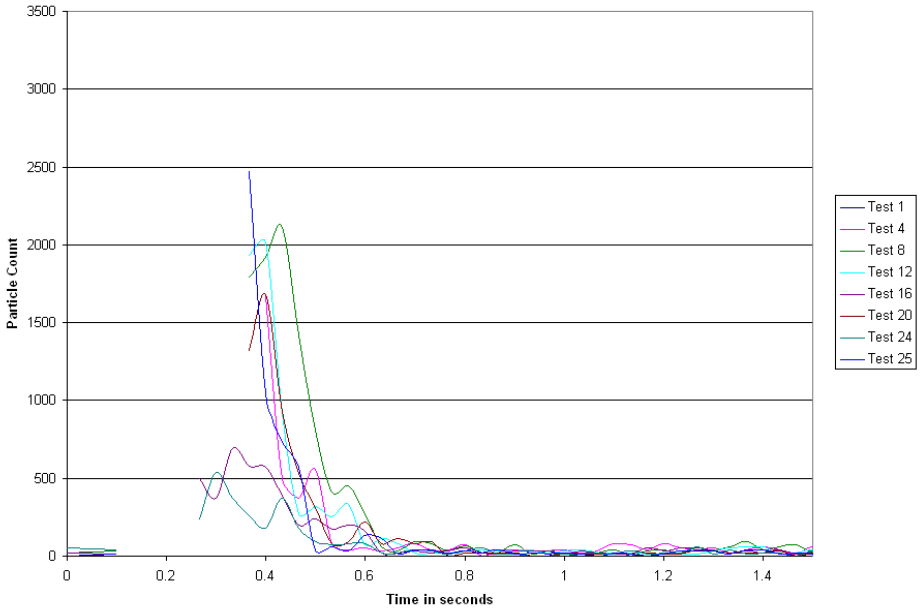

Figure 6.4.18.
Effect of build-up time on Lanxide filter - long term tests
Particle count: less than 100 microns
95 psi regeneration pressure, 5 cm/s face velocity, 20 min build-up time

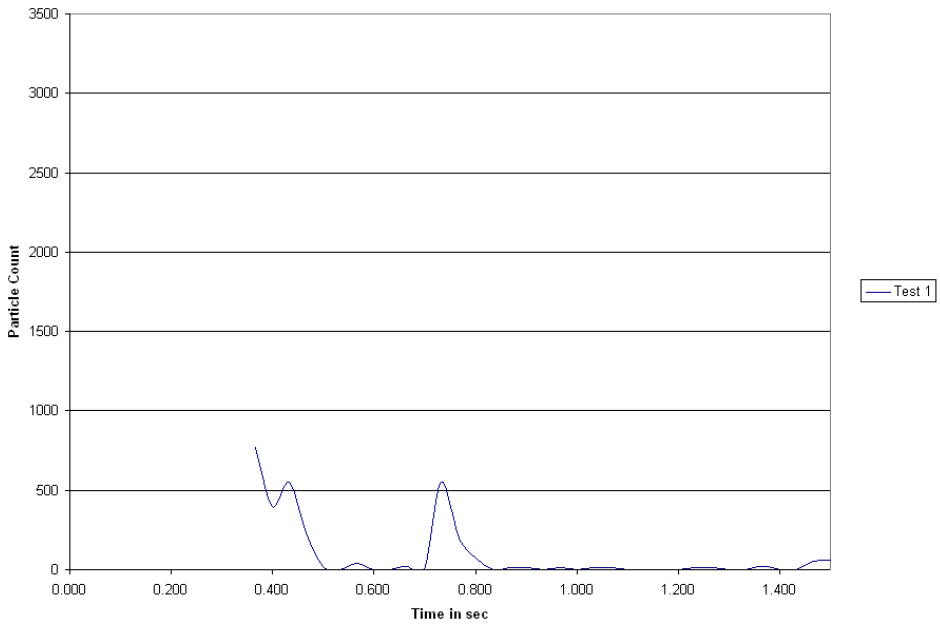

Figure 6.4.19.
Effect of build-up time on Lanxide filter - long term tests
Particle count: less than 100 microns
95 psi regeneration pressure, 5 cm/s face velocity, 45 min build-up time

Note: Particle count analysis was not performed on 45 min build-up tests - 2,3,4 & 5 and 90 min build-up test 1, because the filter did not regenerate at the camera's region of view.

6.4.5 The thickness of ash deposit during build-up

The ash thickness is a function of the build-up variables. The face velocity and the build-up time are two important parameters of build-up variables. It is observed that in shorter build-up time the ash cake is thin (in 10 min and 20 min), while in longer build-up time (45 min and 90 min) the ash cake is thick. (Table 6.4.1)

6.4.6 The type of regeneration:

The ash deposited on the filter surface was thin for the 10 min and the 20 min build-up time cases and the resultant regeneration type was thin type regeneration. The 45 min and the 90 min had thick type ash. the 45 min resulted in thick type regeneration. In both the longer build-up conditions, the filter stopped regenerating. (Table 6.4.1)

6.4.7 Crack initiation Time:

The crack initiation time is low for the 10 min and the 20 min build-up conditions. In both 45 min and 90 min conditions it was not possible to observe the crack initiation time since the filter failed to regenerate (partially as well as wholly) in the camera's image capturing region. The failure to regenerate is indicative of the ash cake strength during these conditions. (Table 6.4.1)

6.4.8 Surface Quality:

The ash on the surface after repeated cycles of regeneration was observed to be thin patchy residuals, for the 10 min and the 20 min build-up time intervals. This can be attributed to the thin type regeneration occurring under these conditions. The 20 min condition had relatively more ash compared to the 10 min build-up time. The 45 min and 90 min build-up time resulted in thick ash growth. The 90 min failed to regenerate and had a thick coating of ash on its surface. The 45 min regenerated for the first cycle thoroughly. But from the second cycle onwards there was thick residual ash on the top portions of the filter, and finally stopped regenerating.

The 90 min and 45 min conditions are not suitable for regeneration process. They can be excluded based on their failure to regenerate even in the first few cycles. The 10 min and the 20 min conditions regenerate repetitively. But they are characterized by thin ash cake formation and thin ash regeneration. This type of ash formation and regeneration is associated with larger small particles. This is also not desirable, especially at higher temperatures when sintering occurs.

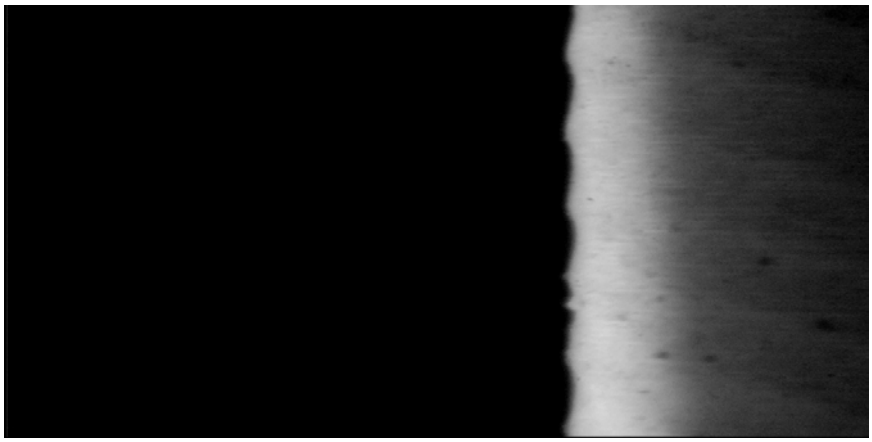

Test 1
Clean Filter

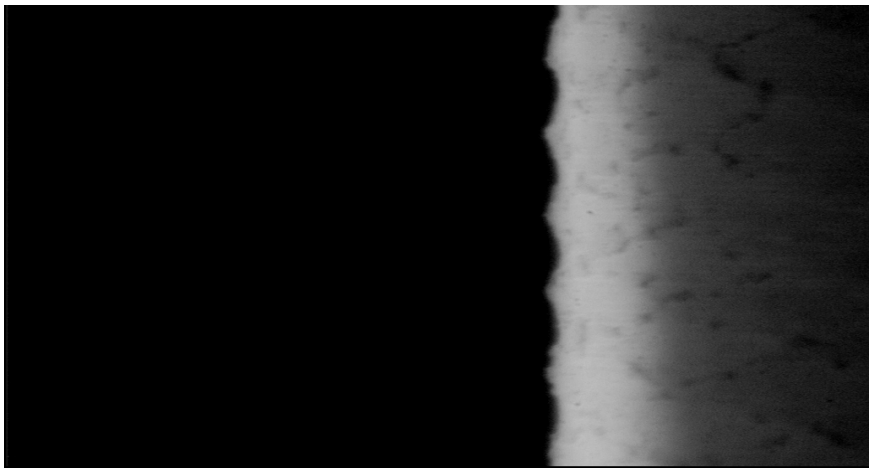

Test 6
Filter Slightly Dirty

Figure 6.4.20a
Effect of build-up time on Lanxide filter
Surface quality during long term test cycles
95 psi regeneration pressure, 5 cm/s face velocity, 10 min build-up time. (Contd.)

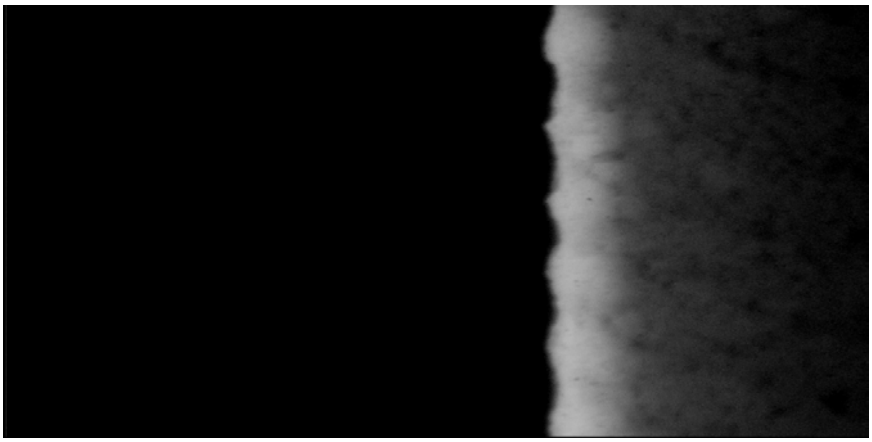

Test 12
Residual ash on
ridges

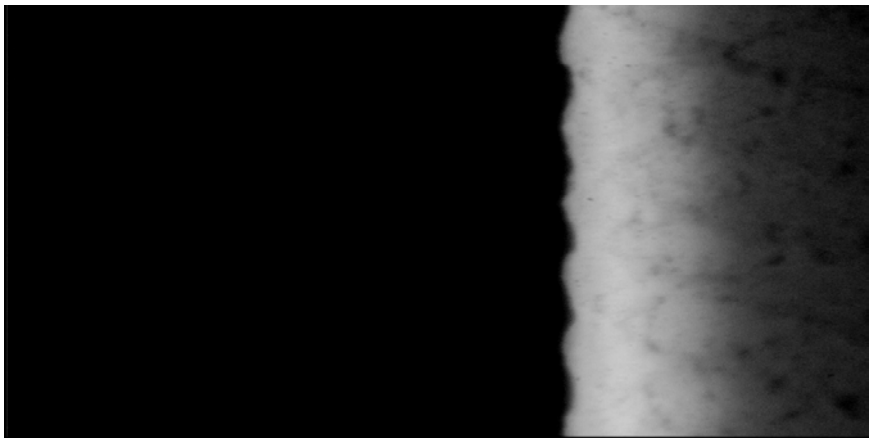

Test 15
Residual ash on
ridges

Figure 6.4.20b
Effect of build-up time on Lanxide filter
Surface quality during long term test cycles
95 psi regeneration pressure, 5 cm/s face velocity, 10 min build-up time.

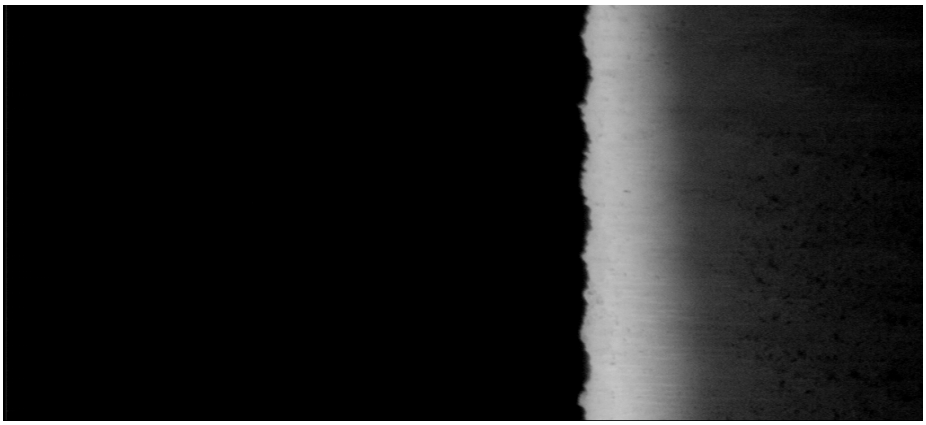

Test 1
Clean filter

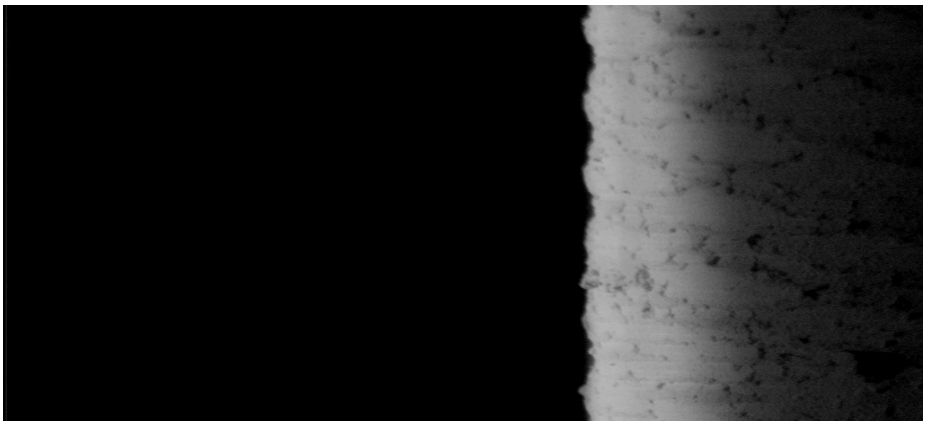

Test 4
Little
residual

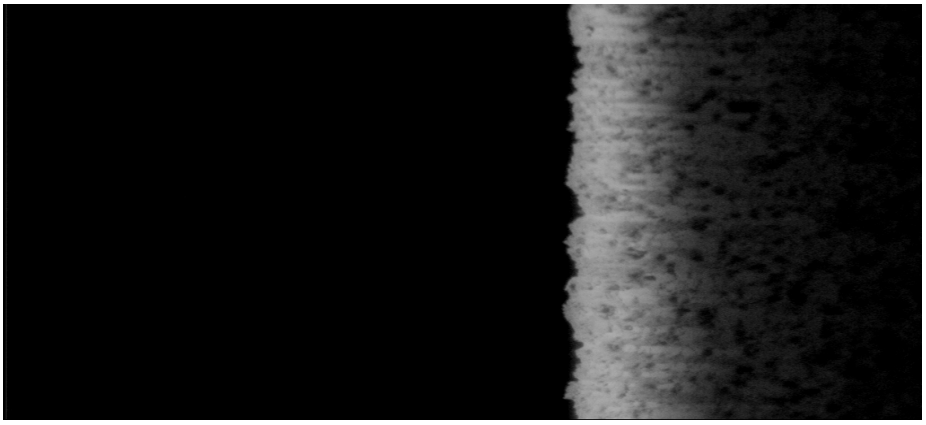

Test 8
Residual ash
typical of thin
ash

Figure 6.4.21a
Effect of build-up time on Lanxide filter
Surface quality during long term test cycles
95 psi regeneration pressure, 5 cm/s face velocity, 20 min build-up time. (Contd.)

Test 16
More thin
ash type

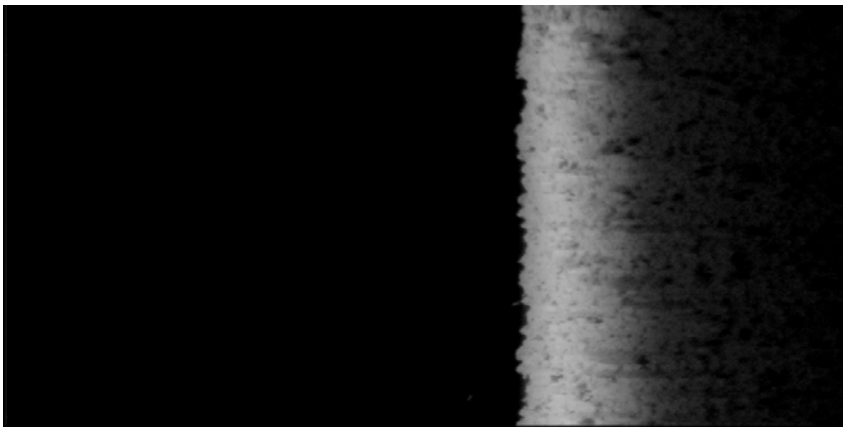

Test 20
Dirty

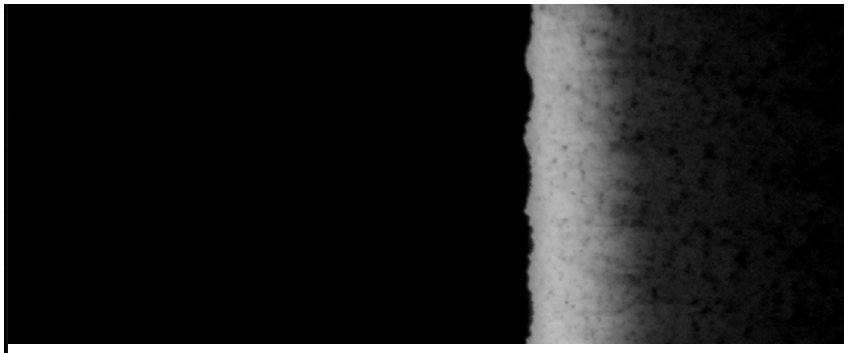

Test 25
Dirty

Figure 6.4.21b.
Effect of build-up time on Lanxide filter
Surface quality during long term test cycles
95 psi regeneration pressure, 5 cm/s face velocity, 20 min build-up time.

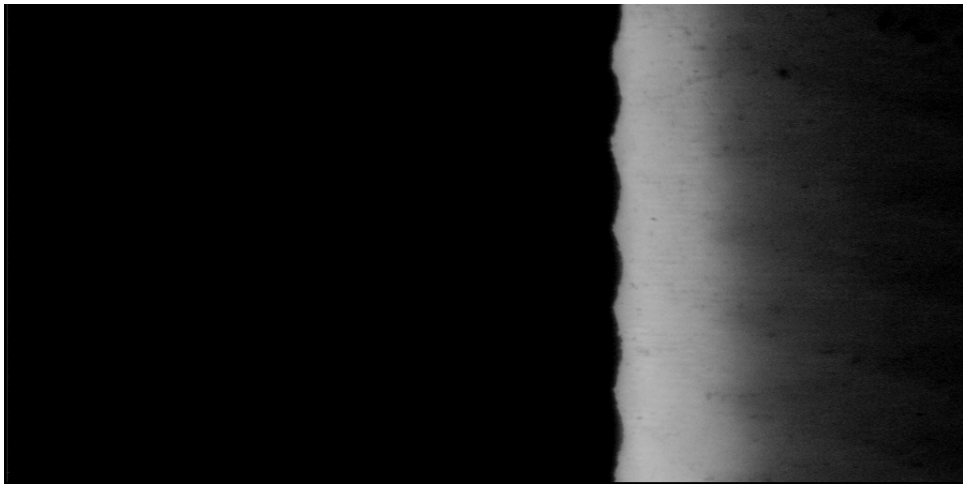

Test 1
clean

Figure 6.4.22.
Effect of build-up time
Surface quality during long term test cycles
95 psi regeneration pressure, 5 cm/s face velocity, 45 min build-up time.

NOTE:

In tests 2,3 and 4 for the 45 min condition, the filter did not regenerate on top where the camera's region of view existed. In test 5, the filter did not regenerate totally

In test 1 for 90 min condition the filter did not regenerate totally.

6.5 Comparison of the effect of filter type - low permeability (Lanxide®) vs. high permeability (Pall®) filter.

All the tests discussed in sections 6.2, 6.3 and 6.4 were all performed on a particular type of filter (brand name: Lanxide®). In order to study the effect of different type of filter another commercially available filter (brand name: Pall®) was tested under similar conditions. The Pall filter was first tested for the base condition and the 7cm/s condition (face velocity as the variable), and results obtained were compared with the results from Lanxide filter. The Pall filter was found to perform better than the Lanxide filter. The Pall filter lasted for more tests when compared to the Lanxide filter when it was subjected to 7cm/s face velocity, 95 psi regeneration pressure and 20 min build-up time. A study to compare filters regeneration characteristics was performed. The permeability of both the filters was measured as a function of pressure drop across a clean filter for increasing clean air flowing through their walls. Also the tests in which Lanxide filter exhibited difficulties in regenerating or stopped regenerating were chosen as the tests to be compared. This was done since we had seen better performance by Pall filter in the 7cm/s - face velocity condition in which Lanxide filter did not perform well.

Five tests were performed in all, on the Pall filter. The tests that were performed are:

1. Face velocity of 5 cm/s, a reservoir pressure of 95 psig, and a build-up time of 20min, (Base condition)
2. Face velocity of 7 cm/s, a reservoir pressure of 95 psig, and a build-up time of 20min, (Higher face velocity)

3. Face velocity of 5 cm/s, a reservoir pressure of 80 psig, and a build-up time of 20min, (Low regeneration Pressure)
4. Face velocity of 5 cm/s, a reservoir pressure of 95 psig, and a build-up time of 45min, (Longer build-up time)
5. Face velocity of 5 cm/s, a reservoir pressure of 95 psig, and a build-up time of 90min, (Longer build-up time)

In this section the results from the tests performed on both the filter to get their pressure drop (permeability) across clean filters is first discussed. Then other surface regeneration characteristics are discussed.

6.5.1 Pressure drop across clean filter

The filters were tested without ash fluidization to measure the pressure drop across a clean filter as a function of face velocity. Tests were performed on a clean filter (without any ash) to measure the pressure drop as a function of velocity. In these tests the regeneration pulse was not employed, only the build-up air was used. The flow conditions were regulated to flow from the chamber (without fluidizing ash) through the filter and exhausted. The face velocity of the flow was varied from 2 cm/s to 9 cm/s and the pressure drop measured. The Lanxide and Pall filters were subjected to similar tests and results obtained. Graphs were plotted for pressure drop vs. face velocity.

The pressure drop observed is the pressure difference between the filter and chamber. In the Lanxide filter the pressure drop is found to decrease linearly with increase in face velocity, while in the Pall filter the pressure drop is relatively small compared to the Lanxide filter. The measurements of permeability for the low

permeability filter are beyond the accuracy of the instrumentation, especially at the lower velocities. Pall filter reaches a maximum pressure drop of -0.12 psi at about 8.5 cm/s flow. This behavior indicated that the permeability of Lanxide filter is low compared to the Pall filter.

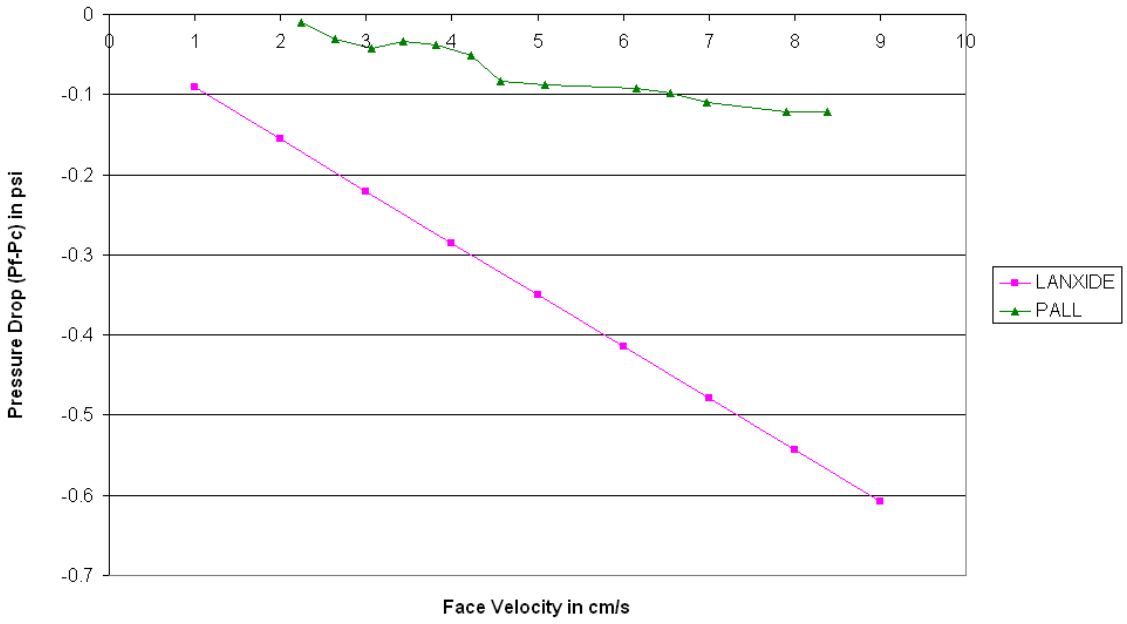

Figure 6.5.1.
Pressure Drop (Pf-Pc) variation across clean Lanxide and Pall filters for varying face velocities.

6.5.2 Number of test cycles and reason for ending

The Pall filter lasted for larger number of cycles without deterioration compared to the Lanxide filter. The Pall filter lasted longer in tests in which both the filters stopped regenerating, especially the 7cm/s condition and the 90 min build-up time condition. In the 45 min build-up time condition The Lanxide filter stopped regenerating after 5 cycles while the Pall filter continued to regenerate even after 16 cycles. In cases where both the filters continued to regenerate (base condition and 80 psi regeneration cases), the Lanxide filter deteriorated more when compared to the Pall filter. The Pall filter performs better in this regard compared to the Lanxide filter.

Filter		Number of cycles	Stopped due to	Ash Thickness in mm	Type of Regeneration	Crack initiation Time	Surface Quality
MAIN CONDITION 95 psi REG. PRESSURE, 5cm/s FACEVELOCITY, 20 min BUILDUP TIME							
Pall	Begin	22	Repetitive Regeneration	1.75-2.1	Thick	0.117	very clean
	During			1.75-2.1	Thick	0.117-0.13	very thin coating
	End			2.1-2.1	Thick	0.1-0.117	residual ash
Lanxide	Begin	25	Repetitive Regeneration	0.7-1.05	Thin	0.1-0.13	clean
	During			0.35-0.35	Thin	0.117-0.13	patchy residuals
	End			0.35-0.525	Thin	0.117-0.15	more residual

Filter		Number of cycles	Stopped due to	Ash Thickness in mm	Type of Regeneration	Crack initiation Time	Surface Quality
MAIN CONDITION 95 psi REG. PRESSURE, **7cm/s FACEVELOCITY**, 20 min BUILDUP TIME							
Pall	Begin	15	**Stopped Regenerating**	1.75	Thick	0.2	Clean
	During			1.4	Thick	0.1833-0.267	Clean, except for thick Patch
	End			1.75	Thick	0.1833-0.267	Didn't regenerate
Lanxide	Begin	7	**Stopped Regenerating**	1.75	Thick	0.2167	clean
	During			1.4	Thick	0.2-0.25	clean
	End			1.75	Thick	0.2833	big patches, stopped

Filter		Number of cycles	Stopped due to	Ash Thickness in mm	Type of Regeneration	Crack initiation Time	Surface Quality
MAIN CONDITION 95 psi REG. PRESSURE, 5cm/s FACEVELOCITY, **45 min BUILDUP TIME**							
Pall	Begin	16	Repetitive Regeneration	0.5	Thick	0.2167	very clean
	During			3.15-3.5	Thick	0.2-0.25	Thin dust Layer
	End			3.15	Thick	0.2833	Ash dust on craters
Lanxide	Begin	5	**Stopped Regenerating**	2.5	Thick	0.117	
	During						*Didn't regen. On top*
	End						Stopped Regenerating

Filter		Number of cycles	Stopped due to	Ash Thickness in mm	Type of Regeneration	Crack initiation Time	Surface Quality
MAIN CONDITION 95 psi REG. PRESSURE, 5cm/s FACEVELOCITY, **90 min BUILDUP TIME**							
Pall	Begin	3	**Stopped Regenerating**	2.1	Thick	0.2167	very clean
	During						
	End			5.6	Thick	0.2833	Ash dust on craters
Lanxide	Begin	1	**Stopped Regenerating**				
	During						*Didn't Regenerate*
	End						

Filter		Number of cycles	Stopped due to	Ash Thickness in mm	Type of Regeneration	Crack initiation Time	Surface Quality
MAIN CONDITION **80 psi REG. PRESSURE**, 5cm/s FACEVELOCITY, 20 min BUILDUP TIME							
Pall	Begin	24	Repetitive Regeneration	1.75	Thick	0.117	clean
	During			1	Part Thick/Thin	0.1-0.117	some residual ash
	End			1	Thin	0.117	more residual ash
Lanxide	Begin	24	**repeated partial regen.**	0.7-1.4	Thin	0.1-0.1667	very clean
	During			0.35	Thin	0.117-0.133	residaul ash on ridges
	End			0.175	Thin	0.117-0.133	repeated partial regen.

Table 6.5.1.
Comparative table of regeneration characteristics, between the filters

6.5.3 Increase of chamber pressure (P_c) during the build-up phase

On comparing the chamber pressure increase between Pall and Lanxide filters, the Pall filter reached the same magnitude of chamber pressure increase as the Lanxide filter in a larger number of test cycles. This indicates that the Pall filter took a longer time to build the same amount of residual ash or to resist the regeneration as the Lanxide filter. This is evident on observing the comparative plots 6.5.2 to 6.5.6.

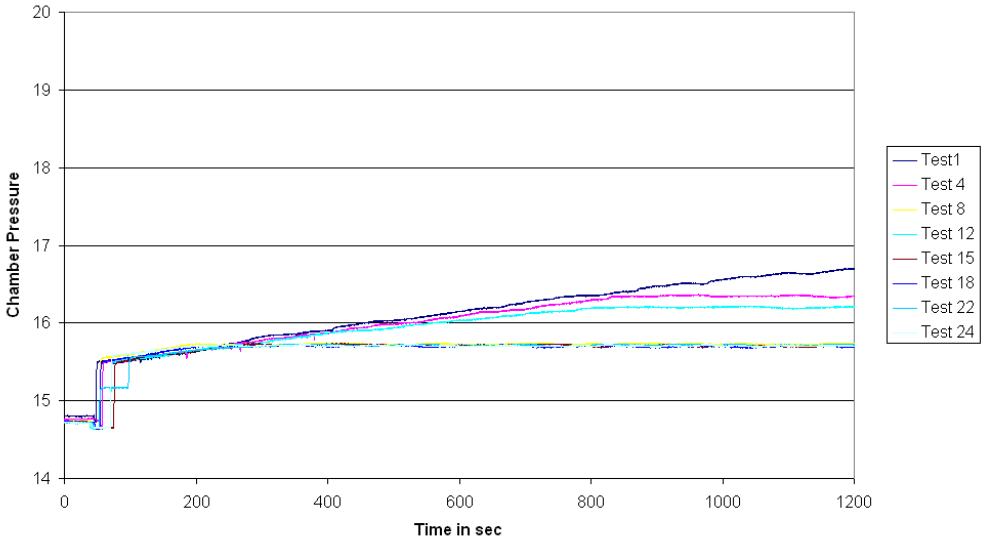

A

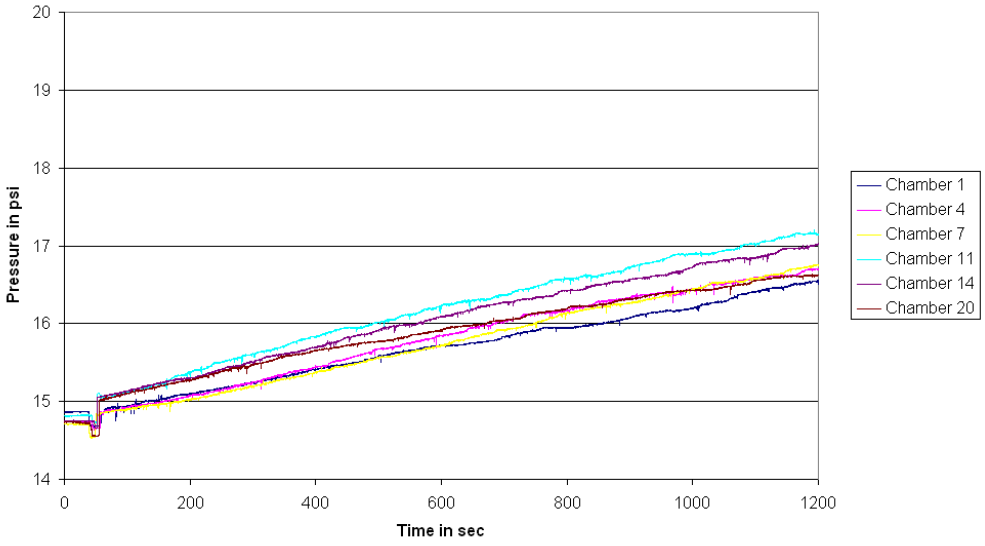

B

Figure 6.5.2.
Lanxide filter (plot A) vs. Pall filter (plot B)
Comparative Plot of chamber pressure increase during build-up
95 psi regeneration pressure, 5 cm/s face velocity, 20 minute build-up time

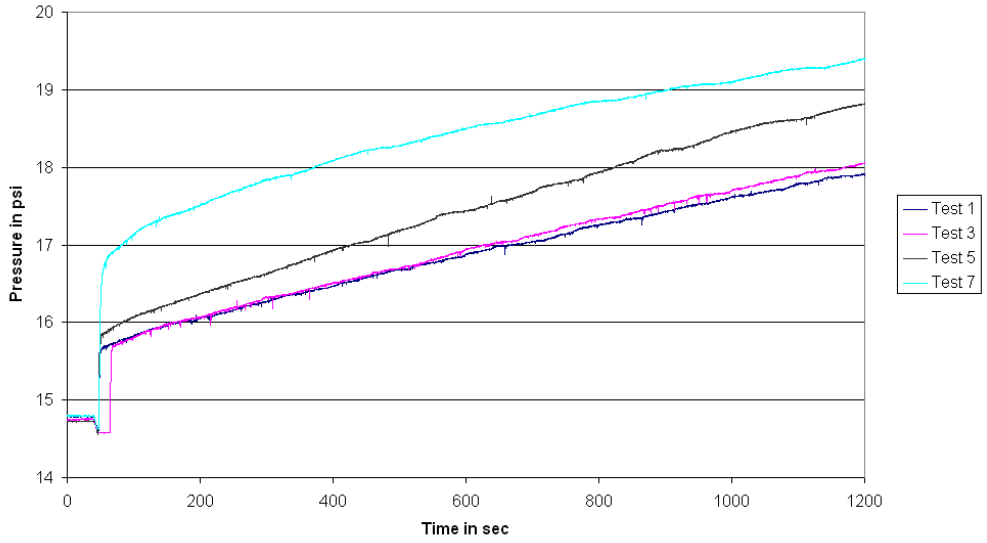

A

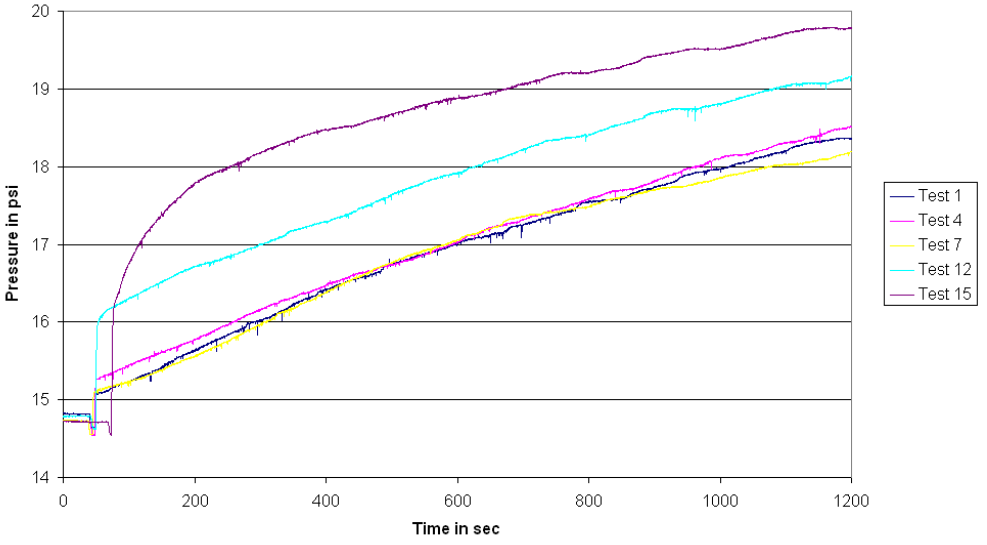

B

Figure 6.5.3.
Lanxide filter (plot A) vs. Pall filter (plot B)
Comparative Plot of chamber pressure increase during build-up
95 psi regeneration pressure, 7 cm/s face velocity, 20 minute build-up time

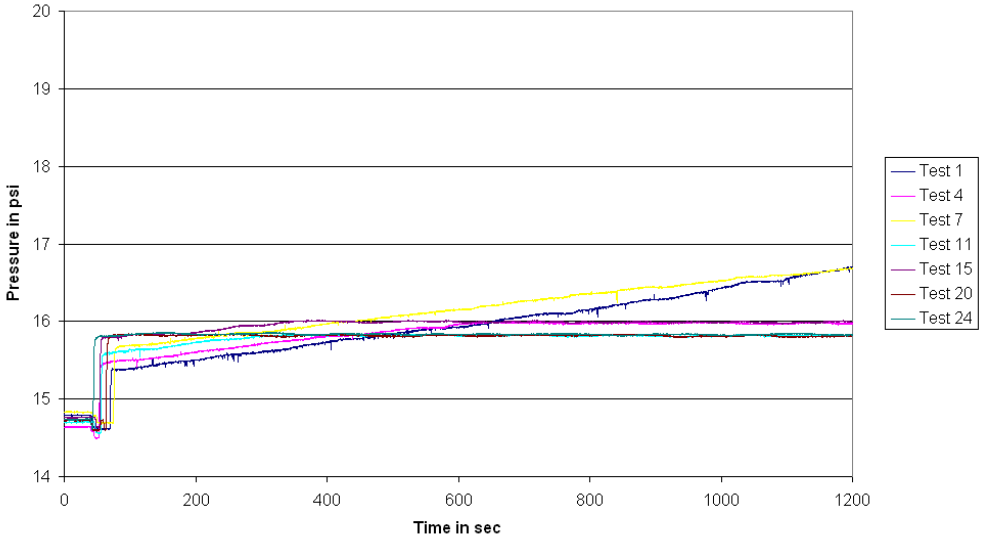

A

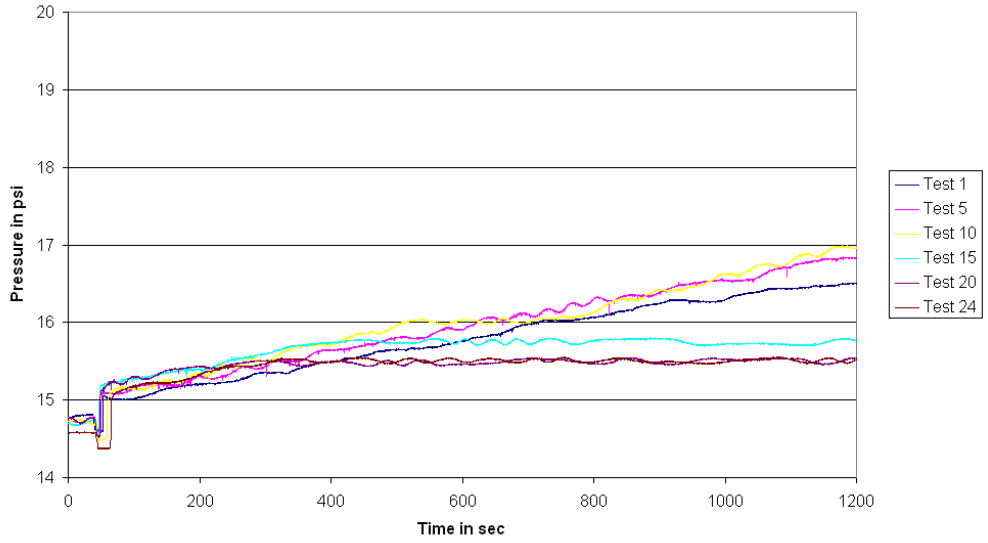

B

Figure 6.5.4.
Lanxide filter (plot A) vs. Pall filter (plot B)
Comparative Plot of chamber pressure increase during build-up
80 psi regeneration pressure, 5 cm/s face velocity, 20 minute build-up time

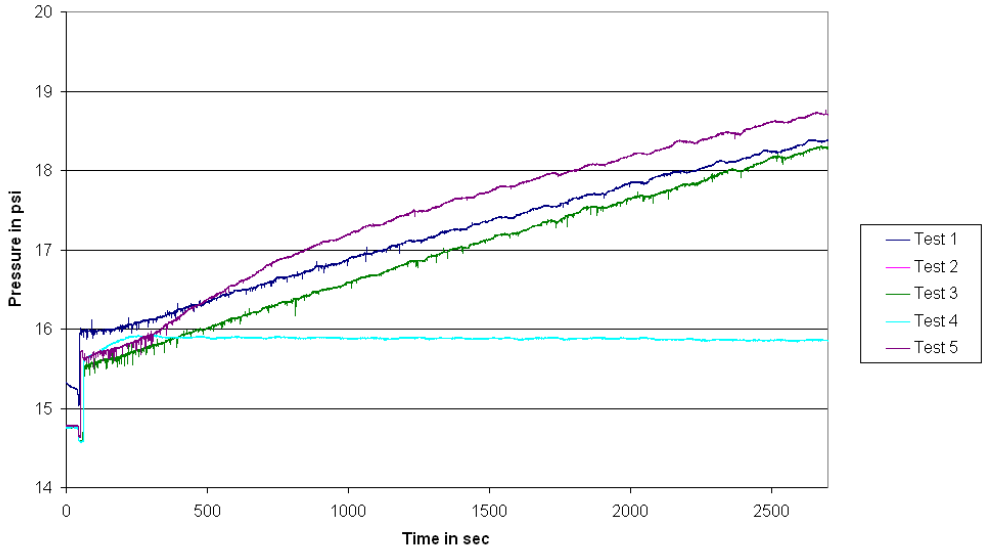

A

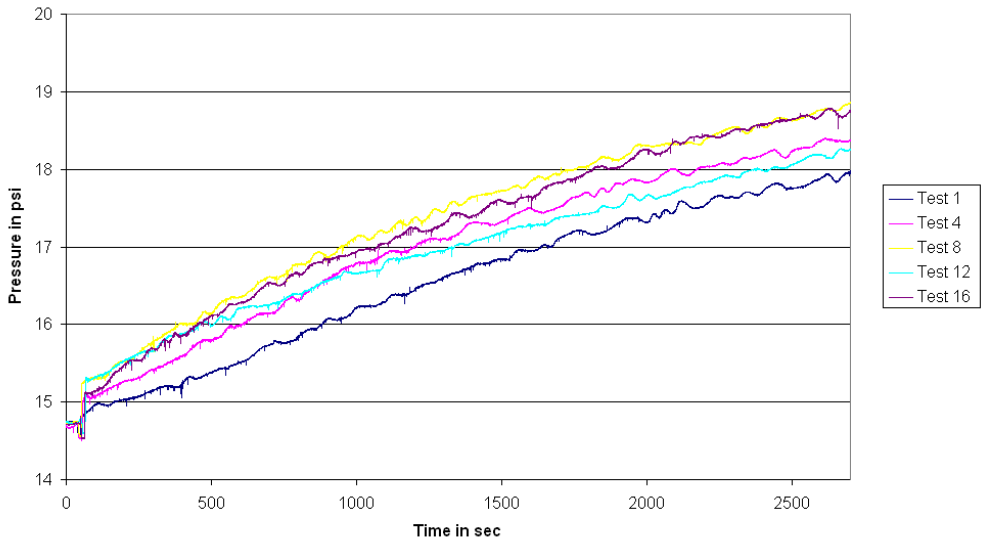

B

Figure 6.5.5.
Lanxide filter (plot A) vs. Pall filter (plot B)
Comparative Plot of chamber pressure increase during build-up
95 psi regeneration pressure, 5 cm/s face velocity, 45 minute build-up time

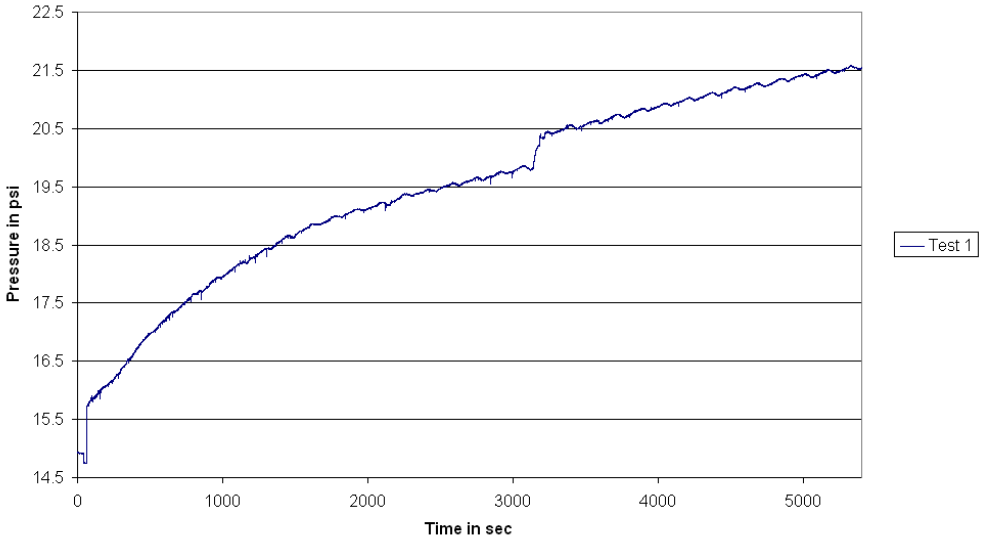

A

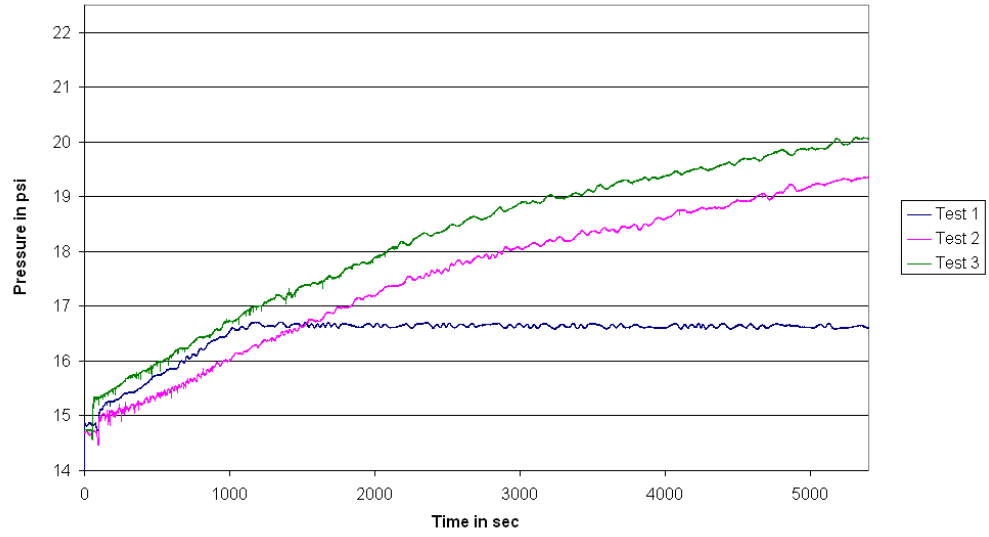

B

Figure 6.5.6.
Lanxide filter (plot A) vs. Pall filter (plot B)
Comparative Plot of chamber pressure increase during build-up
95 psi regeneration pressure, 5 cm/s face velocity, 90 minute build-up time

6.5.4 Pressure difference, ΔP (P_f-Pc), between filter (P_f) and chamber (Pc) during regeneration

A comparative study on the pressure difference curves of the two filters was performed. Figures 6.5.7 to 6.5.11 are the pressure difference curves obtained during regeneration phase of the testing. The Pall filter lasted a higher number of test cycles compared to the Lanxide filter, while accumulating similar residual ash measures. This is highlighted especially in tests where both filters stopped regenerating. The Pall filter lasted more number of cycles under similar testing conditions. A detailed discussion based on the ΔP characteristics is presented in the subsections.

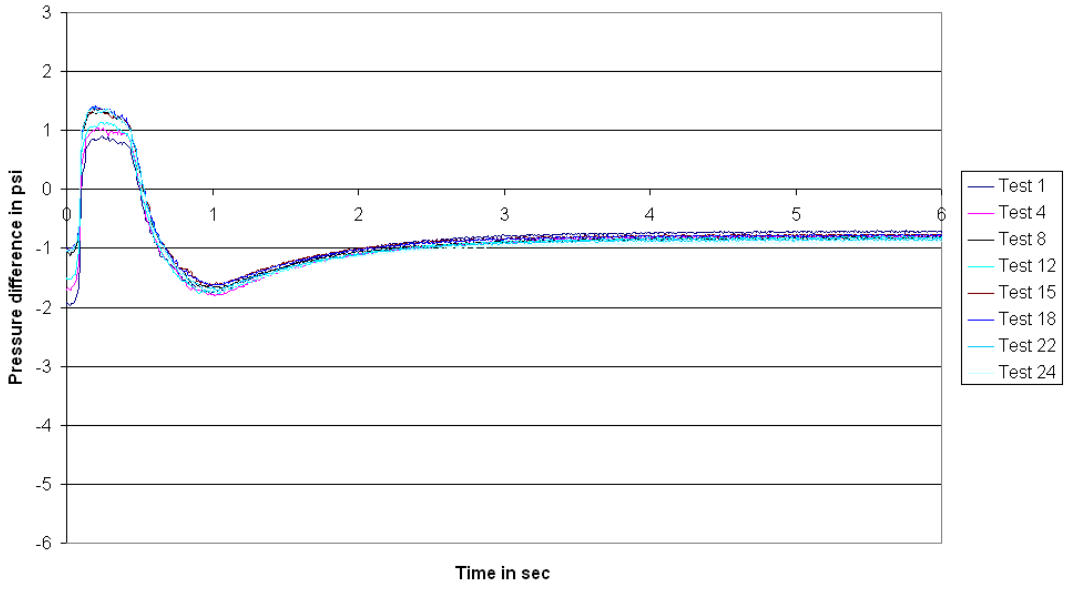

A

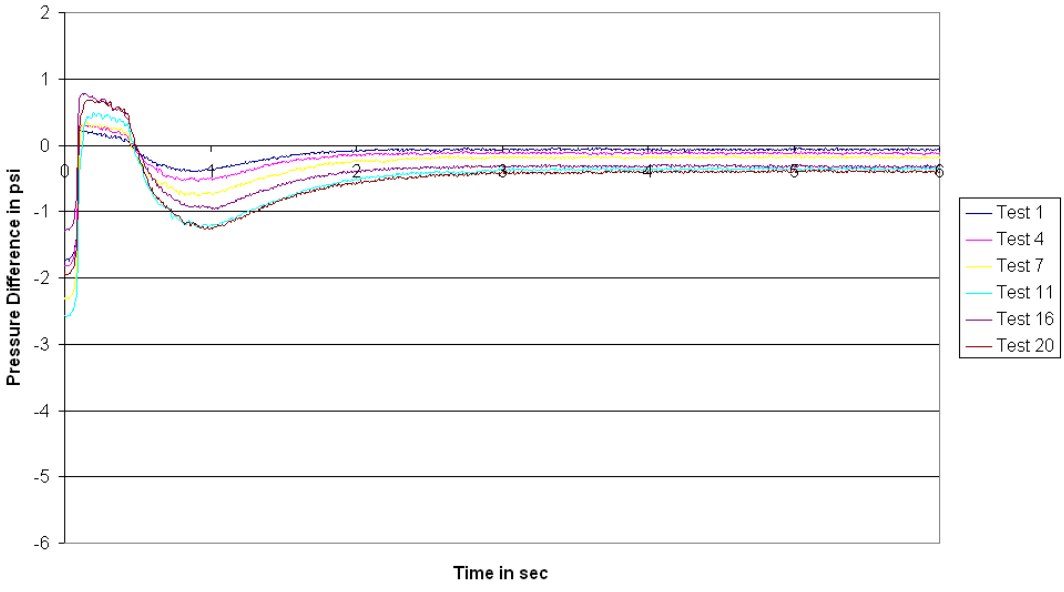

B

Figure 6.5.7.
Lanxide filter (plot A) vs. Pall filter (plot B)
Comparative plot of pressure difference (ΔP: Pf-Pc) change during regeneration
95 psi regeneration pressure, 5 cm/s face velocity, 20 minute build-up time

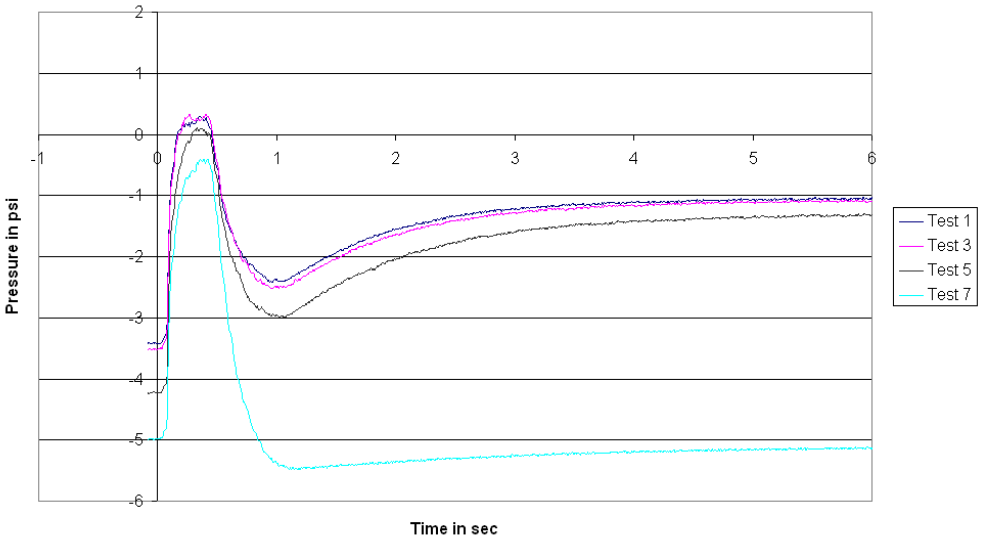

A

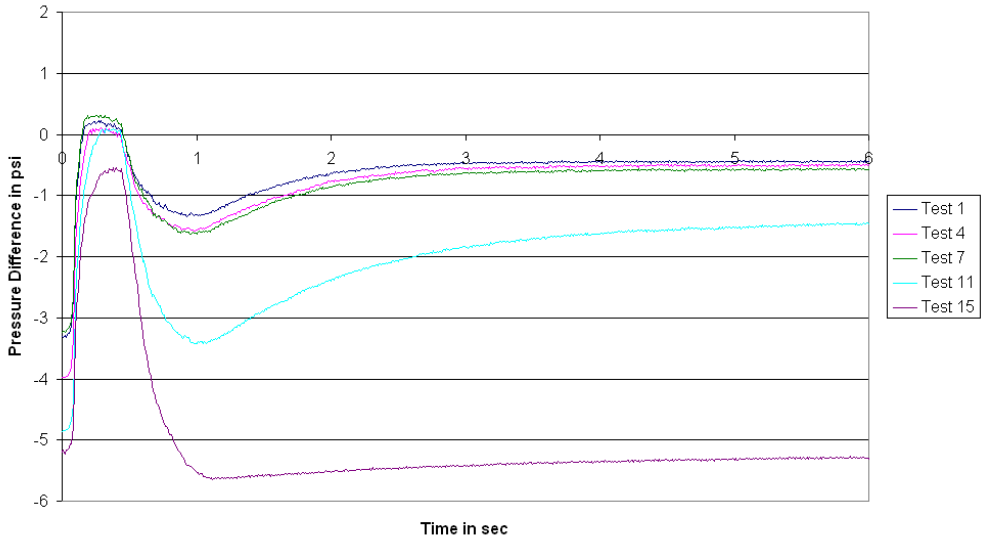

B

Figure 6.5.8.
Lanxide filter (plot A) vs. Pall filter (plot B)
Comparative plot of pressure difference (ΔP: Pf-Pc) change during regeneration
95 psi regeneration pressure, 7 cm/s face velocity, 20 minute build-up time

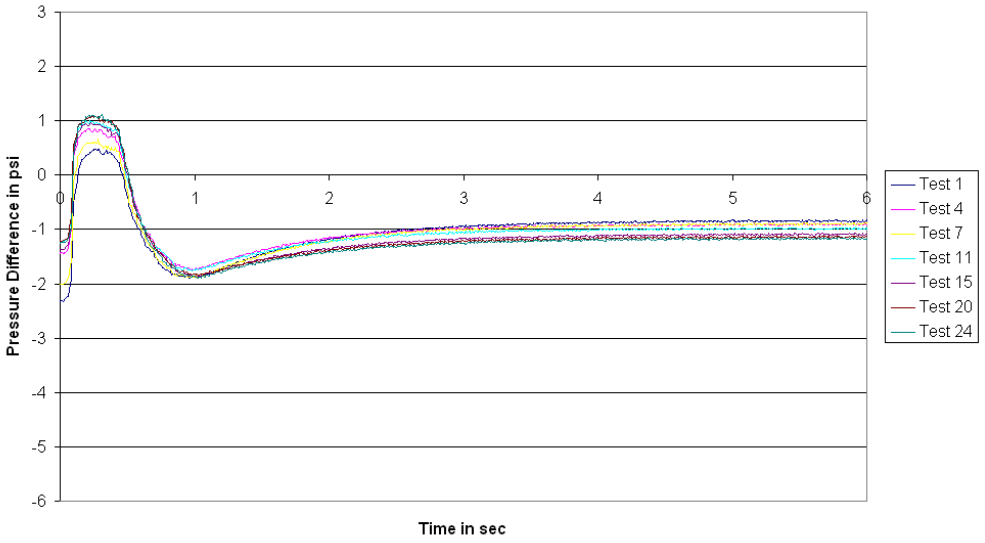

A

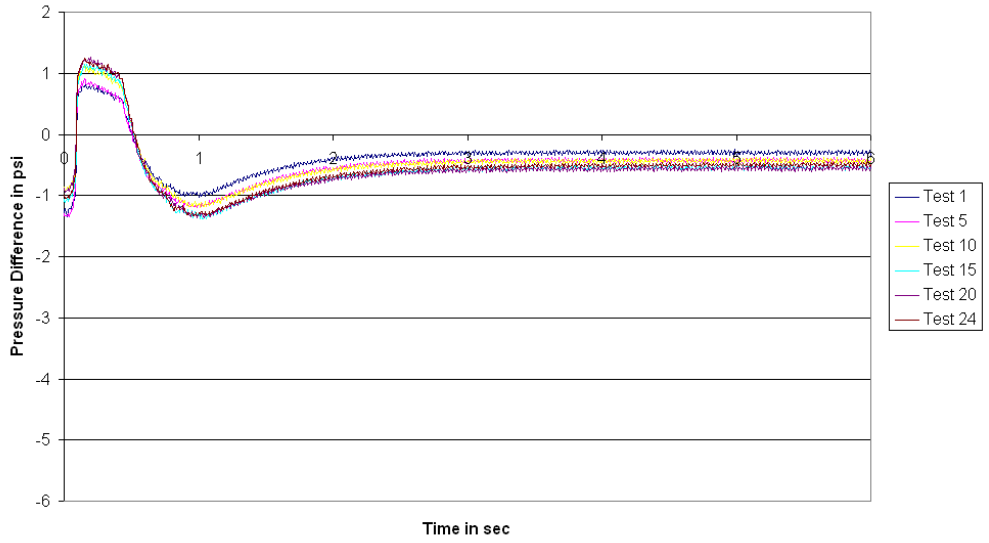

B

Figure 6.5.9.
Lanxide filter (plot A) vs. Pall filter (plot B)
Comparative plot of pressure difference (ΔP: Pf-Pc) change during regeneration
80 psi regeneration pressure, 5 cm/s face velocity, 20 minute build-up time

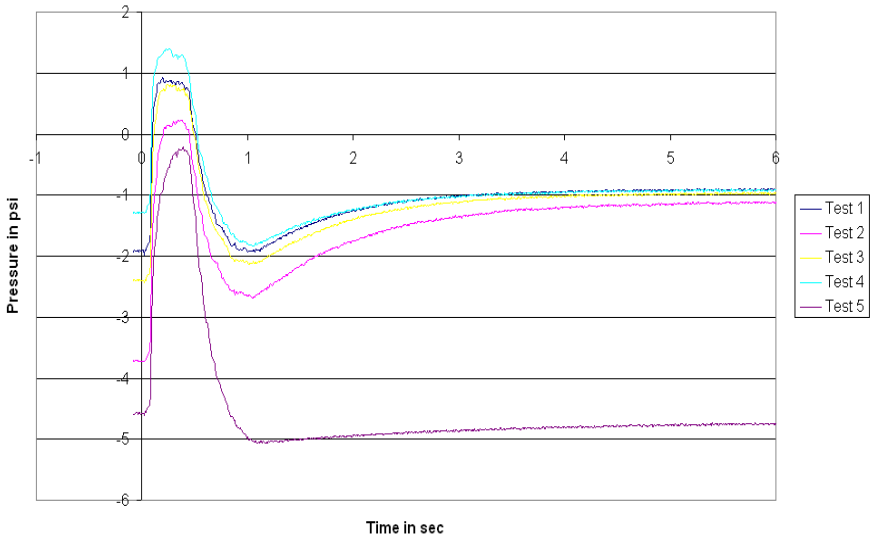

A

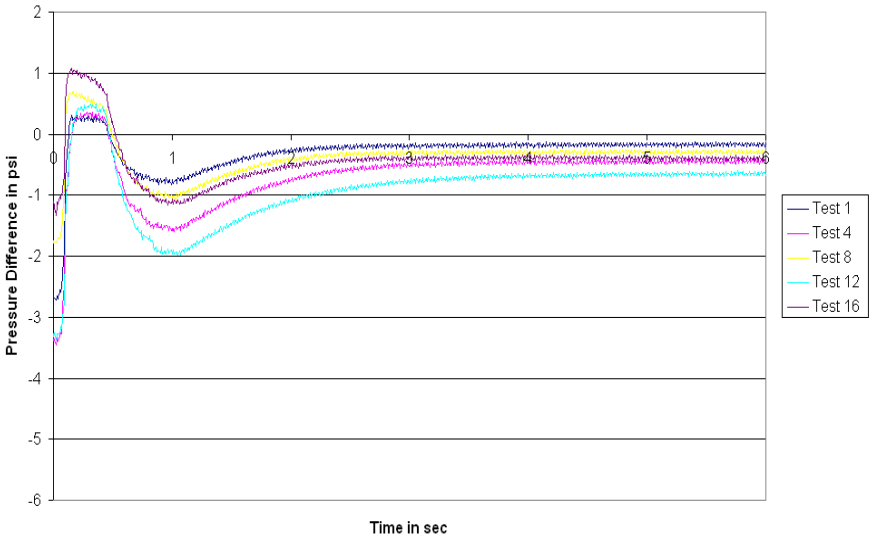

B

Figure 6.5.10.
Lanxide filter (plot A) vs. Pall filter (plot B)
Comparative plot of pressure difference (ΔP: Pf-Pc) change during regeneration
95 psi regeneration pressure, 5 cm/s face velocity, 45 minute build-up time

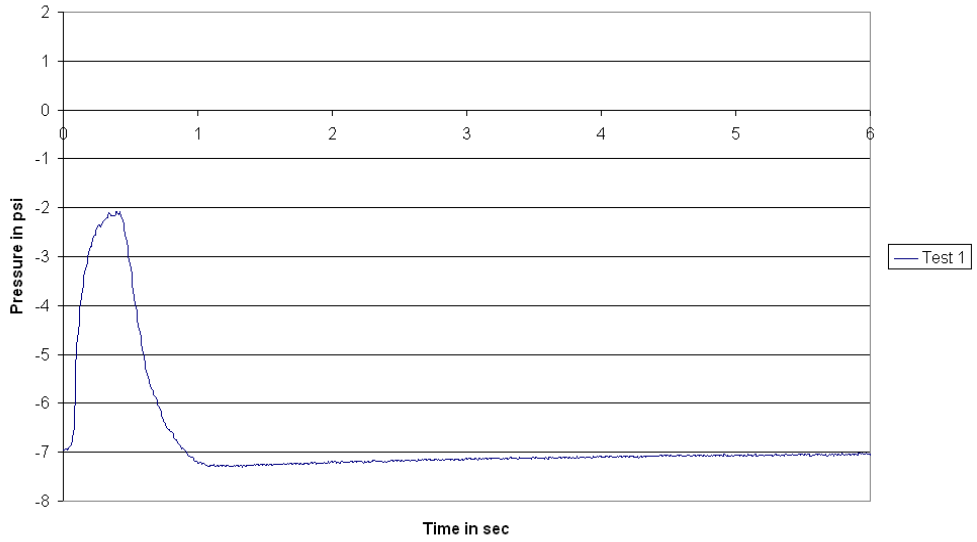

A

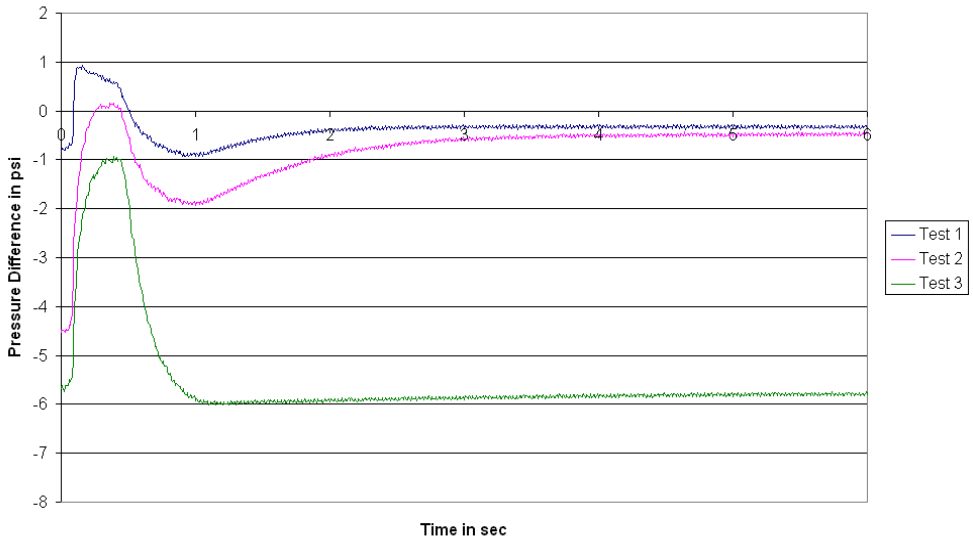

B

Figure 6.5.11.
Lanxide filter (plot A) vs. Pall filter (plot B)
Comparative plot of pressure difference (ΔP: Pf-Pc) change during regeneration
95 psi regeneration pressure, 5 cm/s face velocity, 90 minute build-up time

For all the ΔP factors discussed in the following sub-sections, the associated plots are presented in the appendices A, B and C. Appendix A contains the comparative plots for the 80 psi regeneration pressure condition. Appendix B contains plots for the BASE (5cm/s) and the 7 cm/s face velocity conditions. Appendix C contains plots for the 45 min and the 90 min build-up conditions.

a. $\Delta P_{initial}$

The $\Delta P_{initial}$ value for both the Pall and Lanxide filters are about the same in nearly all conditions. In the 80 psi condition, the pressure drop is lower for Pall filter compared to Lanxide filter. In the 45 min build-up condition the Lanxide filter and Pall filter show similar profiles, but it should be noted that the Pall filter lasted for 16 tests without stopping to regenerate, while the Lanxide filter stopped regenerating in its 5^{th} test. There are no significant differences in the initial pressure drop under the same build-up conditions.

b. ΔP_{final}

The ΔP_{final} value is an indicator of how effective the cleaning is after the regeneration. A low magnitude ΔP_{final} value indicates lesser resistance to flow, which means more efficient ash removal. In comparing the two filters, it should be noted that the Pall filter has inherently a high permeability and low pressure drop, compared to the Lanxide filter. Since the permeability of the filter is a summing factor in the ΔP_{final} value, the results discussed should account for this also. The Pall filter, when compared to Lanxide filter has lower ΔP-final value in all the conditions. Also it should be considered that the Pall filter lasted more number of cycles, especially in the 7 cm/s face velocity, the

45 min build-up and the 90 min build-up conditions. The results on a first glance indicate that the Pall filter is cleaner relative to the Lanxide filter. The cleaning factor (F) should be able to determine this better as it looks at a relative scale based on the pressure drop of a clean filter.

c. ΔP_{max}

The $\Delta P_{max}$is slightly higher for the Lanxide filter in nearly all cases the comparative study was performed. In the 80 psi condition, the results were reversed with the Pall filter displaying higher ΔP_{max} compared to Lanxide filter. But the value in Pall filter was only marginally higher. While testing the same filter with different parametric conditions it was observed that the easier the regeneration process was the higher the ΔP-maximum value. It is possible the low permeability may have a direct effect on the pressure difference between the filter and the chamber. In this study it has been observed that the Pall filter performed much better overall in terms of the number of cycles the filter lasts without building up residual ash.

d. ΔP_{min}

The ΔP_{min} values is associated with the regeneration process because of the direct relation ship between its magnitude and the re-entrainment velocity. If its magnitude is low the re-entrainment velocity is expected to be low. The magnitude of the the ΔP_{min} values for the Pall filter is lower compared to Lanxide filter in all the tests compared. It is expected that Lanxide filter to have more particle re-entrained during the transient phase between regeneration and filtration.

e. Efficiency η:

On studying the plots A5, A6, B5, B6, C5 and C6, which are the comparative efficiency plots for Pall and Lanxide filters, it is observed that the Pall filter has higher efficiencies in all test conditions. The Pall filter builds thicker ash during filtration and therefore has higher initial ΔP. The Pall filter has lower final pressure difference (ΔP_{final}) and both these factors combined causes higher efficiencies. It is important to note that the efficiency is a measure of the resistance overcome by the regeneration pulse.

f. Cleaning Factor F:

The cleaning factor when measured with respect to a new filter (F_N) and the cleaning factor when measured with respect to a cleaned filter (F_C),are plotted for all the conditions (refer Figures A7, A8, B7, B8, C7 and C8). The factor F is a measure of how clean the filter is relative to its original conditions, and is the ratio of final pressure drop to the pressure drop across a clean filter. Since it is measured in the form of pressure difference, a higher pressure difference indicates more resistance. The higher the F value the higher the residual ash relative its original condition. The Pall filter has either lower or equal F values compared to Lanxide filter. Even in cases where the values are equal the Pall filter represents a longer number of test cycles, example 45 minute build-up condition: Pall - 16 tests, continued regenerating; Lanxide - 5 tests, stopped regenerating. In most other cases the Pall filter has lower F value and this indicates efficient cleaning.

6.5.5 Distribution of particles less than 100 microns during regeneration

The particle count observed in the following test conditions, (base, 7cm/s face velocity, and the 45 & 90 minute build-up) is lower for the Pall filter compared to Lanxide filter. Pall filter has desirable characteristics in these conditions since more particle count means more probability for re-entrainment. The low particle count in Pall filter can be attributed to its thick ash build-up and regeneration in all these test conditions.

The particle count is high and about the same in both the filters for the 80 psi regeneration conditions. For this particular condition the ash the regeneration type is thin or partially thick-thin type in both filters. This type of regeneration is not desirable.

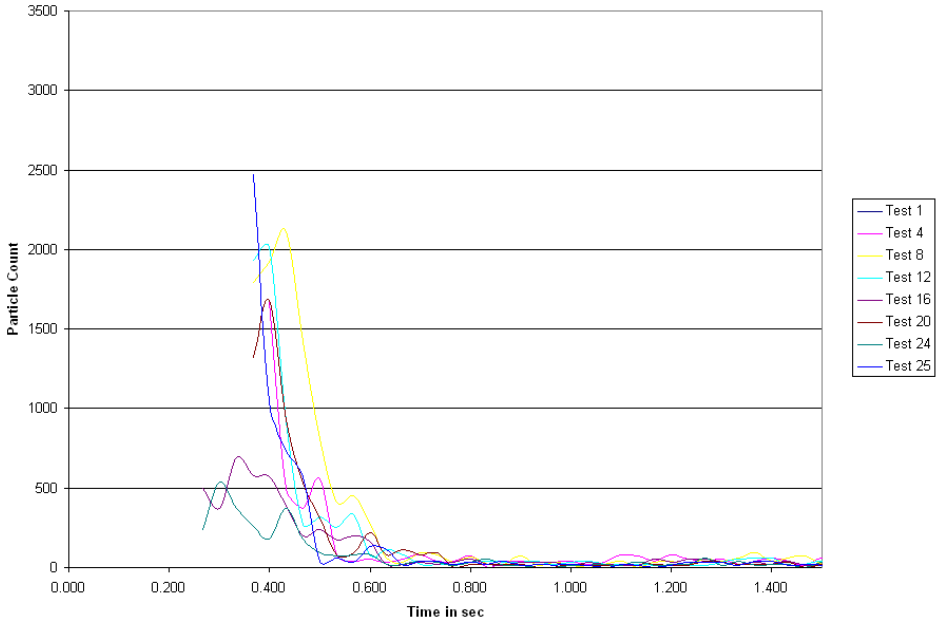

A

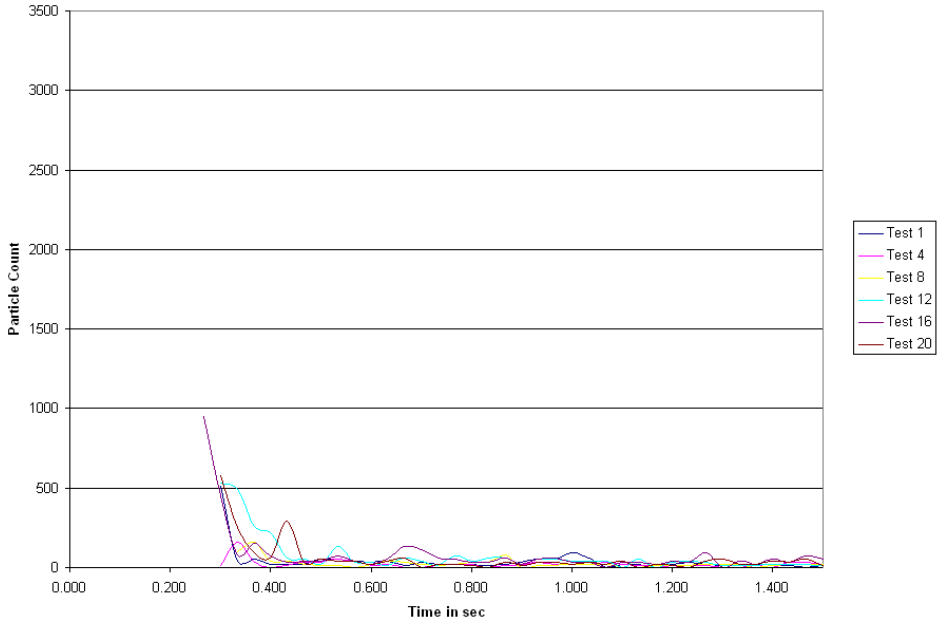

B

Figure 6.5.12.
Lanxide filter (plot A) vs. Pall filter (plot B)
Particle count: less than 100 microns
95 psi regeneration pressure, 5 cm/s face velocity, 20 min build-up time

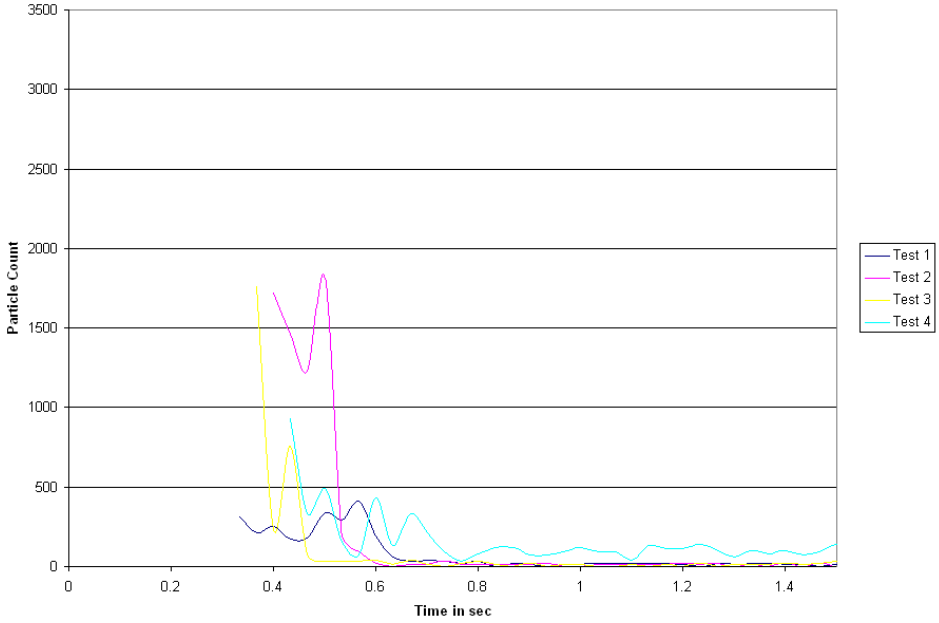

A

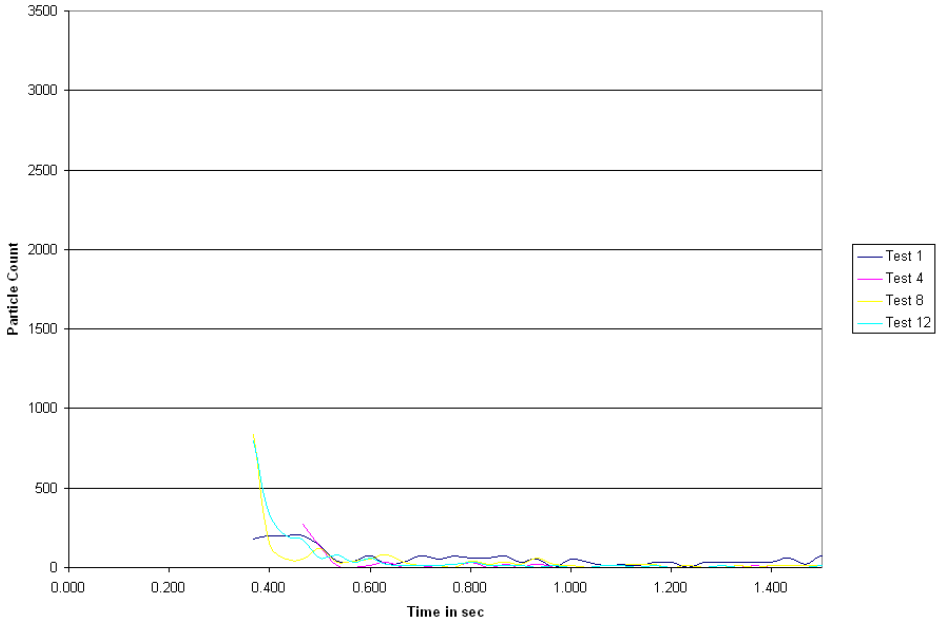

B

Figure 6.5.13.
Effect of high face velocity on Lanxide filter (plot A) vs. Pall filter (plot B)
Particle count: less than 100 microns
95 psi regeneration pressure, 7 cm/s face velocity, 20 min build-up time

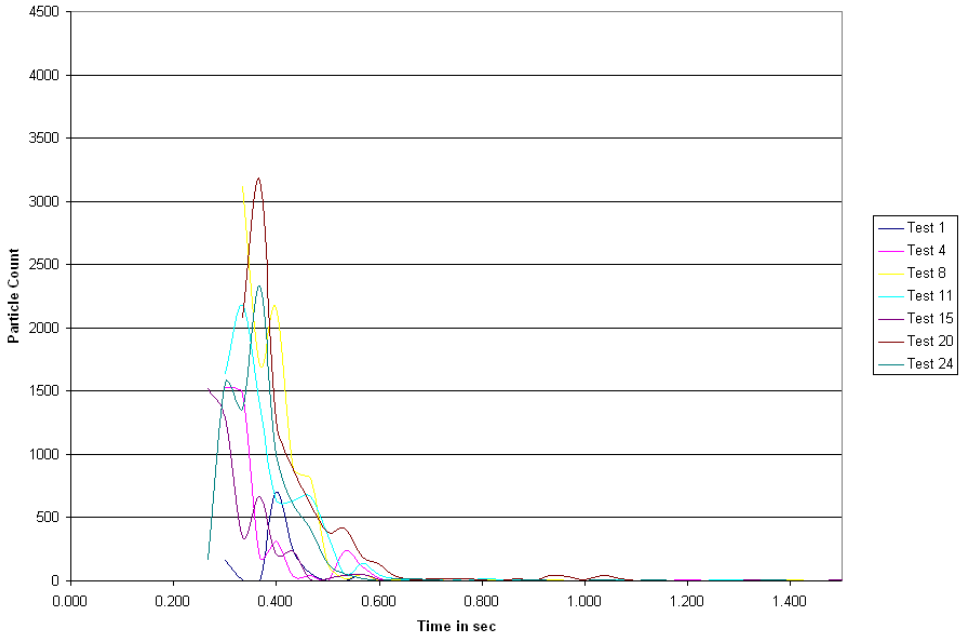

A

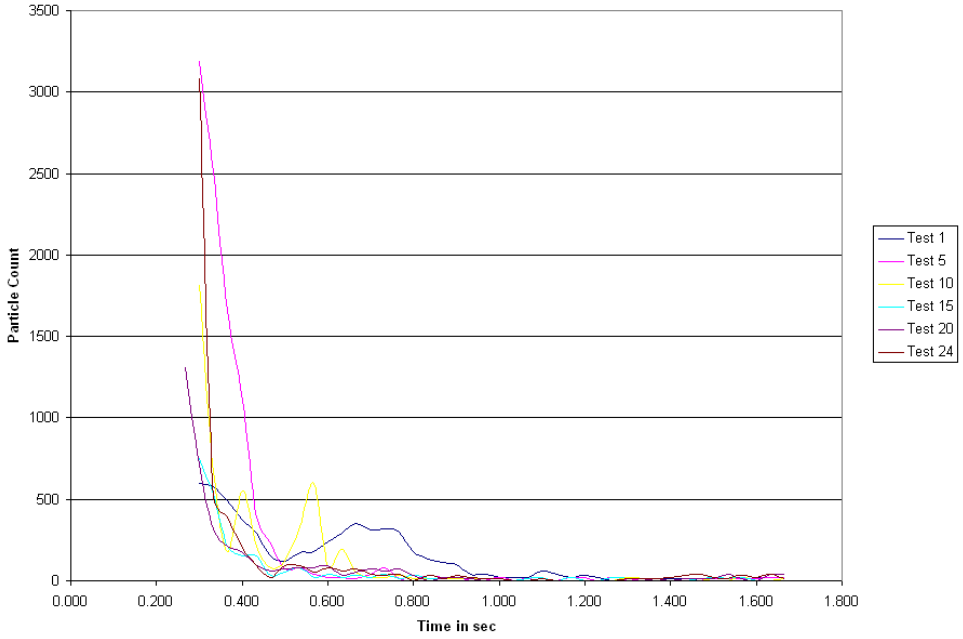

B

Figure 6.5.14.
Effect of low reg. pressure on Lanxide filter (plot A) vs. Pall filter (plot B)
Particle count: less than 100 microns
80 psi regeneration pressure, 5 cm/s face velocity,20 min build-up time

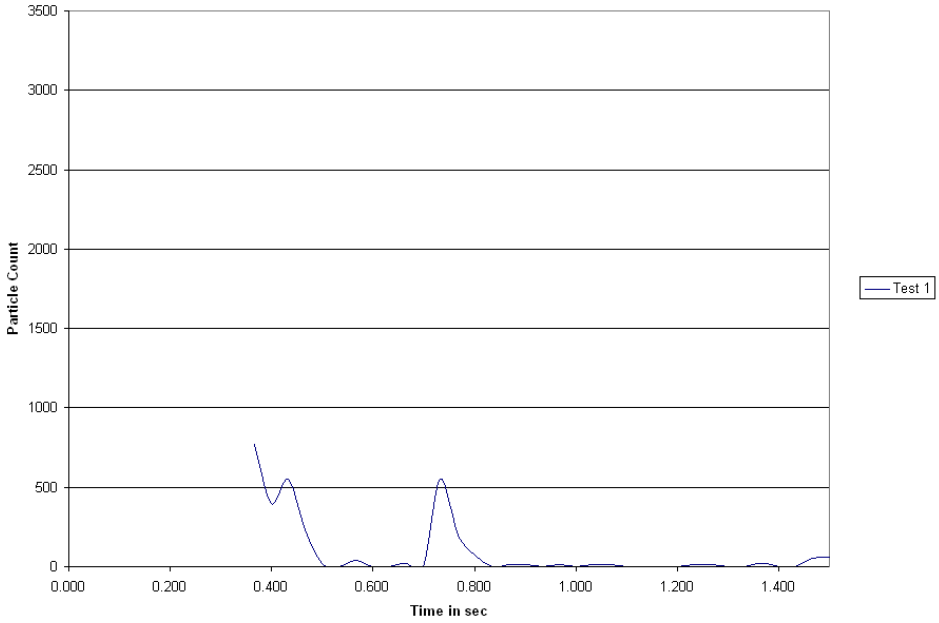

A

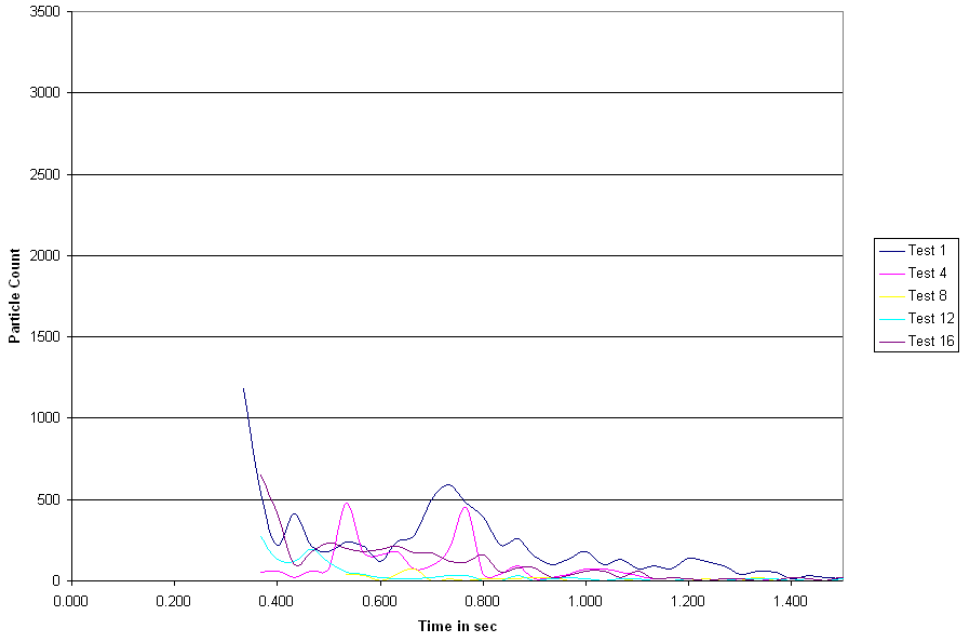

B

Figure 6.5.15.
Effect of build-up time on Lanxide filter (plot A) vs. Pall filter (plot B)
Particle count: less than 100 microns
95 psi regeneration pressure, 5 cm/s face velocity, 45 min build-up time

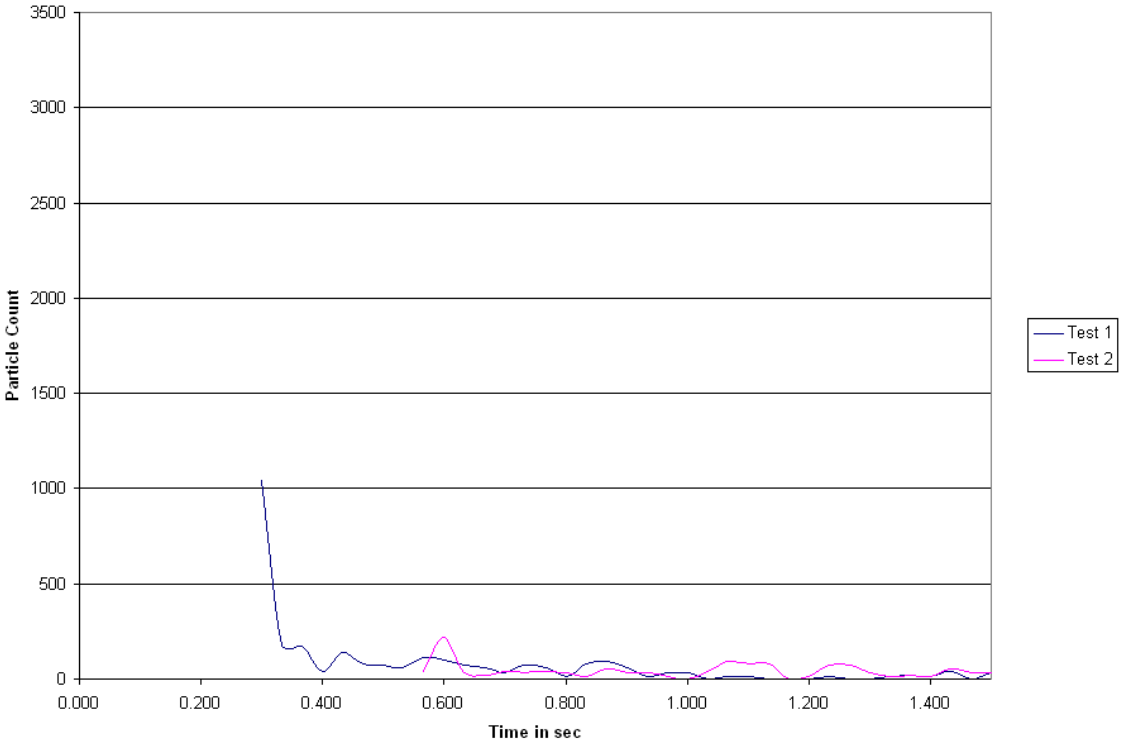

Figure 6.5.16.
Effect of build-up time on Lanxide filter (plot A) vs. Pall filter (plot B)
Particle count: less than 100 microns
95 psi regeneration pressure, 5 cm/s face velocity, 90 min build-up time

NOTE:
In test 1 for 90 min condition Lanxide filter did not regenerate totally, so particle count is NOT available.

6.5.6 The thickness of ash deposit during build-up

Pall filter builds up thicker ash compared to Lanxide filter, in general. This indicated that the permeability characteristics might have an influence on the ash build-up.

6.5.7 The type of regeneration

The type of regeneration is predominantly thick type in Pall filter except for the 80 psi regeneration condition in which the regeneration was partially thick/thin type and thin type regeneration. Lanxide filter exhibited thin type regeneration in the base and the 80 psi regeneration pressure conditions. In both these conditions the flow conditions caused thin ash build-up. The thin type regeneration is not desirable as they leave thin residual layers. Both filters built thick ash for the 7 cm/s face velocity, and the 45 & 90 minute build-up time conditions.

6.5.8 Crack initiation time

The crack initiation time is about the same for both Pall and Lanxide filters, for all the conditions observed.

6.5.9 Surface quality:

The surface quality deterioration rate for the Pall filter is much lower when compared to the Lanxide filter. The whole objective behind all the testing is to identify conditions for which the residual ash accumulation and surface quality deterioration rate is low. From this perspective the behavior of Pall filter is desirable compared to Lanxide

filter. The details are presented in Table 6.5.1 and also images of surface quality are presented in Figures 6.5.17 to 6.5.26.

In the number of test cycles each filter lasted with similar amount of deterioration the Pall filter showed better performance. From Table 6.5.1 the number of test cycles each filter lasted gives ample evidence of this. It is more evident in the 7 cm/s face velocity condition, the 45 min and the 90 min build-up conditions. In these conditions the Pall filter lasted for longer number of cycles (without stopping to regenerate), when compared to Lanxide filter. The surface quality deterioration is another factor in which the Pall filter performed better than the Lanxide filter. Pall filter showed much lower surface deterioration under the same testing conditions.

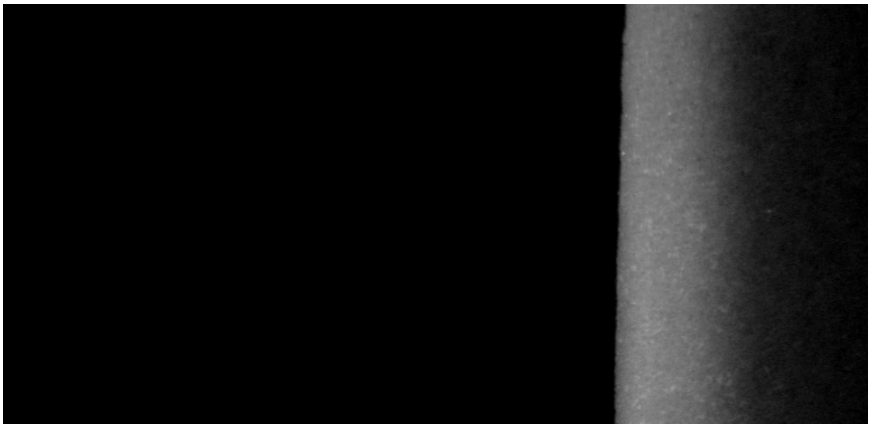

Test 1
Clean Filter

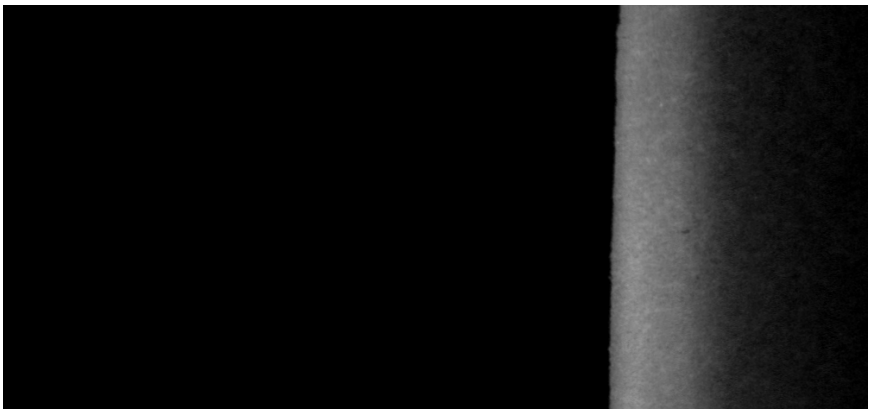

Test 4
Clean Filter

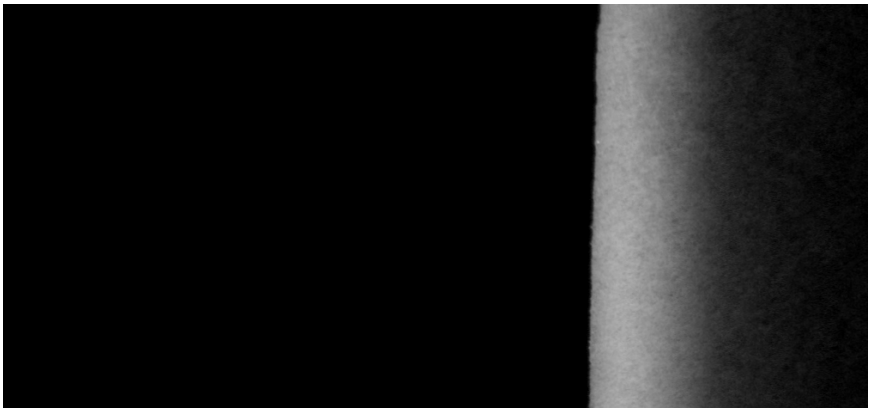

Test 8
Slightly unclean
Filter

Figure 6.5.17a
Surface quality during long term test cycles - Pall filter
95 psi regeneration pressure, 5 cm/s face velocity, 20 min build-up time. (Contd.).

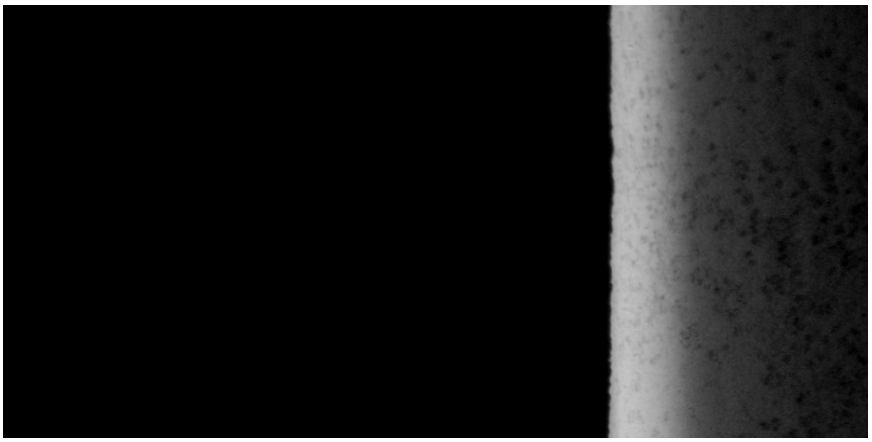

Test 12
Unclean Filter

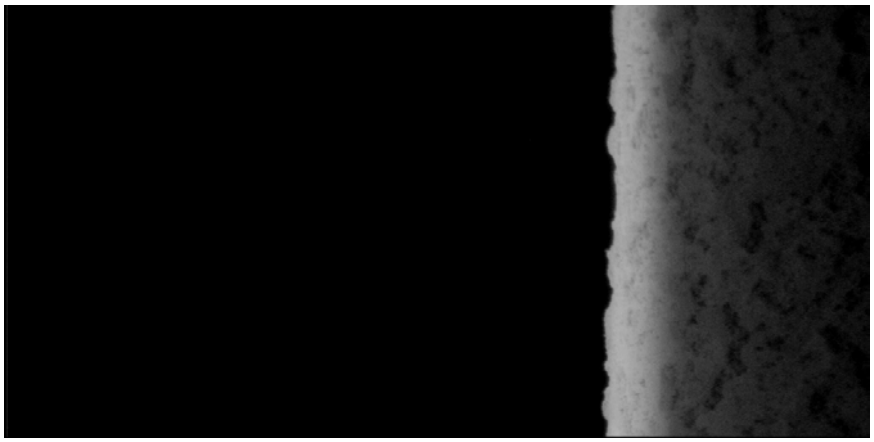

Test 16
Residual Ash

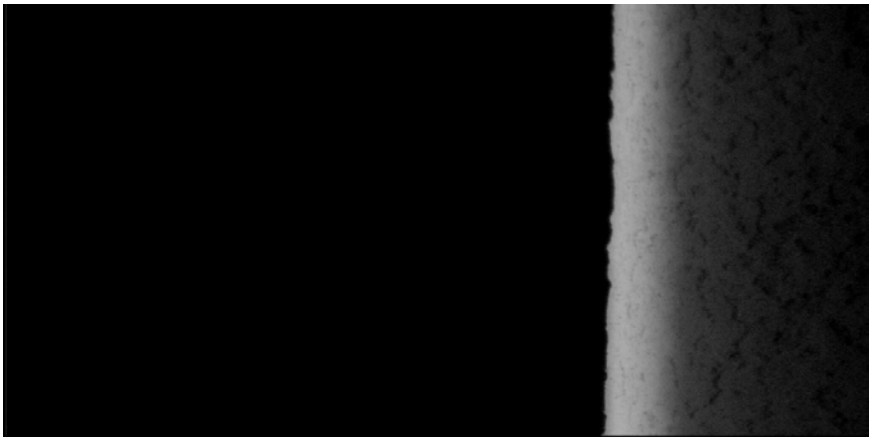

Test 20
Residual Ash

Figure 6.5.17b
Surface quality during long term test cycles - Pall filter
95 psi regeneration pressure, 5 cm/s face velocity, 20 min build-up time.

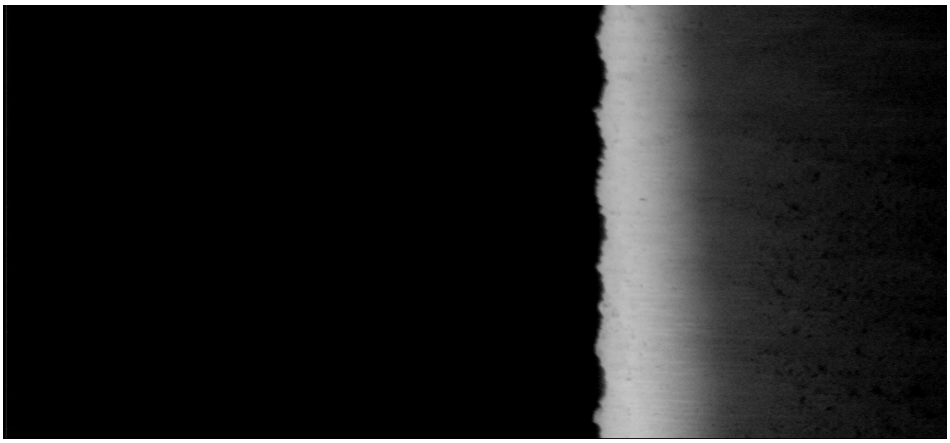

Test 1
Clean Filter

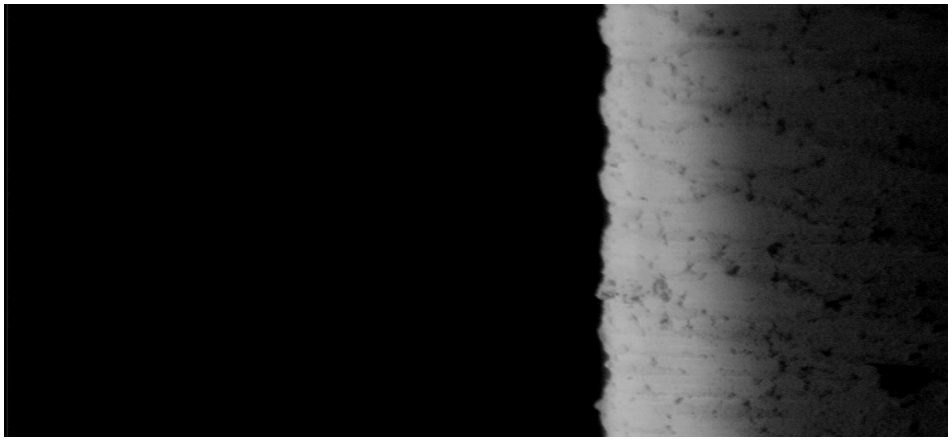

Test 4
Little
Residual

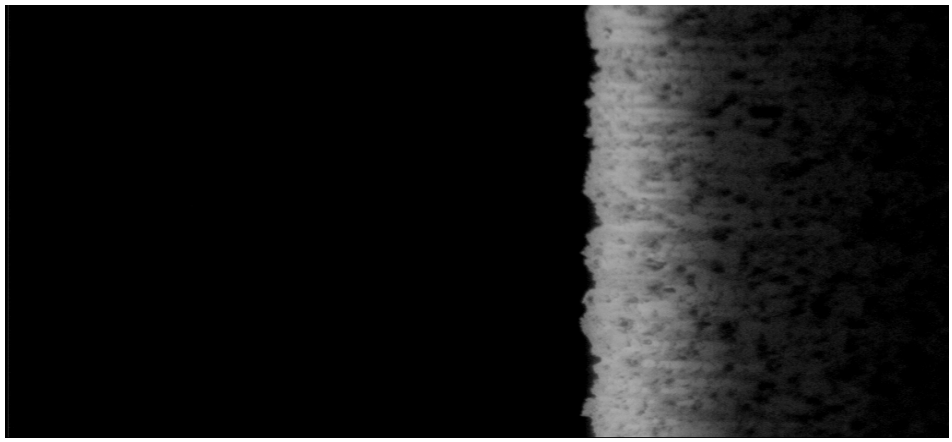

Test 8
Residual ash
typical of thin
ash

Figure 6.5.18a
Surface quality during long term test cycles - Lanxide filter
95 psi regeneration pressure, 5 cm/s face velocity, 20 min build-up time. (Contd.)

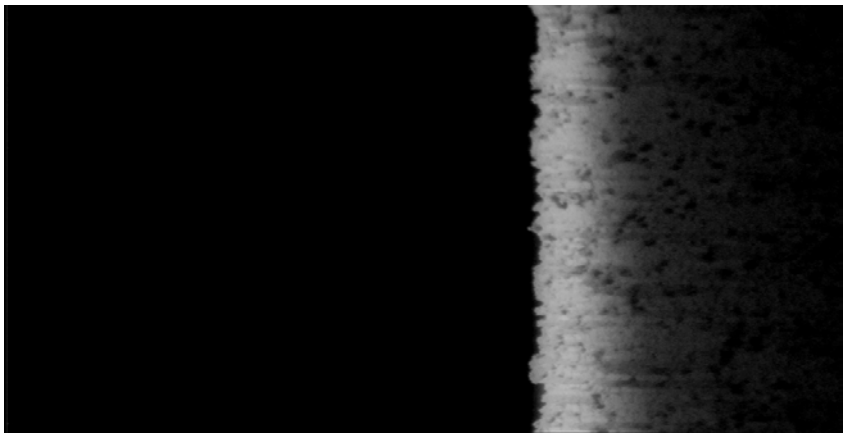

Test 16
More thin
ash type

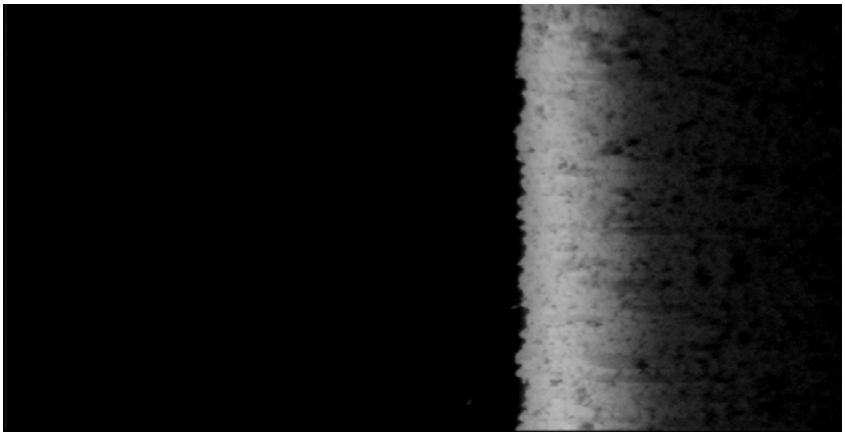

Test 20
Dirty
Filter

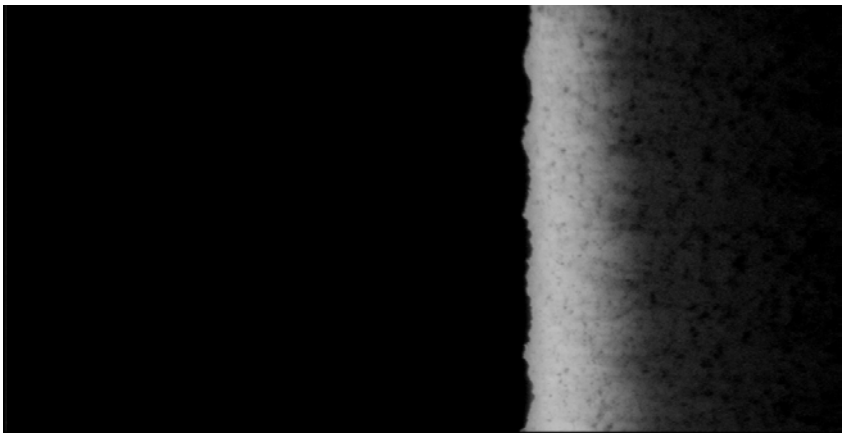

Test 25
Dirty
Filter

Figure 6.5.18b
Surface quality during long term test cycles - Lanxide filter
95 psi regeneration pressure, 5 cm/s face velocity, 20 min build-up time

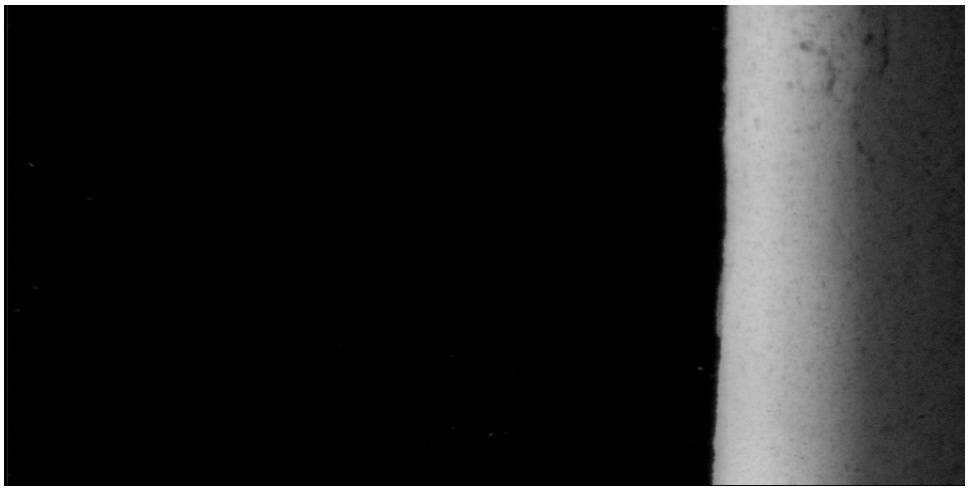

Test 1
Slightly
unclean Filter

Test 4
Residual Ash
Patch

Figure 6.5.19a
Surface quality during long term test cycles - Pall filter
95 psi regeneration pressure, 7 cm/s face velocity, 20 min build-up time. (Contd.)

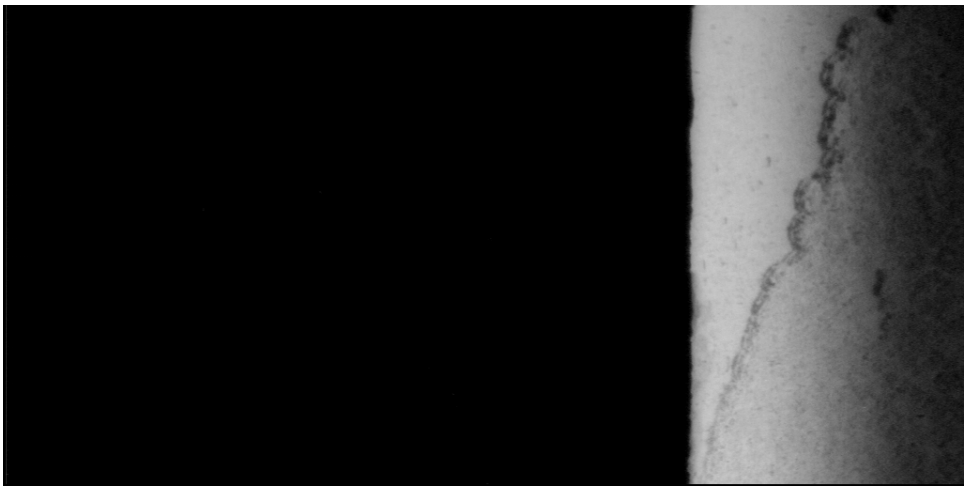

Test 8
Residual Ash
Patch

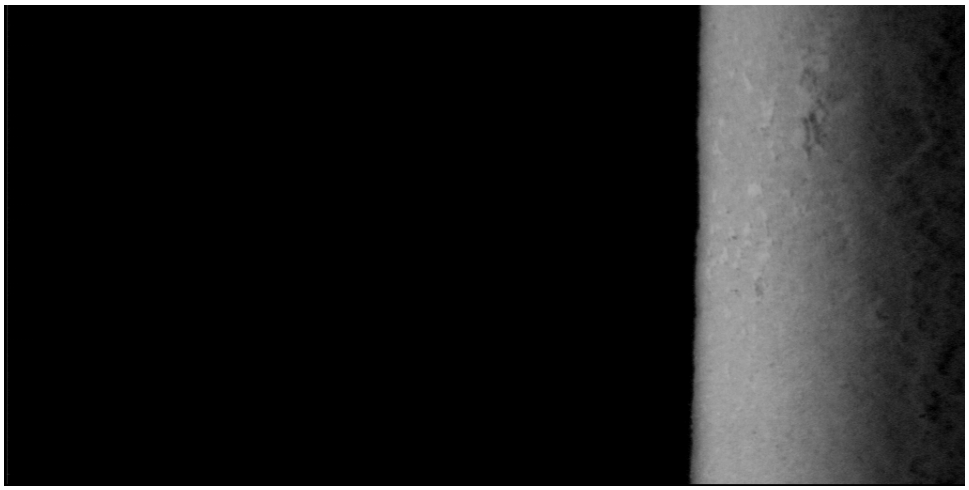

Test 12
Small Patchy Residuals

Figure 6.5.19b
Surface quality during long term test cycles - Pall filter
95 psi regeneration pressure, 7 cm/s face velocity, 20 min build-up time.

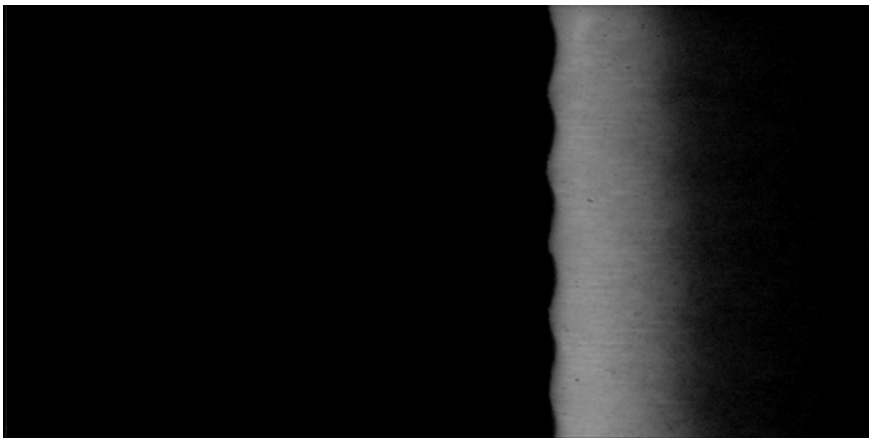

Test 1
Clean Filter

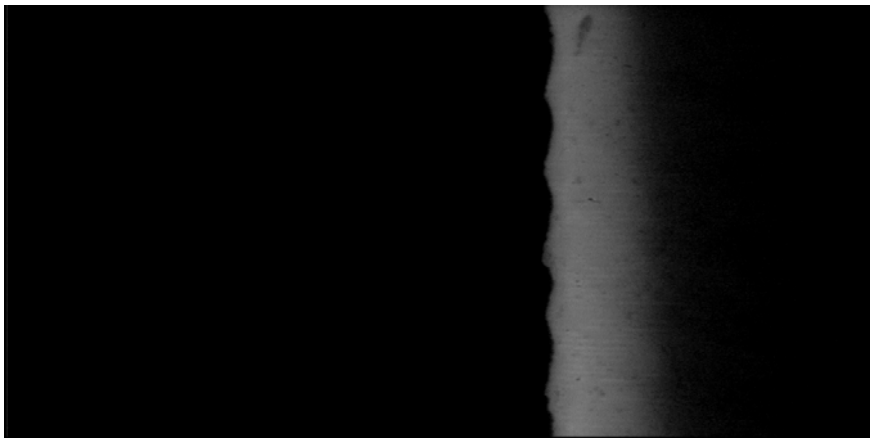

Test 3
Some Residual
Ash

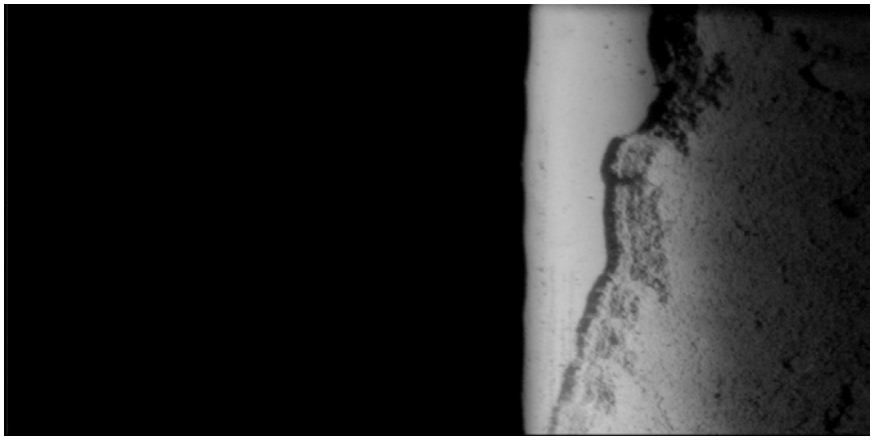

Test 4
Thick Residual
Layer

Figure 6.5.20a
Surface quality during long term test cycles - Lanxide filter
95 psi regeneration pressure, 7 cm/s face velocity, 20 min build-up time. (Contd.)

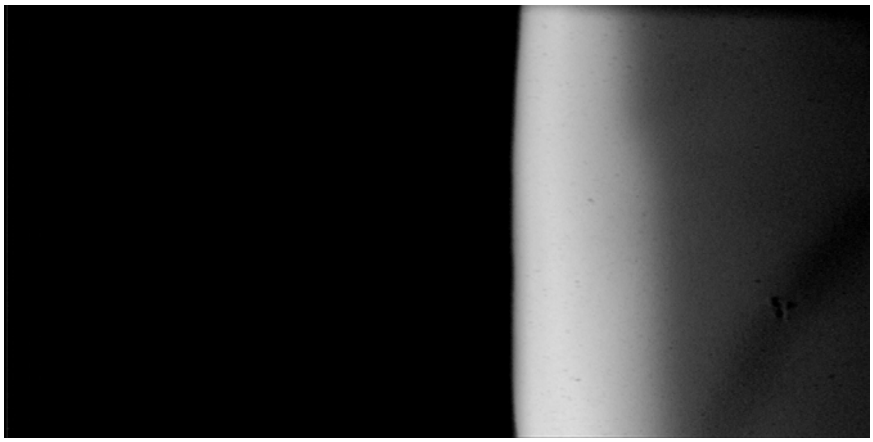

A

B

Test 6, No regeneration observed when comparing the images
A at 0.0 sec and B at 1.5 sec

Figure 6.5.20b
Surface quality during long term test cycles - Lanxide filter
95 psi regeneration pressure, 7 cm/s face velocity, 20 min build-up time.

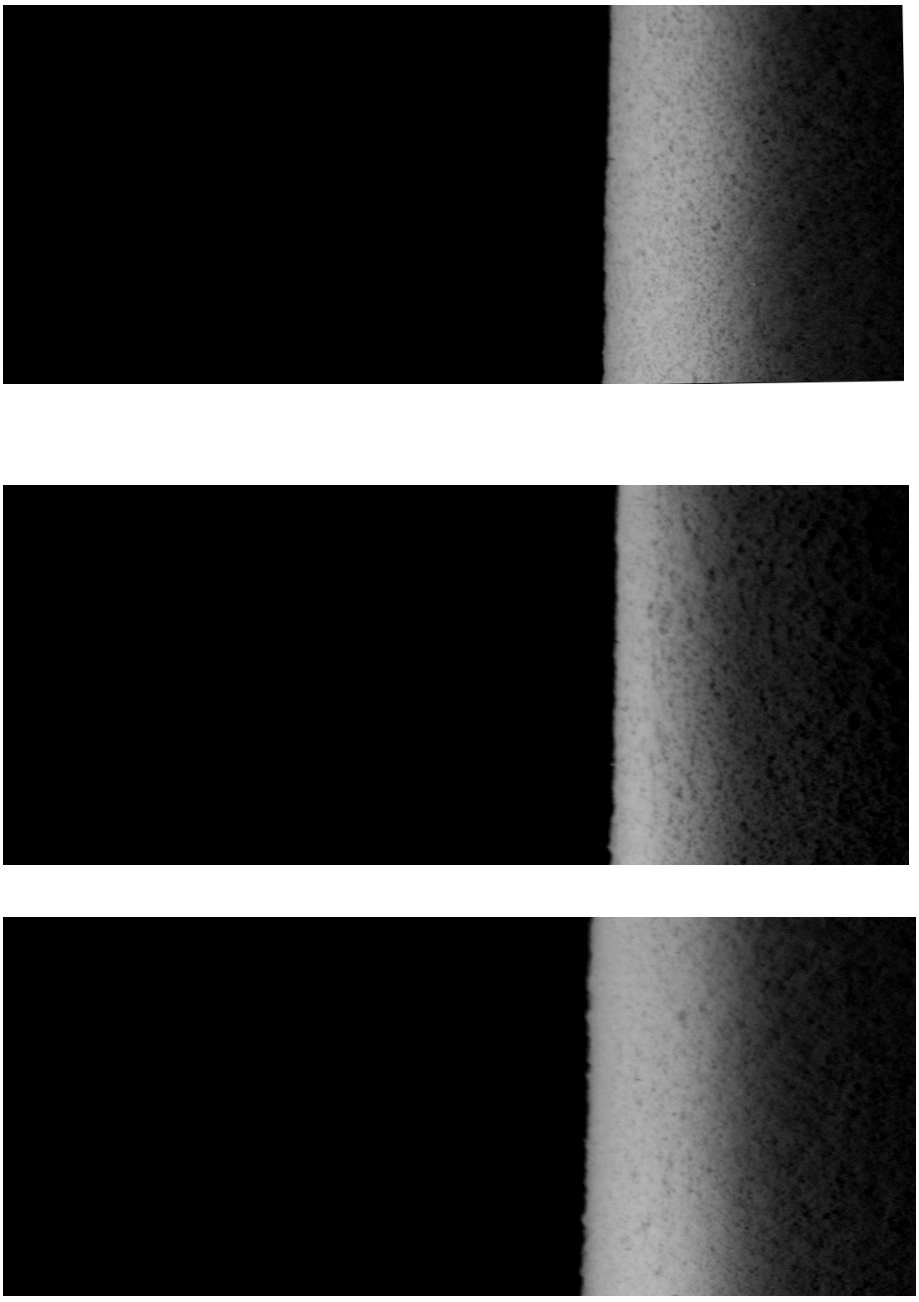

Figure 6.5.21a
Surface quality during long term test cycles - Pall filter
80 psi regeneration pressure, 5 cm/s face velocity, 20 min build-up time. (Contd.)

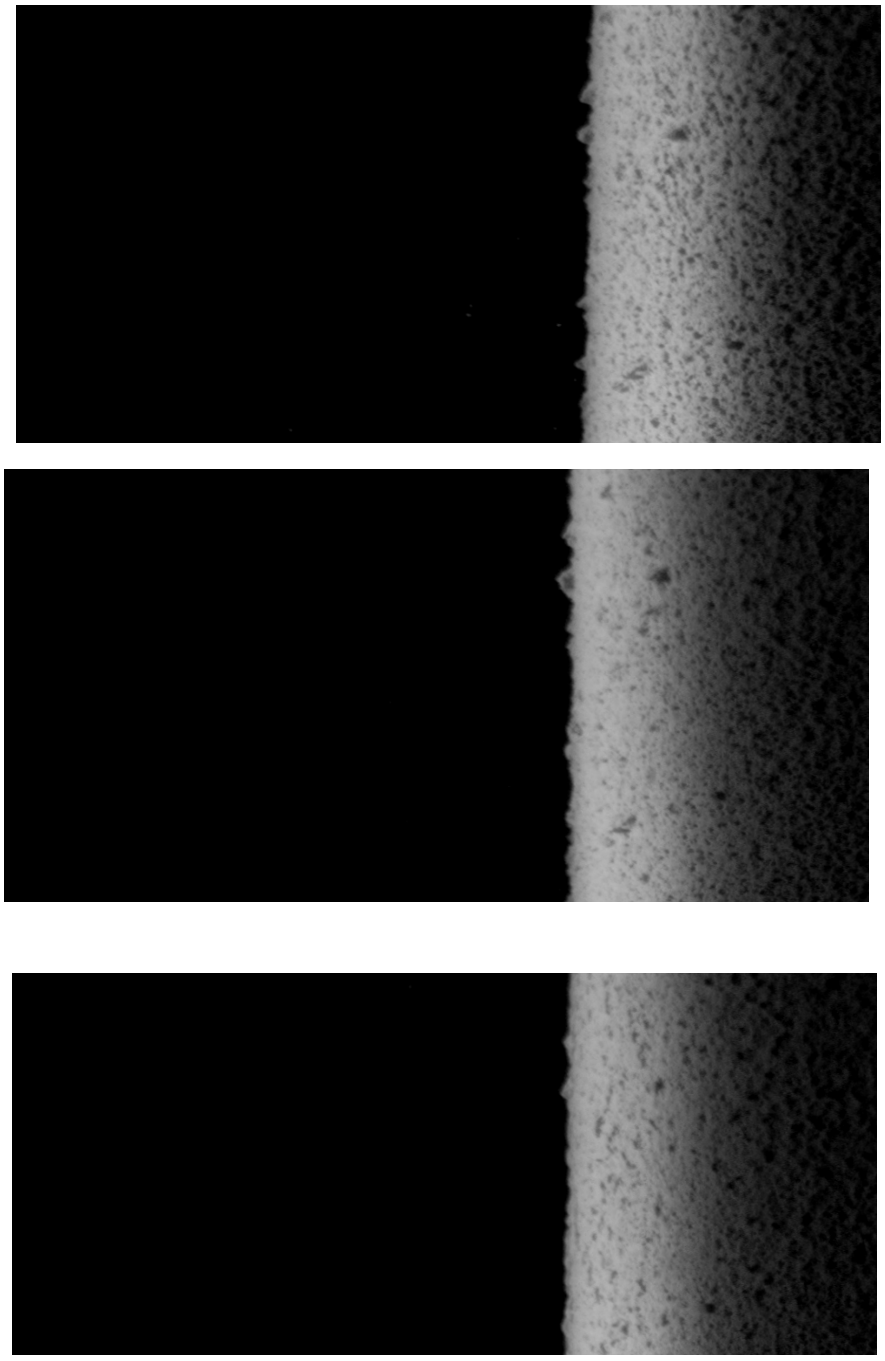

Figure 6.5.21b
Surface quality during long term test cycles - Pall filter
80 psi regeneration pressure, 5 cm/s face velocity, 20 min build-up time.

Test 1
Clean Filter

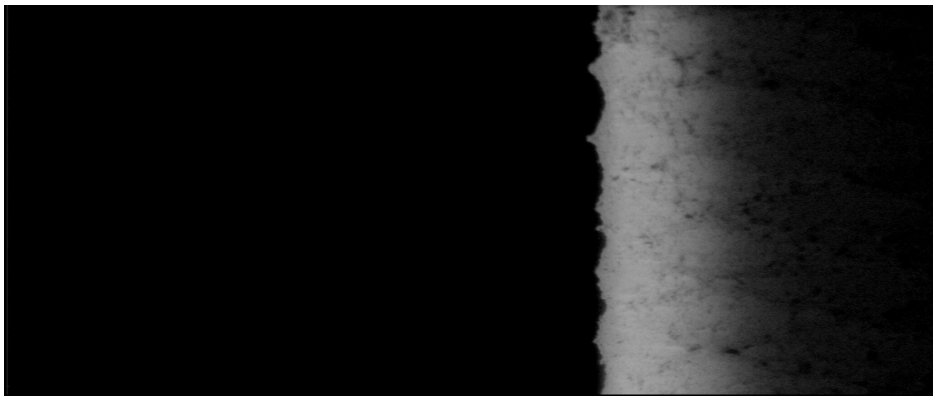

Test 4
Ash on Ridges

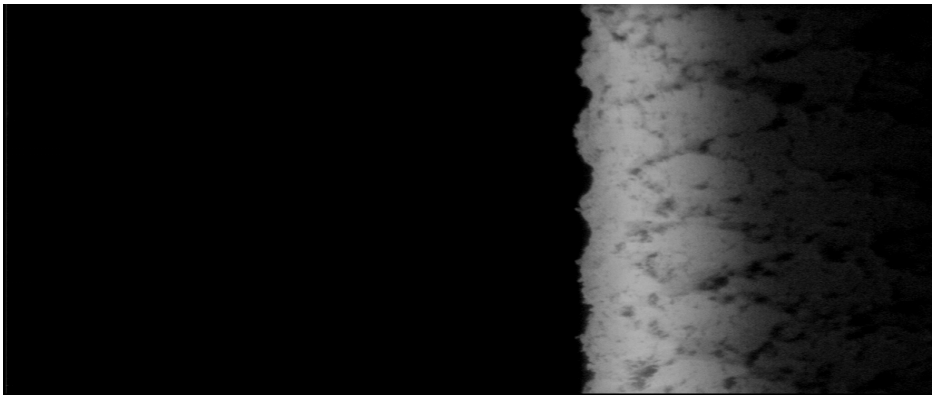

Test 8
Ash on
Ridges

Figure 6.5.22a
Surface quality during long term test cycles - Lanxide filter
80 psi regeneration pressure, 5 cm/s face velocity, 20 min build-up time. (Contd.)

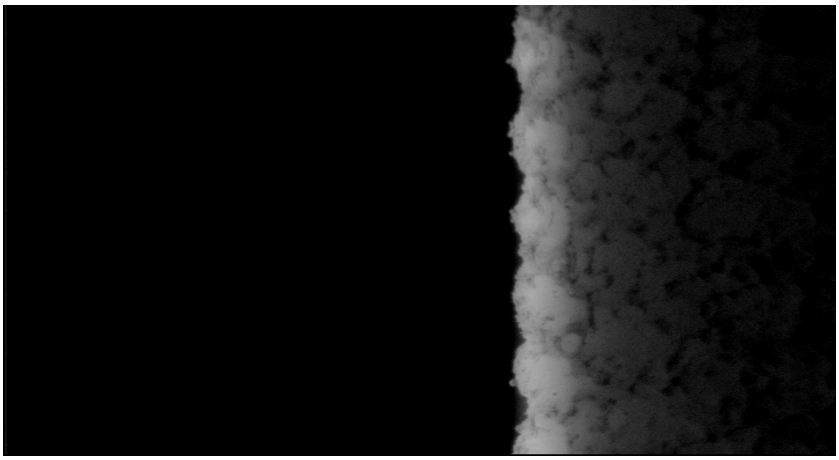

Test 15
More Ash on
Ridges

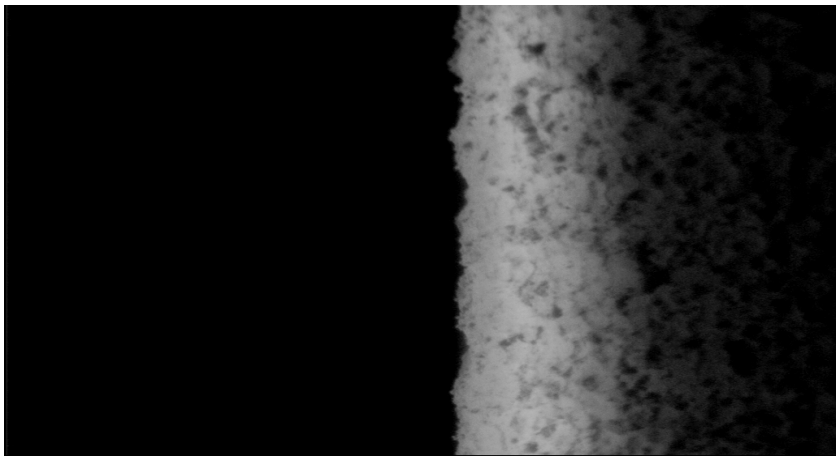

Test 24
Thin
Residual

Figure 6.5.22b
Surface quality during long term test cycles - Lanxide filter
80 psi regeneration pressure, 5 cm/s face velocity, 20 min build-up time.

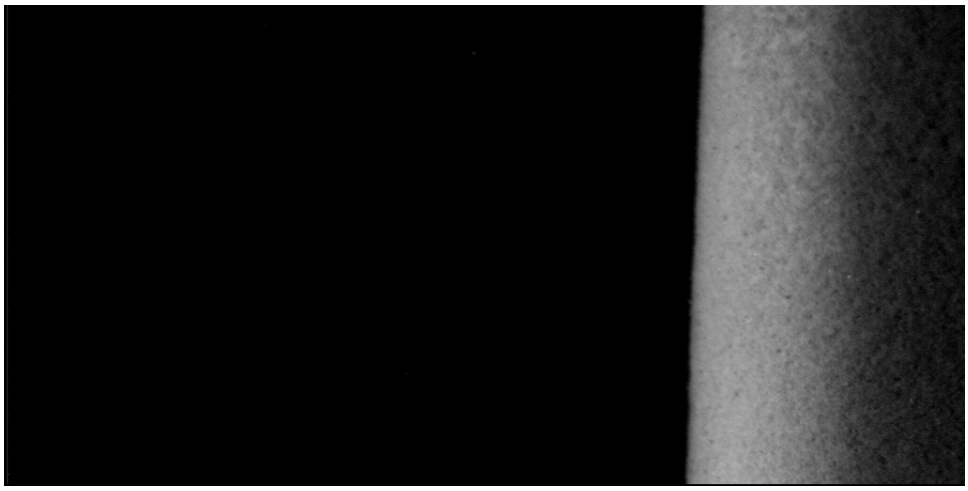

Test 1
Clean Filter

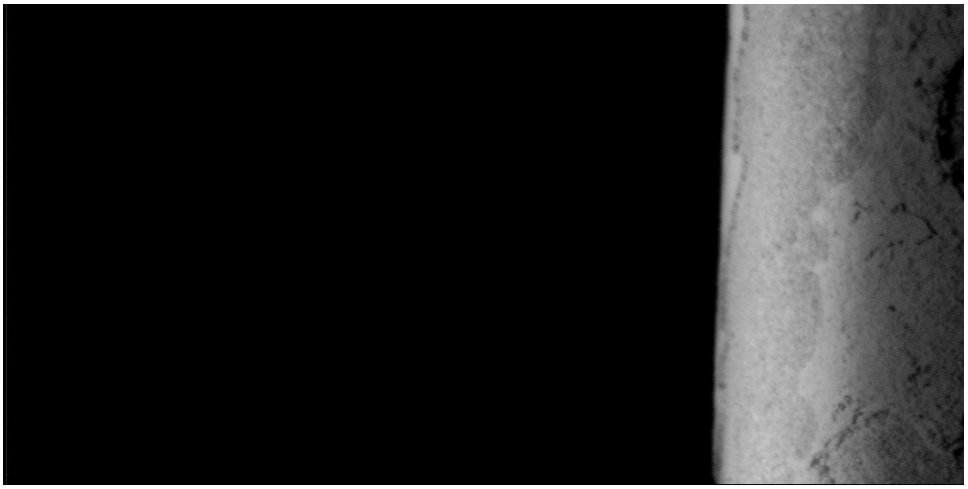

Test 8
Patchy Residuals

Figure 6.5.23a
Surface quality during long term test cycles - Pall filter
95 psi regeneration pressure, 5 cm/s face velocity, 45 min build-up time. (Contd.)

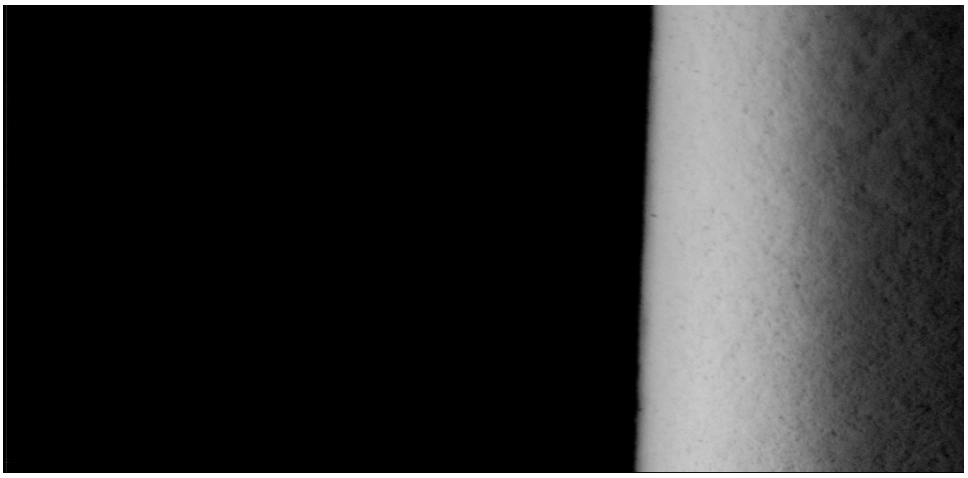

Test 12
Thin Residual Layer

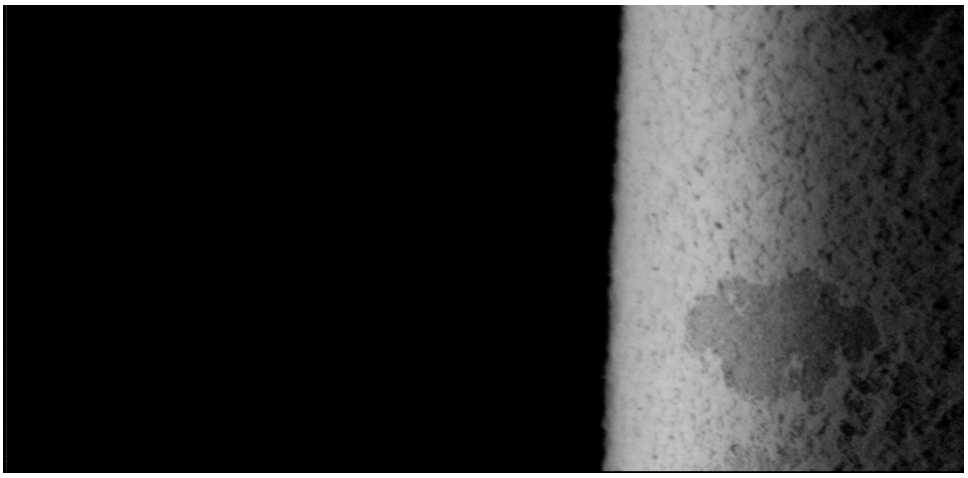

Test 16
Patchy Residuals

Figure 6.5.23b
Surface quality during long term test cycles - Pall filter
95 psi regeneration pressure, 5 cm/s face velocity, 45 min build-up time.

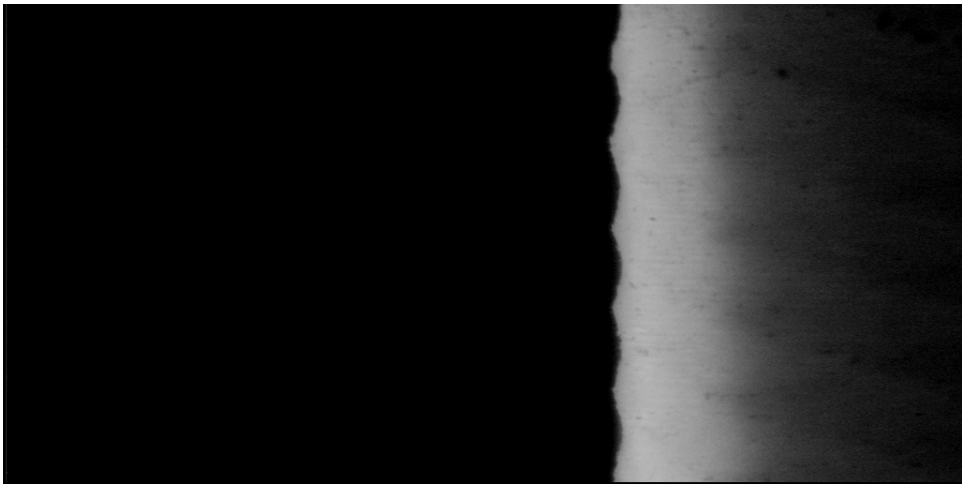

Test 1
Clean

Figure 6.5.24.
Surface quality during long term test cycles - Lanxide filter
95 psi regeneration pressure, 5 cm/s face velocity, 45 min build-up time.

NOTE:
In tests 2,3 and 4 for the 45 min condition, the filter did not regenerate on top where the camera's region of view existed. In test 5, the filter did not regenerate totally

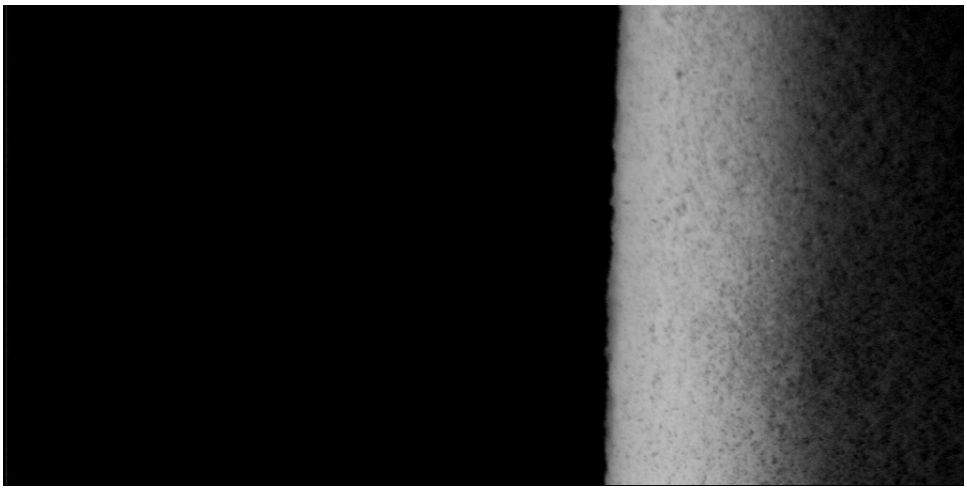

Test 1
Clean

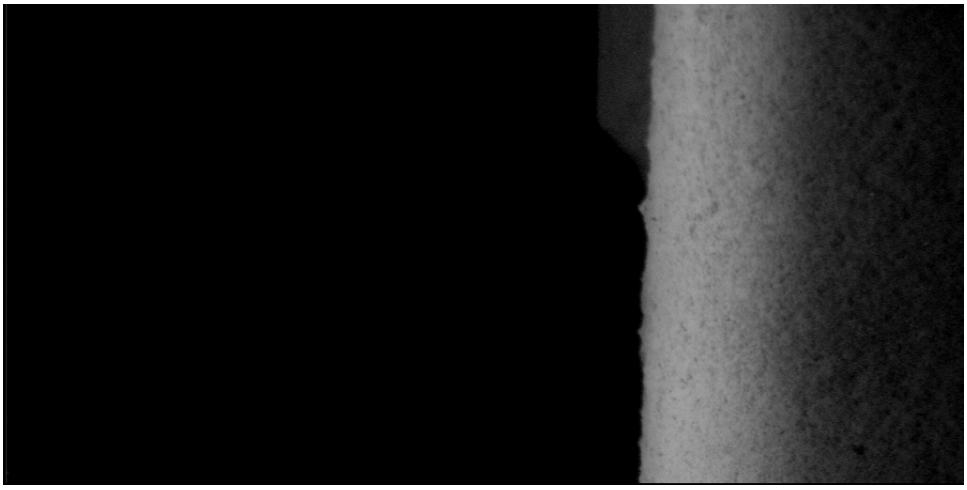

Test 2
Clean

Figure 6.5.25
Surface quality during long term test cycles - Pall filter
95 psi Regeneration Pressure, 5 cm/s face velocity, 90 min build up time

NOTE: 95 psi Regeneration Pressure, 5 cm/s face velocity, 90 min build up time

1. Pall filter failed to regenerate on its 3rd test cycle.
2. Lanxide filter failed to regenerate in its 1st test cycle

Chapter 7

Particle Re-entrainment

7.0 Introduction

In Chapter 2, while discussing the surface regeneration process, the transient pressure pulse was divided into three parts: 1) zero (gauge) pressure part, 2) positive pressure part and 3) negative pressure part. In the first part, the pressure in the filter element is zero (gauge), and this corresponds to the delay time just before pulse jet is activated. In the second part, the reverse pulse dislodges the dust cake on the surface of the filter element. The third part, having a longer time period, was defined as the "interim process" between the pulse jet cleaning and normal filtration. During this period, the transient pressure inside the filter element is much lower than the outside of the filter element. The interim process may cause a fraction of particles removed to re-deposit on the candle surface. This re-deposition of the ash particles was termed as the "ash re-entrainment".

While analyzing the images of the surface regeneration process, acquired during the "long term tests", particle re-entrainment was observed in several tests. Re-entrainment of ash particles was observed more frequently in tests using the Pall filter, compared to tests using the Lanxide filter.

7.1 Particle tracking and velocity estimation

The imaging system acquires samples the regeneration process and acquires images every 1/60 seconds. Since the ash particles move at high velocities, their paths are defined by capturing a series of images. The particle's position is captured at

intermediate points along its path, in successive images. When the successive image frames are added through a logical OR operation, the track of the particle (Figure 7.1.1) is obtained. From the resultant image the velocities and the orientation are estimated.

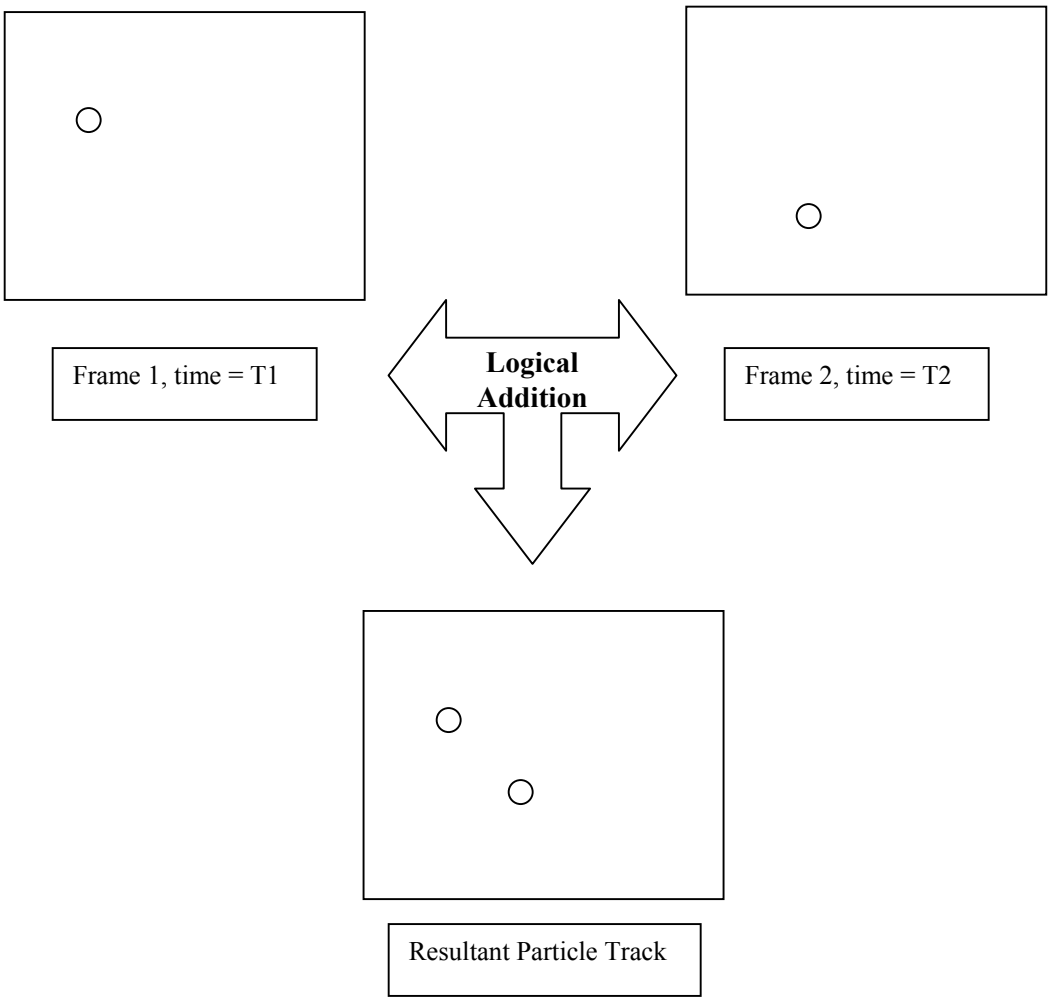

Figure 7.1.1
Representation of image addition through logical operation to obtain particle tracks

The distance traveled and orientation of the particle is calculated from its pixel coordinates at successive time frames. This estimation is done, by employing simple coordinate geometry techniques. The particle is assumed to travel linearly between successive frames lines. Particle velocity is calculated by dividing the displacement between each frame by the time between each frame.

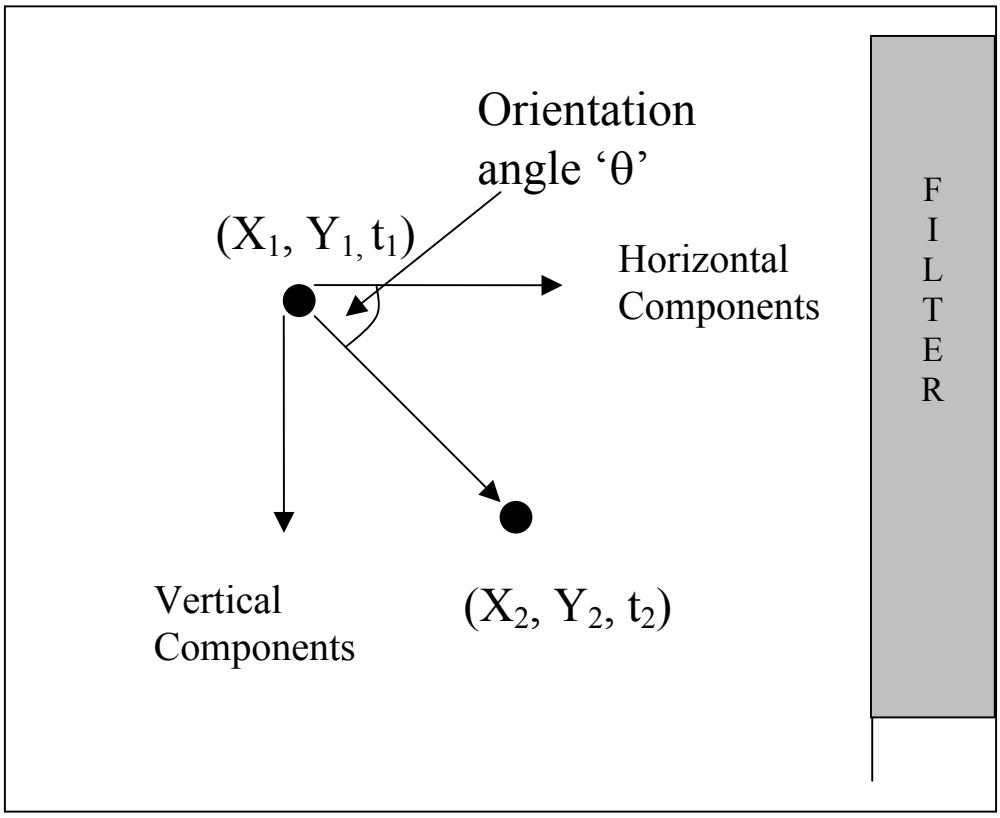

Figure 7.1.2
Schematic of particle displacement and orientation estimation

7.2 Particle re-entrainment in "long-term tests" in RTTF

On observing particle re-entrainment, the analysis of the images was performed to obtain

(a) the image of the particle tracks,

(b) the velocities and orientation.

In addition, from the time information, the test conditions and the related pressure drop, (ΔP – between the filter and the chamber), the re-entrainment was studied and correlated with the pulse cleaning process. As expected, all re-entrainment occurred during the interim process.

Theoretically, the pressure drop ΔP has a direct effect on the particle's horizontal velocity and therefore on its overall orientation and velocity. A large negative pressure drop will impart horizontal forces on the particles towards the filter. The pressure drop data during the re-entrainment was obtained along with the re-entrainment image, the average particle velocities and the orientation.

7.2.1 Particle re-entrainment in the Lanxide filter

In this section, particle re-entrainment in the Lanxide filter is discussed. The images of particle re-entrainment, the pressure drop (ΔP) during that regeneration, and the average velocities & orientation of the particle for observations made in the Lanxide filter are presented. The cases presented are

(a) Lanxide filter - base condition, 3rd test cycle, images from 0.65 to 0.73 sec.

(b) Lanxide filter -base condition, 21st test cycle, images from 0.65 to 0.72 sec

(c) Lanxide filter, 80 psi regeneration pressure, 9th test cycle, images from 0.65 to 0.75 sec

(d) Lanxide filter, 120 psi regeneration pressure, 4th test cycle, images from 0.83 to 0.92 sec

(e) Lanxide filter, 120 psi regeneration pressure, 10th test cycle, images from 0.68 to 0.72 sec

The particle track image and the corresponding pressure drop plot are presented for each of the cases. The negative pressure difference between the filter and chamber (ΔP), during the interim process causes the re-entrainment of the particles. The maximum value of this negative ΔP, was defined as the minimum ΔP in Chapter 6. The values of minimum ΔP, and the pressure difference values at the start and end of the re-entrainment sequence are presented, along with the averaged velocities and orientations, as a table. All related observations have been presented in the next two sub-sections.

a Lanxide filter - base condition, 3rd test cycle, images from 0.65 to 0.73 sec

In this test, a particle is observed moving towards the filter from 0.65 sec to 0.73 sec. The time period corresponds to the interim process, and re-entrainment is observed to occur even before the ΔP value reaches its minimum value. The particle is estimated to move towards the filter, with a velocity of 395.81 mm/sec and an angle of 70.82°.

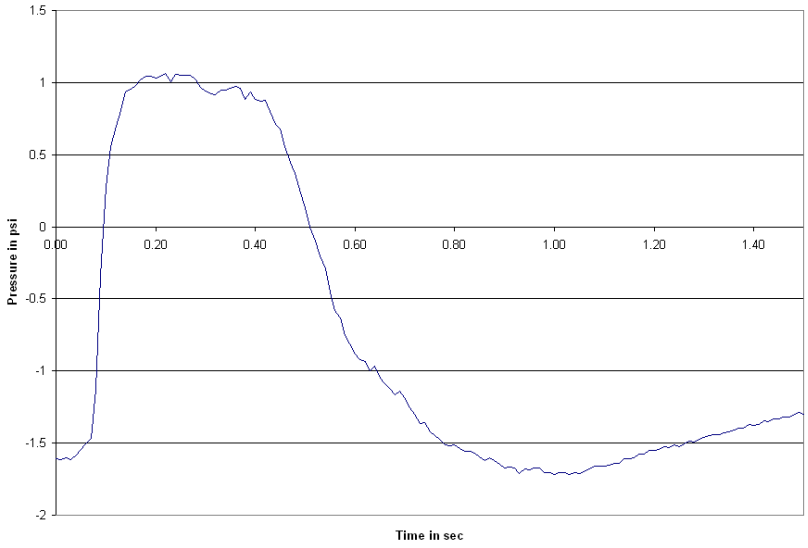

Figure 7.2.1
Pressure drop (ΔP) across the filter for Lanxide filter,
base condition, 3rd test cycle, images from 0.65 to 0.72 sec

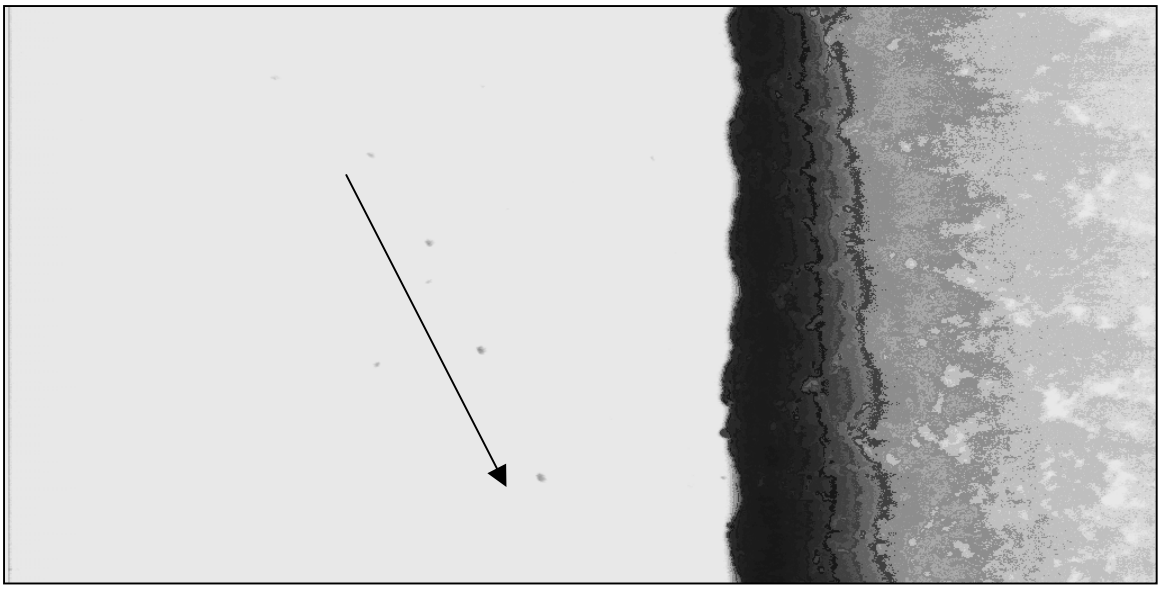

Figure 7.2.2
Image of particle re-entrainment - Lanxide filter
base condition, 3rd test cycle, images from 0.65 to 0.73 sec

Track	Particle Size (μ)	Minimum Pressure (Δp-min)	Start Pressure (psi)	End Pressure (psi)	Horizontal Velocity Component (mm/sec)	Vertical Velocity Component (mm/sec)	Velocity (mm/sec)	Orientation (θ) in degrees
1	560	-1.72	-1.05	-1.36	123.90	372.75	395.81	70.82

Table 7.2.1
Particle size, pressure conditions, velocities and orientations - Lanxide filter,
base condition, 3rd test cycle, images from 0.65 to 0.72 sec

b. Lanxide filter - base condition, 21st test cycle, images from 0.65 to 0.72 sec

In this test, a particle is observed moving towards the filter from 0.65 sec to 0.72 sec. The time period corresponds to the interim process, and re-entrainment is observed to occur even before the ΔP value reaches its minimum value. The particle takes a curved path, the velocities are estimated assuming linear trajectory between image frames. The particle is estimated to move towards the filter, with a velocity of 261 mm/sec and an angle of 71.81°.track.

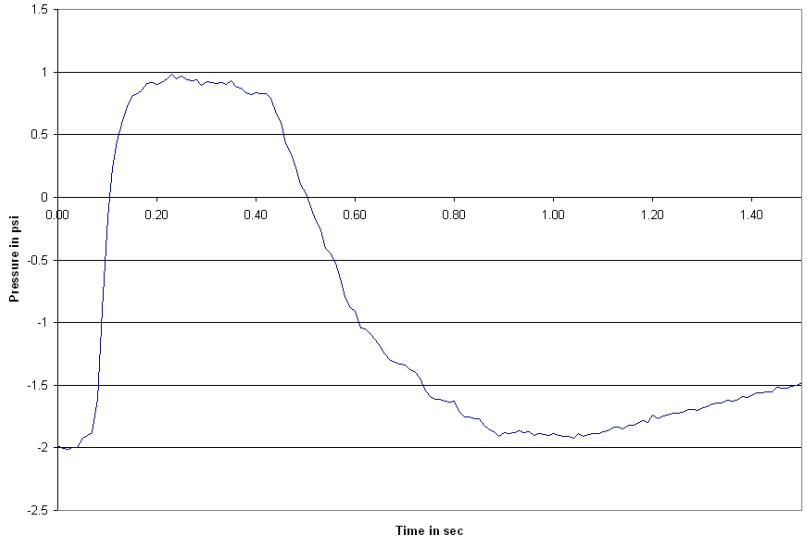

Figure 7.2.3
Pressure drop (ΔP) across the filter for Lanxide filter
base condition, 21st test cycle, images from 0.65 to 0.72 sec

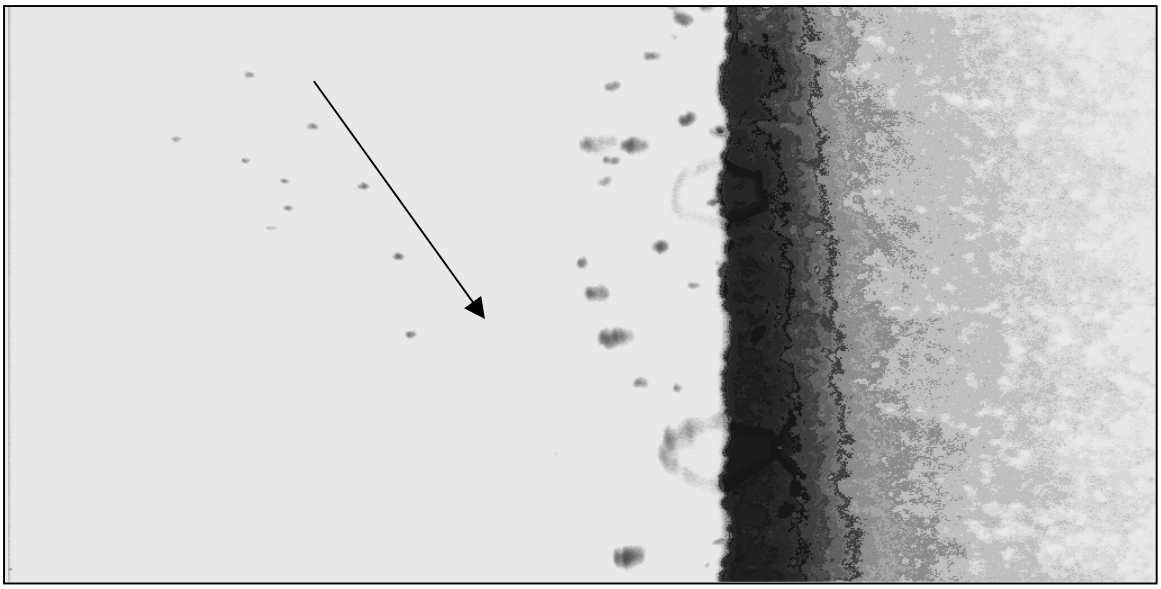

Figure 7.2.4
Image of particle re-entrainment - Lanxide filter
base condition, 21st test cycle, images from 0.65 to 0.72 sec

Track	Particle Size (μ)	Minimum Pressure (Δp-min)	Start Pressure (psi)	End Pressure (psi)	Horizontal Velocity Component (mm/sec)	Vertical Velocity Component (mm/sec)	Velocity (mm/sec)	Orientation (θ) in degrees
1	490	-1.93	-1.19	-1.59	75.60	245.70	261.00	71.81

Table 7.2.2
Particle size, pressure conditions, velocities and orientations - Lanxide filter,
base condition, 21st test cycle, images from 0.65 to 0.72 sec

c. Lanxide filter, 80 psi regeneration pressure, 9th test cycle, images from 0.65 to 0.75 sec

In this test, a particle is observed moving towards the filter from 0.65 sec to 0.75 sec. The time period corresponds to the interim process, and re-entrainment is observed to occur even before the ΔP value reaches its minimum value. The particle is estimated to move towards the filter, with a velocity of 297 mm/sec and an angle of 69.93°.

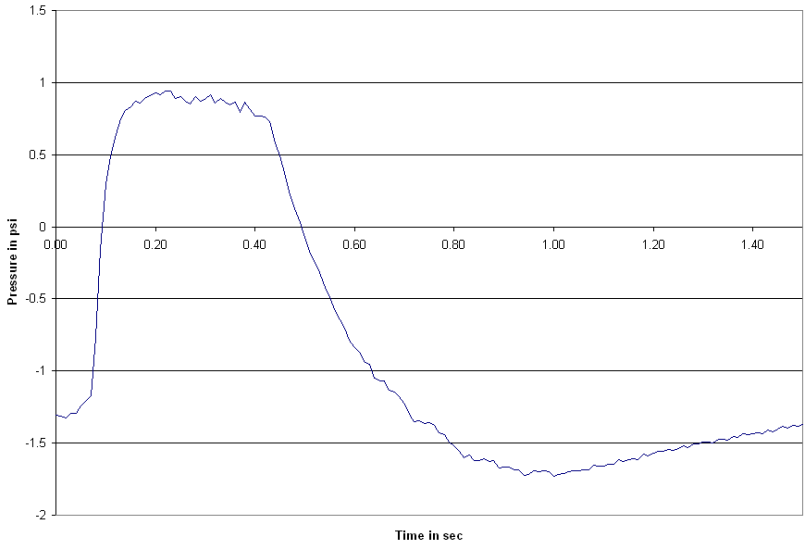

Figure 7.2.5
Pressure drop (ΔP) across the filter for Lanxide filter,
80 psi regeneration pressure, 9th test cycle, images from 0.65 to 0.75 sec

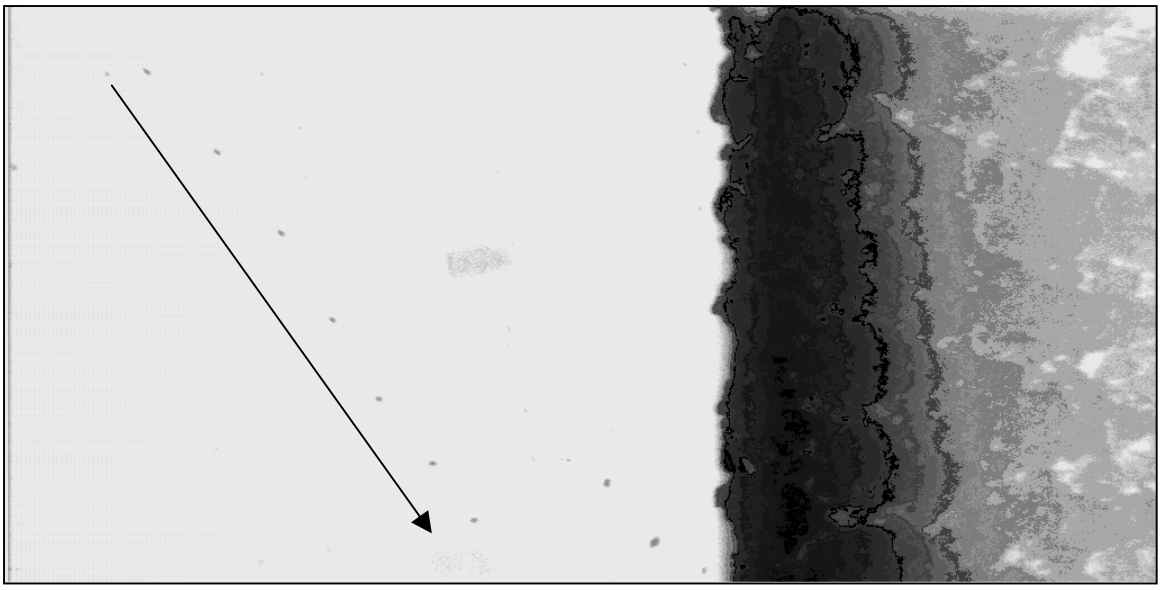

Figure 7.2.6
Image of particle re-entrainment - Lanxide filter
80 psi regeneration pressure, 9th test cycle, images from 0.65 to 0.75 sec

Track	Particle Size (μ)	Minimum Pressure (Δp-min)	Start Pressure (psi)	End Pressure (psi)	Horizontal Velocity Component (mm/sec)	Vertical Velocity Component (mm/sec)	Velocity (mm/sec)	Orientation (θ) in degrees
1	280	-1.73	-1.35	-1.07	101.50	278.60	297.00	69.93

Table 7.2.3
Particle size, pressure conditions, velocities and orientations - Lanxide filter,
80 psi regeneration pressure, 9th test cycle, images from 0.65 to 0.75 sec

d. Lanxide filter, 120 psi regeneration pressure, 4th test cycle, images from 0.83 to 0.92 sec

In this test, two particles are observed moving towards the filter from 0.83 sec to 0.92 sec. The time period corresponds to the interim process, and re-entrainment is observed to occur just before the ΔP value reaches its minimum value. The particle in track 1 is estimated to move towards the filter, with a velocity of 251.31 mm/sec and an angle of 45.71°. The particle in track 2 is estimated to move towards the filter, with a velocity of 211.30 mm/sec and an angle of 27.11°.

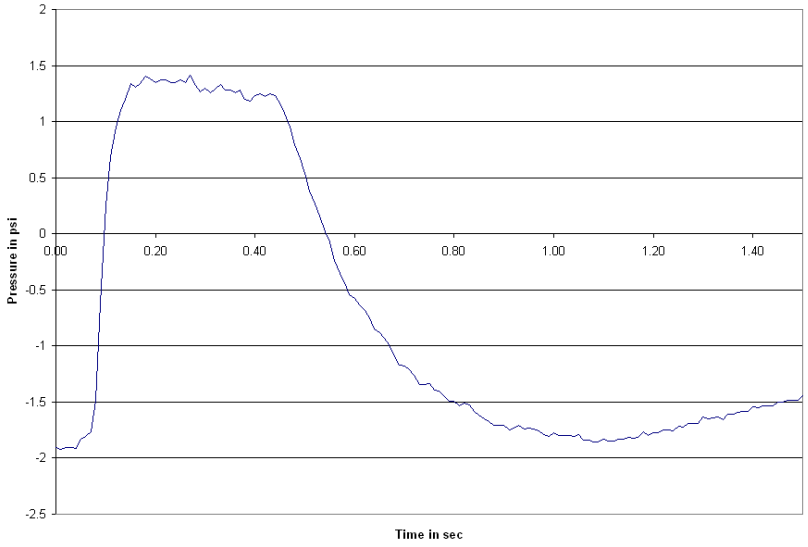

Figure 7.2.7
Pressure drop (ΔP) across the filter for Lanxide filter
120 psi regeneration pressure, 4th test cycle, images from 0.83 to 0.92 sec

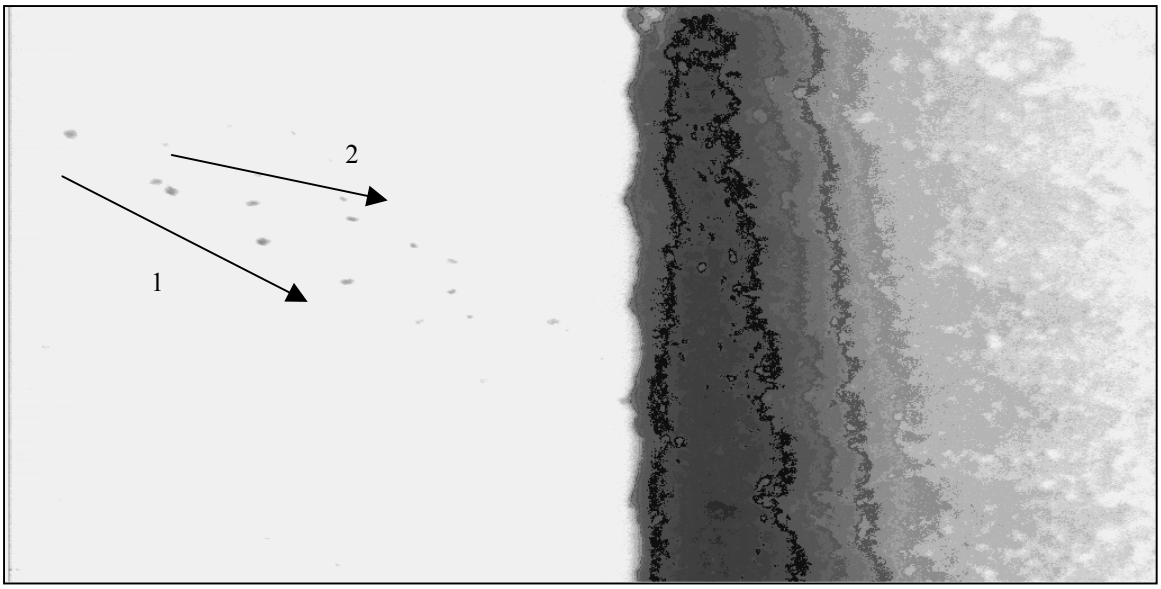

Figure 7.2.8
Image of particle re-entrainment - Lanxide filter
120 psi regeneration pressure, 4th test cycle, images from 0.83 to 0.92 sec

Track	Particle Size (μ)	Minimum Pressure (Δp-min)	Start Pressure (psi)	End Pressure (psi)	Horizontal Velocity Component (mm/sec)	Vertical Velocity Component (mm/sec)	Velocity (mm/sec)	Orientation (θ) in degrees
1	560	-1.86	-1.52	-1.72	174.30	180.60	251.31	45.71
2	490	-1.86	-1.52	-1.72	183.40	98.00	211.30	27.11

Table 7.2.4
Particle size, pressure conditions, velocities and orientations - Lanxide filter,
120 psi regeneration pressure, 4th test cycle, images from 0.83 to 0.75 sec

e. Lanxide filter, 120 psi regeneration pressure, 10th test cycle, images from 0.68 to 0.72 sec

In this test, a particle is observed moving towards the filter from 0.68 sec to 0.72 sec. The time period corresponds to the interim process, and re-entrainment is observed to occur even before the ΔP value reaches its minimum value. The particle is estimated to move towards the filter, with a velocity of 300.96 mm/sec and an angle of 70.56°.

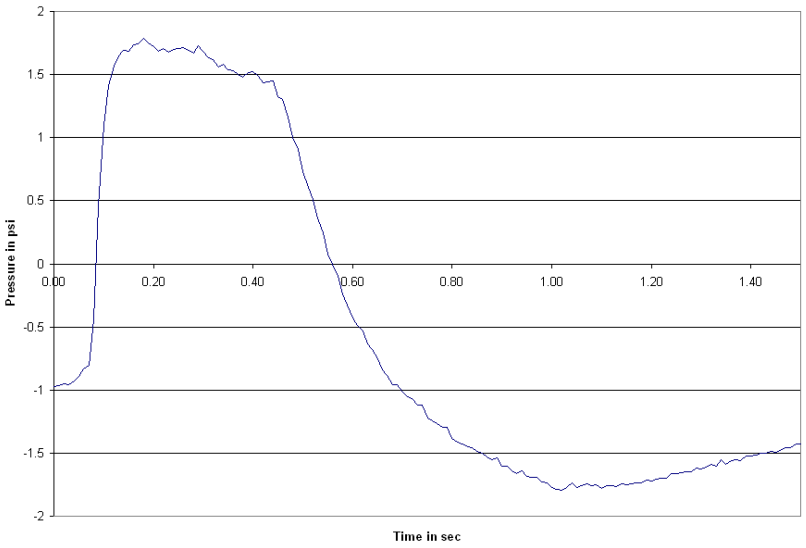

Figure 7.2.9
Pressure drop (ΔP) across the filter for Lanxide filter
120 psi regeneration pressure, 10th test cycle, images from 0.68 to 0.72 sec

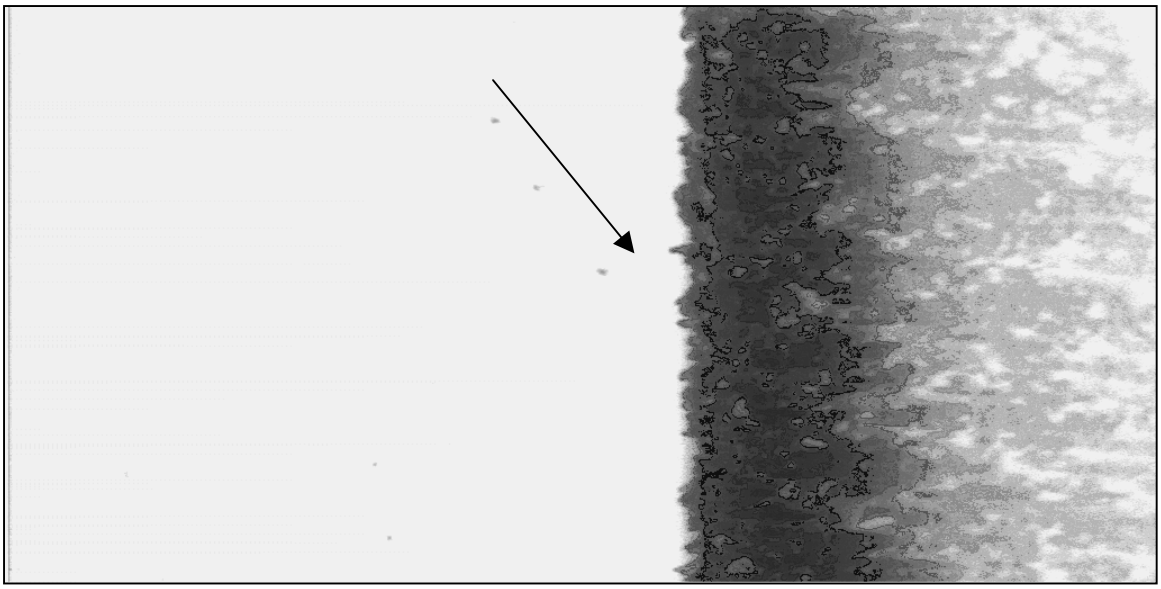

Figure 7.2.10
Image of particle re-entrainment - Lanxide filter
120 psi regeneration pressure, 10th test cycle, images from 0.68 to 0.72 sec

Track	Particle Size (μ)	Minimum Pressure (Δp-min)	Start Pressure (psi)	End Pressure (psi)	Horizontal Velocity Component (mm/sec)	Vertical Velocity Component (mm/sec)	Velocity (mm/sec)	Orientation (θ) in degrees
1	420	-1.79	-1.49	-1.55	100.80	283.50	300.96	70.56

Table 7.2.5
Particle size, pressure conditions, velocities and orientations - Lanxide filter,
120 psi regeneration pressure, 10th test cycle, images from 0.68 to 0.72 sec

7.2.2 Particle re-entrainment in Pall filter

In this section, particle re-entrainment in Pall filter is discussed. The images of particle re-entrainment, the pressure drop (ΔP) during that regeneration, and the average velocities & orientation of the particle for observations made in Pall filter are presented. The cases presented are

(a) Pall filter - base condition, 1st test cycle, images from 0.55 to 0.65 sec

(b) Pall filter - base condition, 18th test cycle, images from 0.57 to 0.63 sec

(c) Pall filter - base condition, 18th test cycle, images from 0.88 to 0.98 sec

(d) Pall filter - base condition, 18th test cycle, images from 1.05 to 1.15 sec

(e) Pall filter, 80 psi regeneration pressure, 3rd test cycle, images from 0.68 to 0.88 sec

(f) Pall filter, 80 psi regeneration pressure, 3rd test cycle, images from 1.03 to 1.13 sec

(g) Pall filter, 7cm/s face velocity, 1st test cycle, images from 0.85 to 0.92 sec

(h) Pall filter, 7cm/s face velocity, 1st test cycle, images from 0.93 to 1.03 sec

(i) Pall filter, 7cm/s face velocity, 13th test cycle, images from 0.75 to 0.87 sec

(j) Pall filter, 90 min build-up time, 1st test cycle, images from 0.80 to 0.88 sec

The image of particle track and the corresponding pressure drop plot are presented for each of the cases. The values of minimum ΔP, and the ΔP values at the star and end of the re-entrainment sequence, are presented along with the averaged velocities and orientations, as a table.

(a) Pall filter - base condition, 1st test cycle, images from 0.55 to 0.65 sec

In this test, three particles are observed moving towards the filter from 0.55 sec to 0.65 sec. The time period corresponds to the interim process, and re-entrainment is observed to occur even before the ΔP value reaches its minimum value. The particle in track 1 is estimated to move towards the filter, with a velocity of 315.26 mm/sec and an angle of 49.99°. The particle in track 2 is estimated to move towards the filter, with a velocity of 339.09 mm/sec and an angle of 55.22°. The particle in track 2 is estimated to move towards the filter, with a velocity of 330.46 mm/sec and an angle of 61.29°.

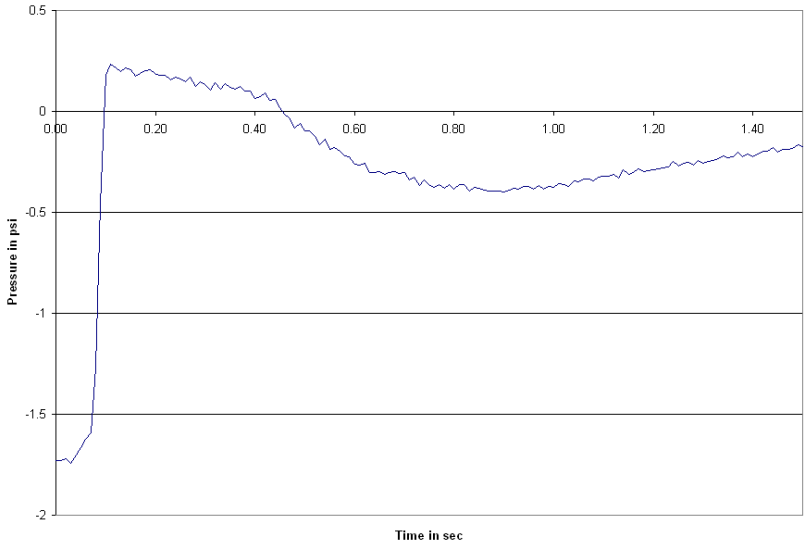

Figure 7.2.11
Pressure drop (ΔP) across the filter for Pall filter
base condition, , 1st test cycle, images from 0.55 to 0.65 sec

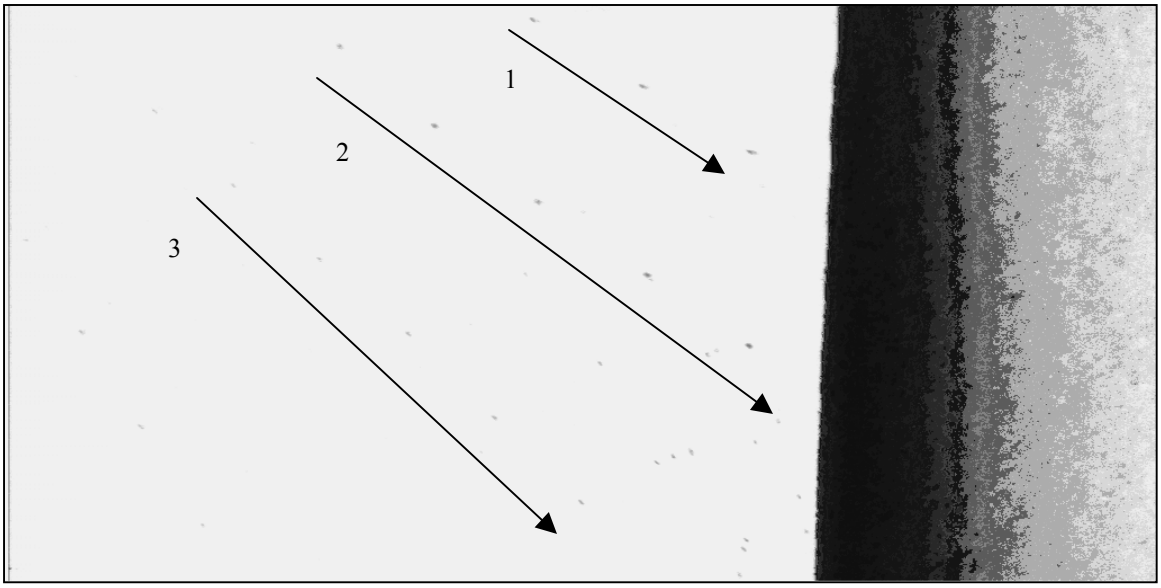

Figure 7.2.12
Image of particle re-entrainment - Pall filter
base condition, , 1st test cycle, images from 0.55 to 0.65 sec

Track	Particle Size (μ)	Minimum Pressure (Δp-min)	Start Pressure (psi)	End Pressure (psi)	Horizontal Velocity Component (mm/sec)	Vertical Velocity Component (mm/sec)	Velocity (mm/sec)	Orientation (θ) in degrees
1	490	-0.40	-0.19	-0.30	202.65	241.50	315.26	49.99
2	560	-0.40	-0.19	-0.30	193.2	278.25	339.09	55.22
3	420	-0.40	-0.19	-0.30	158.55	289.80	330.46	61.29

Table 7.2.6
Particle size, pressure conditions, velocities and orientations - Pall filter
base condition, , 1st test cycle, images from 0.55 to 0.65 sec

(b) Pall filter - base condition, 18th test cycle, images from 0.57 to 0.63 sec

In this test, a particle is observed moving towards the filter from 0.57 sec to 0.63 sec. The time period corresponds to the interim process, and re-entrainment is observed to occur even before the ΔP value reaches its minimum value. The particle is estimated to move towards the filter, with a velocity of 341.56 mm/sec and an angle of 84.64°.

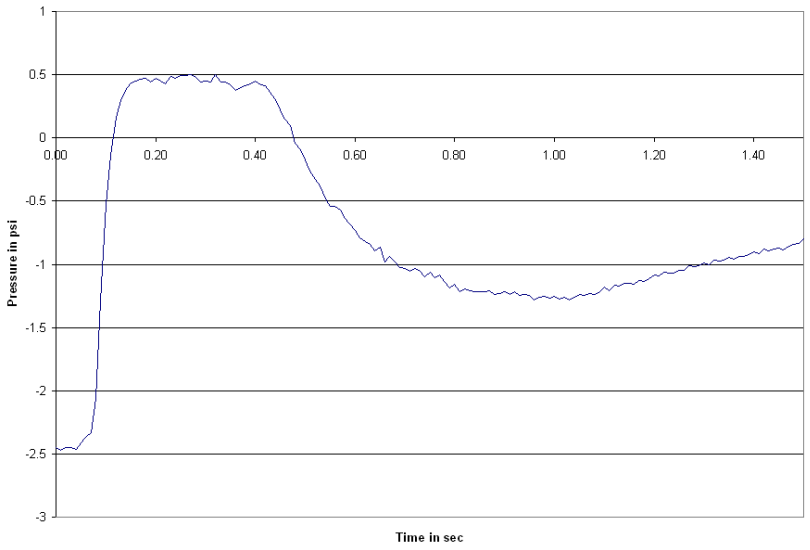

Figure 7.2.13
Pressure drop (ΔP) across the filter for Pall filter
base condition, 18th test cycle, images from 0.57 to 0.63 sec

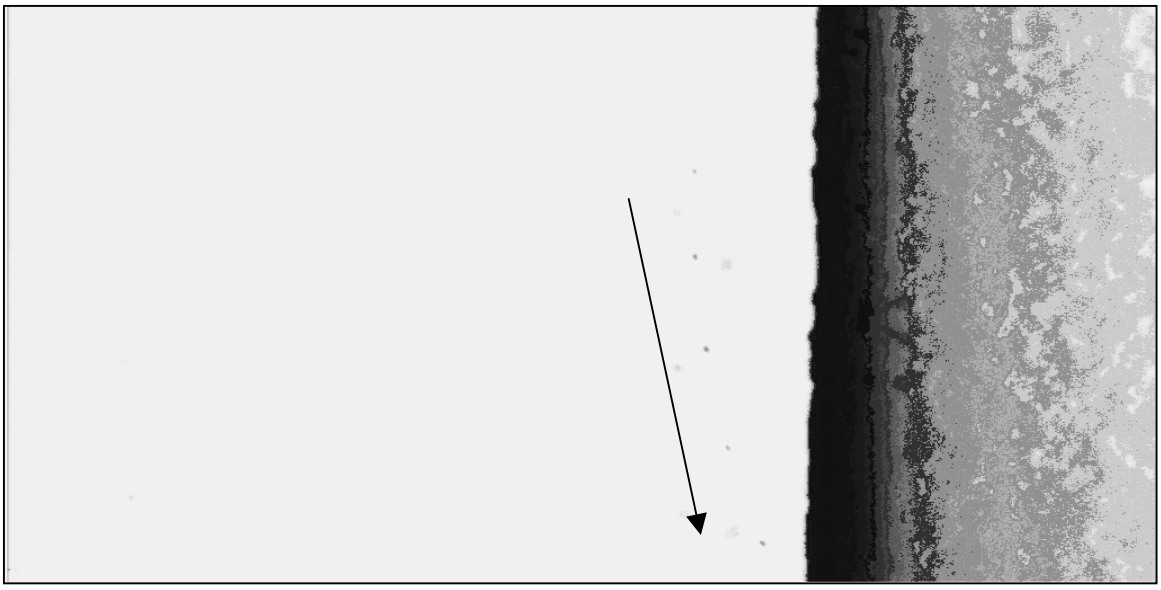

Figure 7.2.14
Image of particle re-entrainment - Pall filter
base condition, 18th test cycle, images from 0.57 to 0.63 sec

Track	Particle Size (μ)	Minimum Pressure (Δp-min)	Start Pressure (psi)	End Pressure (psi)	Horizontal Velocity Component (mm/sec)	Vertical Velocity Component (mm/sec)	Velocity (mm/sec)	Orientation (θ) in degrees
1	490	-1.28	-0.57	-0.85	32.55	339.15	341.50	84.64

Table 7.2.7
Particle size, pressure conditions, velocities and orientations - Pall filter
base condition, 18th test cycle, images from 0.57 to 0.63 sec

(c) Pall filter - base condition, 18th test cycle, images from 0.88 to 0.98 sec

In this test, three particles are observed moving towards the filter from 0.88 sec to 0.98 sec. The time period corresponds to the interim process, and re-entrainment is observed to occur just before the ΔP value reaches its minimum value. The particle in track 1 is estimated to move towards the filter, with a velocity of 227.66 mm/sec and an angle of 83.74°. The particle in track 2 is estimated to move towards the filter, with a velocity of 352.42 mm/sec and an angle of 76.56°. The particle in track 2 is estimated to move towards the filter, with a velocity of 294.04 mm/sec and an angle of 74.78°.

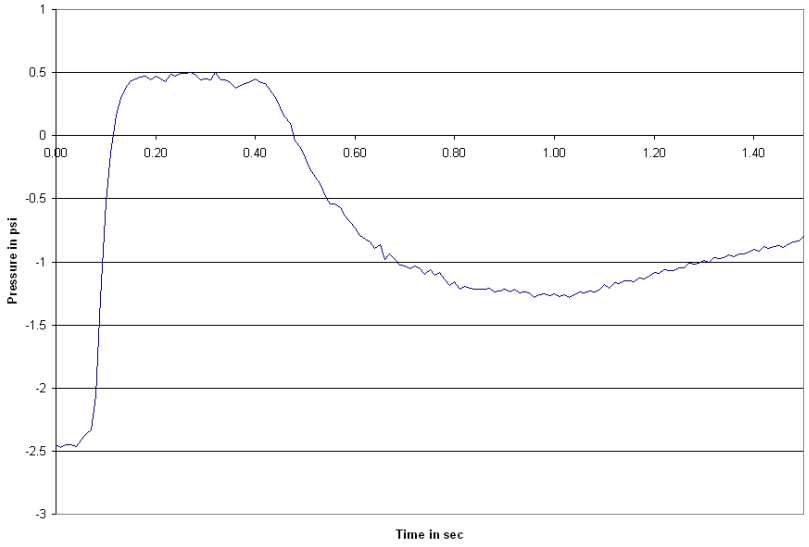

Figure 7.2.15
Pressure drop (ΔP) across the filter for Pall filter
base condition, 18th test cycle, images from 0.88 to 0.98 sec

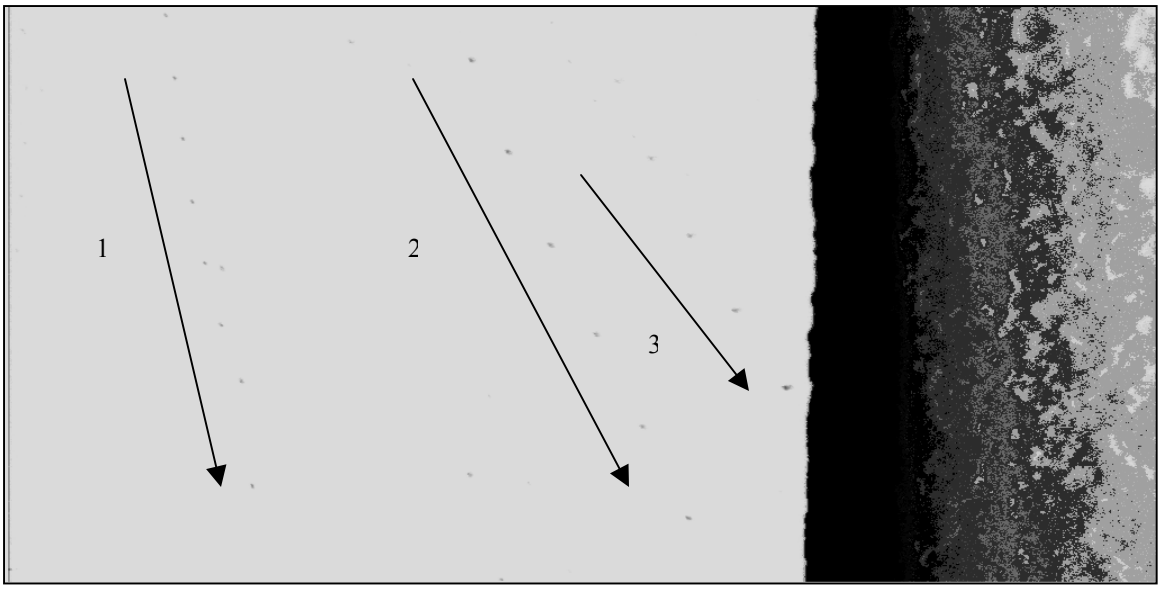

Figure 7.2.16
Image of particle re-entrainment - Pall filter
base condition, 18th test cycle, images from 0.88 to 0.98 sec

S.No	Particle Size (μ)	Minimum Pressure (Δp-min)	Start Pressure (psi)	End Pressure (psi)	Horizontal Velocity Component (mm/sec)	Vertical Velocity Component (mm/sec)	Velocity (mm/sec)	Orientation (θ) in degrees
1	280	-1.28	-1.24	-1.25	24.15	226.10	227.66	83.74
2	420	-1.28	-1.24	-1.25	81.90	342.72	352.42	76.56
3	420	-1.28	-1.24	-1.25	77.18	283.50	294.04	74.78

Table 7.2.8
Particle size, pressure conditions, velocities and orientations - Pall filter
base condition, 18th test cycle, images from 0.88 to 0.98 sec

(d) Pall filter - base condition, 18th test cycle, images from 1.05 to 1.15 sec

In this test, two particles are observed moving towards the filter from 1.05 sec to 1.15 sec. The time period corresponds to the interim process, and re-entrainment is observed to occur just when the ΔP value reaches its minimum value. The particle in track 1 is estimated to move towards the filter, with a velocity of 270.31 mm/sec and an angle of 60.83°. The particle in track 2 is estimated to move towards the filter, with a velocity of 246.77 mm/sec and an angle of 82.57°.

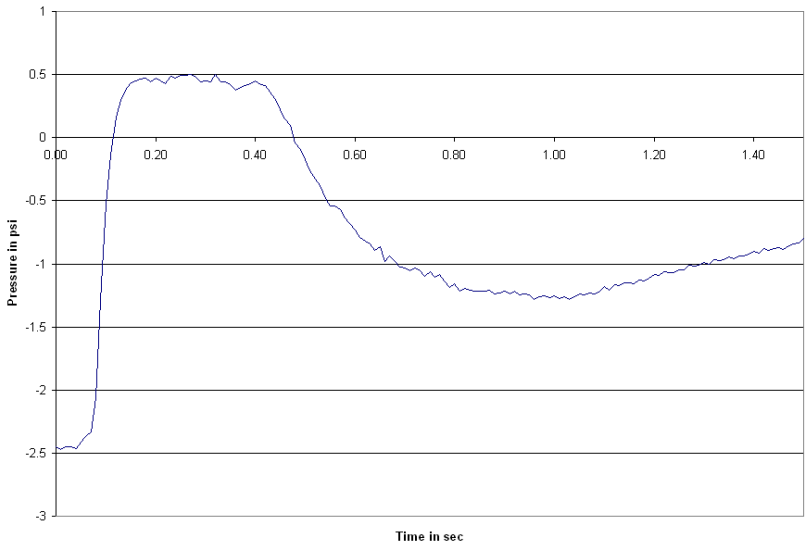

Figure 7.2.17
Pressure drop (ΔP) across the filter for Pall filter
base condition, 18th test cycle, images from 1.05 to 1.15 sec

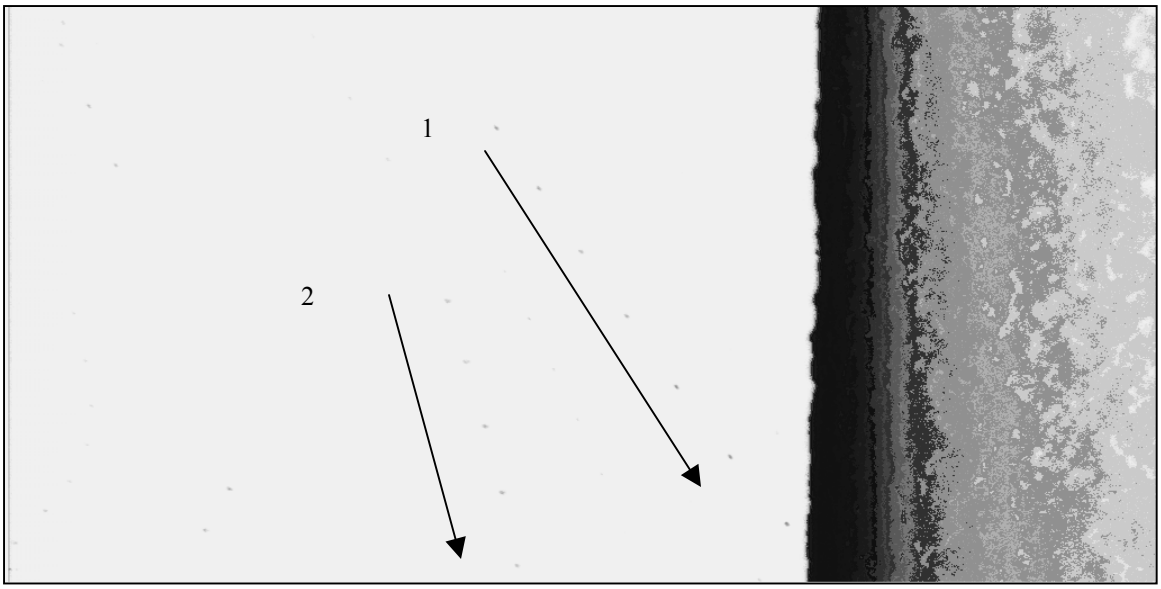

Figure 7.2.18
Image of particle re-entrainment - Pall filter
base condition, 18th test cycle, images from 1.05 to 1.15 sec

S.No	Particle Size (μ)	Minimum Pressure (Δp-min)	Start Pressure (psi)	End Pressure (psi)	Horizontal Velocity Component (mm/sec)	Vertical Velocity Component (mm/sec)	Velocity (mm/sec)	Orientation (θ) in degrees
1	280	-1.28	-1.24	-1.15	91.00	245.00	270.31	60.83
2	280	-1.28	-1.24	-1.15	31.50	244.65	246.77	82.57

Table 7.2.9
Particle size, pressure conditions, velocities and orientations - Pall filter
base condition, 18th test cycle, images from 1.05 to 1.15 sec

(e) Pall filter, 80 psi regeneration pressure, 3rd test cycle, images from 0.68 to 0.88 sec

In this test, two particles are observed moving towards the filter from 0.68 sec to 0.88 sec. The time period corresponds to the interim process, and re-entrainment is observed to occur even before the ΔP value reaches its minimum value. The particle in track 1 is estimated to move towards the filter, with a velocity of 264.25 mm/sec and an angle of 75.45°. The particle in track 2 is estimated to move towards the filter, with a velocity of 147.34 mm/sec and an angle of 73.97°.

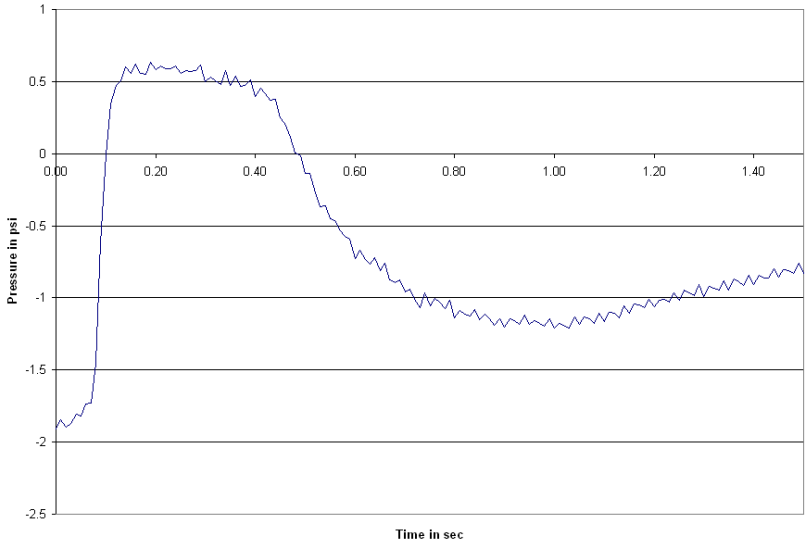

Figure 7.2.19
Pressure drop (ΔP) across the filter for Pall filter
80 psi regeneration pressure, 3rd test cycle, images from 0.68 to 0.88 sec

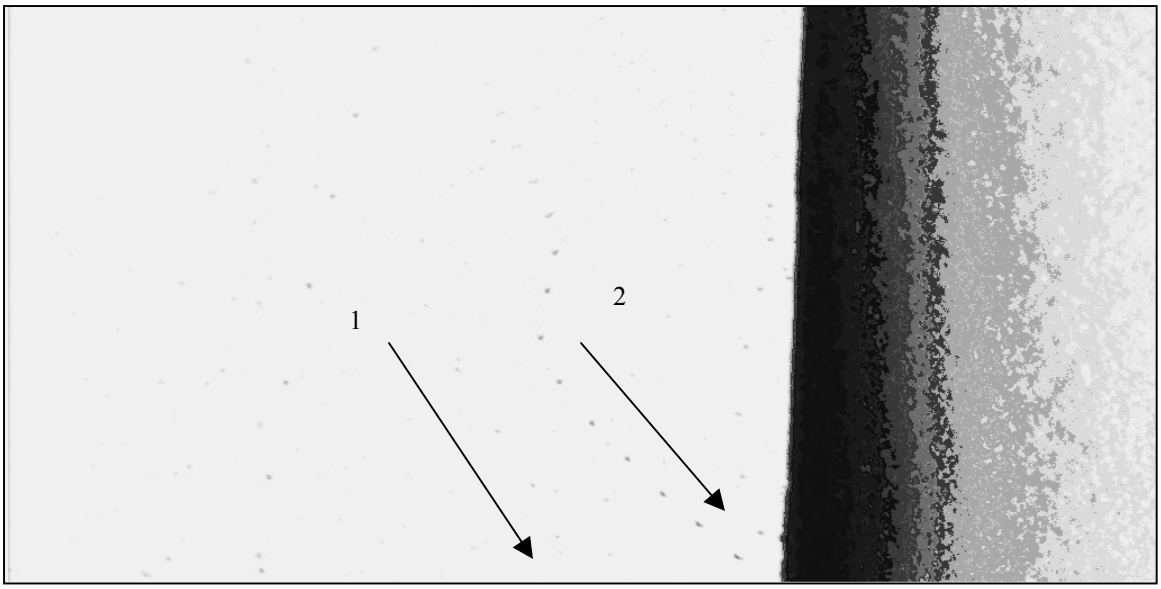

Figure 7.2.20
Image of particle re-entrainment - Pall filter
80 psi regeneration pressure, 3rd test cycle, images from 0.68 to 0.88 sec

Track	Particle Size (μ)	Minimum Pressure (Δp-min)	Start Pressure (psi)	End Pressure (psi)	Horizontal Velocity Component (mm/sec)	Vertical Velocity Component (mm/sec)	Velocity (mm/sec)	Orientation (θ) in degrees
1	140	-1.21	-0.89	-1.19	60.90	256.20	264.25	75.45
2	490	-1.21	-0.89	-1.19	38.85	137.76	147.34	73.97

Table 7.2.10
Particle size, pressure conditions, velocities and orientations - Pall filter
80 psi regeneration pressure, 3rd test cycle, images from 0.68 to 0.88 sec

(f) Pall filter, 80 psi regeneration pressure, 3rd test cycle, images from 1.03 to 1.13 sec

In this test, three particles are observed moving towards the filter from 1.03 sec to 1.13 sec. The time period corresponds to the interim process, and re-entrainment is observed to occur just when the ΔP value reaches its minimum value. The particle in track 1 is estimated to move towards the filter, with a velocity of 208.07 mm/sec and an angle of 62.06°. The particles in track 2 & 3 are estimated to move towards the filter, with a velocity of 95.64 mm/sec and an angle of 62.77°, and 141.90 mm/sec and an angle of 65.24°, respectively.

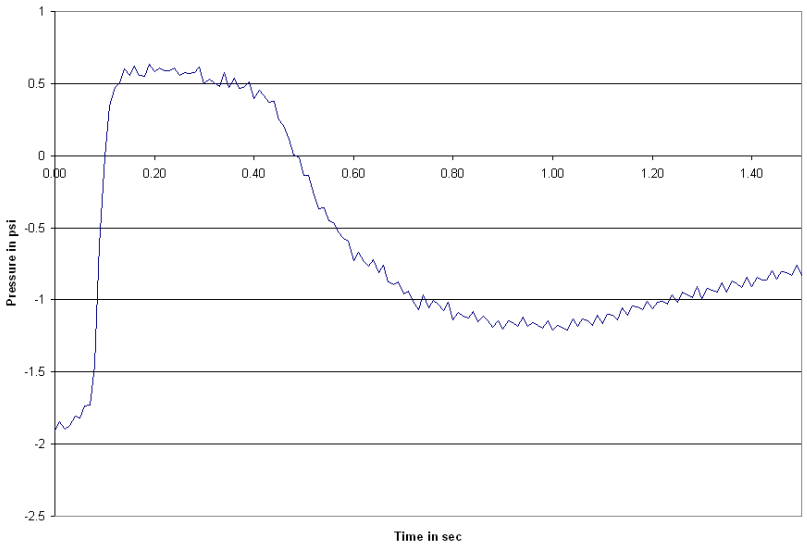

Figure 7.2.21
Pressure drop (ΔP) across the filter for Pall filter
80 psi regeneration pressure, 3rd test cycle, images from 1.03 to 1.13 sec

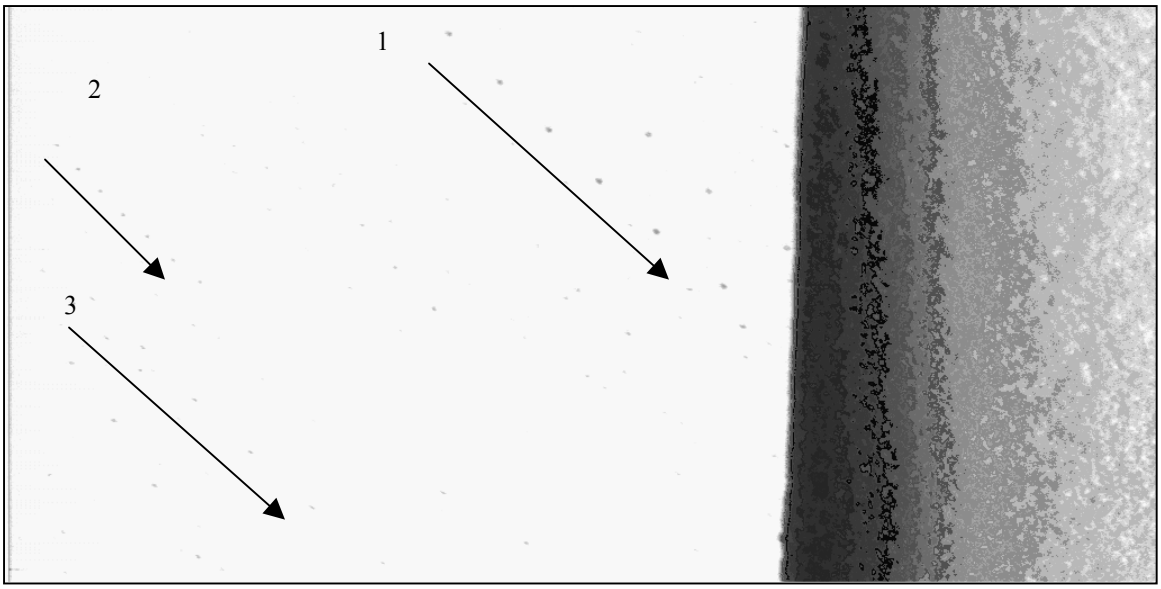

Figure 7.2.22
Image of particle re-entrainment - Pall filter
80 psi regeneration pressure, 3rd test cycle, images from 1.03 to 1.13 sec

Track	Particle Size (μ)	Minimum Pressure (Δp-min)	Start Pressure (psi)	End Pressure (psi)	Horizontal Velocity Component (mm/sec)	Vertical Velocity Component (mm/sec)	Velocity (mm/sec)	Orientation (θ) in degrees
1	350	-1.21	-1.21	-1.14	97.13	183.75	208.07	62.06
2	210	-1.21	-1.21	-1.14	43.68	84.84	95.64	62.71
3	280	-1.21	-1.21	-1.14	59.50	128.80	141.90	65.24

Table 7.2.11
Particle size, pressure conditions, velocities and orientations - Pall filter
80 psi regeneration pressure, 3rd test cycle, images from 1.03 to 1.13 sec

(g) Pall filter, 7cm/s face velocity, 1st test cycle, images from 0.85 to 0.92 sec

In this test, three particles are observed moving towards the filter from 0.85 sec to 0.92 sec. The time period corresponds to the interim process, and re-entrainment is observed to occur even before ΔP reaches its minimum value. The particle in track 1 is estimated to move towards the filter, with a velocity of 555.77 mm/sec and an angle of 80.67°. The particles in track 2 & 3 are estimated to move towards the filter, with a velocity of 441.12 mm/sec and an angle of 84.18°, and 298.31 mm/sec and an angle of 70.11°, respectively.

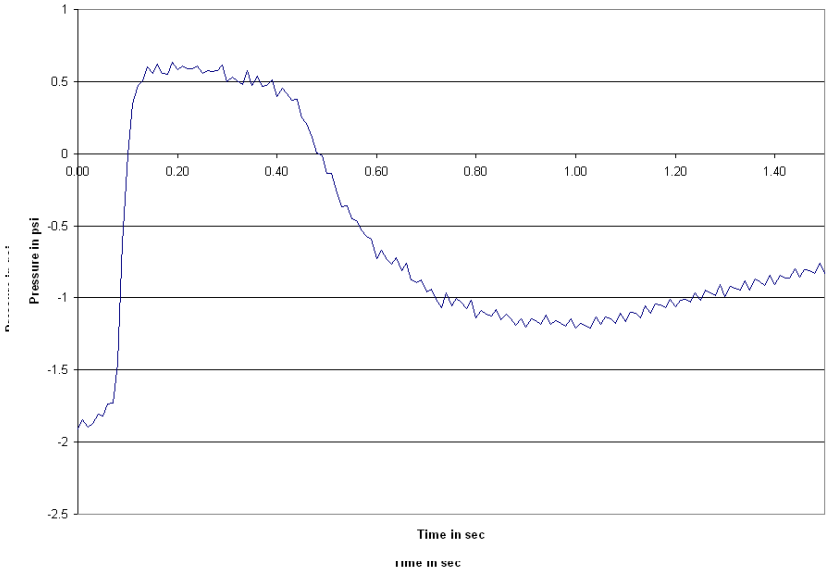

Figure 7.2.23
Pressure drop (ΔP) across the filter for Pall filter
7cm/s face velocity, 1st test cycle, images from 0.85 to 0.92 sec

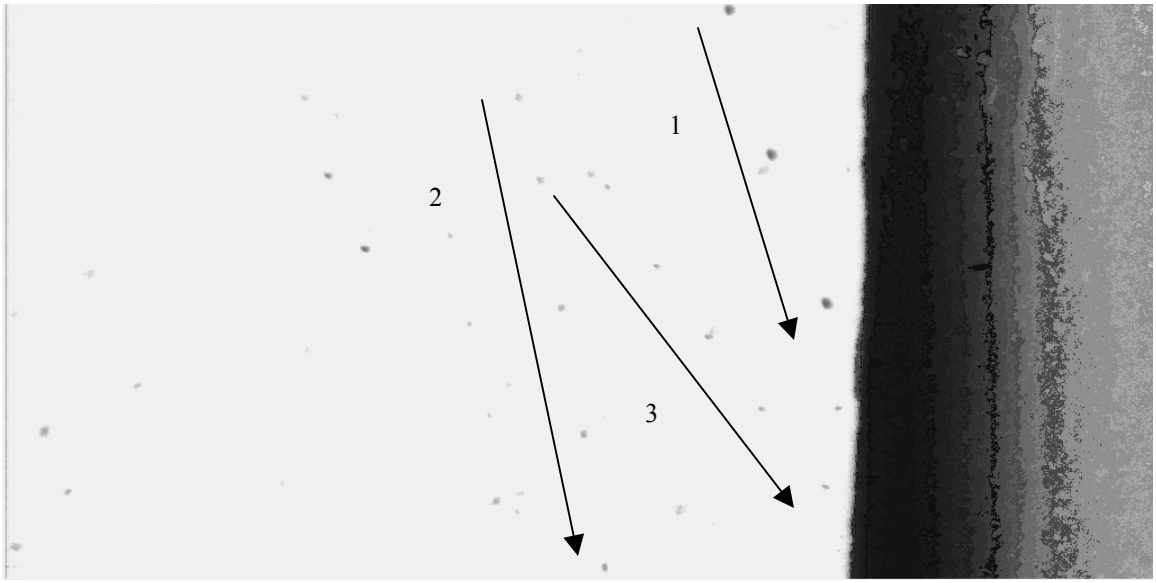

Figure 7.2.24
Image of particle re-entrainment - Pall filter
7cm/s face velocity, 1st test cycle, images from 0.85 to 0.92 sec

S.No	Particle Size (μ)	Minimum Pressure (Δp-min)	Start Pressure (psi)	End Pressure (psi)	Horizontal Velocity Component (mm/sec)	Vertical Velocity Component (mm/sec)	Velocity (mm/sec)	Orientation (θ) in degrees
1	910	-1.34	-1.28	-1.31	90.30	548.10	555.77	80.67
2	490	-1.34	-1.28	-1.31	42.53	438.90	441.12	84.18
3	490	-1.34	-1.28	-1.31	101.33	280.35	298.31	70.11

Table 7.2.12
Particle size, pressure conditions, velocities and orientations - Pall filter
7cm/s face velocity, 1st test cycle, images from 0.85 to 0.92 sec

(h) Pall filter, 7cm/s face velocity, 13th test cycle, images from 0.75 to 0.87 sec

In this test, three particles are observed moving towards the filter from 0.75 sec to 0.87 sec. The time period corresponds to the interim process, and re-entrainment is observed to occur even before ΔP reaches its minimum value. The particle in track 1 is estimated to move towards the filter, with a velocity of 368.89 mm/sec and an angle of 64.60°. The particles in track 2 & 3 are estimated to move towards the filter, with a velocity of 313.49 mm/sec and an angle of 59.70°, and 415.84 mm/sec and an angle of 66.80°, respectively.

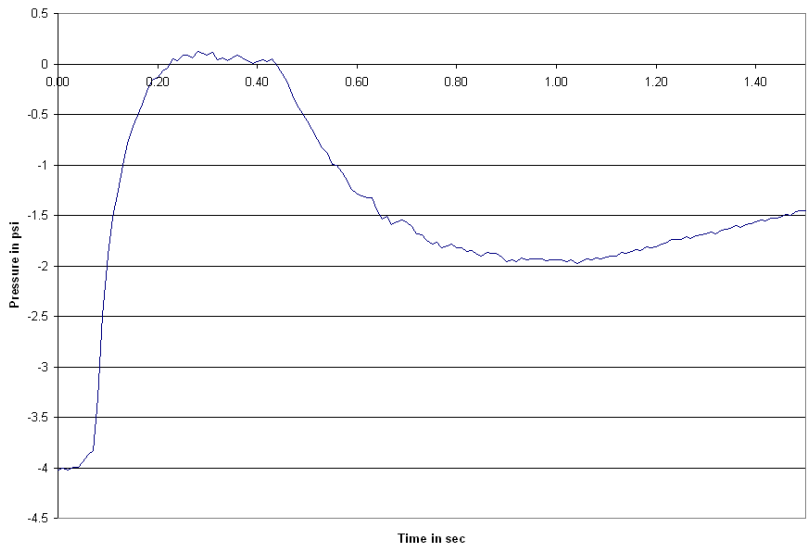

Figure 7.2.25
Pressure drop (ΔP) across the filter for Pall filter
7cm/s face velocity, 13th test cycle, images from 0.75 to 0.87 sec

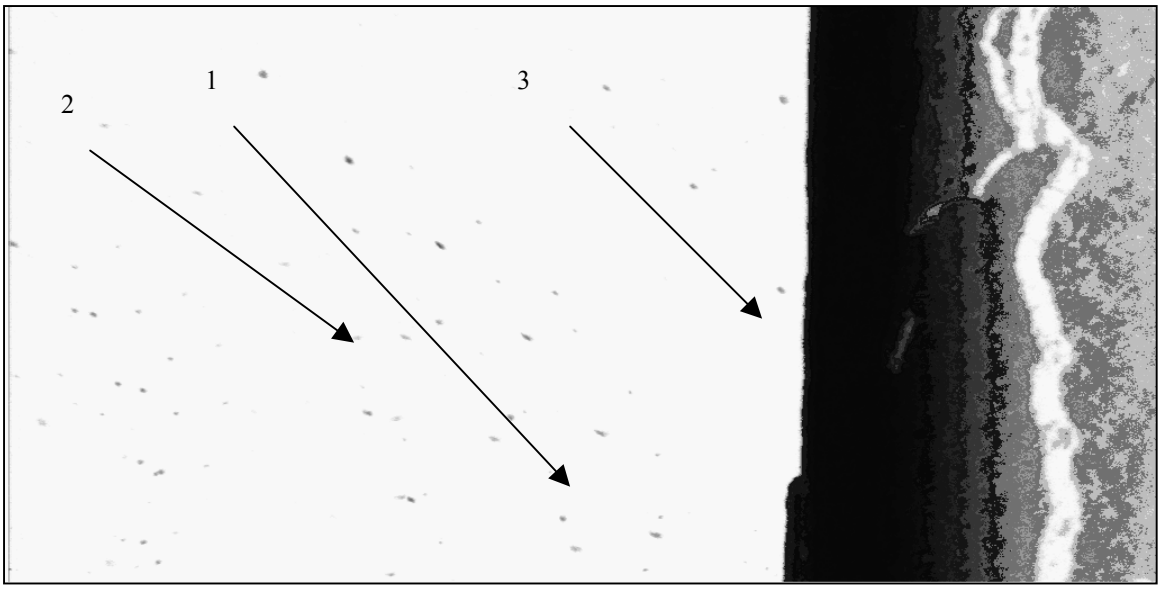

Figure 7.2.26
Image of particle re-entrainment - Pall filter
7cm/s face velocity, 13th test cycle, images from 0.75 to 0.87 sec

Track	Particle Size (μ)	Minimum Pressure (Δp-min)	Start Pressure (psi)	End Pressure (psi)	Horizontal Velocity Component (mm/sec)	Vertical Velocity Component (mm/sec)	Velocity (mm/sec)	Orientation (θ) in degrees
1	700	-1.97	-1.79	-1.88	158.03	332.85	368.69	64.60
2	315	-1.97	-1.79	-1.88	157.50	270.20	313.49	59.70
3	420	-1.97	-1.79	-1.88	163.80	382.20	415.84	66.80

Table 7.2.13
Particle size, pressure conditions, velocities and orientations - Pall filter
7cm/s face velocity, 13th test cycle, images from 0.75 to 0.87 sec

(j) Pall filter, 90 min build-up time, 1st test cycle, images from 0.80 to 0.88 sec

In this test, two particles are observed moving towards the filter from 0.80 sec to 0.88 sec. The time period corresponds to the interim process, and re-entrainment is observed to occur even before ΔP reaches its minimum value. The particle in track 1 is estimated to move towards the filter, with a velocity of 218.60 mm/sec and an angle of 68.50°. The particle in track 2 is estimated to move towards the filter, with a velocity of 162.33 mm/sec and an angle of 50.94°.

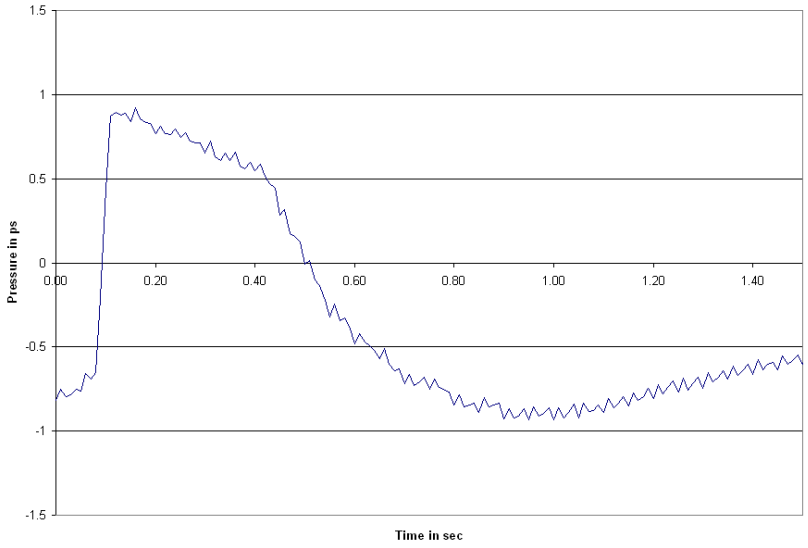

Figure 7.2.27
Pressure drop (ΔP) across the filter for Pall filter
90 min build-up time, 1st test cycle, images from 0.80 to 0.88 sec

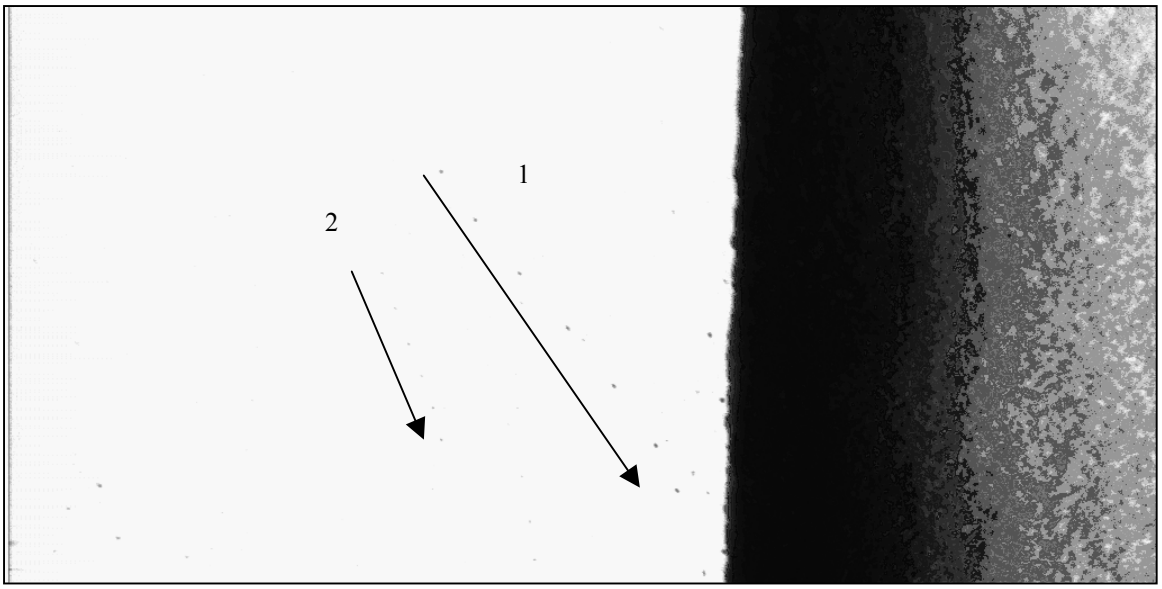

Figure 7.2.28
Image of particle re-entrainment - Pall filter
90 min build-up time, 1st test cycle, images from 0.80 to 0.88 sec

Track	Particle Size (μ)	Minimum Pressure (Δp-min)	Start Pressure (psi)	End Pressure (psi)	Horizontal Velocity Component (mm/sec)	Vertical Velocity Component (mm/sec)	Velocity (mm/sec)	Orientation (θ) in degrees
1	350	-0.93	-0.89	-0.83	80.22	203.28	218.60	68.50
2	210	-0.93	-0.89	-0.83	21.84	125.16	162.33	50.94

Table 7.2.14
Particle size, pressure conditions, velocities and orientations - Pall filter
90 min build-up time, 1st test cycle, images from 0.80 to 0.88 sec

7.3 Summary

The particle re-entrainment behavior during the interim process was observed and analyzed. The re-entrainment was always observed to occur between the maximum and minimum ΔP values in the plot of pressure difference between the filter and the chamber, during regeneration. The images were processed to obtain the tracks of the particle and, its velocity & orientation established. However, correlation between the ΔP value and the velocities & orientation, could not be established with the current data.

Chapter 8

Conclusions

8.0 Conclusions

The objective of this research was to develop a comprehensive understanding of the surface regeneration process at room temperatures, and to determine optimal conditions for efficient surface regeneration in the room temperature testing facility (RTTF). The results from the room temperature tests will be helpful in predicting, to an extent, the nature of results in high temperature tests. RTTF was utilized to perform tests on candle filter(s) to study candle filter surface regeneration.

Among the parameters that affect the regeneration characteristics, the following - (1) regeneration pressure, (2) face velocity of build up air, and (3) time of ash layer build-up, were identified as the key parameters and tests performed to study the effect of each of these parameters. The filter type also affects the regeneration process, therefore two brands of filters, "Lanxide-PRD-66$^{\rightarrow}$" and "Pall-442T$^{\rightarrow}$", were tested and compared. The "base" test upon which all other tests are compared was performed with a regeneration pressure of 95 psig, face velocity of 5 cm/s and a build-up time of 20 minutes.

8.0.1 Effect of regeneration pressure

The regeneration pulse pressure imparts stresses on the ash-cake and dislodges it. Cleaning efficiency is expected to increase with increasing the regeneration pulse pressure. The regeneration pressures used in the study were (a) 80 psig, (b) 95 psig, (c) 120 psig and (d) 145 psig. The 95 psig condition, as mentioned earlier was taken as the

base condition. The results were discussed in section 6.3 and a comparative table (Table 8.0.1) is used to arrive at conclusions.

The performance of the filter, based on regeneration pressure, is not readily distinguishable as in the other two parameters. The face velocity and the build-up time chosen always resulted in thin ash layer depositions. Failure of filter to regenerate is the easiest way to distinguish the performances, but in all the four pressure conditions the filters continued to regenerate continuously. This can be partially attributed to the build-up conditions. All four conditions displayed thin ash build-up and regeneration. The particle count during regeneration was high, due to thin ash regeneration, in all four conditions.

Among the four pressure values, the 80 psig condition displayed more undesirable characteristics. This was especially highlighted by - repeated partial regeneration, relatively high and increasing cleaning factors, and relatively high deterioration of the filter surface quality. A stronger build-up condition could result in increased difficulty for the filter to regenerate. 95 psig condition displayed similar regeneration characteristics as 80 psig, but had relatively lower surface deterioration. The cleaning factor value was low and constant. The 120 psig and the 145 psig pressure conditions, displayed the most desirable surface regeneration characteristics, among all four conditions. Surface deterioration was very low and the filter had thin and sparse residual ash on its surface, in these cases.

Since both 120 psig and 145 psig regeneration pressure conditions perform similarly, 120 psig can be preferred over 145 psig as the optimal regeneration pressure. The same amount of cleaning is achieved with lower energy expenditure.

8.0.2 Effect of face velocity

The face velocity is the velocity at which the air stream mixed with ash dust passes the wall of the candle filter. Face velocity affects the density, thickness, compaction and strength of the ash cake. The face velocities employed in the study were (a) 3 cm/s, (b) 5 cm/s and (c) 7cm/s. A face velocity of 5 cm/s was taken as the base condition. The results were discussed in section 6.4 and a comparative table (Table 8.0.2) is used to arrive at conclusions.

The 7 cm/s condition affected the filters performance the most. The filter failed to regenerate on the 7^{th} cycle, while the 3 cm/s and 5 cm/s conditions continued to regenerate. The chamber pressure increase was highest in the 7 cm/s condition. The pressure difference during the interim process was large and could have caused a lot of particle re-entrainment. The cleaning factor was large and kept increasing with each cycle for 7 cm/s condition. The crack initiation time was longest for the 7 cm/s condition and the filter built thick residual ash cakes. The 7 cm/s face velocity is not desirable for efficient filter regeneration.

Among the 3 cm/s and 5 cm/s face velocity conditions, there was not much difference in their performance. Surface deterioration was about the same for both conditions (after 15 cycles). Both conditions built thin ash and displayed thin ash regeneration. A major drawback in both these conditions was the significantly higher particle count, due to thin type ash deposition.

A face velocity of 5 cm/s can be preferred over 3 cm/s, as the optimal face velocity. Although they exhibit similar performances, a higher face velocity will help in quicker filtration with a smaller filtration system, saving time and energy.

8.0.3 Effect of build-up time

The time interval between successive regenerations is the build-up time. A increase in build-up time results in more ash being collected on the surface of the filter and increased compaction of the ash cake. The build-up time used in the study were (a) 10 min, (b) 20 min, (c) 45 min and (d) 90 min. The 20 min build-up time was used as the base condition. The results were discussed in section 6.5 and a comparative table (Table 8.0.3) is used to arrive at conclusions.

The filter failed to regenerate on the 5^{th} cycle for the 45 min build-up and in the 1^{st} cycle for the 90 min build up conditions. As expected, a longer build-up time built stronger and thicker ash cakes, which caused difficulties in regeneration process. The two longer build-up conditions resulted in increased chamber pressures and large negative ΔP_{min} values that further deteriorate the cleaning action of the pulse jet. Their cleaning factors were larger and increasing. They built strong residual ash cakes that failed to regenerate. The crack initiation time was long in the 45 min condition and could not be observed in the 90 min condition (failed to regenerate even in 1^{st} cycle). The 45 min and 90 min build-up time are not desirable for efficient filter regeneration.

The 10 min and 20 min build-up times exhibited similar performances. Surface deterioration was about the same for both conditions (after 15 cycles). Both conditions built thin ash and displayed thin ash regeneration. A major drawback in both these conditions was the significantly higher particle count, due to thin type regeneration.

The 20 min build-up time imparts similar cleaning, less frequently, as compared to the 10 min build-up time. Therefore 20 min build-up time can be chosen as the optimal cleaning build-up time interval.

8.0.4 Effect of filter type

Two branded filters, "Lanxide-PRD-66$^{\rightarrow}$" and "Pall-442T$^{\rightarrow}$", were the filters compared to study the effect of filter type. The Lanxide filter was observed to be a low permeability filter and the Pall filter was the high permeability filter. Five comparative tests were performed in all. The testing conditions chosen were the ones that made the surface regeneration harder in Lanxide filter. The tests that were performed are:

1. Face velocity of 5 cm/s, a reservoir pressure of 95 psig, and a build-up time of 20min, (Base condition)
2. Face velocity of 7 cm/s, a reservoir pressure of 95 psig, and a build-up time of 20min, (Higher face velocity)
6. Face velocity of 5 cm/s, a reservoir pressure of 80 psig, and a build-up time of 20min, (Low regeneration Pressure)
7. Face velocity of 5 cm/s, a reservoir pressure of 95 psig, and a build-up time of 45min, (Longer build-up time)
8. Face velocity of 5 cm/s, a reservoir pressure of 95 psig, and a build-up time of 90min, (Longer build-up time).

The results were discussed in section 6.6 and a comparative table (Table 8.0.4) is used to arrive at conclusions.

The Pall filter performed better than the Lanxide filter in all the limiting cases. The Pall filter lasted longer than the Lanxide filter, in conditions when both filters failed to regenerate - 7 cm/s face velocity and 90 min build-up time conditions. The Lanxide filter failed to regenerate on the 5^{th} cycle in the 45 min build-up condition, while the Pall filter lasted for 16 cycles, and continued to regenerate. The values of the cleaning factors and ΔP_{min} were consistently better in the Pall filter, compared to the Lanxide filter. The surface quality deterioration was lower for the Pall filter and performed better than the Lanxide filter. The Pall filter should be preferred to the Lanxide filter, based on the test results.

The objective of this research in determining the optimal regeneration parameters was met. The other important results achieved through this research were,

(i) the room temperature tests have helped in designing the high temperature tests,

(ii) the inconsistency associated with the reservoir pressure was identified and a solution proposed

(iii) the development of a particle counting/classifying program using MATLAB

(iv) the evidence of particle re-entrainment during the interim process.

Characteristics	Testing Condition			
	80 psi Regeneration Pressure	95 psi Regeneration Pressure	120 psi Regeneration Pressure	145 psi Regeneration Pressure
Number of Test Cycles	24	25	14	15
Reason for Ending	Repeated Partial Regeneration	Repetitive Regeneration	Repetitive Regeneration	Repetitive Regeneration
Chamber Pressure (Pc) Increase during the build up phase	Increases (upto 17 psi)	Increases (upto 17 psi)	Increases (upto 16.5 psi)	Increases (upto 16 psi)
ΔP-Minimum	Low Magnitude (negative sign)	Low Magnitude (negative sign)	Low Magnitude (negative sign)	Low Magnitude (negative sign)
ΔP-final	Low & Constant (negative sign)	Low & Constant (negative sign)	Low & Constant (negative sign)	Increases
Cleaning Factor F	Increases	Low & Constant	Low & Constant	Low & Constant
Distribution of particles less than 100 microns	High	High	High	High
The thickness of ash deposit during buildup	Thin	Thin	Thin	Thin
The type of regeneration	Thin	Thin	Thin	Thin
Crack initiation Time	Low	Low	Low	Low
Surface Quality	Clean to Residual, Partial Regeneration, High Deterioration	Clean to Thin Residual, Medium Deterioration	**Mostly Clean, Low Deterioration**	**Mostly Clean, Low Deterioration**

Table 8.0.1 Comparative table: effect of regeneration pressure

Charateristics	Testing Condition		
	3 cm/s Face Velocity	**5 cm/s Face Velocity**	**7 cm/s Face Velocity**
Number of Test Cycles	15	25	7
Reason for Ending	Repetitive Regeneration	Repetitive Regeneration	Stopped Regenerating
Chamber Pressure (Pc) Increase during the build up phase	Little Increase (upto 16 psi)	Increases (upto 17 psi)	Significant Increase (19 psi)
ΔP-Minimum	Low Magnitude (negative sign)	Low Magnitude (negative sign)	Large Magnitude (negative sign)
ΔP-final	Low & Constant (negative sign)	Low & Constant (negative sign)	Increases
Cleaning Factor F	Low & Constant	Low & Constant	Large & Increases
Distribution of particles less than 100 microns	High	High	Low
The thickness of ash deposit during buildup	Thin	Thin	Thick
The type of regeneration	Thin	Thin	Thick
Crack initiation Time	Low	Low	Long
Surface Quality	Thin Residual Ash	Clean to Thin Residual, Medium Deterioration	Thick Residual Ash that stopped Regenerating

Table 8.0.2 Comparative table: effect of face velocity

Characteristics	Testing Condition			
	10 min Build-up Time	20 min Build-up Time	45 min Build-up Time	90 min Build-up Time
Number of Test Cycles	15	25	5	1
Reason for Ending	Repeated Partial Regeneration	Repetitive Regeneration	Stopped Regenerating	Stopped Regenerating
Chamber Pressure (Pc) Increase during the build up phase	Increases (upto 17 psi)	Increases (upto 17 psi)	Significant Increase (19 psi)	Significant Increase (21.5 psi)
ΔP-Minimum	Low Magnitude (negative sign)	Low Magnitude (negative sign)	Large Magnitude (negative sign)	Large Magnitude (negative sign)
ΔP-final	Low & Constant (negative sign)	Low & Constant (negative sign)	Increases	Increases
Cleaning Factor F (new)	Low & Constant	Low & Constant	Large & Increases	Large & Increases
Cleaning Factor F (cleaned)	Low & Constant	Low & Constant	Large & Increases	Large & Increases
Distribution of particles less than 100 microns	High	High	Low	Not Observable
The thickness of ash deposit during buildup	Thin	Thin	Thick	Thick
The type of regeneration	Thin	Thin	Thick	Thick
Crack initiation Time	Low	Low	Not Observable	Not Observable
Surface Quality	Thin Patchy Residuals	Clean to Thin Residual, Medium Deterioration	Thick Residual that did not regenerate	Thick Residual that did not regenerate

Table 8.0.3 Comparative table: effect of build-up time

Characteristics	Testing Conditions									
	Base		80 psi Regeneration Pressure		7 cm/s Face Velocity		45 min Cycle Period		90 min Cycle Period	
Filter Permeability	Low	High	Low	High	Low	High	Low	High	Low	High
Number of Test Cycles	25	22	24	24	7	15	5	16	1	3
Reason for Ending	Repetitive Regeneration	Repetitive Regeneration	Repeated Partial Regeneration	Repetitive Regeneration	Stopped Regenerating	Stopped Regenerating	Stopped Regenerating	Repetitive Regeneration	Stopped Regenerating	Stopped Regenerating
Chamber Pressure (Pc) Increase during the build up phase	Increases (upto 17 psi)	Increases (upto 17 psi)	Increases (upto 17 psi)	Increases (upto 17 psi)	Significant Increase (19 psi)	Significant Increase (20 psi)	Significant Increase (19 psi)	Significant Increase (19 psi)	Significant Increase (21.5 psi)	Significant Increase (20 psi)
ΔP-Minimum	Large Magnitude (negative sign)	Low Magnitude (negative sign)	Large Magnitude (negative sign)	Low Magnitude (negative sign)	Large Magnitude (negative sign)	Low Magnitude (negative sign)	Large Magnitude (negative sign)	Low Magnitude (negative sign)	Large Magnitude (negative sign)	Low Magnitude (negative sign)
ΔP-final	Large Magnitude (negative sign)	Low Magnitude (negative sign)	Large Magnitude (negative sign)	Low Magnitude (negative sign)	Large Magnitude (negative sign)	Low Magnitude (negative sign)	Large Magnitude (negative sign)	Low Magnitude (negative sign)	Large Magnitude (negative sign)	Low Magnitude (negative sign)
Cleaning Factor F	Higher	Lower	Higher	Lower	Higher	Lower	Higher	Lower	Higher	Lower
Distribution of particles less than 100 microns	High	Low	High	High	High	Low	Low	Low	Not Observable	Low
The thickness of ash deposit during buildup	Thin	Thick	Thin	Thick	Thick	Thick	Thick	Thick	Thick	Thick
The type of regeneration	Thin	Thick	Thin	Thin	Thick	Thick	Thick	Thick	Not Observable	Thick
Crack initiation Time	Low	Low	Low	Low	Long	Long	Thick & Not Observable	Long	Not Observable	Long
Surface Quality	Relativley more Deterioration	Lesser Deterioration	Relativley more Deterioration	Lesser Deterioration	Thick Residual Ash that stopped Regenerating	Thick Residual Ash that stopped Regenerating	Thick Residual that did not regenerate	Residual Dust Layer	Thick Residual that did not regenerate	Thick Residual that did not regenerate
Constant Conditions	Base Conditions		Face velocity, Cycle period		Regeneration pressure, Cycle period		Regeneration pressure, Face Velocity		Regeneration pressure, Face Velocity	

Table 8.0.4 Comparative table: effect of filter type

APPENDIX A

Comparative plot of Lanxide filter vs. Pall filter

80 psi regeneration pressure, 5 cm/s face velocity, 20 minute build-up

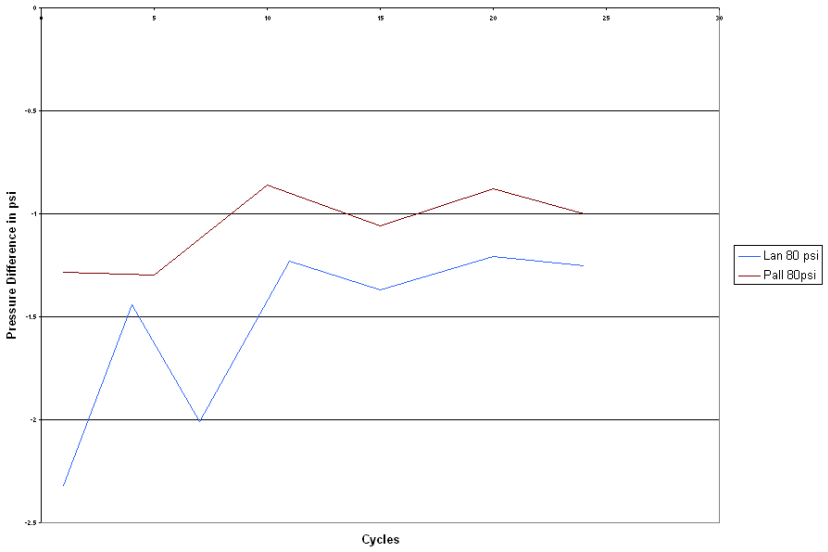

Figure A.1.
Lanxide filter vs. Pall filter
Comparative plot of initial pressure difference ($\Delta P_{initial}$) during regeneration
80 psi regeneration pressure, 5 cm/s face velocity, 20 minute build-up time

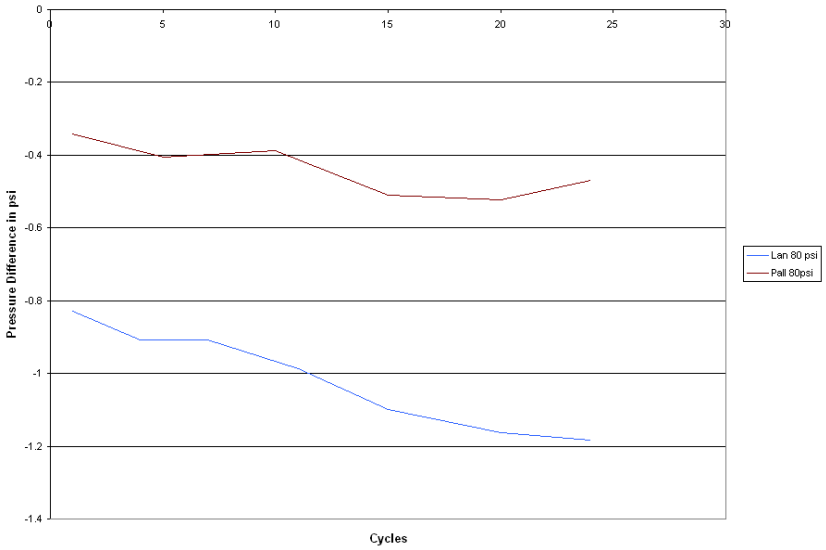

Figure A.2.
Lanxide filter vs. Pall filter
Comparative plot of final pressure difference (ΔP_{final}) during regeneration
80 psi regeneration pressure, 5 cm/s face velocity, 20 minute build-up time

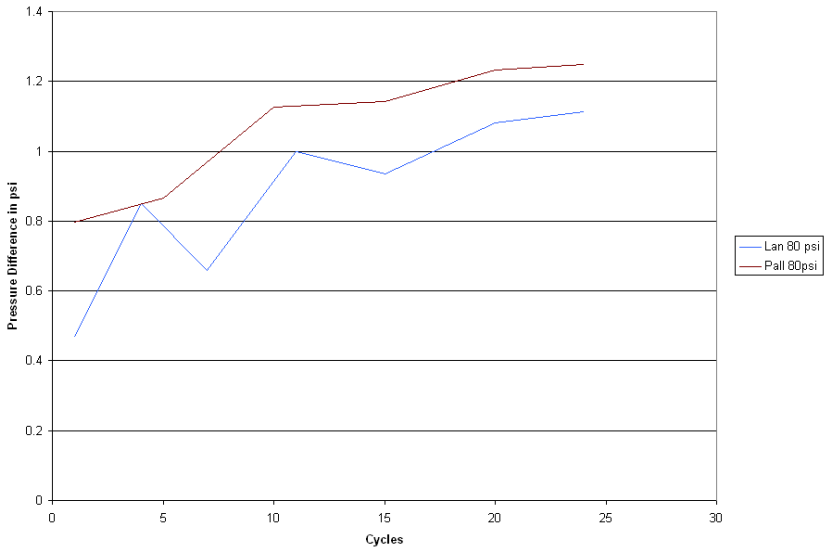

Figure A.3.
Lanxide filter vs. Pall filter
Comparative plot of maximum pressure difference (ΔP_{max}) during regeneration
80 psi regeneration pressure, 5 cm/s face velocity, 20 minute build-up time

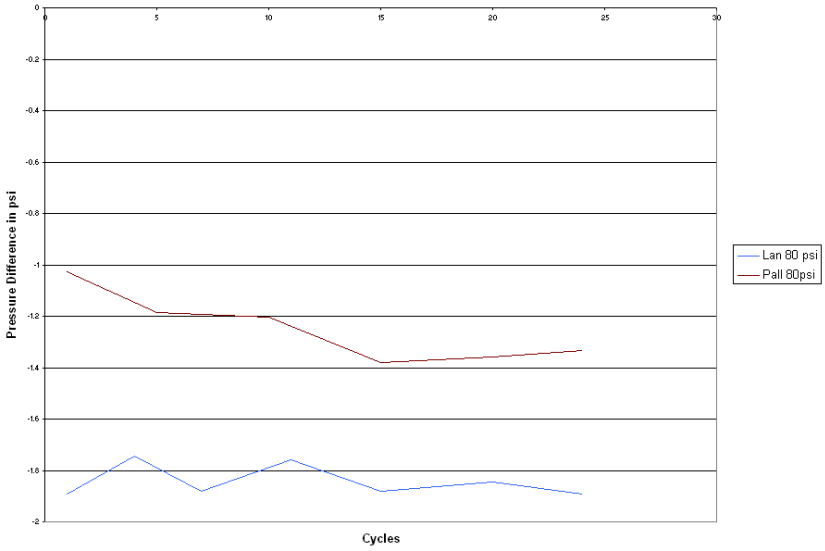

Figure A.4.
Lanxide filter vs. Pall filter
Comparative plot of minimum pressure difference (ΔP_{min}) during regeneration
80 psi regeneration pressure, 5 cm/s face velocity, 20 minute build-up time

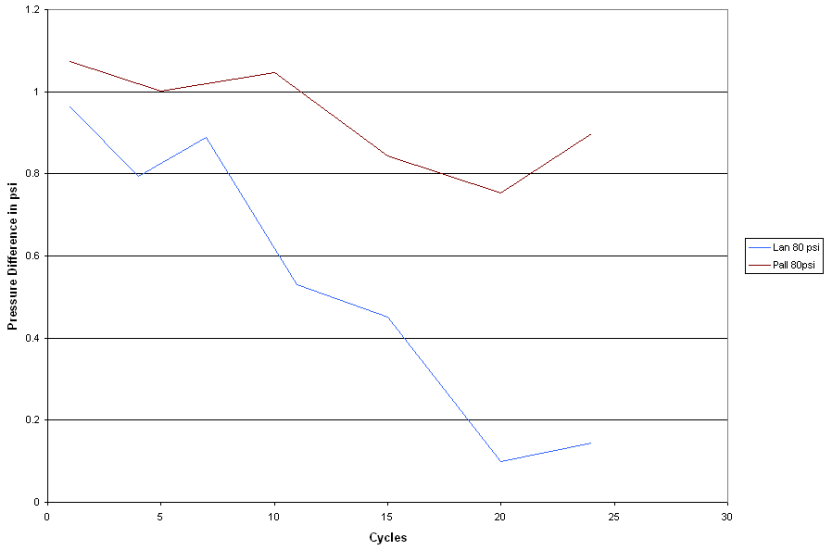

Figure A.5.
Lanxide filter vs. Pall filter
Comparative plot of efficiency-cleaned (η_C) during regeneration
80 psi regeneration pressure, 5 cm/s face velocity, 20 minute build-up time

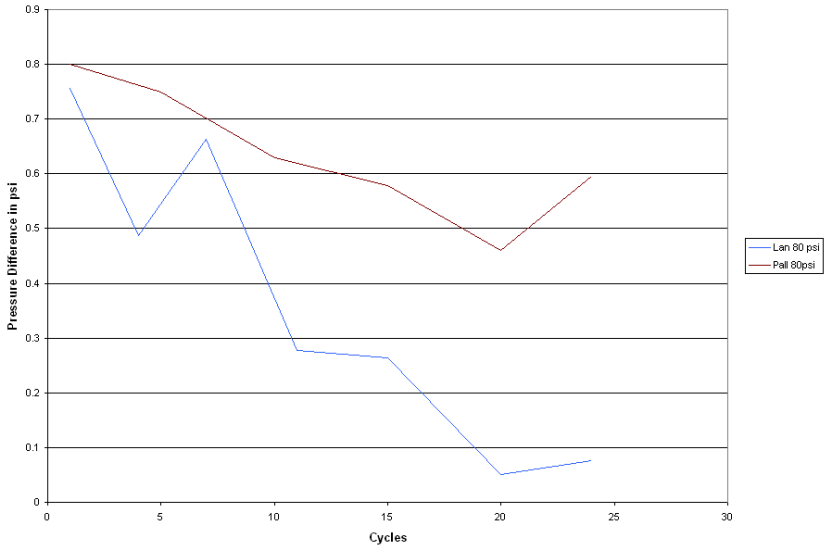

Figure A.6.
Lanxide filter vs. Pall filter
Comparative plot of efficiency-new ($\eta_{N)}$ during regeneration
80 psi regeneration pressure, 5 cm/s face velocity, 20 minute build-up time

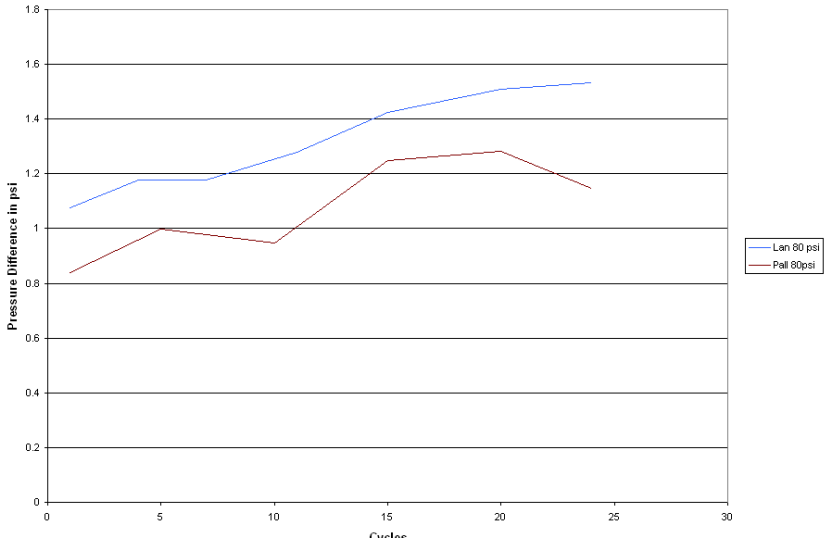

Figure A.7.
Lanxide filter vs. Pall filter
Comparative plot of cleaning factor-cleaned (F_C) during regeneration
80 psi regeneration pressure, 5 cm/s face velocity, 20 minute build-up time

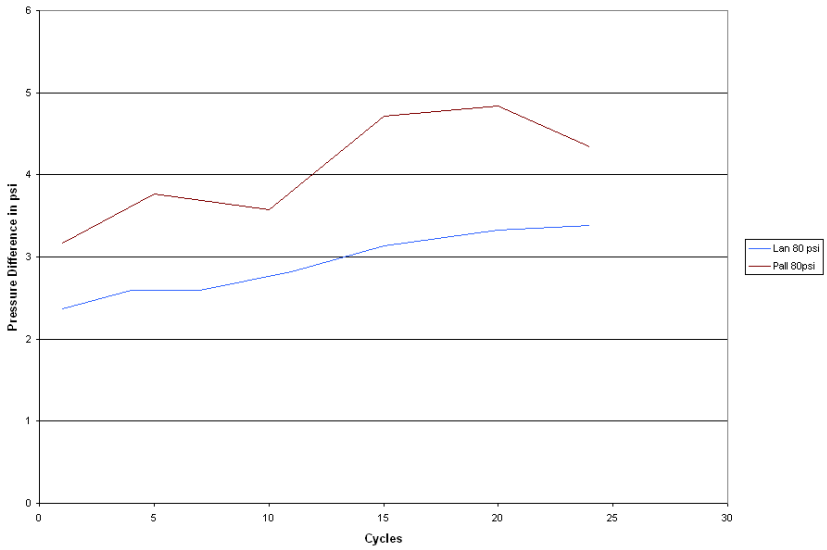

Figure A.8.
Lanxide filter vs. Pall filter
Comparative plot of cleaning factor-new (F_N) during regeneration
80 psi regeneration pressure, 5 cm/s face velocity, 20 minute build-up time

APPENDIX B

Comparative plot of Lanxide filter vs. Pall filter

95 psi regeneration pressure, 5 & 7cm/s face velocity, 20 minute build-up time

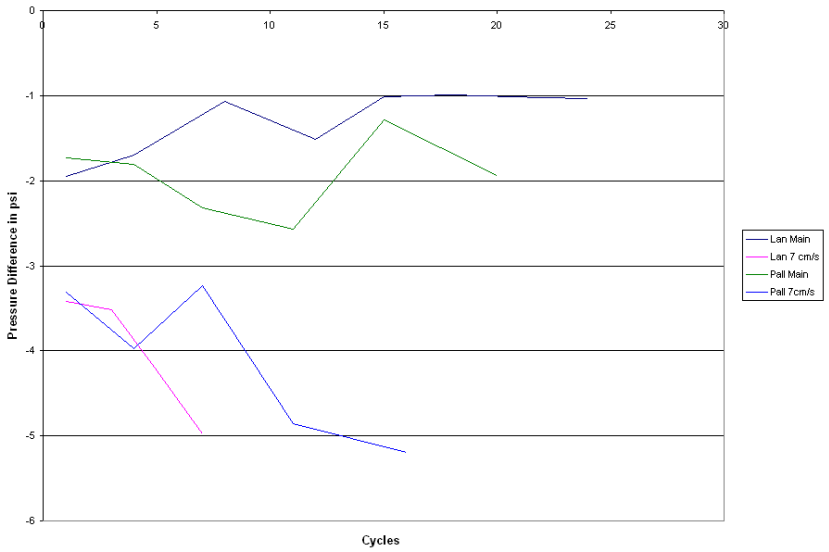

Figure B.1.
Lanxide filter vs. Pall filter
Comparative plot of initial pressure difference ($\Delta P_{initial}$) during regeneration
95 psi regeneration pressure, 5 & 7 cm/s face velocity, 20 min build-up time

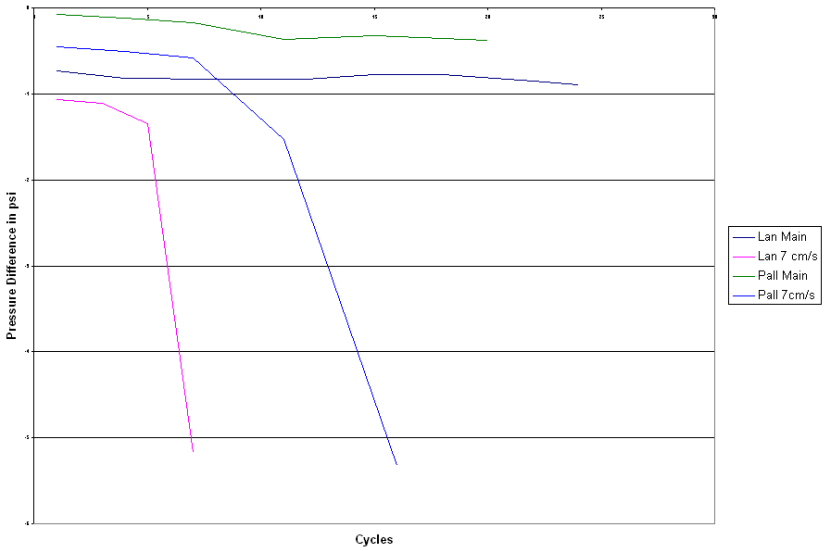

Figure B.2.
Lanxide filter vs. Pall filter
Comparative plot of final pressure difference (ΔP_{final}) during regeneration
95 psi regeneration pressure, 5 & 7 cm/s face velocity, 20 min build-up time

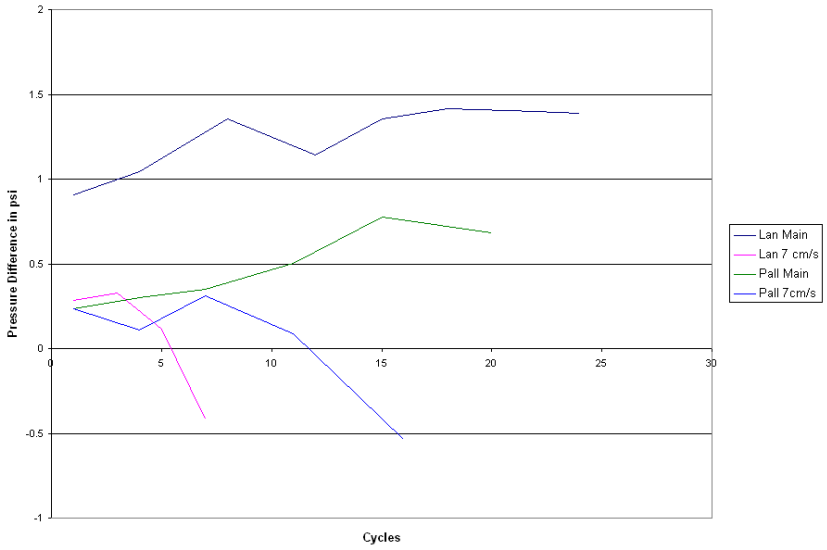

Figure B.3.
Lanxide filter vs. Pall filter
Comparative plot of maximum pressure difference (ΔP_{max}) during regeneration
95 psi regeneration pressure, 5 & 7 cm/s face velocity, 20 min build-up time

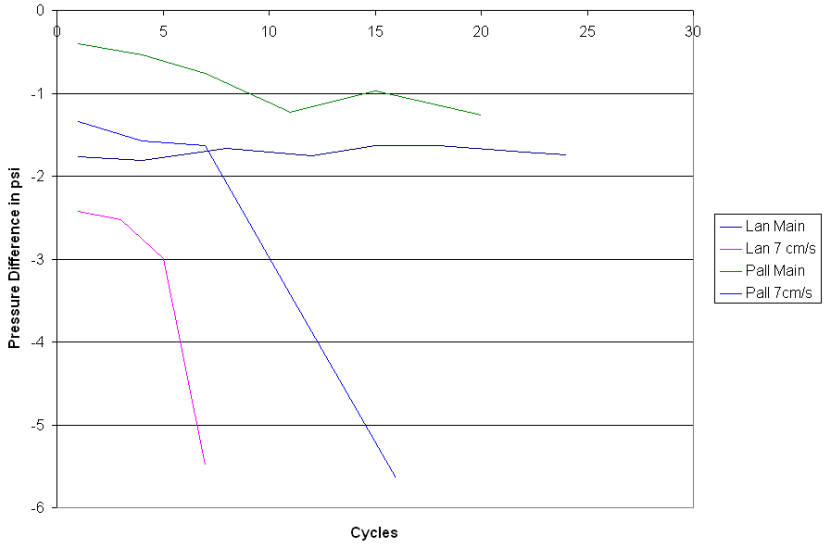

Figure B.4.
Lanxide filter vs. Pall filter
Comparative plot of minimum pressure difference (ΔP_{min}) during regeneration
95 psi regeneration pressure, 5 & 7 cm/s face velocity, 20 min build-up time

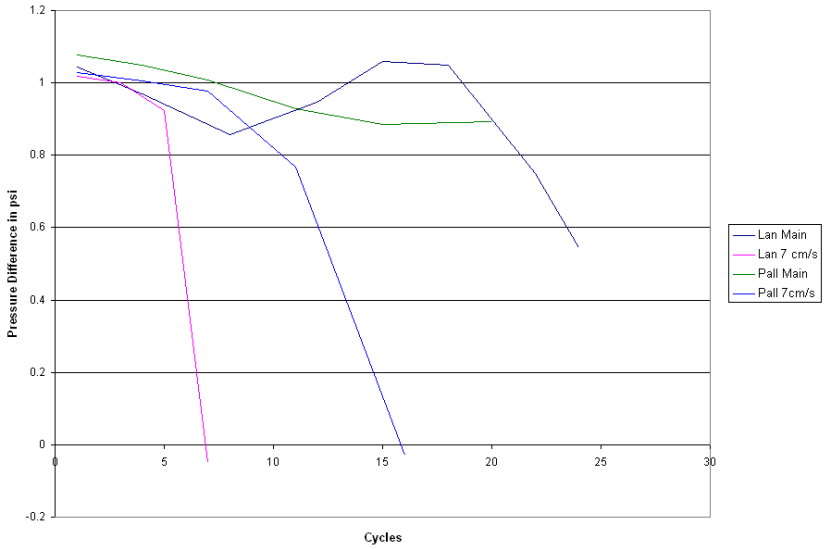

Figure B.5.
Lanxide filter vs. Pall filter
Comparative plot of efficiency-cleaned (η_C) during regeneration
95 psi regeneration pressure, 5 & 7 cm/s face velocity, 20 min build-up time

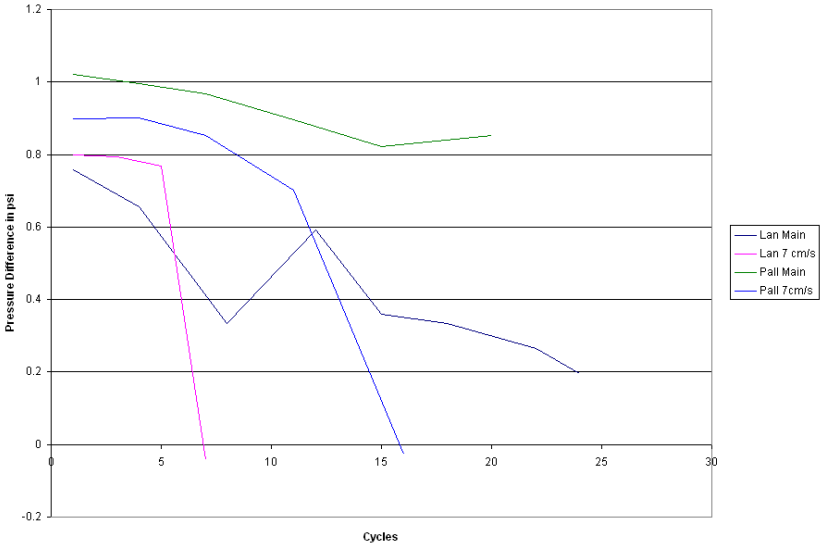

Figure B.6.
Lanxide filter vs. Pall filter
Comparative plot of efficiency-new ($\eta_{N)}$ during regeneration
95 psi regeneration pressure, 5 & 7 cm/s face velocity, 20 min build-up time

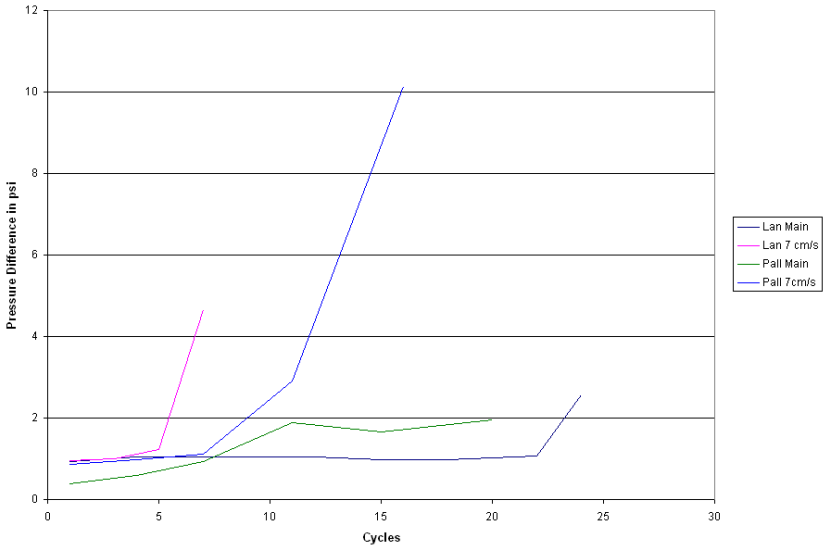

Figure B.7.
Lanxide filter vs. Pall filter
Comparative plot of cleaning factor-cleaned (F_C) during regeneration
95 psi regeneration pressure, 5 & 7 cm/s face velocity, 20 min build-up time

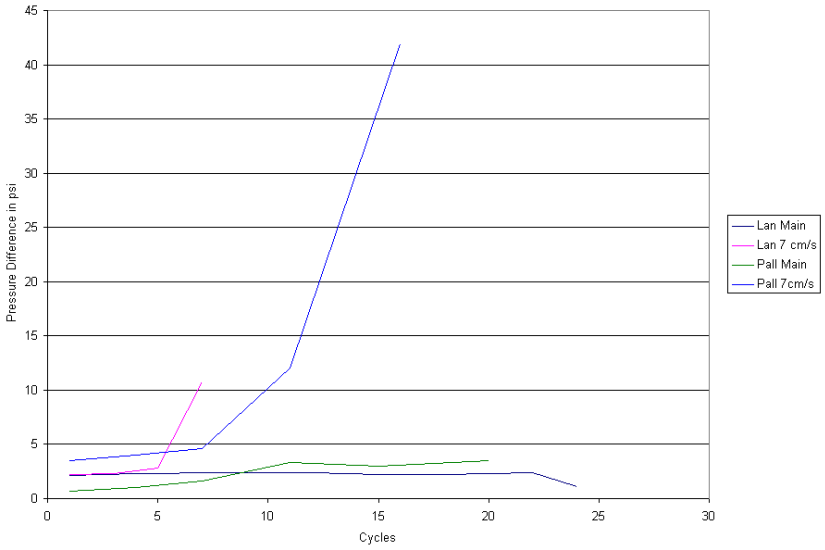

Figure B.8.
Lanxide filter vs. Pall filter
Comparative plot of cleaning factor-new (F_N) during regeneration
95 psi regeneration pressure, 5 & 7 cm/s face velocity, 20 min build-up time

APPENDIX C

Comparative plot of Lanxide filter vs. Pall filter

95 psi regeneration pressure, 5 cm/s face velocity, 45 & 90 min build-up time

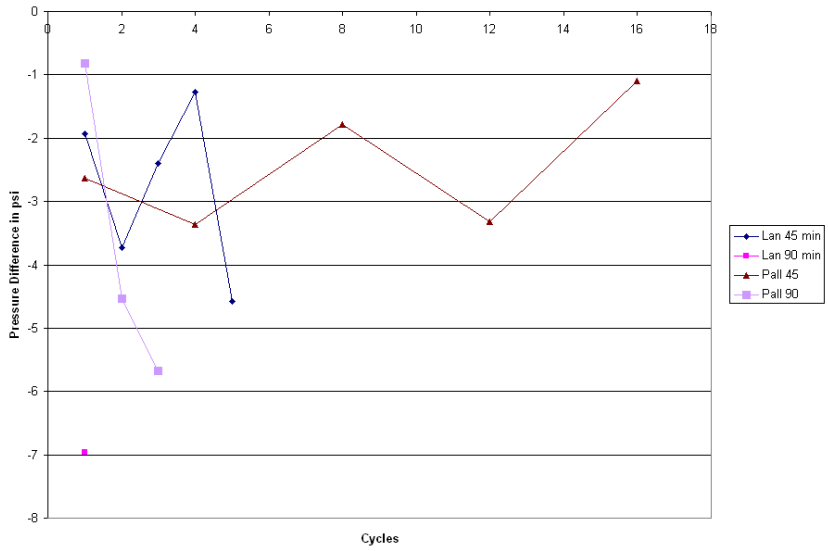

Figure C.1.
Lanxide filter vs. Pall filter
Comparative plot of initial pressure difference ($\Delta P_{initial}$) during regeneration
95 psi regeneration pressure, 5 cm/s face velocity, 45 & 90 min build-up time

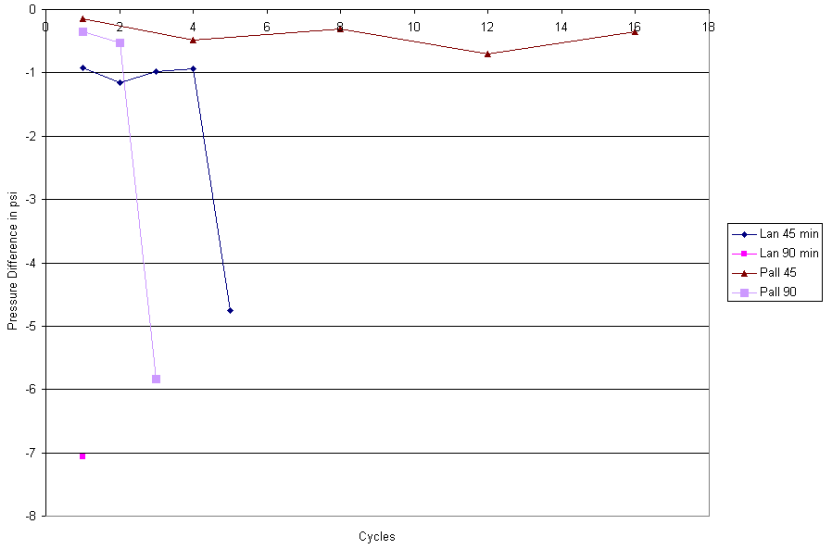

Figure C.2.
Lanxide filter vs. Pall filter
Comparative plot of final pressure difference (ΔP_{final}) during regeneration
95 psi regeneration pressure, 5 cm/s face velocity, 45 & 90 min build-up time

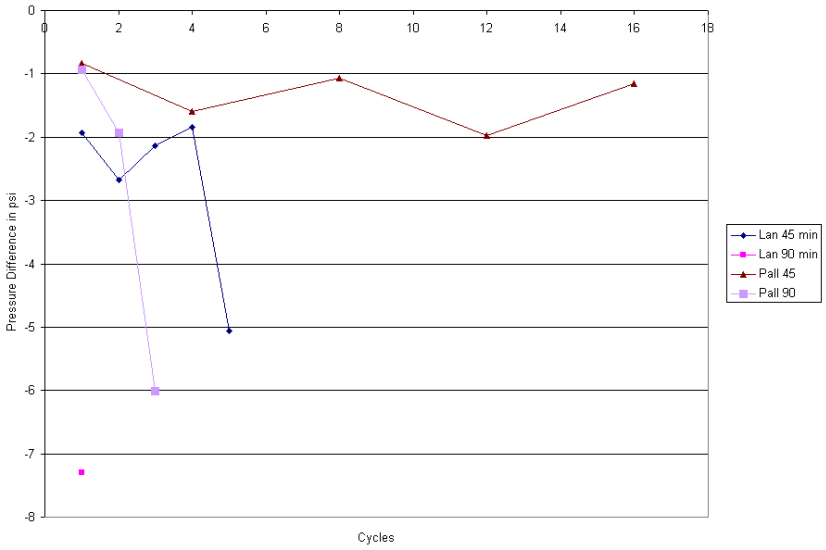

Figure C.3.
Lanxide filter vs. Pall filter
Comparative plot of maximum pressure difference (ΔP_{max}) during regeneration
95 psi regeneration pressure, 5 cm/s face velocity, 45 & 90 min build-up time

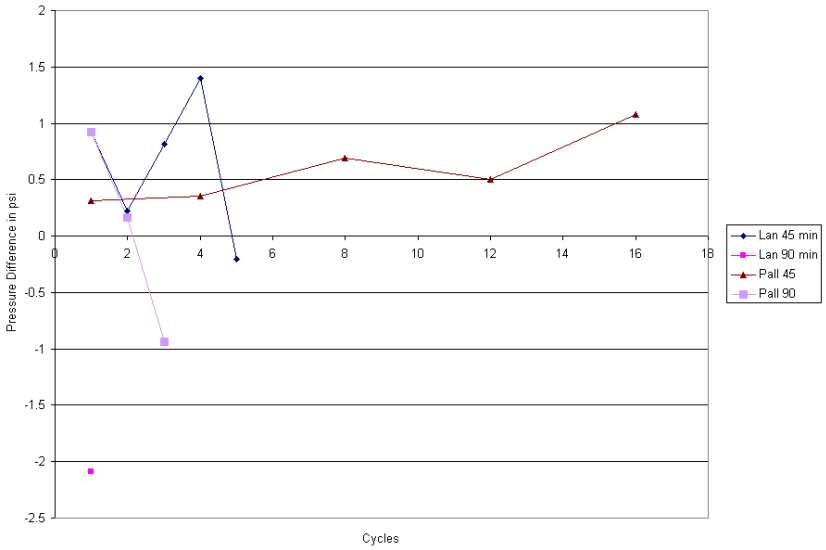

Figure C.4.
Lanxide filter vs. Pall filter
Comparative plot of minimum pressure difference (ΔP_{min}) during regeneration
95 psi regeneration pressure, 5 cm/s face velocity, 45 & 90 min build-up time

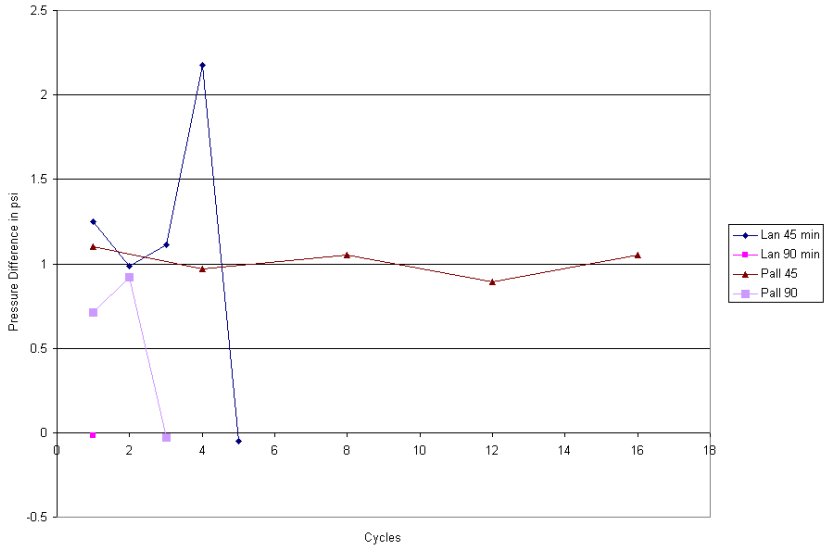

Figure C.5.
Lanxide filter vs. Pall filter
Comparative plot of efficiency-cleaned (η_C) during regeneration
95 psi regeneration pressure, 5 cm/s face velocity, 45 & 90 min build-up time

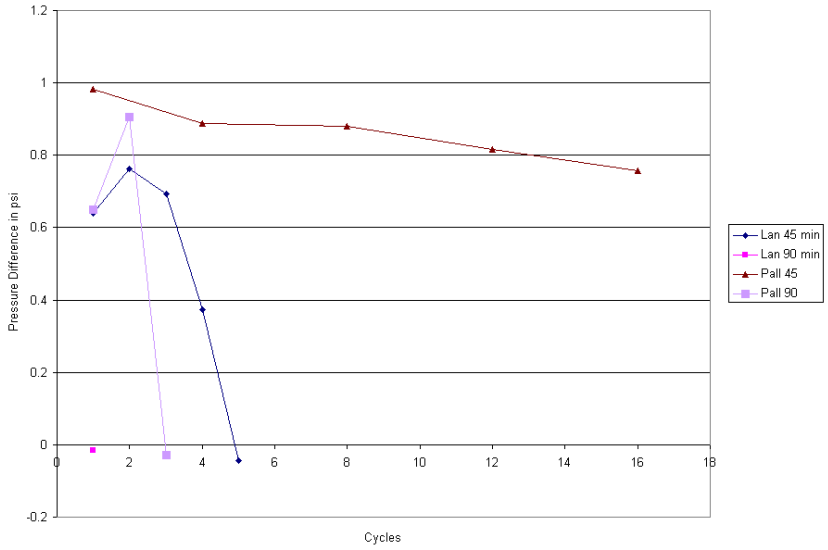

Figure C.6.
Lanxide filter vs. Pall filter
Comparative plot of efficiency-new ($\eta_{N)}$ during regeneration
95 psi regeneration pressure, 5 cm/s face velocity, 45 & 90 min build-up time

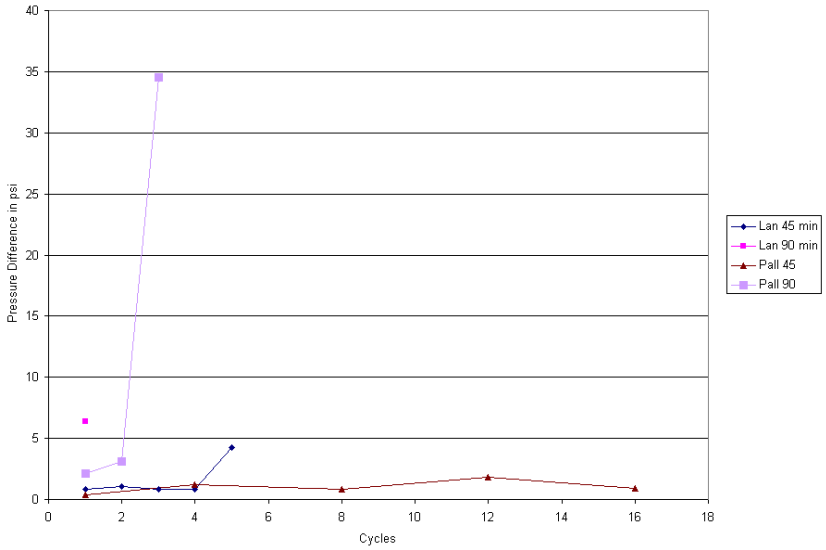

Figure C.7.
Lanxide filter vs. Pall filter
Comparative plot of cleaning factor-cleaned (F_C) during regeneration
95 psi regeneration pressure, 5 cm/s face velocity, 45 & 90 min build-up time

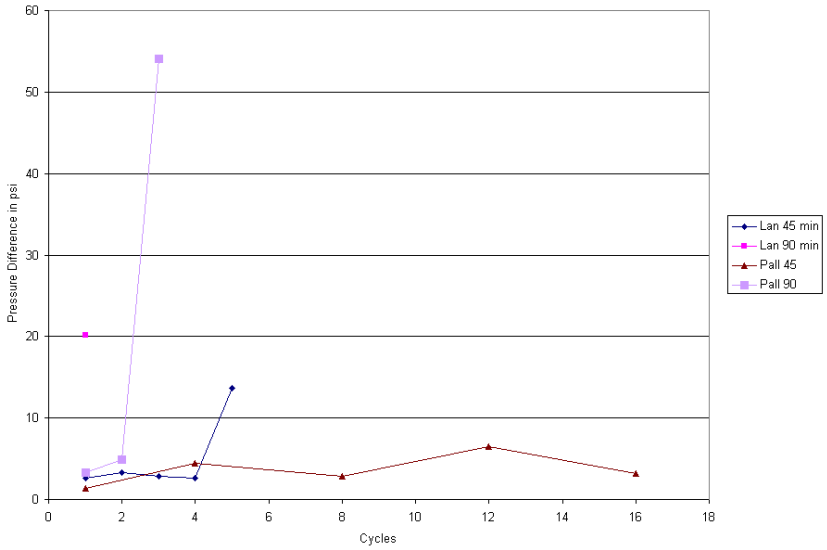

Figure C.8.
Lanxide filter vs. Pall filter
Comparative plot of cleaning factor-new (F_N) during regeneration
95 psi regeneration pressure, 5 cm/s face velocity, 45 & 90 min build-up time

References

1. Christ, A., Giernoth, B.,and Renz, U., “Possible Improvements to the Back-Pulse Cleaning of Ceramic Candle Filters", ASME Fluidized Bed Combustion, Volume-1, 1995, pp. 241-250.
2. Berbner, S., and Lofler, F.,, “Pulse Jet Cleaning of Rigid Filter Elements at High Temperatures”, Gas Cleaning at High Temperatures, Chapman and Hall, 1993, pp. 225-243.
3. Berbner, S., and Pilz, T.,, “Characterization of the Filtration and Regeneration Behaviour of Rigid Ceramic Barrier Filters at High Temperatures”, Powder Technology, 86, 1996, pp. 103-111.
4. Chiang, Ta-Kuan, “Regeneration Characteristics of a Rigid Barrier Filter”, Symposium on High Temperature Particulate Cleanup for Advanced Coal-Based Power Systems, DOE/EPRI, Birmingham, AL, April 20-23, 1998
5. Cicero Daniel C., Dennis, Richard A., Geiling, Donald W., and Schmidt, Dale K., “Hot- gas cleanup for coal-based gas turbines”, Mechanical Engineering, September, 1994, pp. 70-75.
6. Dennis R., McMahon, T., Dorchak, T., and Chaing, T., “U.S. Department of Energy’s High-Temperature and High-Pressure Particulate Cleanup Program for Advanced Coal-Based Power Systems”, High Temperature Gas Cleaning Volume II, 1999, G. Braun ems GmbH, pp. 303-314.
7. Duo, W, Grace, J.R, et al “The Role of Filter Cake in Hot Gas Cleaning with Ceramic Filters", Industrial Engineering Chemistry, 1999, Vol. 38, pp. 260-269.

8. Ji, Z., Meng, X., Shi, M., and Ding, F., "The Interim Process between Pulse-backing Cleaning and Normal Filtration Processes of Ceramic Filter", High Temperature Gas Cleaning Volume II, 1999, G. Braun ems GmbH, pp. 211-219.
9. Kanaoka, C., Amornkitbamrung, M, Kishima, T., "Cleaning Mechanism of Dust from Ceramic Filter Element", High Temperature Gas Cleaning Volume II, 1999, G. Braun ems GmbH, pp. 142-152.
10. Kang, B.S-J., Johnson, E.K., and Gregory, S., "Basic Candle Filter Surface Regeneration Investigation", High Temperature Gas Cleaning Volume II, 1999, G. Braun ems GmbH, pp. 153-163.
11. Koch, D., Schulz, K., Seville, J., and Clift, R., "Regeneration of Rigid Ceramic Filters", Gas Cleaning at High Temperatures, Chapman and Hall, 1993, pp. 244-265.
12. Koch, D., Seville, J., and Clift, R., "Dust Cake Detachment from Gas Filters", Powder Technology, 86, 1996, pp. 21-29.
13. Laux, S., Giernoth, B., Bulak, H., and Renz, U., "Aspects of Pulse-Jet Cleaning of Ceramic Filter Elements", Gas Cleaning at High Temperatures, Chapman and Hall, 1993, pp. 203-224.
14. Lippert, T.E., et. al., "Development of Hot Gas Cleaning Systems for Advanced, Coal-Based Gas Turbine Cycles", Journal of Engineering for Gas Turbines and Power, Vol. 115, July 1993, pp. 658-664.
15. Natesan, K., "Materials Performance in Advanced Combustion Systems", Journal of Engineering for Gas Turbines and Power, April 1994, Vol. 116, pp. 331-337.

16. Newby, R. A., and Bannister, R. L., "Advanced Hot Gas Cleaning System for Coal Gasification Processes", Journal of Engineering for Gas Turbines and Power, Vol. 116, April 1994, pp. 338-344.
17. Quimby, J. M. and Kumar, K. S., "Hot Gas Cleanup for Advanced Power Generation System", Gas Cleaning at High Temperatures, Chapman and Hall, 1993, pp. 66-85.
18. Raask E.,″ *Mineral Impurities in coal combustion* ″, Hemisphere Publishing corporation, 1985.
19. Seville, J.P.K., "Particulate Removal II - Overview", High Temperature Gas Cleaning Volume II, G. Braun ems GmbH, pp. 131-141.
20. Stringer, J., Leitch, A. J., "Ceramic Candle Filter Performance at the Grimethorpe (UK) Pressurized Fluidized Bed Combustor", Journal of Engineering for Gas Turbines and Power, April 1992, Vol. 114, pp. 371-379.
21. Beattie, C.J.C., and Withers, C. J., "Applications of Low Density Ceramic Filters for Gas Cleaning at High Temperatures", Gas Cleaning at High Temperatures, Chapman and Hall, 1993, pp. 173-189
22. Web Source http://www.engr.utk.edu/~cmc/429/appli/appli.html
23. Burnard, G. K., Leitch, A. J., Stringer, J., Clark, R.K., and Holbrow, P., "Operation and Performance of the EPRI hot gas filter at Grimethorpe PFBC Establishment: 1987-1992", Gas Cleaning at High Temperatures, Chapman and Hall, 1993, pp. 88-110
24. Gregory S.P., "Development of instrumentation for the investigation of surface regeneration for candle filters", Thesis (M.S.)--West Virginia University, 2001

PART II - High Temperature Test Facility

A HIGH TEMPERATURE TEST FACILITY FOR STUDYING ASH PARTICLE CHARACTERISTICS OF CANDLE FILTER DURING SURFACE REGENERATION

Introduction

A High Temperature Test Facility (HTTF) was built to investigate the ash characteristics during surface regeneration at high temperatures. The system is capable of conducting surface regeneration tests of a single candle filter at temperatures up to 1500^{o}F. Details of the HTTF apparatus as well as some test results are presented in this report. In order to obtain sequential digital images of ash particle distribution during the surface regeneration process, a high resolution, high-speed image acquisition system was integrated into the HTTF system. The regeneration pressure and the transient pressure difference between the inside of the candle filter and the chamber during regeneration were measured using a high speed PC data acquisition system. The control variables for the high temperature regeneration tests were (1) face velocity, (2) pressure of the back pulse, (3) cyclic ash built-up time and, (4) temperature of the hot gas being filtered.

The High Temperature Test Facility

The HTTF system consists of a chamber, an air preheater, a gas control unit, a water cooling system for pressure sensors, a temperature control unit, a data acquisition system, and an image capturing system, as schematically shown in Figure 2.1.

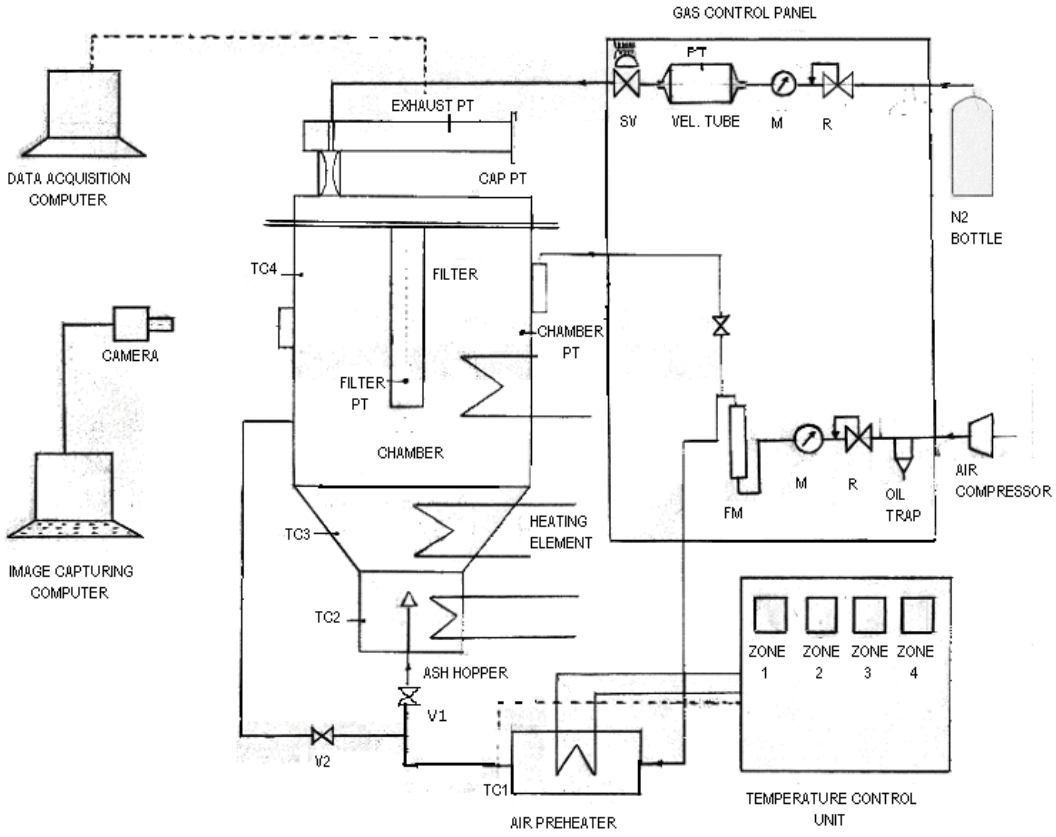

Figure 2.1 The High Temperature Testing Facility

The HTTF chamber is essentially an electrically heated oven which is constructed of stainless steel with heating elements mounted on the outside wall of the steel frame and then covered by a 1.5 inches thick thermal insulation layer of alumina silica. A single filtration element (candle filter) was mounted inside the chamber where the hot gas filtration process took place.

For a typical sequence of surface regeneration tests, a continuous stream of hot air flows through a nozzle in the ash hopper at the bottom of the HTTF. The hot air flow fluidizes the particles in the ash hopper. The fluidized stream of particles then flow

through the chamber and up to the candle filter. The gases then flow through the filter and the ash particles are trapped on the filter surface.

The chamber has a quartz window in each wall. The windows are positioned in sets of two, at two different elevations. The image capturing system takes pictures through one of the windows, while a light source projects a parallel light through the other window at the same elevation. The selection of quartz windows was necessary for its high temperature tolerance as well as its low thermal expansion coefficient. These conditions were necessary in order to avoid failure of the windows during heating and cooling for each test.

All the windows have internal metallic shields which can be opened or closed depending on whether regeneration pictures are to be taken. Continuous gas (air) injection is provided between the shield and the quartz window in order to keep the internal surface clean.

The air preheater is a Pebble Bedded Heat Exchanger (PBHE), which is used to raise the gas (air) to the desired temperature. The PBHE consists of a forty-inch long stainless steel pipe (diameter: 4.25 inch, thickness: 0.135 inch) which is filled with 1/4" diameter alumina-silica balls. The unit is thermally insulated with a three-inch thick layer of a soft-hard combination of alumina-silica.

The gas (air) from the preheater enters the chamber at two points, Figure 2.1. The V1 valve controls the air going to the ash hopper, while the V2 valve controls air going to the side port, thus bypassing the ash hopper. In this way the system can simulate the actual regeneration process in an IGCC or PFBC power plant, i.e., maintaining the flow of gas (air) into the chamber while surface regeneration is taking place. Specifically,

when V1 is opened with V2 closed, the ash is being fluidized and filtration occurs at a specified face velocity. When V2 is opened with V1 closed, the fluidization of the ash is stopped and the concentration of particles in the chamber is significantly reduced while the face velocity is maintained on the filter surface. This allowed the optical system to have a relatively clear path to the filter surface.

The gas control panel has two separate gas lines, one for air and the other for nitrogen. The air line supplies air at the desired flow rate and pressure to the air pre-heater. An oil trap was installed in the air line to ensure an oil-free air for the experiments. This is to avoid two potential problems: combustion at the higher temperatures and oil-caused stickiness in the ash layer not related to the ash characteristics.

The nitrogen line has a pressure regulator to establish a suitable reservoir pressure for the back pulse. A velocity tube was installed with a pressure sensor attached to it. This configuration gives pulse pressure information during the regeneration period. A normally closed solenoid valve in the nitrogen line is triggered by the data acquisition system to start the surface regeneration process.

A temperature control unit was used to keep the air inside the chamber at the desired temperature condition during the test runs. The temperature was controlled through four independent heating zones with a total power rating of 28.8 KW. The first zone is the air preheater with a power rating of 10.8 KW. Zone two is the ash hopper section at the bottom of the chamber with a 3.6 KW heating element attached. Zone three is the middle part of the chamber with a heating element of 7.2 KW. Zone four is the

upper portion of the chamber with a 7.2 KW heating element. Each zone has its own thermocouple connected to the temperature controller.

The HTTF system has pressure sensors placed inside the chamber, the filter, the cap of the chamber, and the exhaust tube of the chamber. Each pressure sensor is water-cooled to prevent damage due to exceeding allowable temperatures. The data acquisition system is used to record all the pressure information from the pressure sensors.

The optical system is consisted of an image capturing system which is capable of recording sequential high resolution pictures (1024 x 512 pixels) of the regeneration process at 60 frames per second for 20 seconds. The imaging acquisition is triggered by a signal coming from the solenoid valve in the nitrogen line. A long-distance microscope lens is attached to the CCD camera and is capable of measuring resolution down to 25 micron at a distance of one meter to the object.

Experimental Procedure

The procedure consists of three main steps. In the first step the filter inside the chamber as well as the internal walls of the chamber and the windows were properly cleaned of any ash before starting a new test. Initially V1 was closed and V2 was opened for the purpose of avoiding any ash fluidization during the heating process.

In the second step the chamber was brought up to the operating temperature. The desired air temperature target for the test was set in zone 4 of the temperature control unit. Temperature readings were recorded at least every half an hour during the heating process, which usually took between 4 and 8 hours. In the third step, when the air inside the chamber had reached a stable temperature at the specified condition, the filtration

process was then commenced. The data acquisition system was then activated, and V1 was opened and V2 was closed. After the filtration period had been completed, V1 was closed and V2 was opened in order to let the free particles settle, while maintaining the specified face velocity on the ash layer. Then two windows were then opened for the image-capturing sequence during the surface regeneration process. The onset of the image capturing sequence was triggered by the signal coming from the solenoid valve. This step was repeated for each cycle during the tests at a specific temperature condition. This sequence of events is shown in Figure 2.3.

Test Matrix

The selected test matrix for the HTTF was based on the test conditions employed for the RTTF. Table 2.1 shows the test matrix employed in this investigation. This test matrix was based on the optimum surface regeneration conditions obtained in the RTTF tests, Part I. Unfortunately, the length of each test run at elevated temperatures was such that a test matrix had to be selected at the beginning of the testing period. There was no time for exploratory tests to determine if there were more appropriate conditions for a study of the surface regeneration process. Consequently, it was determined to use the optimum surface regeneration conditions from the room temperature tests and investigate the effects of higher temperatures on the process relative to the room temperature tests.

Table 2.1 Test Matrix

Test #	Temperature	Face Velocity (cm/s)	Regeneration Press(psi)	Build up time (minutes)	# of regeneration cycles
1	1100	5	95	20	8
2	1200	5	95	20	7
3	1300	5	95	20	8
4	1300	5	95	20	21
5	1300	7	95	20	21
6	1400	5	95	20	21
7	1400	7	95	20	16
8	1500	7	95	20	21

The measurements made during these tests include the chamber pressure and the filter pressure as a function of time. Pictures were obtained for various surface regeneration events. The particulate matter used in this work was a coal ash obtained from the Power System Development Facility (PSDF) at Wilsonville AL. The ash was from an ash hopper and originated from a combustion process, probably a circulating fluidized bed combustion system. Frequently, after a test run, the condition of the ash in the ash hopper was evaluated as to whether the ash remained as a powder or whether "lumps" were forming due to sintering. All tests investigated indicated that no sintering had occurred.

System Performance

Several preliminary tests were conducted on the HTTF system without ash in the system. These tests were at several temperatures, up to 1500^0 F. The purpose for these tests was to investigate the integrity of the system and the performance of the instrumentation at the temperatures selected for the surface regeneration tests.

The pressure sensors displayed a significant drift during the high temperature tests. After each surface regeneration event, the system was at atmospheric pressure when the windows were closed, V2 was closed , and V1 was not yet opened. The system exhaust was always open to the surroundings: therefore, the system reached a uniform (atmospheric) pressure during the re-calibration period, as shown in Figure 2.3. Before this period was established, the final ΔP_f was recorded; and consequently, the residual ash on the filter had survived the surface regeneration process. Therefore this surviving ash layer should have had sufficient strength (cohesiveness) to survive the pressure equilibration process. Also, the ash layer appeared to be unaffected by the calibration period. If the drift for each pressure sensor occurred at essentially a constant rate, then the pressure difference errors for ΔP_i would be about 0.1 (10% of the total time for the drift) multiplied by the difference in the rate of drift for the two pressures readings. The ΔP_f should be relatively accurate as the pressure sensors are calibrated just after the event.. The metal shield covering the windows, with air supplied to the back side, provided clean windows for the CCD camera and the light source. At this time it appears that the HTTF system has performed as required.

Experimental Results

The experimental results for each test condition have the same general set of curves for the ΔP (pressure drop across the filter) verses time. Figure 2.2 illustrates the results for 1400^0 F and a face velocity of 5 cm/sec. The many curves, one for each cycle, tend to fall close to each other and consequently the details of the surface regeneration processes were difficult to observe. For purposes of discussion, the nomenclature shown on Figure 2.3 will form the bases for the following presentation. The room temperature tests showed that when ΔP_{MAX} exceeded zero, the filter surface would be regenerated. This was due to the weak structure of the ash layer. However, at elevated temperatures, the ΔP_{MAX} frequently exceeded zero without the surface being regenerated. It is apparent that at elevated temperatures, the ash layer has a stronger cohesive structure. In addition, the pictures obtained of the regeneration events at elevated temperatures depicted a new regeneration phenomenon. The room temperature tests showed a thin ash, a thick ash, and a transition thick/thin surface regeneration process. These processes are defined as:

Thin ash regeneration - small ash particles appear to explode off the filter surface.
Thick ash regeneration - large "lumps" of ash appear to fall away from the filter surface.
Thick/thin ash regeneration - initially, lumps of ash begin to fall away from the filter surface followed by disintegration of the lumps and an explosion of small articles from the surface.

At higher temperatures, the ash layer appears to have a stronger structure which requires a greater ΔP_{MAX} for removal of the ash layer. When ΔP_{MAX} is insufficient for cleaning, a new phenomenon may occur. During several surface regeneration events, it appears that small particles are being blown out of the strong ash layer structure, as

shown in Figure 2-4. A dusting of the structure may be a more descriptive expression. This phenomenon is denoted as "dust regeneration". Note that thick and thin ash regeneration processes have also been observed at elevated temperatures, as shown in Figures 2.5 and 2.6.

After reviewing the experimental results, a different approach to analyzing the data was employed. The approach selected was based on the effectiveness of surface regeneration. The analysis consisted of investigating the difference between the initial ΔP_i and the final ΔP_f , as shown in Figure 2.3. The quantity ΔP_i represents the initial pressure drop across the filter that is to be reduced during surface regeneration. This quantity represents the pressure drop across the filter due to the filter wall and the ash layer due to the face velocity. The quantity ΔP_f represents the pressure drop across the filter after surface regeneration. Ideally, ΔP_f would represent the pressure drop across a completely clean filter. Therefore, the quantity (ΔPi - ΔP_f) for each surface regeneration event becomes the bases for the ensuing analysis. This quantity is referred to as the "overall pressure drop difference". The more negative this quantity, the greater the surface cleaning. If this quantity is zero, no surface cleaning has occurred, and if this quantity is greater than zero, the ash layer now produces a greater pressure drop than existed initially. The overall pressure drop difference data from cycle-to-cycle is the basic data and the other data is essentially supporting data. Several pictures were taken of the ash layer during surface regeneration at several test conditions. These pictures were successfully employed in the low temperature tests described in Part I. At elevated temperatures, the pictures were used to understand the overall pressure drop difference data. Figure 2.4 illustrates a dust regeneration process for the 16^{th} cycle of the 1400^0F,

5cm/s, test. A thick ash regeneration is shown in Figure 2.5 for the 1st cycle of the 1400^0F, 7cm/s, test. Figure 2.6 shows a thin ash regeneration for the 2nd cycle of the 1400^0F, 7cm/s, test. There were also conditions for which no regeneration occurred.

The rather chaotic behavior of the ash layer during surface regeneration process may be observed at 1400^0 F at both 5 and 7 cm/sec, Figures 2.7 and 2.8. Both sets of curves appear to indicate that the ash layer should reach a certain thickness before the required filter pressure drop is generated to clean the surface. It may be noted that in several cases, the final pressure difference, ΔP_f is greater than the initial pressure difference, ΔPi. There is no ash being fluidized in this time period, see Figure 2.8. The only plausible explanation is that dust regeneration has occurred in such a way that when the dust is drawn back into the ash structure, an ash layer with more flow resistance is formed.

At 1400 ^{0}F, the data for the initial pressure drop, ΔP_i, at 7 cm/s is more uniform from cycle to cycle when compared to the 5 cm/sec data. Because the filtering period was held constant at twenty minutes, more particles were transported to the filter for the 7 cm/sec tests. This in turn produced thicker ash layers which may have led to better surface regeneration performance. The variation of the overall pressure drop difference for the 5 cm/sec tests may be due to: 1) an intermediate ash layer thickness which produced inconsistent surface cleaning, or 2) the low value for the pulse pressures. An interesting additional experiment would have been to have a set of tests at 5cm/s and a 28 minute filtering period. This 28 minute period corresponds to the same amount of ash being deposited on the filter with a face velocity of 5cm/s as a 20 minute period with a face velocity of 7cm/s.

Discussion

A HTTF system has been designed, constructed, and operated at temperatures up to 1500^0F. Temperature and pressure sensors and associated instrumentation for the HTTF system were also developed and made operational. Preliminary filter surface regeneration tests were conducted at temperatures of 1100, 1200, 1300, 1400, and 1500^0F. Test results indicate that the history profiles (ΔP versus time) for the tests are consistant with the general shape of the profiles obtained during the room temperature tests. However, the details in the pressure history curves begin to change at 1300^0F.

Several tests were initially conducted, without ash in the system, from room temperature up to 1500^0F, to ensure the integrity and performance of the system. Then several cyclic ash layer build-up and surface regeneration tests were conducted at 1100, 1200, 1300, 1400, and 1500^0F to complete the initial testing. The test conditions selected correspond to those employed during room temperature tests and are shown in Table 2.1.

The data for each test condition is grouped together so that each test condition may be more easily reviewed. Each group of data contains: 1) the pressure history, 2) the initial pressure drop, 3) the final pressure drop, 4) the maximum pressure drop, 5) the overall pressure drop difference, and 6) several regeneration photographs. The data for the 1300^0F runs are shown in Figures 2.9 through 2.23, the data for the 1400^0F are shown in Figures 2.24 to 2.42, and the data for the run at 1500^0F are shown in Figures 2.43 to 2.49.

The analysis of the data for each temperature condition involves employing essentially the same arguments. Selecting the 1400^0F tests runs as our basis for analysis , it may be noted that the curves in Figure 2.24 (1400^0F,5cm/s) and 2.2.9 (1400^0F, 7cm/s) are essentially of the same shape as the general curve shown in Figure 2.3. The initial

pressure drop, ΔP_i, represents the sum of the pressure drops across the filter wall and ash layer which involves the ash thickness and porosity parameters. If a residual ash layer forms and grows during each cycle, then for a constant face velocity, the ΔP_i should become larger (more negative) with each cycle. As indicated in Figure 2.25 and2.30, no such general trend was observed. However, the ΔP_i also depends on porosity and the effectiveness of the previous surface regeneration event. The ΔP_{MAX} and ΔP_f results are rather erratic. The most interesting results are shown in Figures 2.28 and 2.33. The overall pressure drop difference oscillates between positive and negative values. Recall that the equation for the overall pressure drop difference is $(\Delta P_i - \Delta P_f)$ and both quantities are negative. For surface regeneration to be successful, $|\Delta P_i| > |\Delta P_f|$, which leads to a negative number. However, if $|\Delta P_i| < |\Delta P_f|$, then one obtains a positive number. The pressure drop across the filter in this situation is greater after surface regeneration than before surface regeneration. In this study, the fluidizing air valve, VI, was closed during the regeneration process, see Figure 2.3. Then the only plausible explanation is that dust regeneration occurred and when the dust particles re-entrained in the ash layer, the porosity of the ash layer was reduced. Of course, $|\Delta P_i| = |\Delta P_f|$ implies that nothing occurred during the surface regeneration event.

It should be noted that the ΔP_{MAX} depends on the resistance to flow caused by the thickness of the ash layer. The ΔP_{MAX} is then related to the stresses in the ash layer. If the ash layer is thin, then ΔP_{MAX} will be small and either dust or no regeneration may occur. This may be the situation for many situations. Once the ash layer thickness reaches a critical value, then significant surface cleaning may occur. This concept appears plausible considering cycles 11 and 13 in Figures 2.26 and 2.27 (1400^0F, 5cm/s). This logic is not

apparent for 1400^0F, 7cm/s. This may be due to the fact that the ash thickness was greater for the 7cm/s cycles and the ΔP_{MAX} was, on the average, greater than that for the 5cm/s tests.

Another concept which should be considered is the ΔP_R, shown in Figure 2.3. During surface regeneration, there are two flows into the filter chamber. The flows are the process air (fluidizing air) and the pulse jet gas through the filter. The pressure in the chamber increases, but the pressure increase inside the filter is greater. When the pulse jet stops, the pressure in the filter quickly returns to the downstream pressure. However, the increased pressure in the chamber decreases at a slower rate. Consequently, just after the pulse jet is stopped, there is a short period of excess chamber pressure before ΔP_f is reached. The greater the value of ΔP_R, the greater will be the velocity and the number of the particles being re-entrained. The value for the ΔP_R, on the average, was of greater magnitude for the 7cm/s tests. As alluded to previously, these re-entrained particles may have a significant effect on the strength and/or porosity of the ash layer. The pictures taken of the surface regeneration process are not consistent with the pressure data. Several pictures did not show any surface regeneration effects; however, the pressure data indicated some surface cleaning had occurred.

This discussion of the results for the 1400^0F tests is applicable to the tests at 1300 and 1500^0F.

Future Research

In order to more completely understand the data obtained in these tests, it is estimated that a four person month effort would be required. Such an effort was not

anticipated nor requested in the project proposal. The information required for a detailed analysis would include the following items:

(1) Thickness of ash layer before and after each surface regeneration event,
(2) Particle characteristics at elevated temperatures,
(3) Chamber pressure histories,
(4) Filter pressure histories, and
(5) Pictures of the surface regeneration events.

Item #1 may be obtained from the existing pictures using image enhancement techniques. Also, item#1 would provide the information as to the consistency of the particle flow to the filter. Item #2 would involve heating ash material in the form of cones to selected temperatures. The characteristics of significance would be the ash softening temperature, the shrinkage of the cone, and stickiness of the particles. Items# 3, 4, and 5 already exists and the pictures would require enhancement to insure nothing has been overlooked.

In addition, a new set of tests should be performed with a higher pulse pressure. It is of concern that the selected pulse pressure may represent a condition on the boundary of the "good" range of operating conditions. The rational for suggesting a higher pulse pressure was the increased strength of the ash layer.

Future experimental studies with the HTTF should include modifications to the facility. These modifications involve redesigning the system so that the filter may be more readily replaced and/or removed for cleaning. Also, the ash hopper dimensions should be reduced to insure the proper fluidization of the particles during the high temperature test conditions. An additional study would be to investigate the drift of the pressure signals during the high temperature tests,

Conclusions

A high temperature test facility has been designed and assembled. Temperature and pressure measurement systems have been installed and made operational. The optical equipment developed for the RTTF was installed and made operational. Tests were conducted up to 1500^0F. The surface regeneration process at the selected conditions was investigated. The results of these tests appear to be reasonable on a macroscopic time scale, but rather chaotic on a microscopic time scale. It is the investigators opinion that the HTTF and associated equipment operated as desired and produced reliable results for the conditions selected.

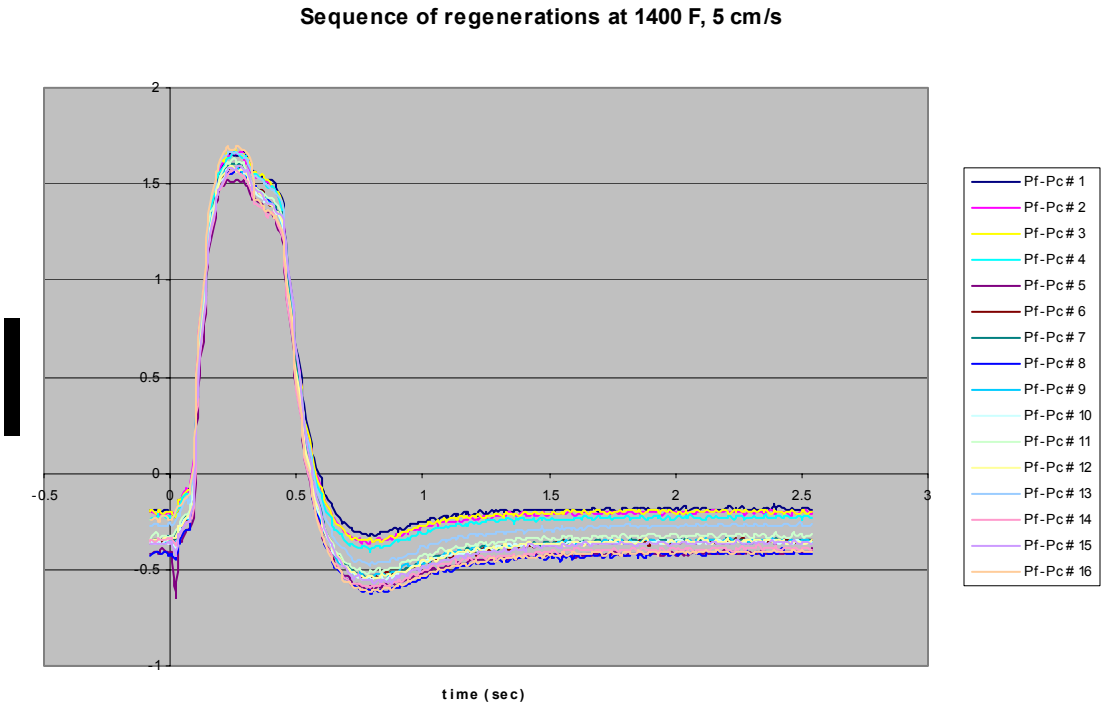

Figure 2.2 ΔP vs. time at 1400 C, 5

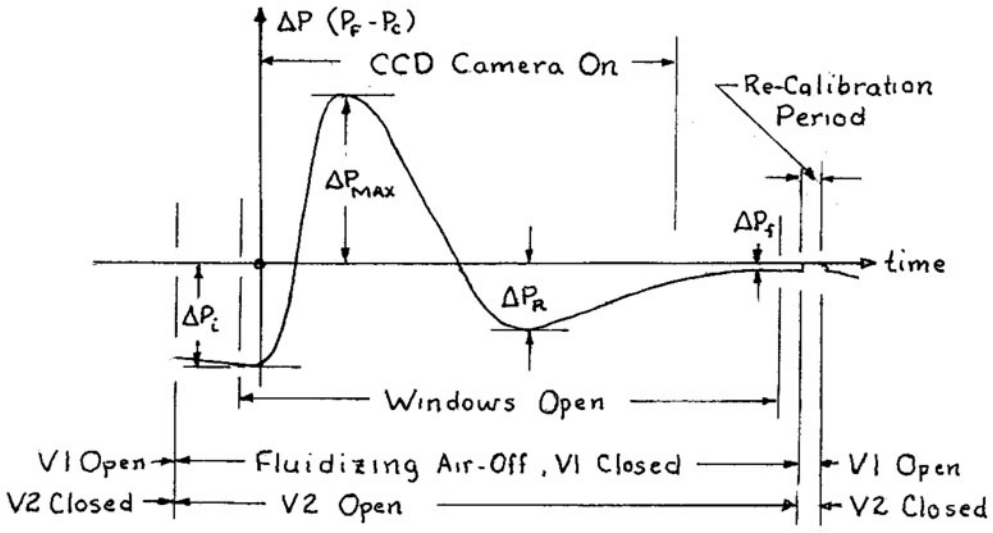

Figure 2.3 Typical curve of pressure drop across the filter

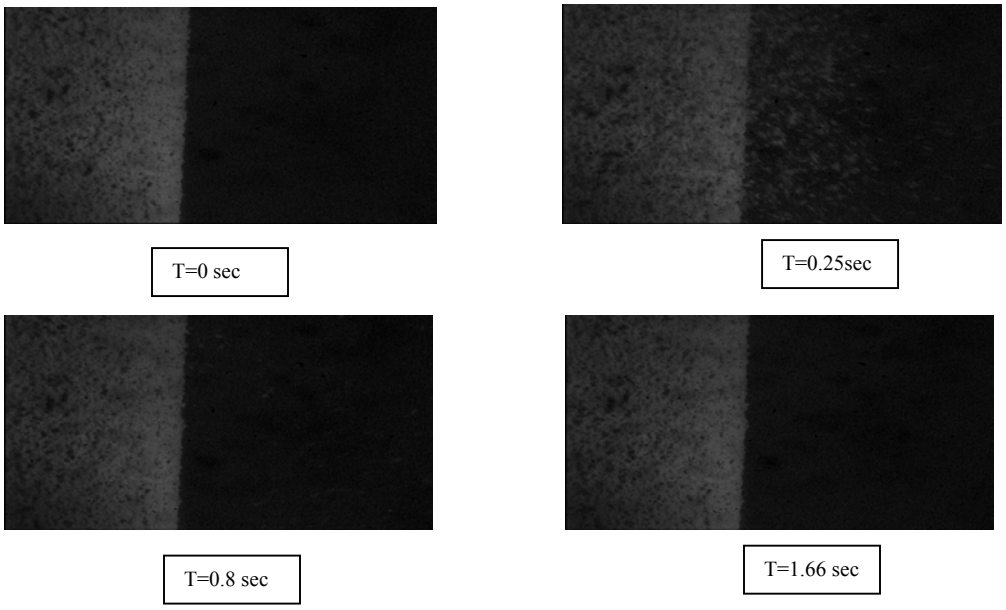

Figure 2.4 Dust regeneration at 16 th cycle, 1400 F, 5 cm/s

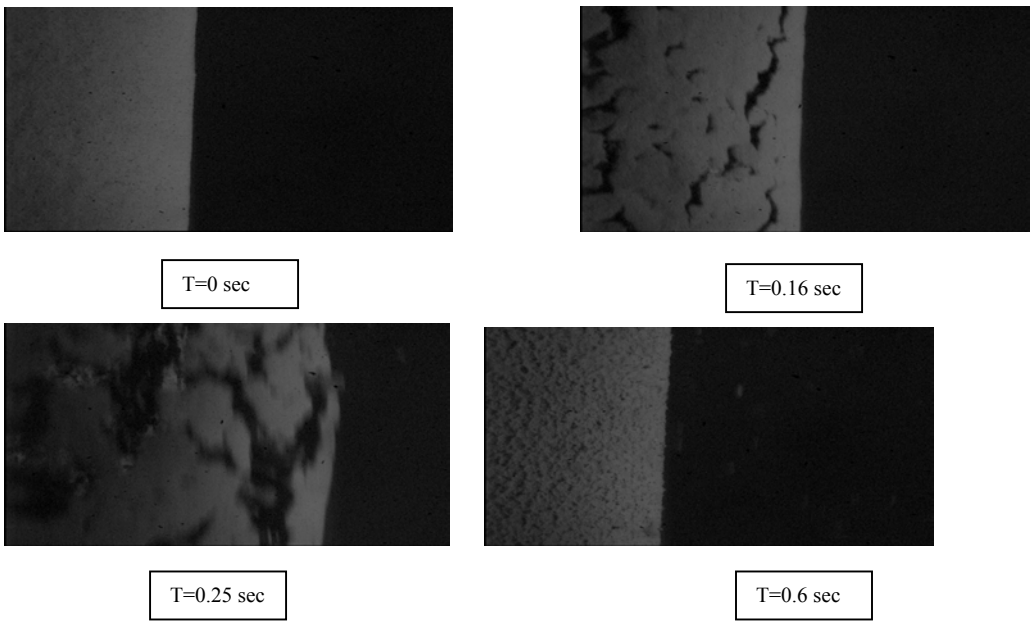

Figure 2.5 Thick ash regeneration at first cycle with residual ash formation. 1400 F, 7 cm/s

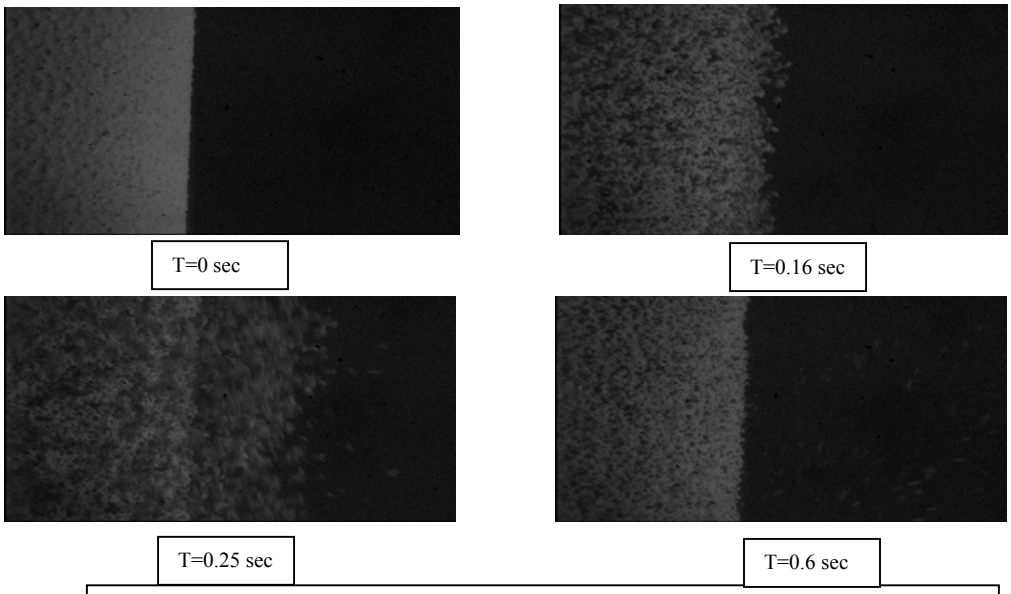

Figure 2.6 Thin ash regeneration at second cycle. 1400 F, 7 cm/s

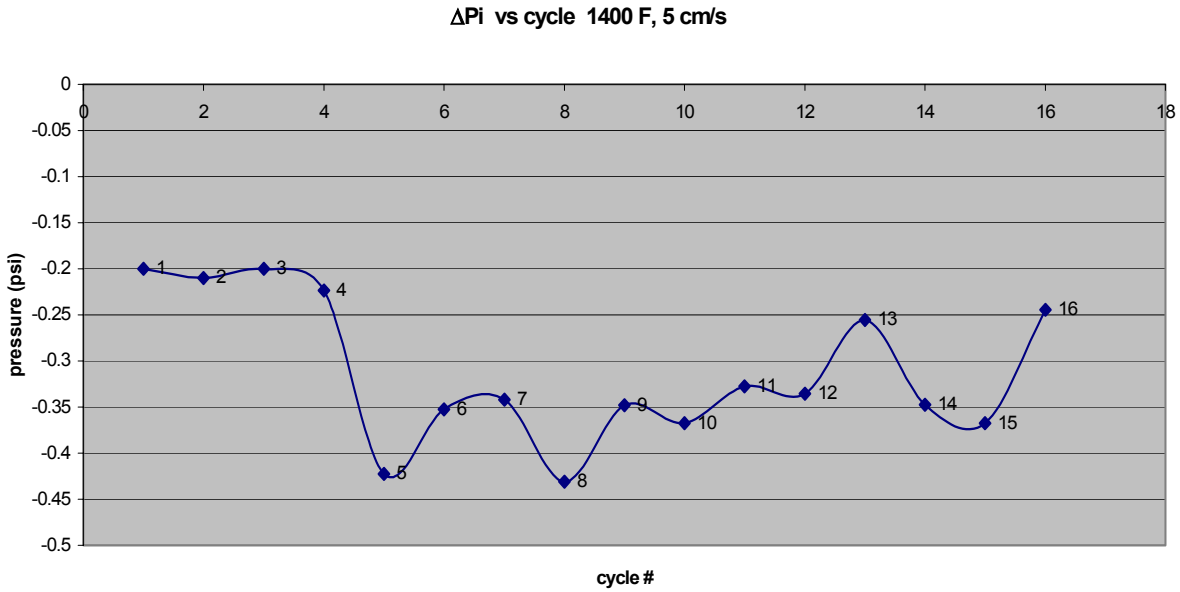

Figure 2.7 a. Initial pressure drop vs time at 1400 F, 5 cm/s

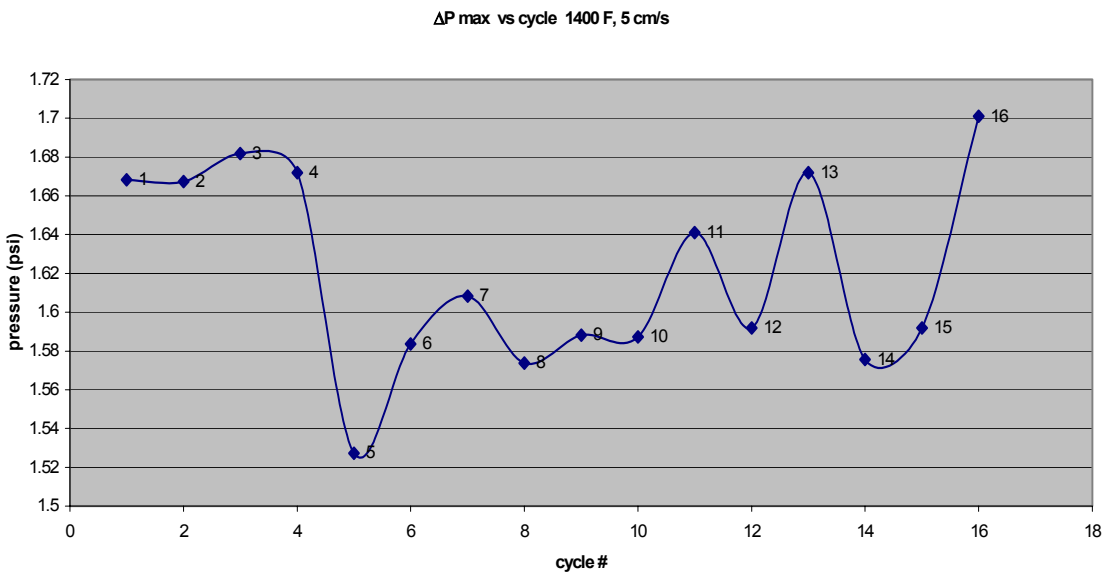

Figure 2.7 b. Maximum pressure drop vs time at 1400 F, 5 cm/s

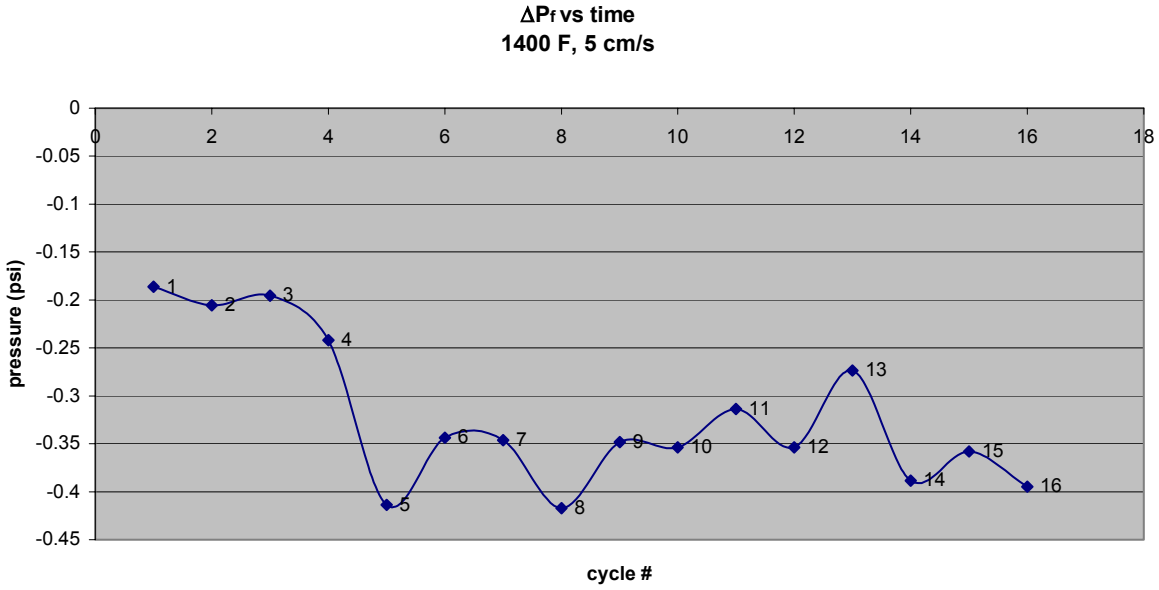

Figure 2.7 c. Final pressure drop vs time at 1400 F, 5 cm/s

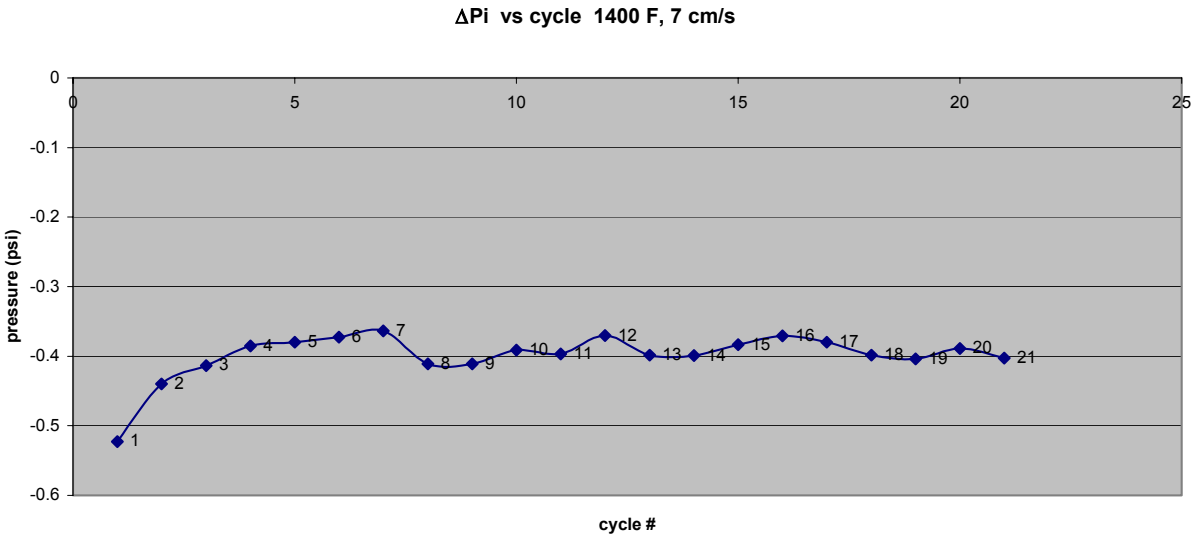

Figure 2.8 a. Initial pressure drop vs time at 1400 F, 7 cm/s

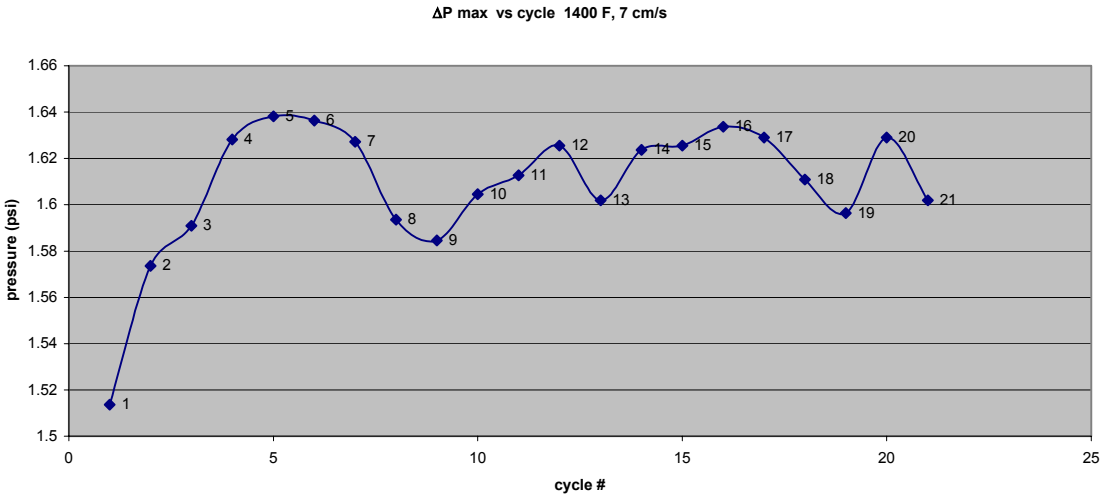

Figure 2.8 b. Maximum pressure drop vs time at 1400 F, 7 cm/s

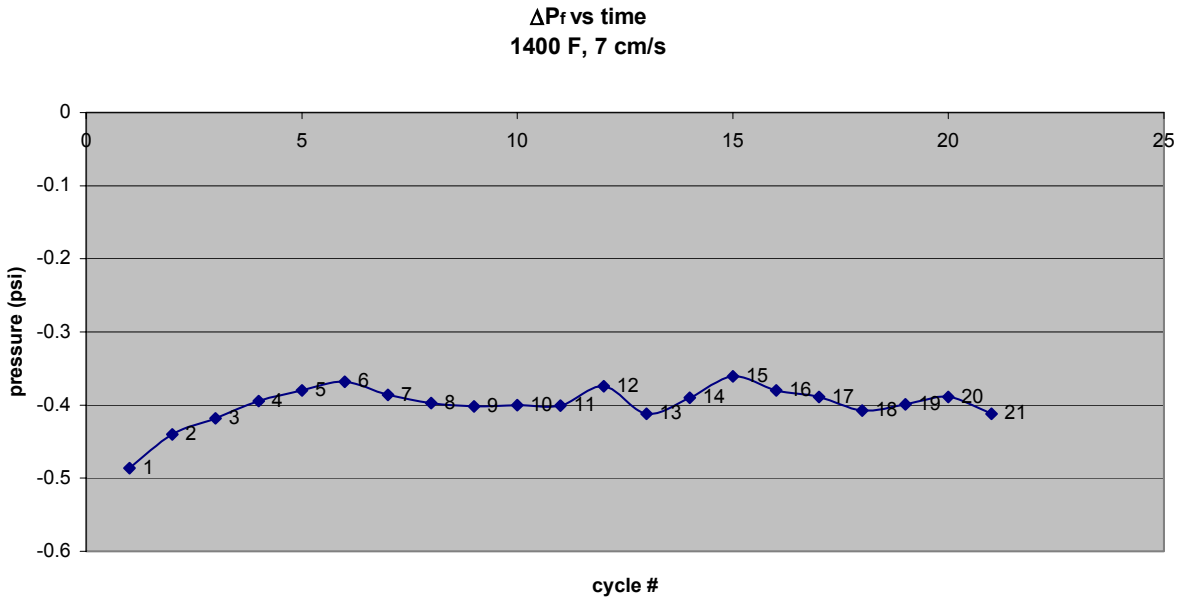

Figure 2.8 c. Final pressure drop vs time at 1400 F, 7 cm/s

Additional Data

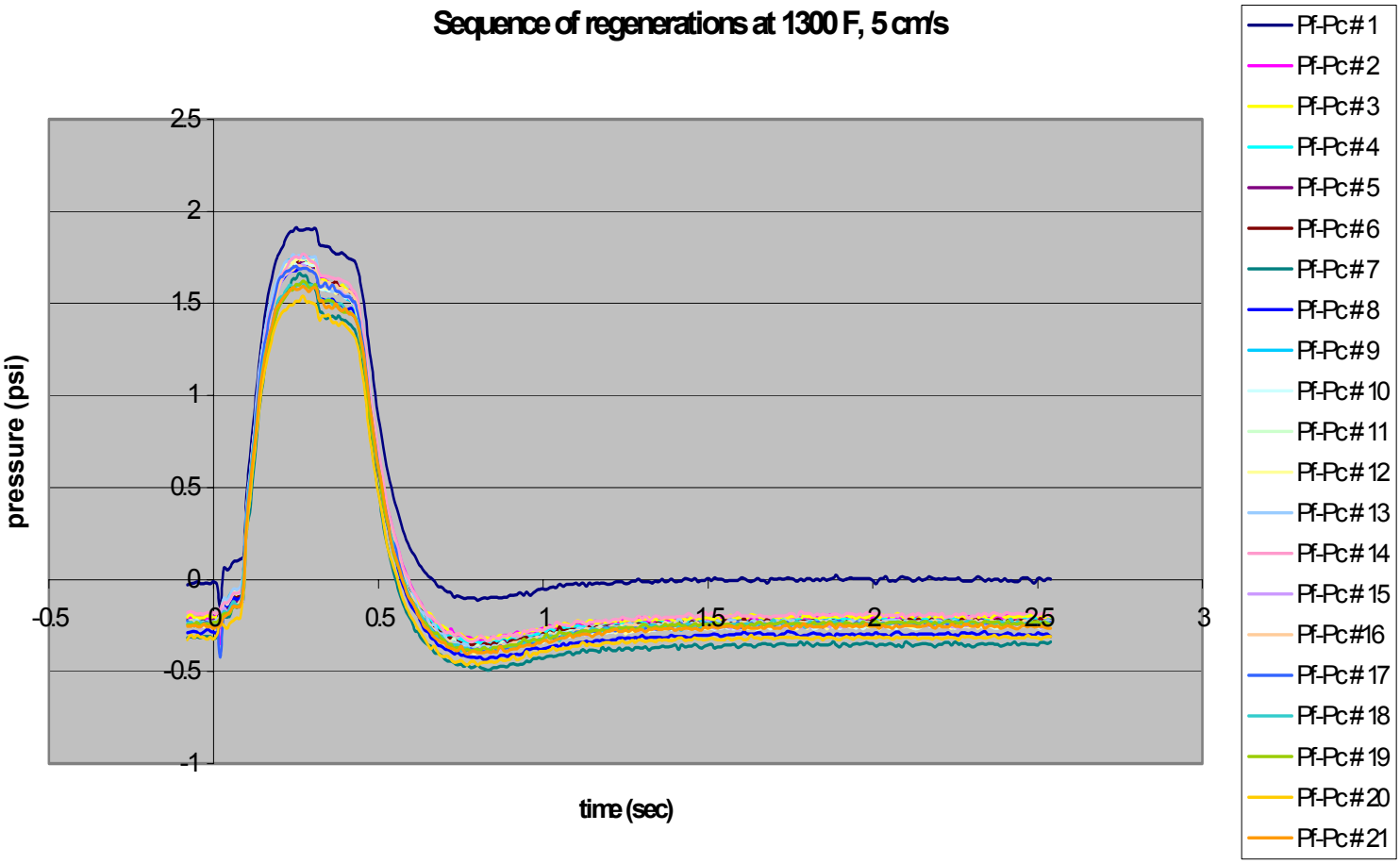

Figure 2.9. Pressure profiles during surface regeneration at 1300 F, 5 cm/s. Long term test.

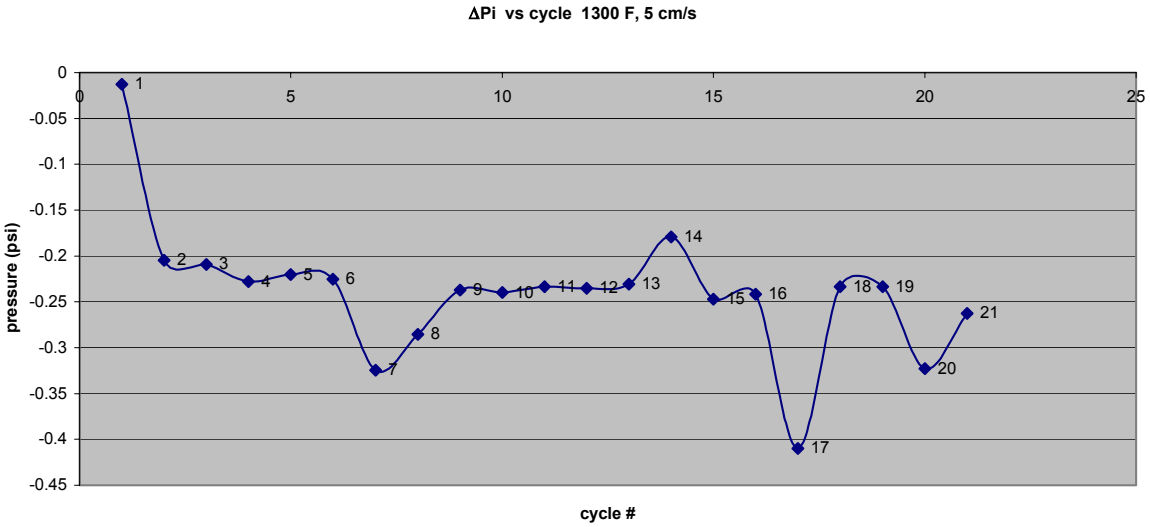

Figure 2.10 Initial pressure drop at 1300 F, 5

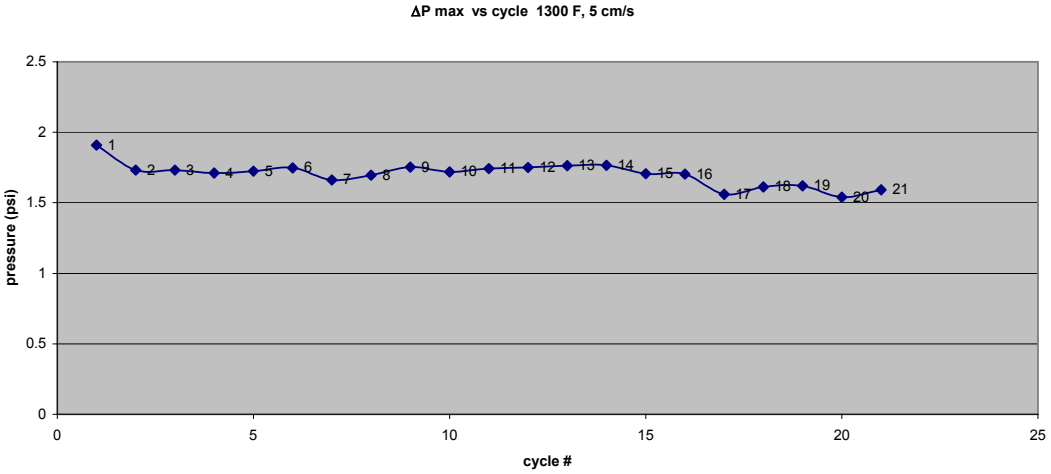

Figure 2.11 Maximum pressure drop at 1300 F, 5 cm/s

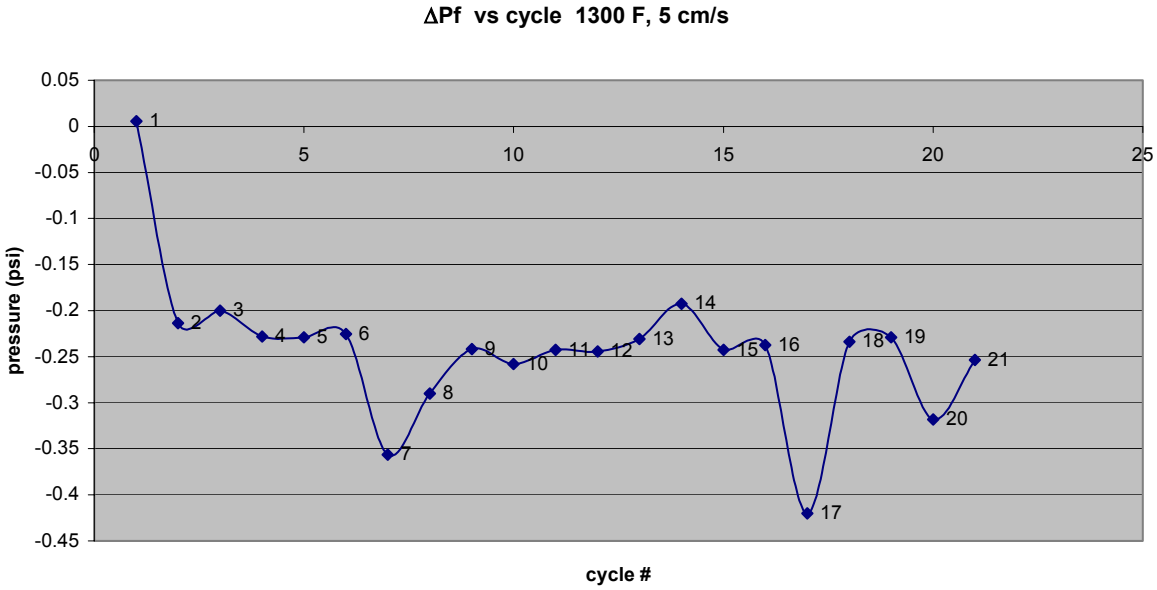

Figure 2.12 Final pressure drop at 1300 F, 5 cm/s

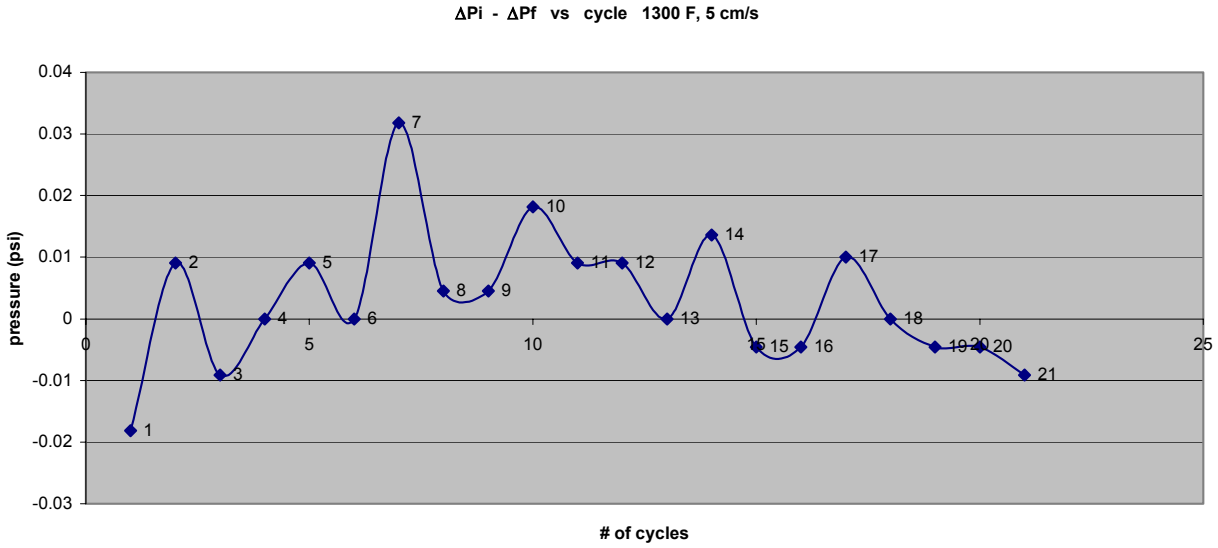

Figure 2.13 Initial – final pressure drop difference at 1300 F, 5 cm/s

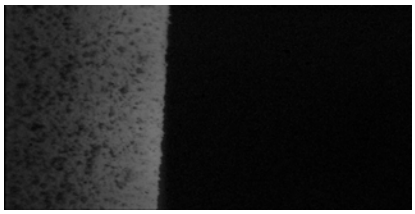

T=0

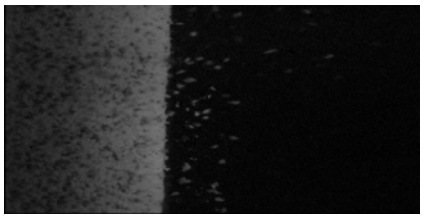

T=0.3

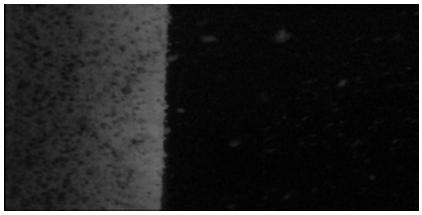

T=0.68

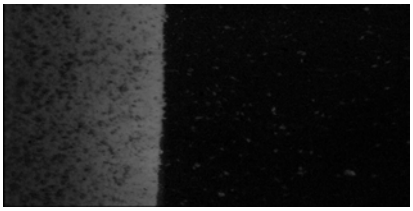

T=0.83

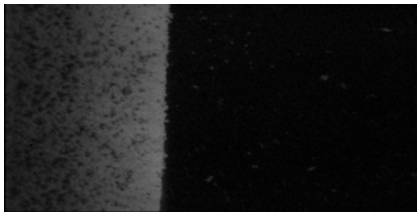

T=1.05

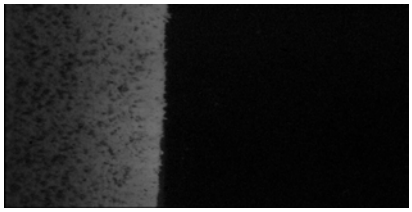

T=1.5

Figure 2.14 Regeneration # 4 at test 1300 F, 5 cm/s

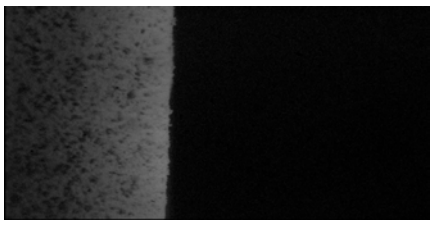

T=0

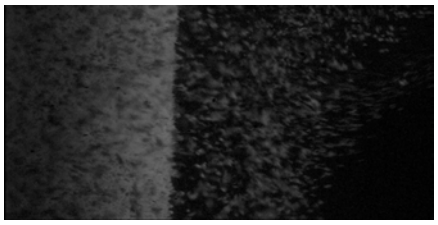

T=0.3

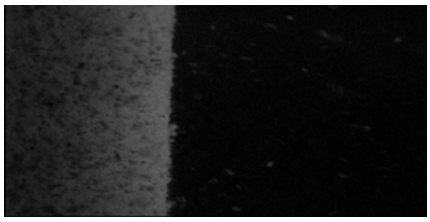

T=0.68

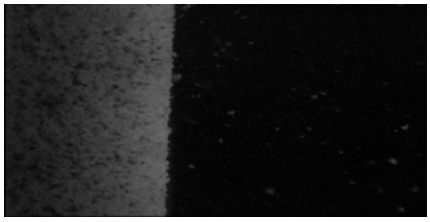

T=0.83

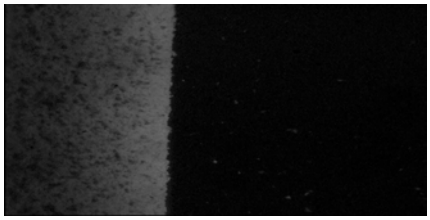

T=1.05

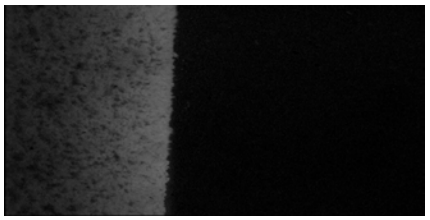

T=1.5

Figure. 2.15 Regeneration # 5 at test 1300 F, 5 cm/s

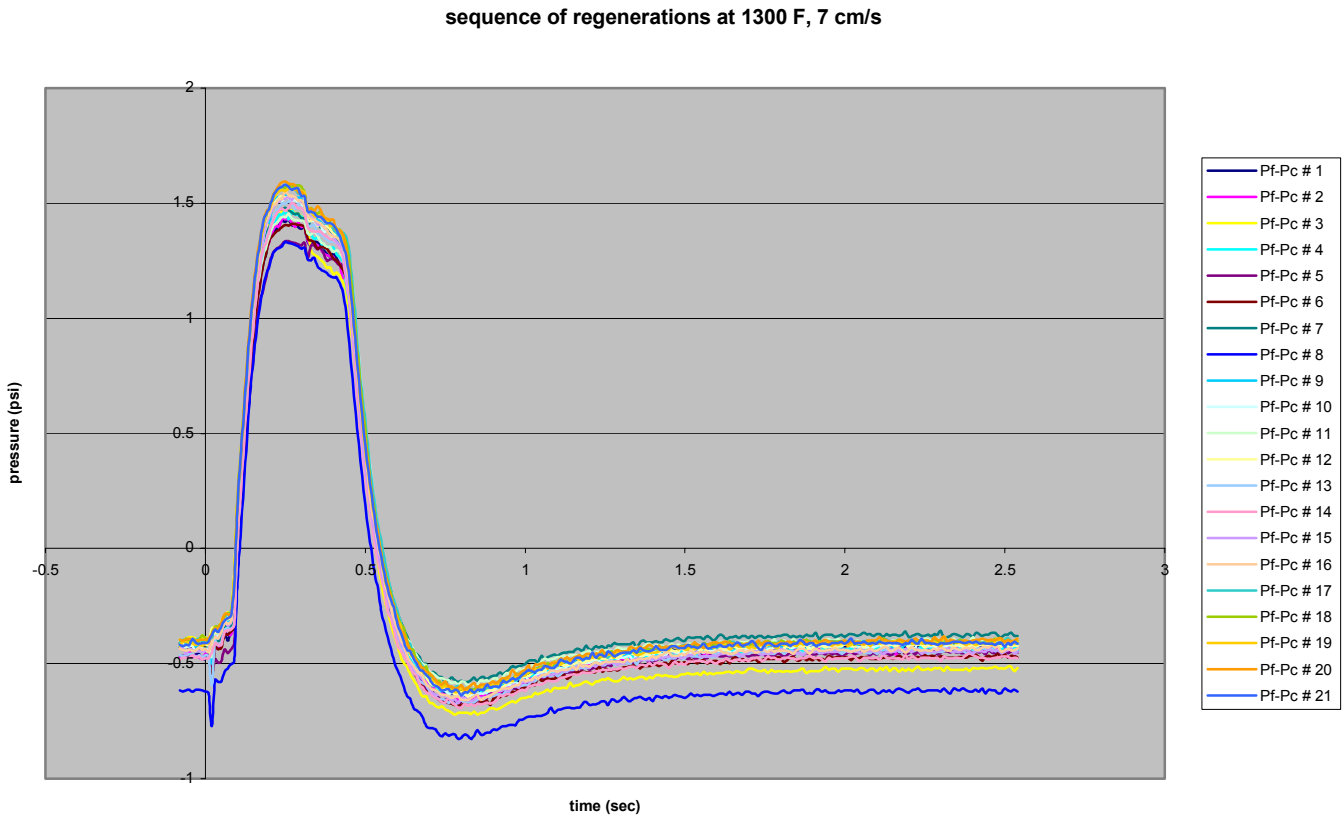

Figure 2.16. Pressure profiles during surface regeneration at 1300 F, 7 cm/s. Long term test

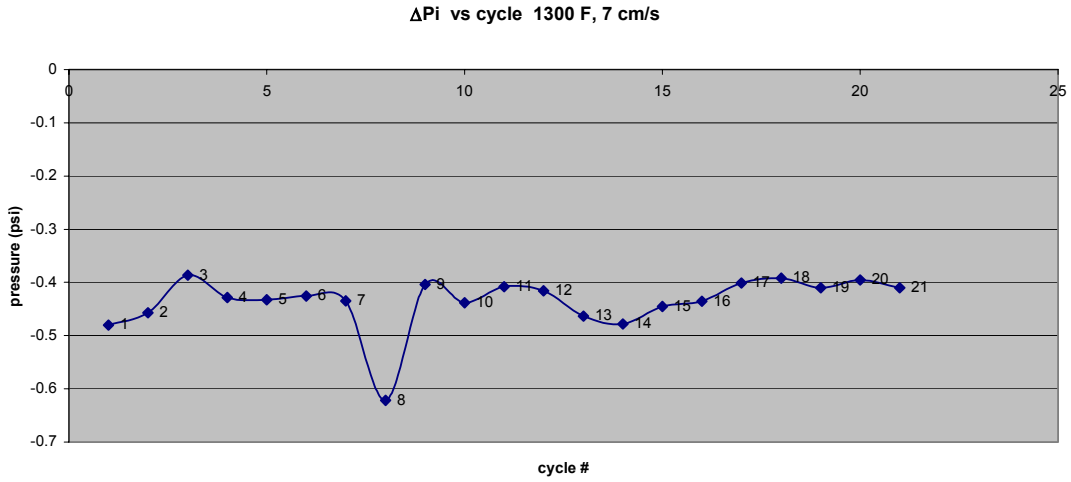

Figure 2.17 Initial pressure drop at 1300 F, 7 cm/s

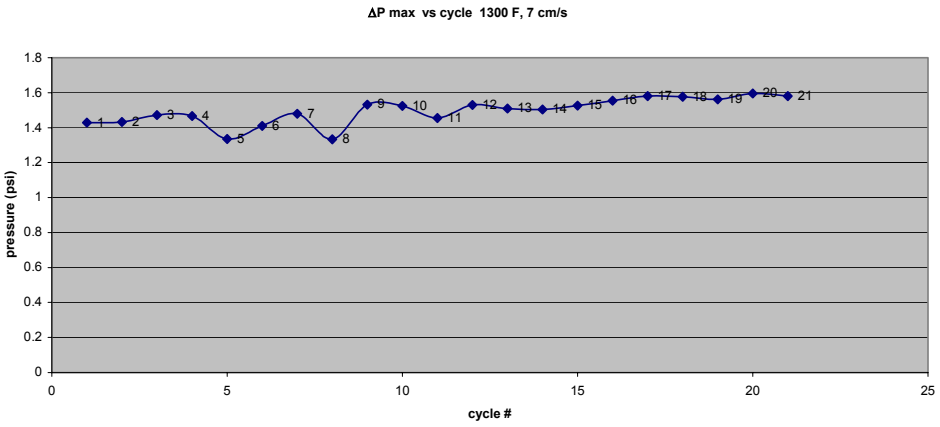

Figure 2.18 Maximum pressure drop at 1300 F, 7 cm/s

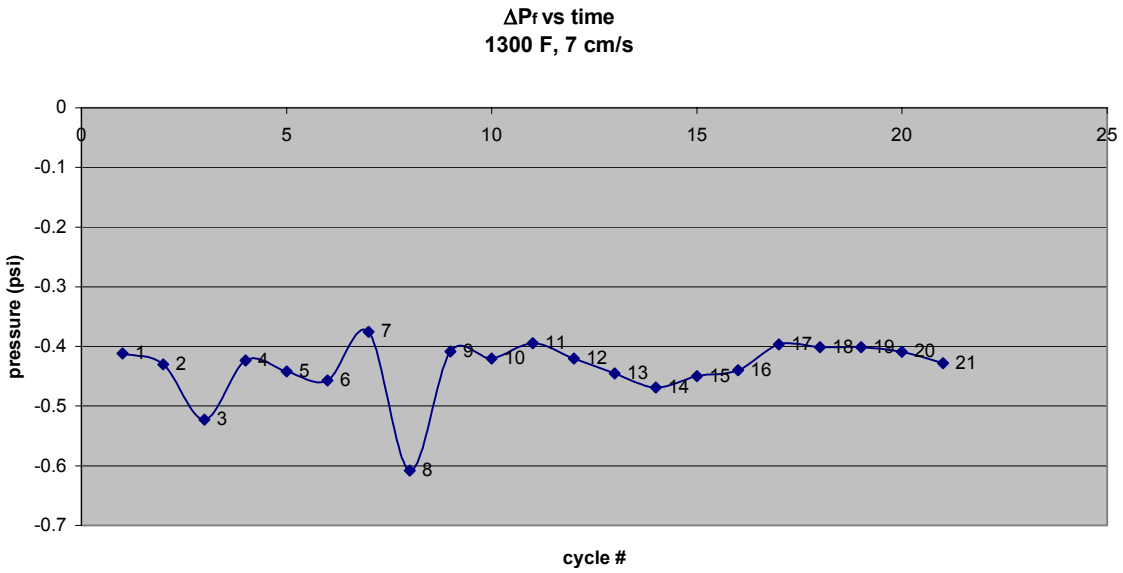

Figure 2.19 Final pressure drop at 1300 F, 7 cm/s

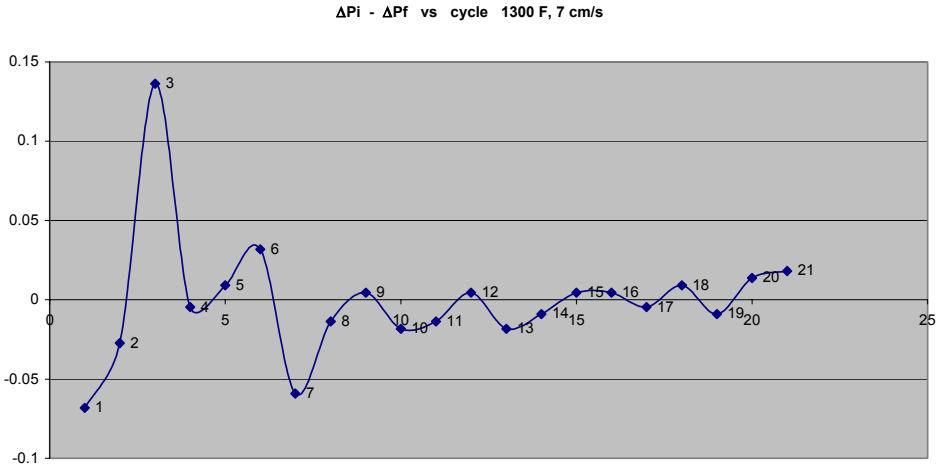

Figure 2.20 Initial – final pressure drop at 1300 F, 7 cm/s

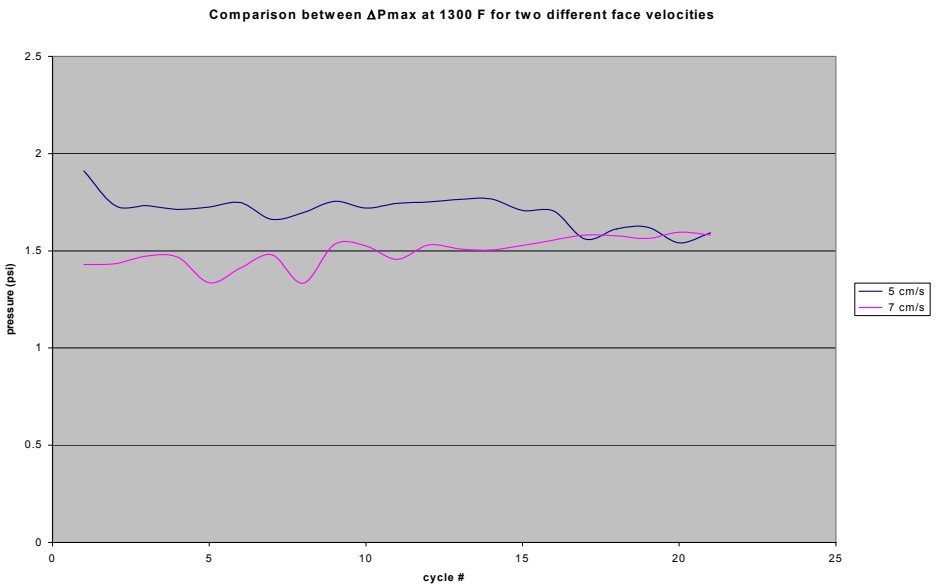

Figure 2..21 Comparison between initial pressure drop at 1300 F for two different face velocities

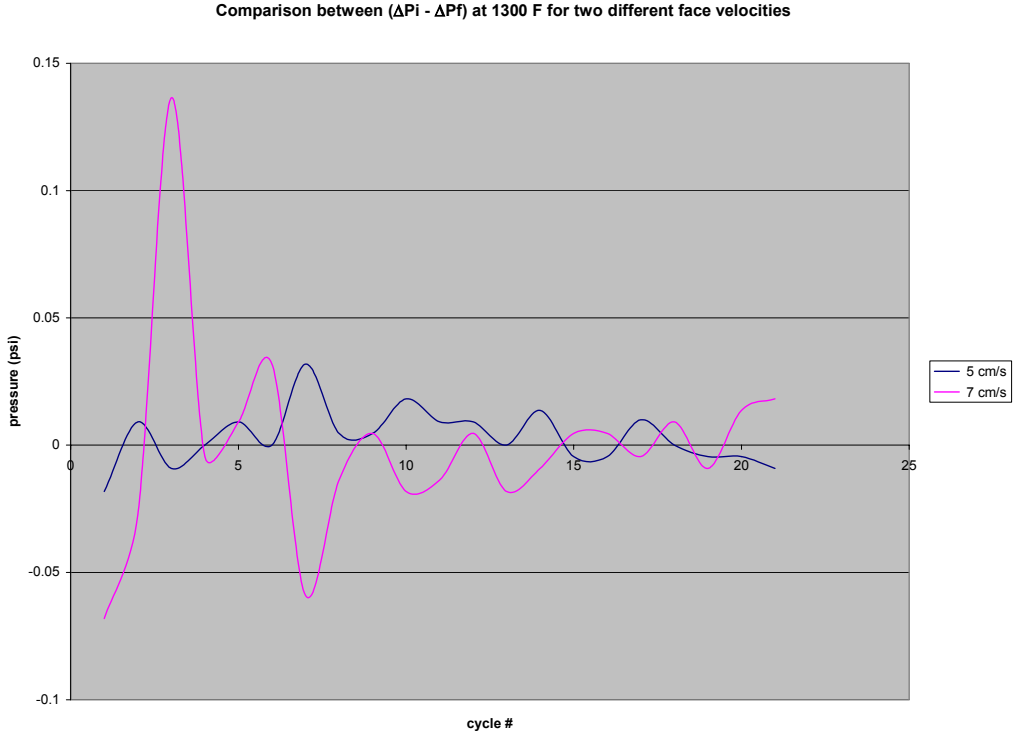

Figure 2.22 Comparison between maximum pressu drop at 1300 F for diferent face velocities

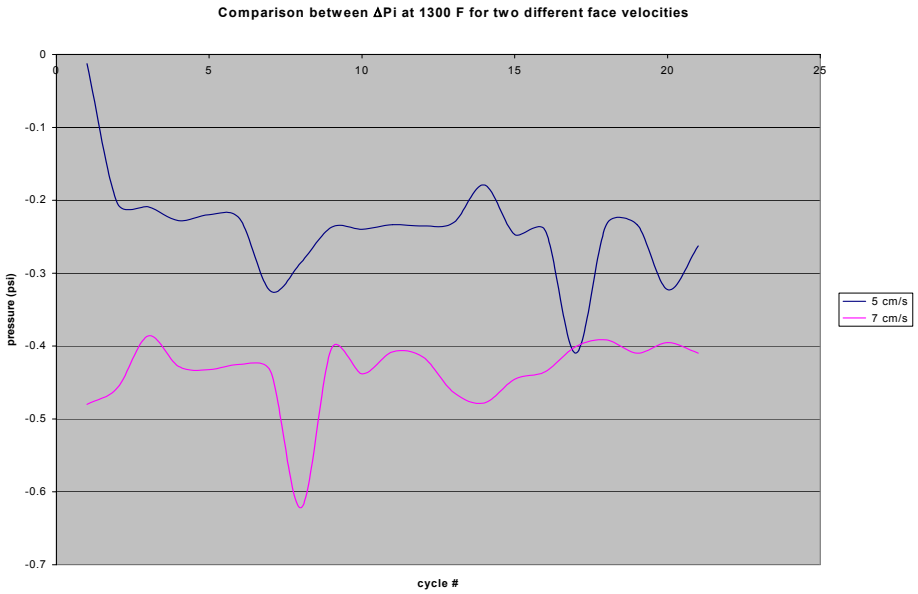

Figure 2.23 Comparison between (initial – final) pressure drop at 1300 F for two different face velocities

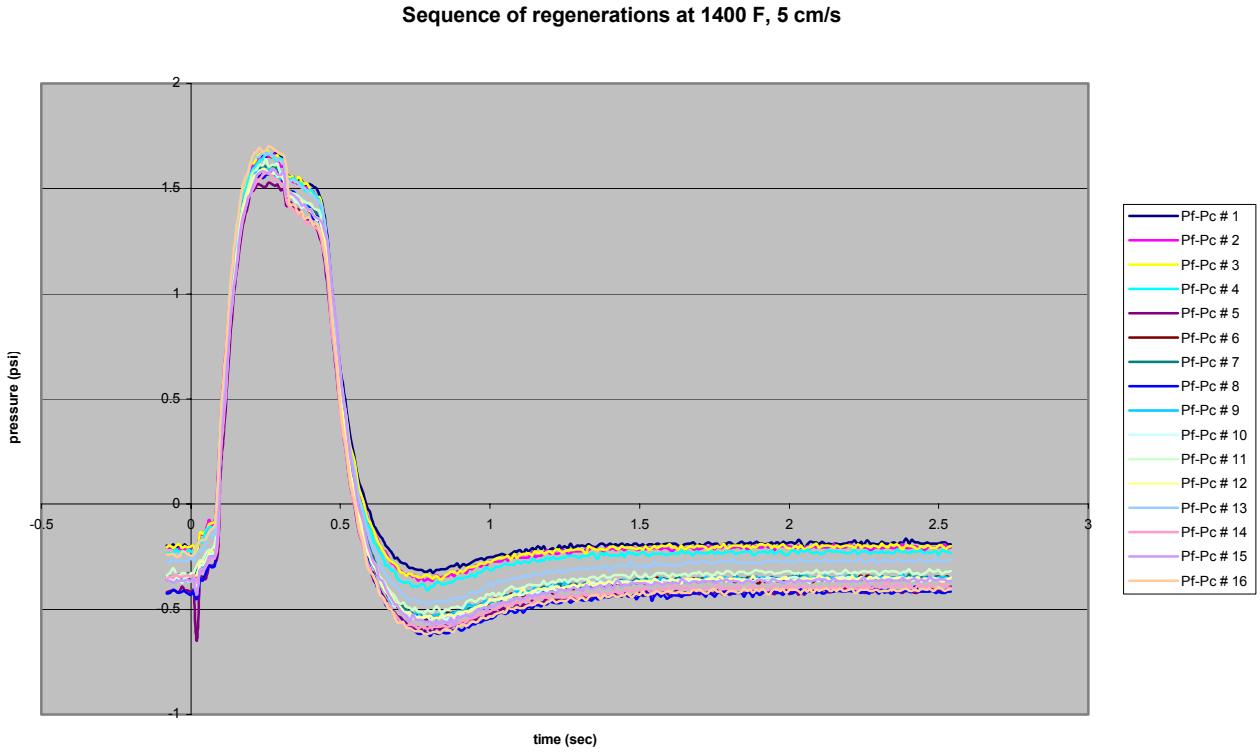

Figure 2.24 Sequence of regenerations at 1400 F, 5 cm/s

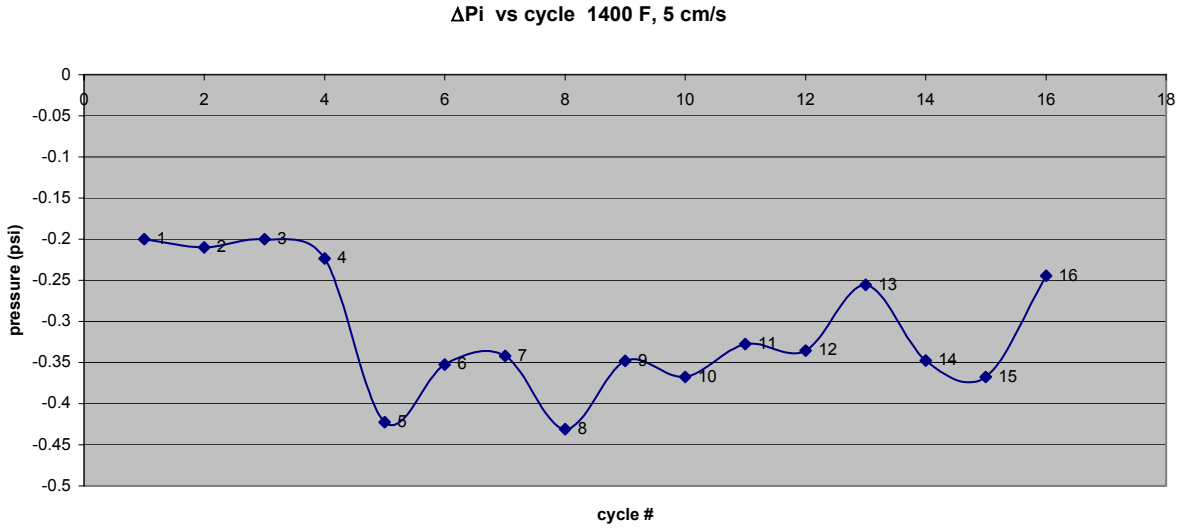

Figure 2.25 Initial pressure drop at 1400 F, 5 cm/s

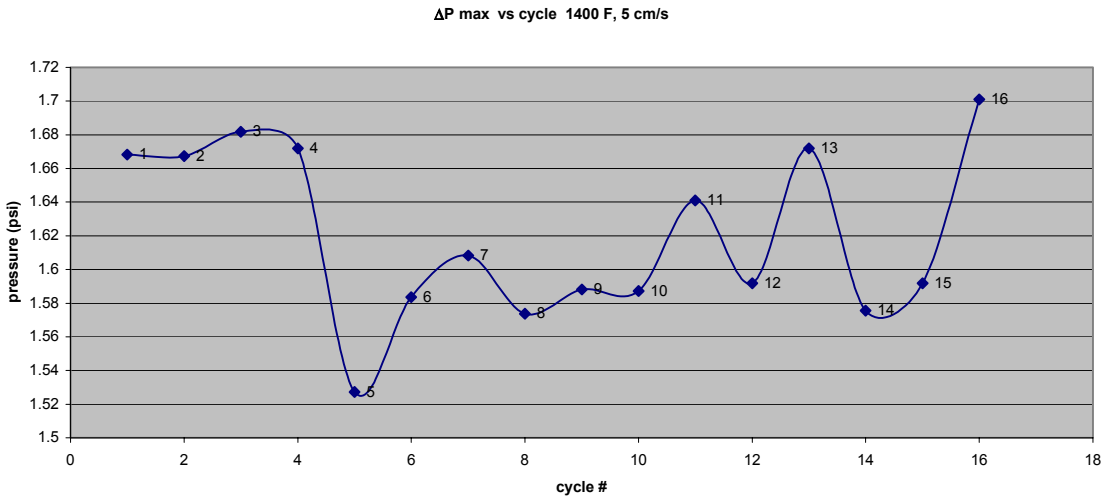

Figure 2.26 Maximum pressure drop at 1400 F, 5 cm/s

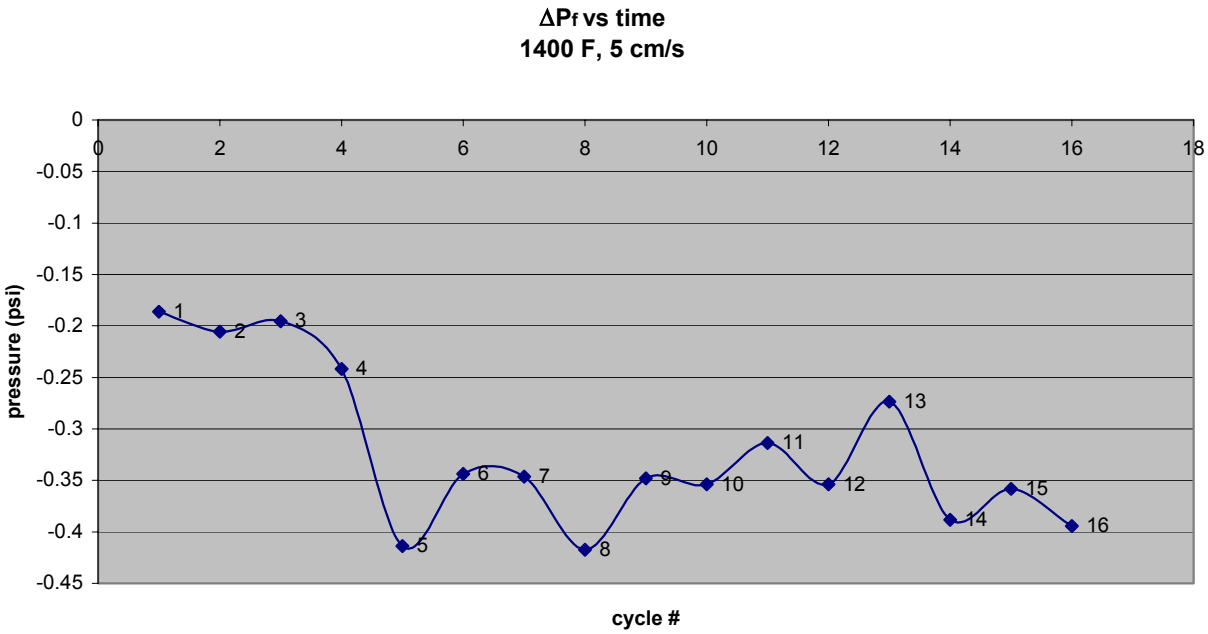

Figure 2.27 Final pressure drop at 1400 F, 5 cm/s

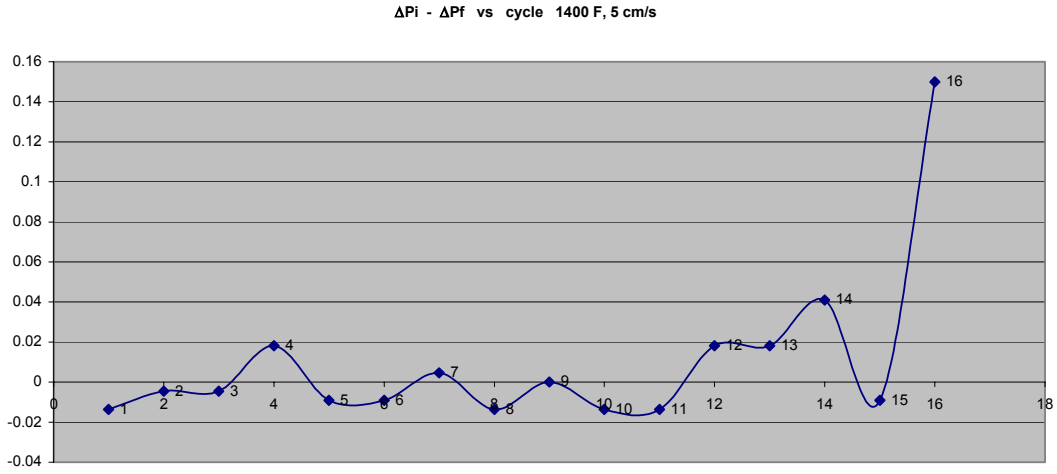

Figure 2.28 Difference between initial pressure drop and final pressure drop at 1400 F, 5 cm/s

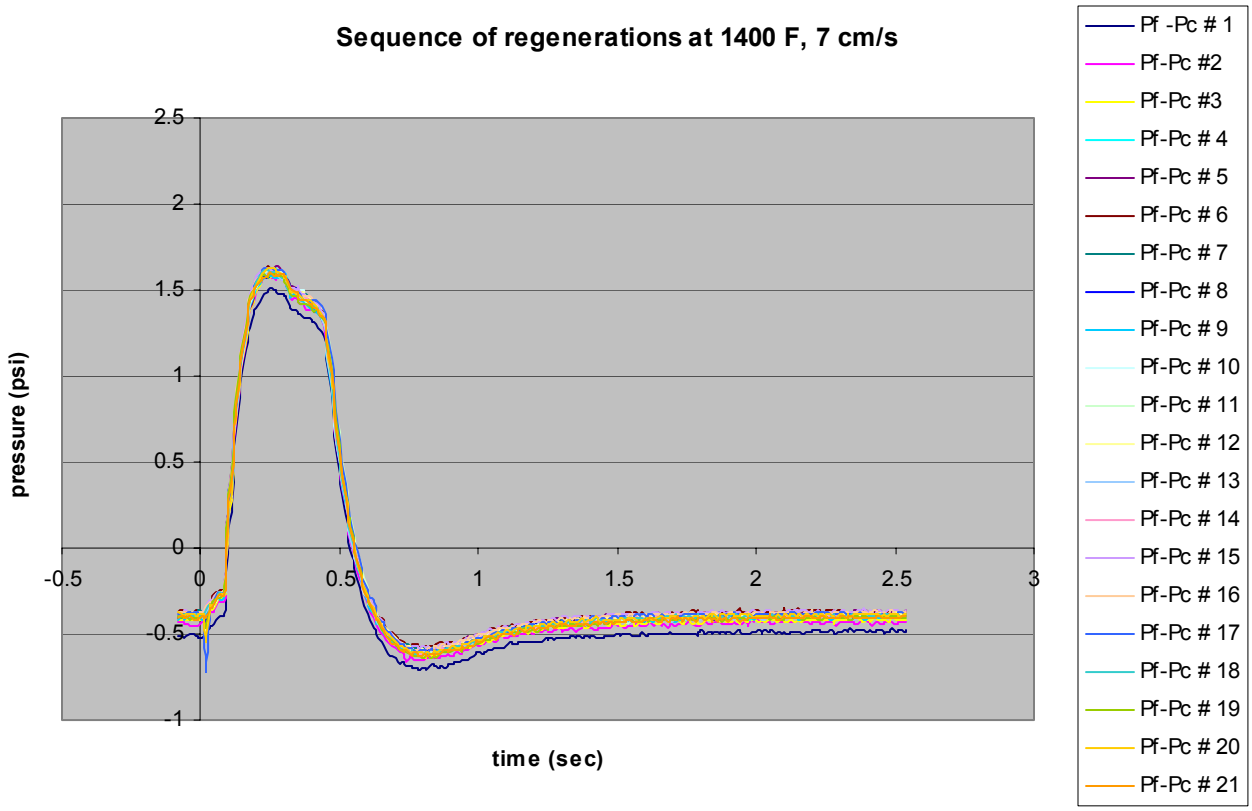

Figure 2.29 Sequence of regenerations at 1400 F, 7 cm/s

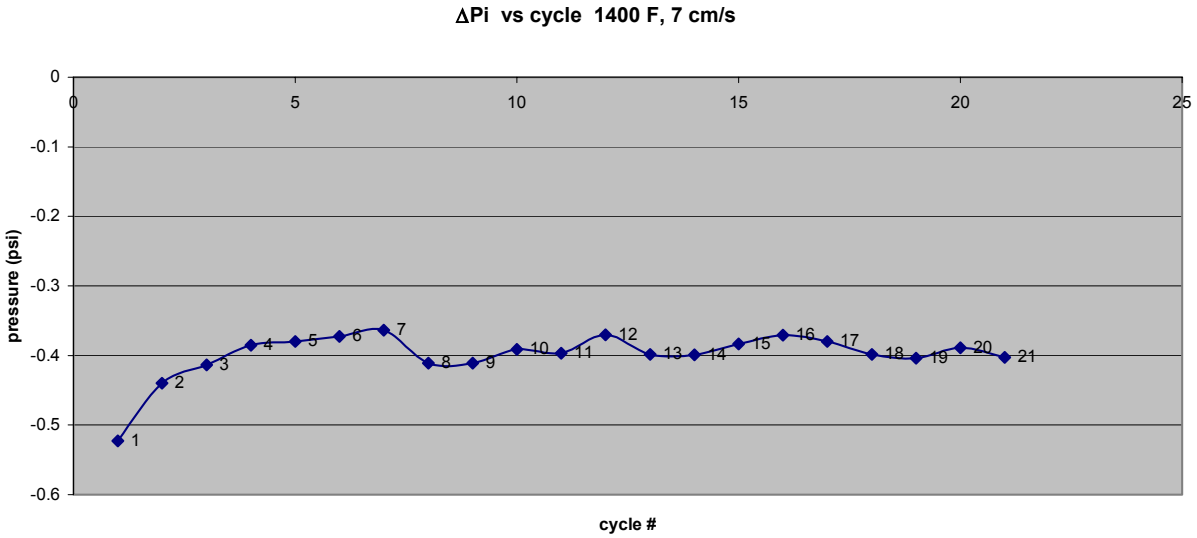

Figure 2.30 Initial pressure drop at 1400 F, 7 cm/s

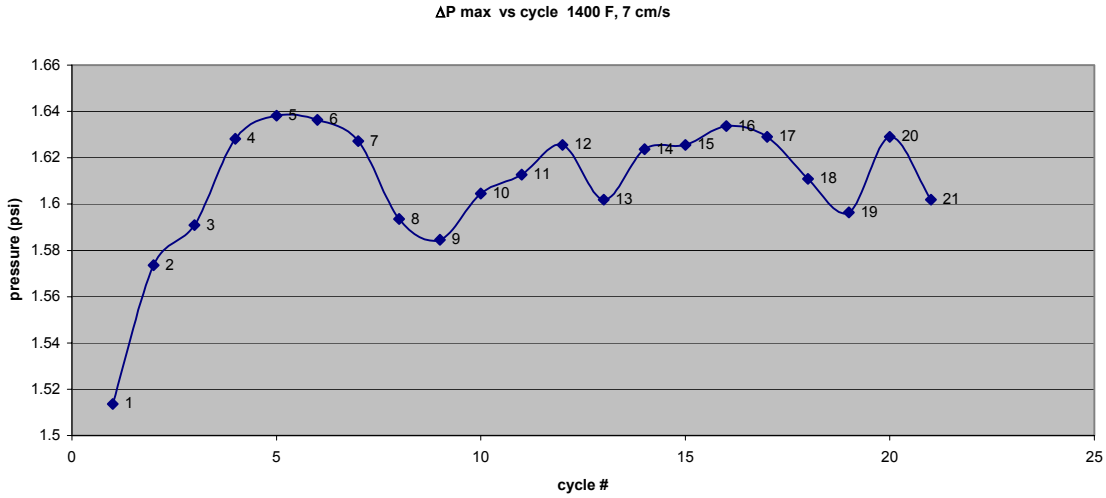

Figure 2.31 Maximum pressure drop at 1400 F, 7 cm/s

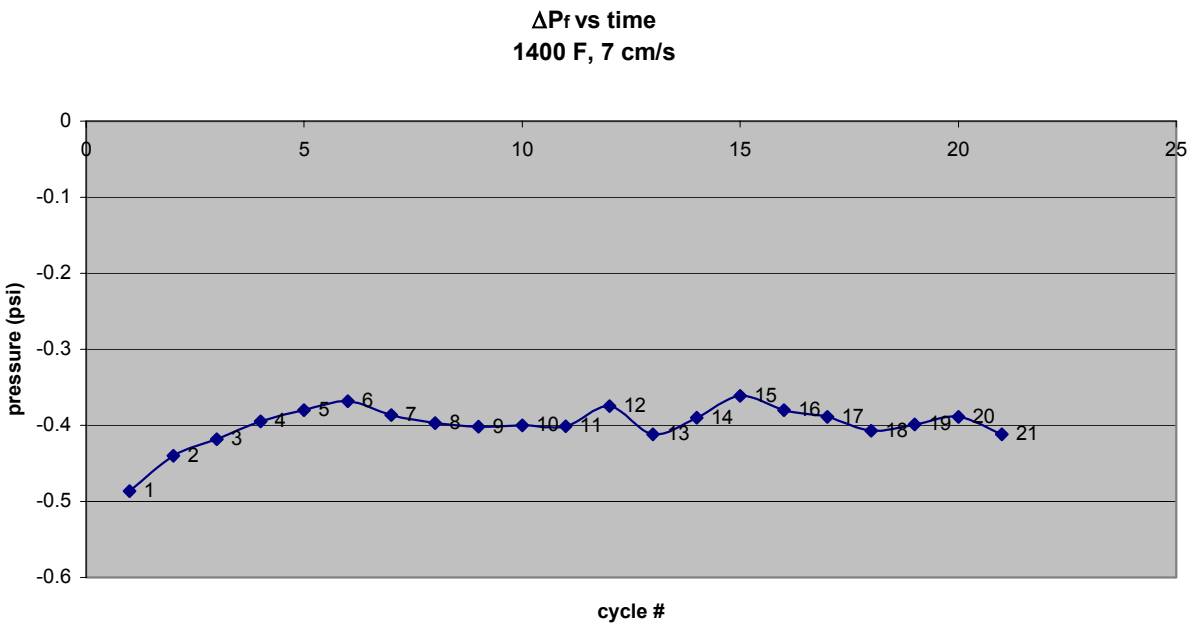

Figure 2.32 Final pressure drop at 1400 F, 7 cm/s

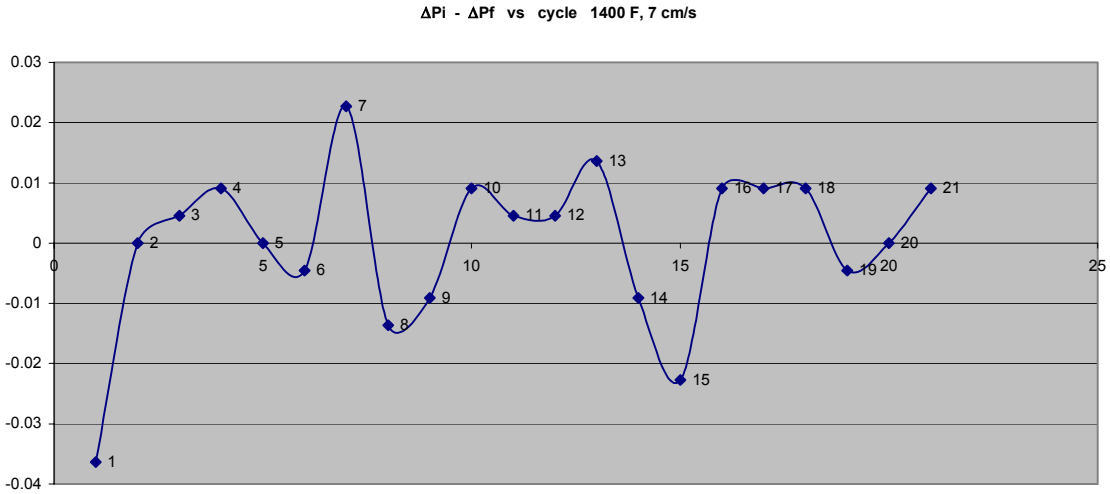

Figure 2.33 Difference between initial and final pressure drop at 1400 F, 7 cm/s

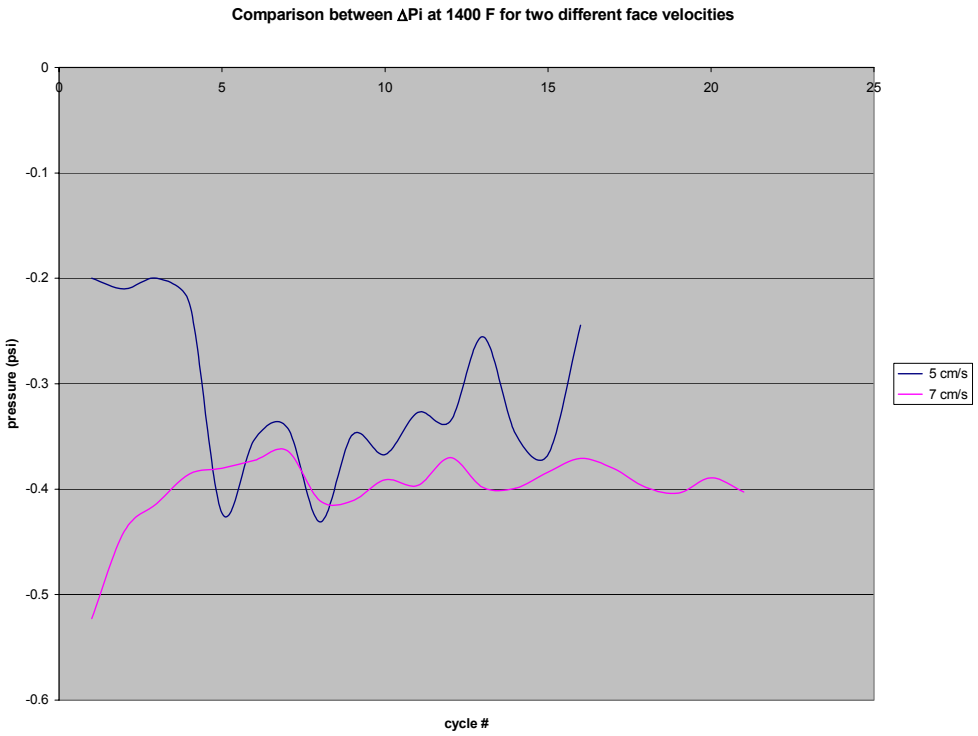

Figure 2.34 Comparison between initial pressure drop at 1400 F for two different face velocities

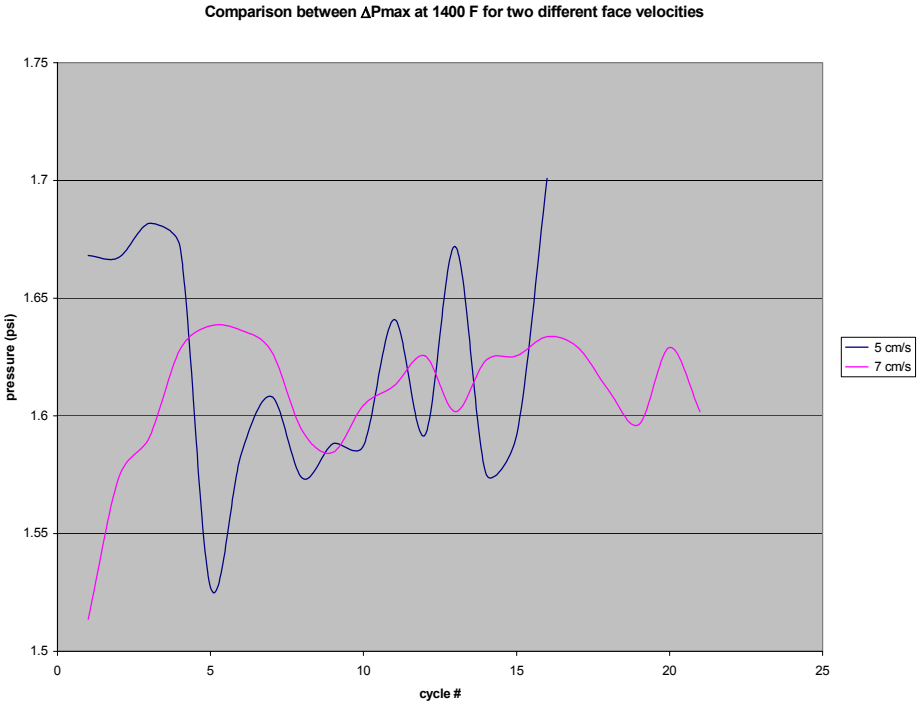

Figure 2.35 Comparison between maximum pressure drop at 1400 F for two different face velocities

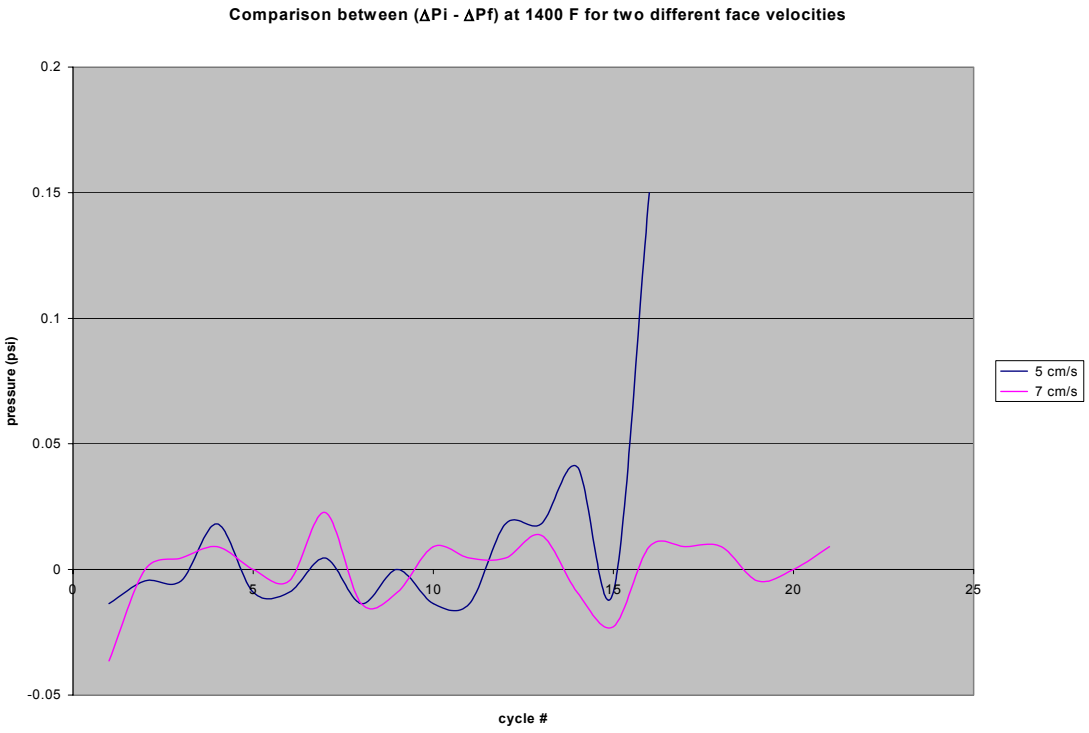

Figure 2.36 Comparison between differences of initial and final pressure drop at 1400 F, for two different velocities

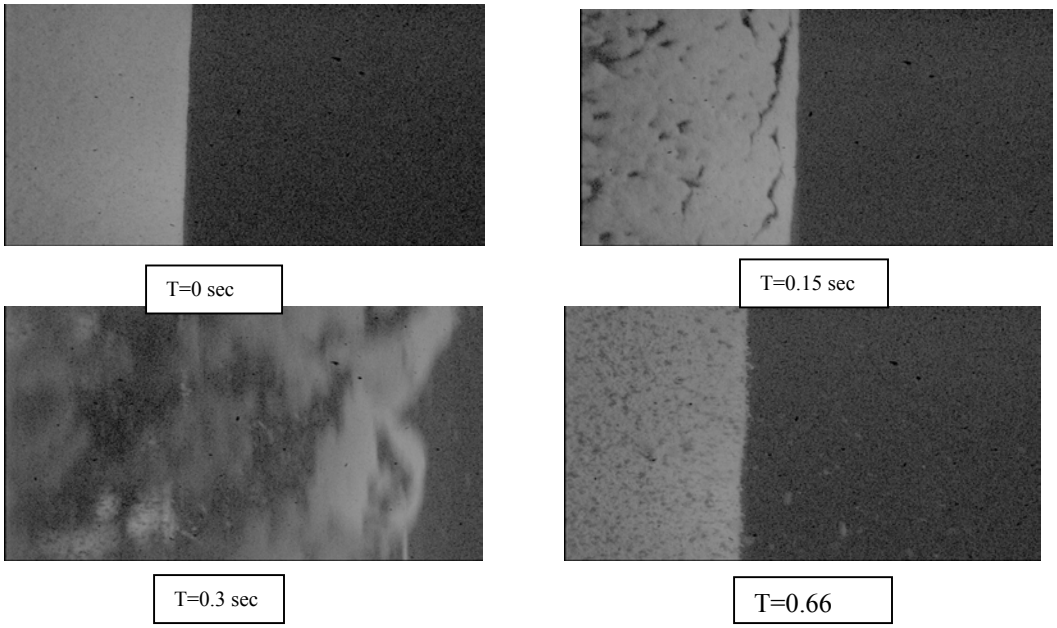

Figure 2.37 Thick ash regeneration at first cycle with residual ash formation. 1400 F, 5 cm/s

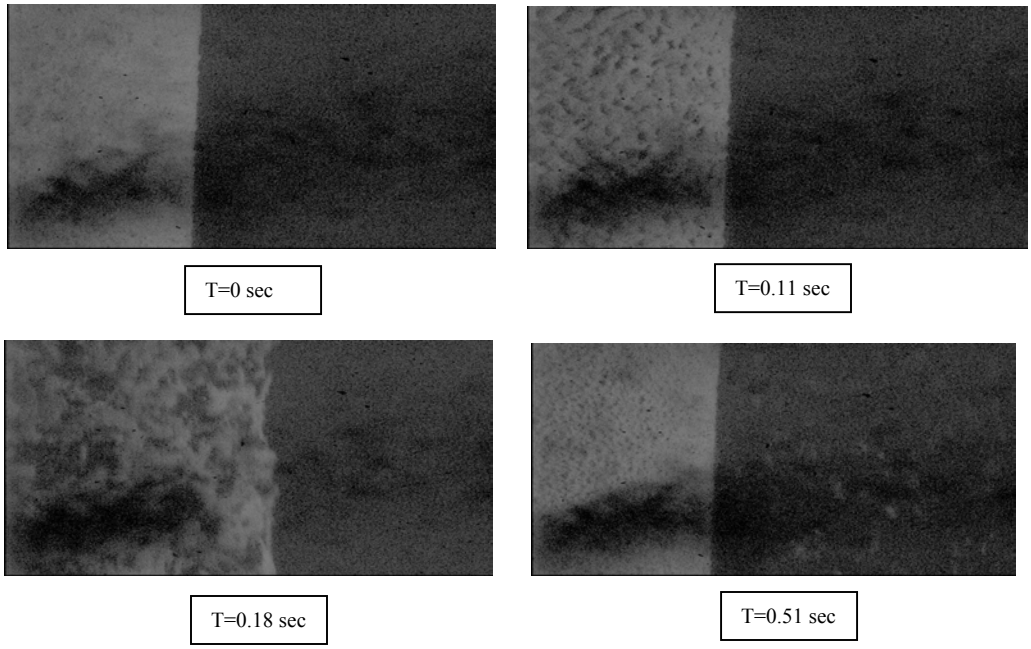

Figure 2.38 Thin ash regeneration at fifh cycle.1400 F, 5 cm/s

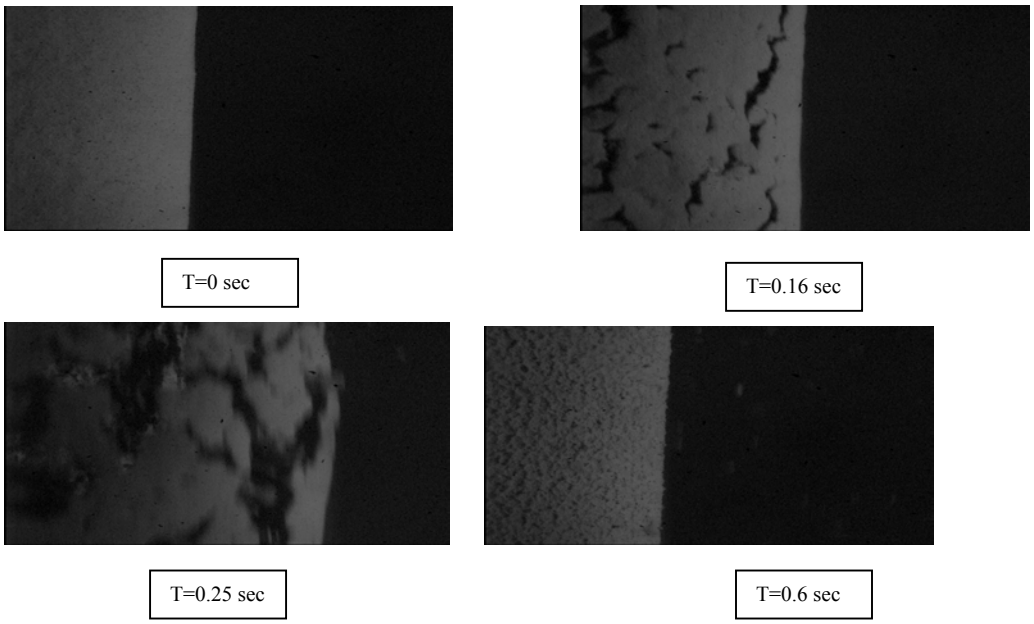

Figure 2.39 Thick ash regeneration at first cycle with residual ash formation. 1400 F, 7 cm/s

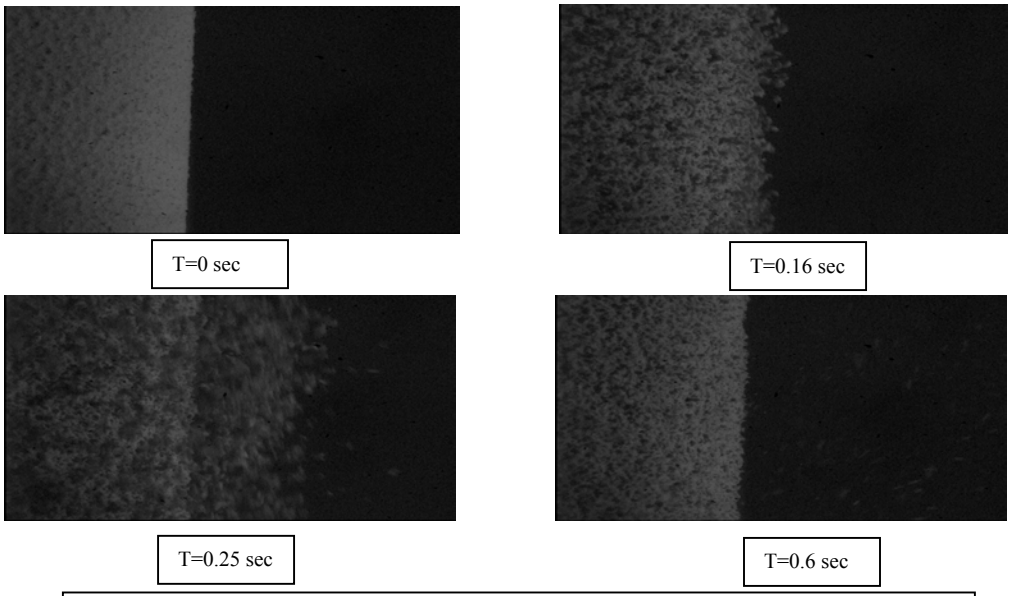

Figure 2.40 Thin ash regeneration at second cycle. 1400 F, 7 cm/s

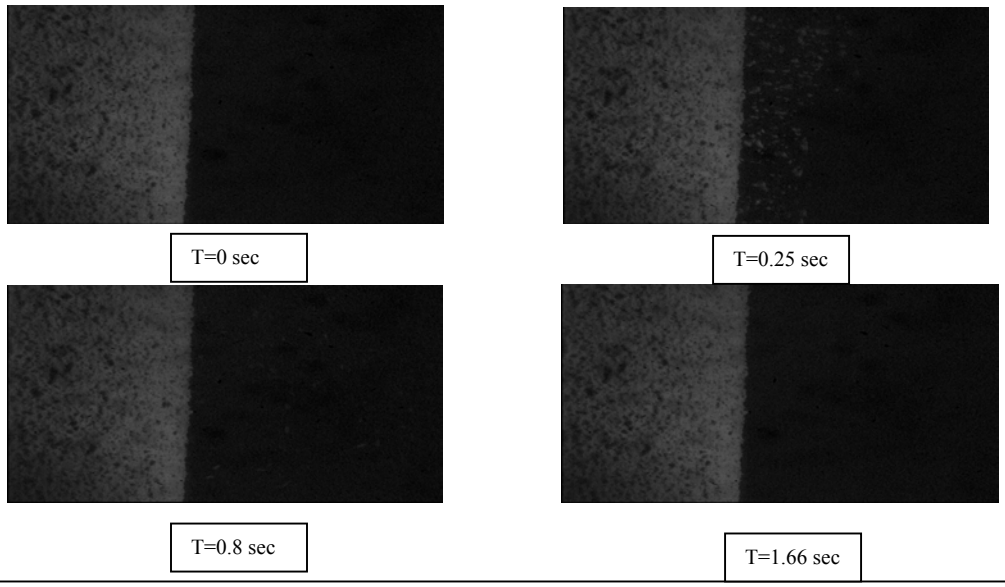

Figure 2.41 No regeneration with very few particles flying out at cycle 15th. 1400 F, 7 cm/s.

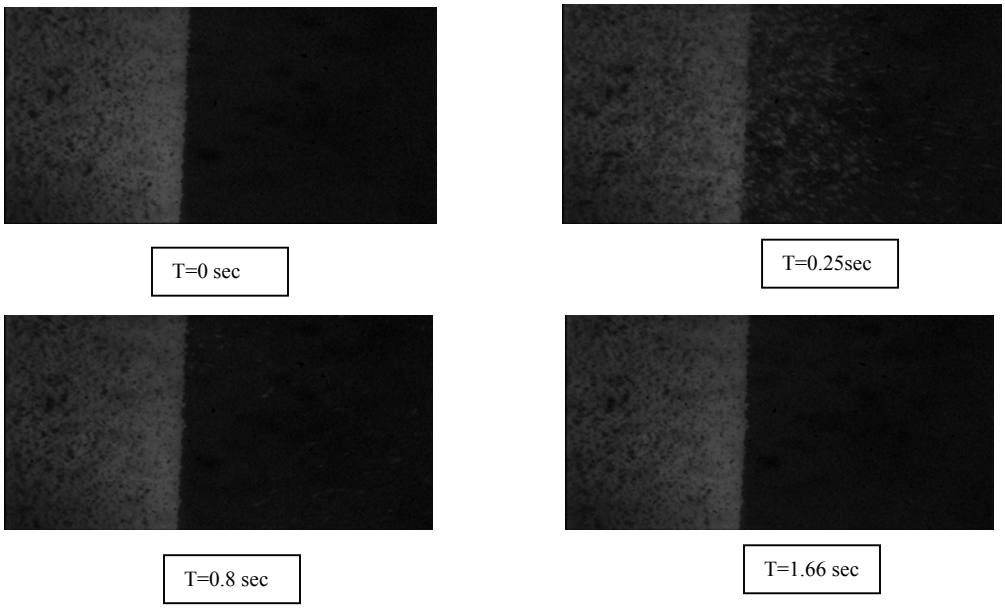

Figure 2.42 No regeneration with big amount of particles flying out at cycle 16 th. 1400 F, 7 cm/s.

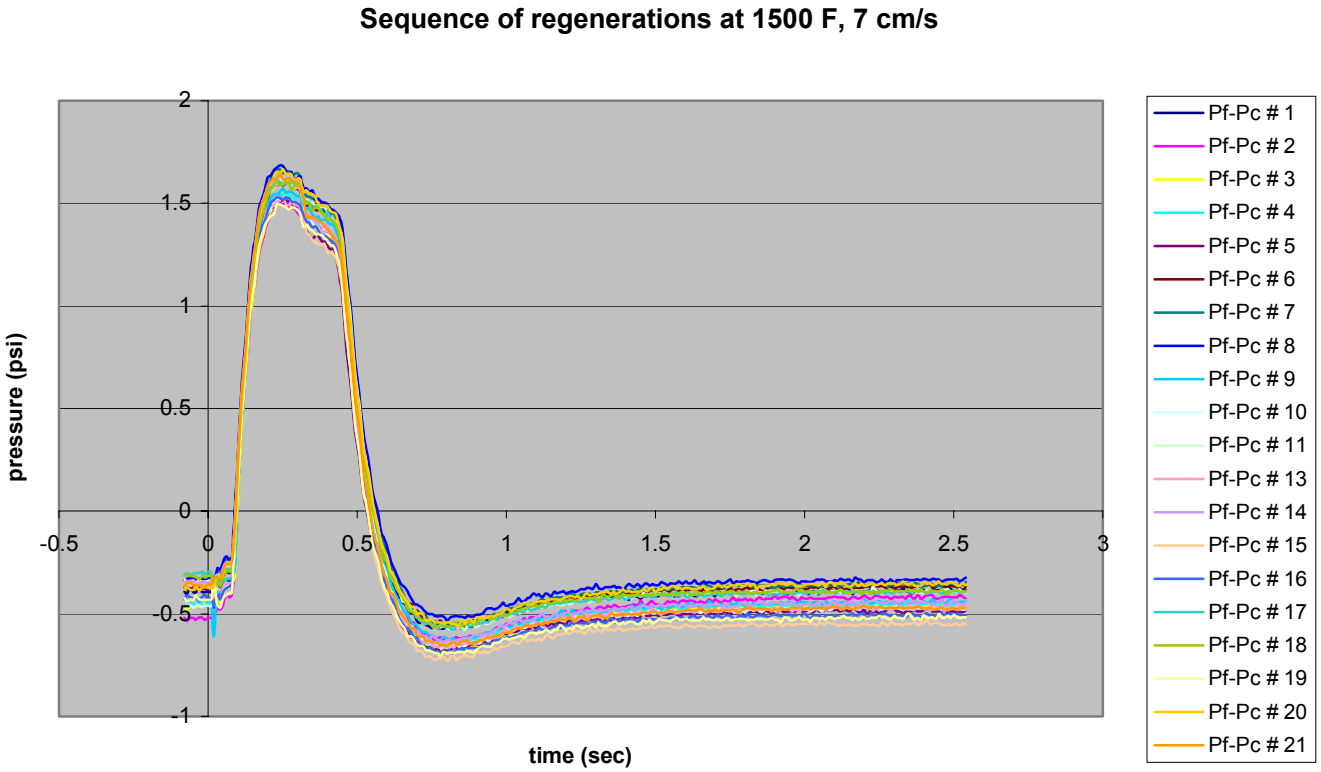

Figure 2.43 Pressure profile for sequence of regenerations at 1500 F, 7cm/s

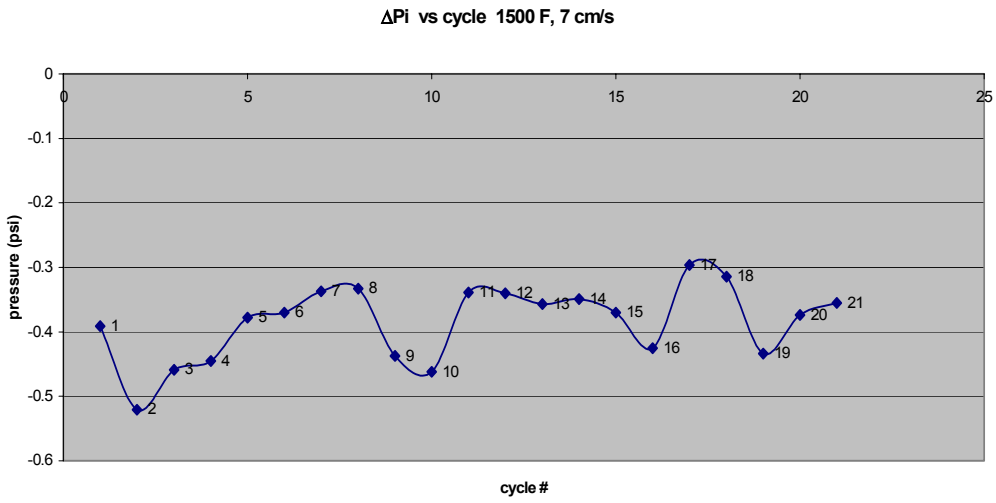

Figure 2.44 Initial pressure drop at 1500 F, 7 cm/s

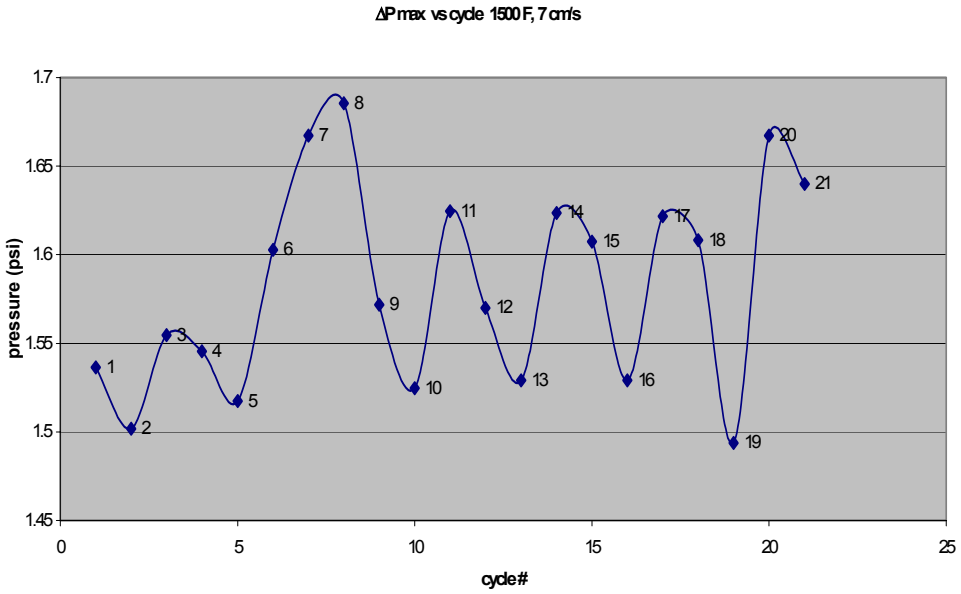

Figure 2.45 Maximum pressure drop at 1500 F, 7 cm/s

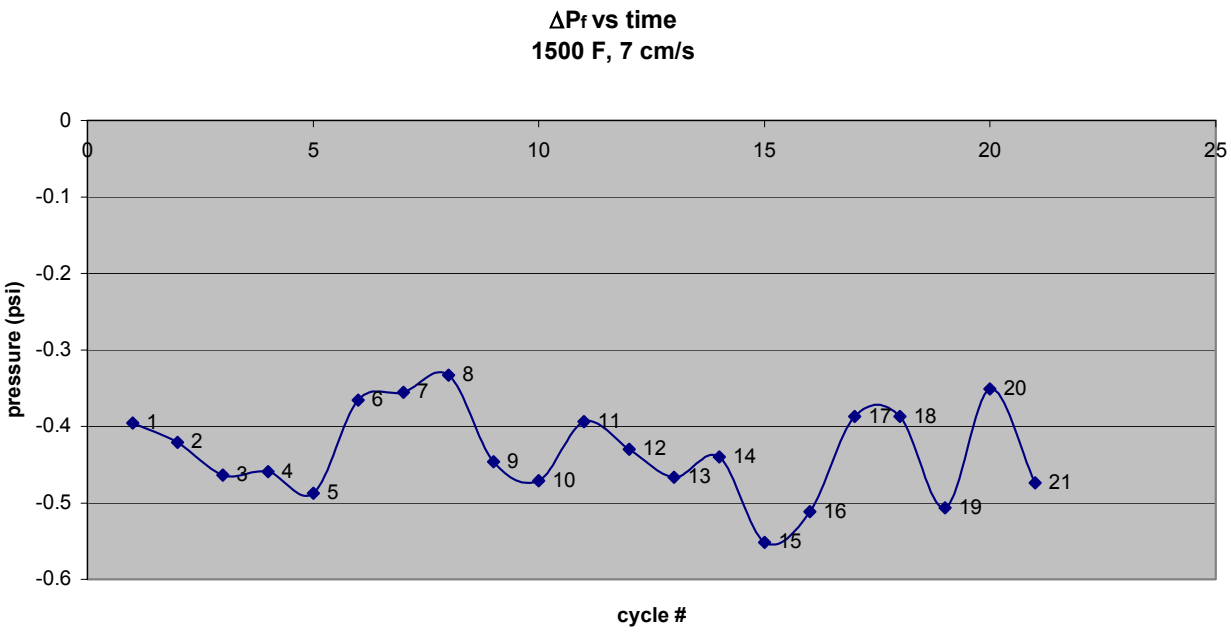

Figure 2.46 Final pressure drop at 1500 F, 7 cm/s

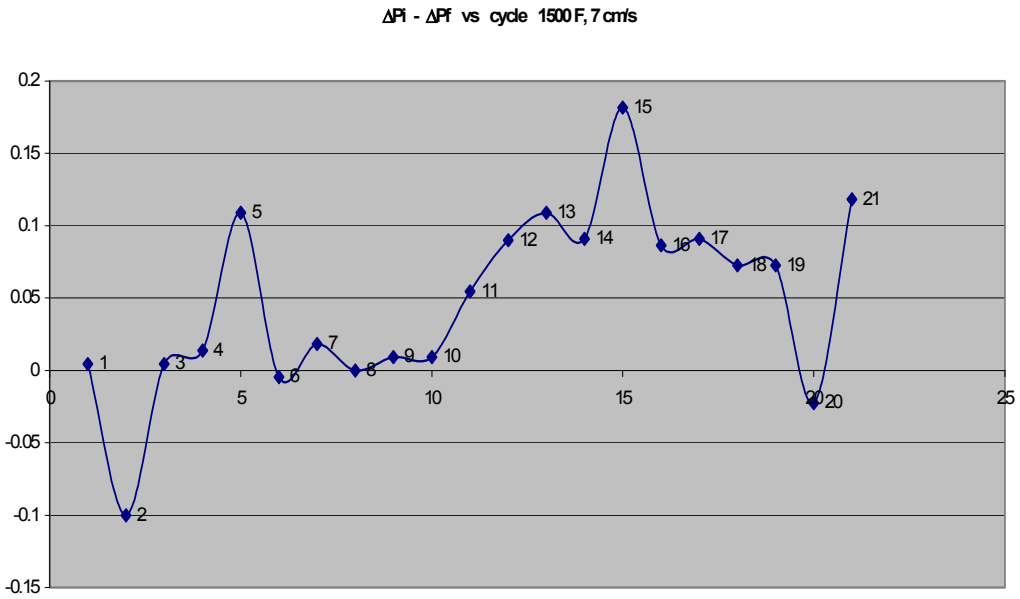

Figure 2.47 Difference between initial and final pressure drop at 1500, 7 cm/s

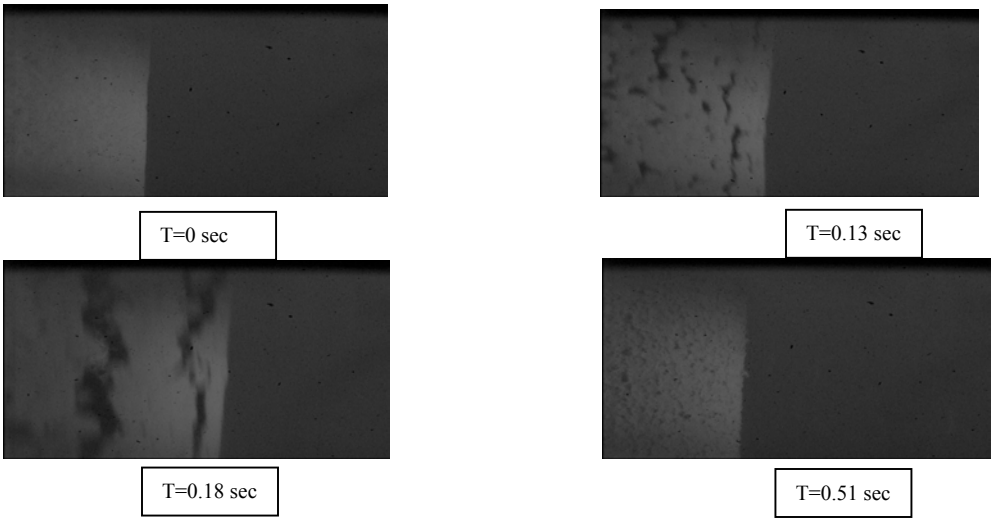

Figure 2.48 Thick ash regeneration at first cycle. 1500 F, 7 cm/s.

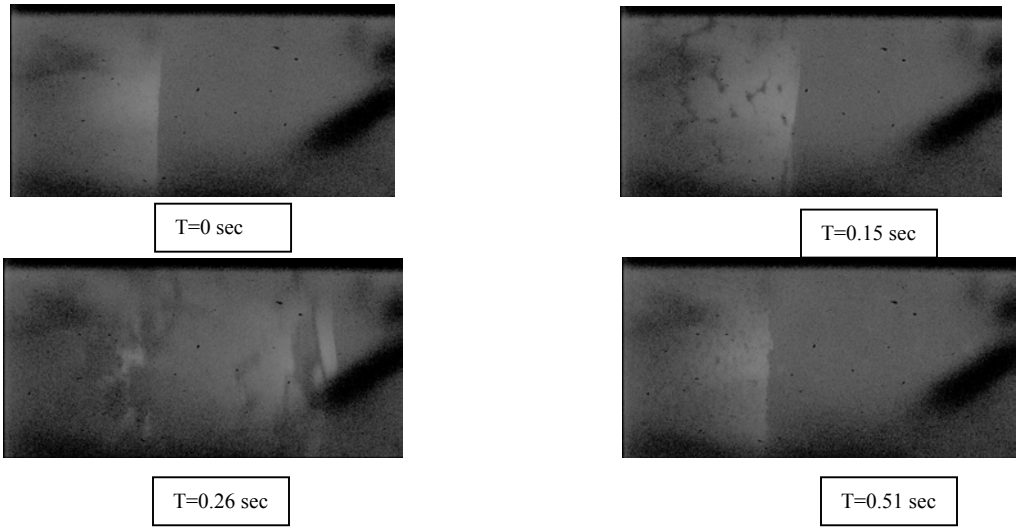

Figure 2.49 Thick ash regeneration at fourth cycle. 1500 F,7 cm/s.